The relationship between docohexanoic acid (DHA) and L-serine, providing an insight into the biochemistry of meningioma.

by

Hayley Hatchell

A thesis submitted in partial fulfilment for the requirements for the degree of
Doctor of Philosophy at the University of Central Lancashire

December, 2017.

Student declaration form

Type of Award   PhD

School   Pharmacy and Biomedical Sciences

I declare that no material contained in the thesis has been used in any other submission for an academic reward and is solely my own work.

No proof-reading service was used in the compilation of this thesis.

Signature of Candidate   _____

Print name: _____

Acknowledgements

Firstly, I would like to thank Brain Tumour North West, Royal Preston Hospital Tissue Bank and Inbetween Ears for their backing throughout this research project. This dissertation would not have been possible without the support from Dr Charles Davis, Dr Tim Dawson, Professor Bob Lea, Kate Ashton and Dave Griffiths. I am sincerely grateful for the experimental skills shared by Dave Griffiths, Dr Iftikar Khan, Dr Kerry Ann Rostron, Dr Andrea Burrows and Dr Sarah Dennison which I have implemented throughout this study.

I am truly indebted and thankful for the continual guidance and advice from Dr Steve Beeton throughout my undergraduate and postgraduate studies. I would also like to show my sincerest thanks to Clare Altham, Fiona Mair and Professor Peter Seville who have made this experience as least stressful as possible! Finally, I would like to show my gratitude to Proffesor Colin Davidson, Dr Frederick Harris and Dr Sarah Dennison for their recommendations over the past 12 months.

In addition to the fond memories I have gained, these individuals have also given me the strength over the past year to continue; Dr Vikesh Chhabria, Shofiya Salim, Murassa Sheikh, Roshini Mathews, Mehak Raja, Joud Sabouni, Muraf Jalab, Dr Iftihar Khan, Dr Sakib Yousaf. I honestly cannot thank you enough!

"It always seems impossible until it's done"

Abstract

As far back as the 1920s, Otto Warburg observed that cancerous cells display an altered state of metabolism surrounding lipid biosynthesis. However, only until recently has metabolic reprogramming been a recognised hallmark of the disease. The number of cancer cases diagnosed is set to triple by 2030, demonstrating the need for disease prevention, improved diagnostic testing and personalised treatment therapies. However, with some cancers occurring in the brain and spinal cord, the type of treatment available can become challenging due to their locality. Such cancer types include meningioma and glioma which are the most common brain tumours diagnosed.

An initial study involving human meningioma tissue revealed unusually high levels of the phosphatidylserine enriched with docosahexaenoic acid (DHA). In this study, the metabolism surrounding lipid biosynthesis was examined to establish if such alterations in lipid profiles were related to an altered state of metabolism. From the results gained, it can be suggested that meningioma does have an altered state of metabolism, evolving around serine as opposed to DHA. From the grade I and grade II meningioma tissues immunochemically examined, positive expressions of pyruvate kinase isoform 2 (PKM2) and phosphoglycerate dehydrogenase (PHGDH) were shown. Therefore, the results demonstrated that within meningioma tissues, serine can allosterically regulate the flux through glycolysis. The association that serine presence alone can alter the metabolic flux was demonstrated in the model organism, *Lipomyces starkeyi*.

Those *L. starkeyi* cells supplemented with serine, displayed a 50% reduction in the amount of radiolabelled acetate taken up during exponential and stationary growth phases. The radiolabelled study also highlighted that with serine presence, *de novo* lipid biosynthesis was altered. Once synthesised, these neutral lipids go on to be

stored in membrane bound organelles. Within the phenotype of cancerous cells, such storage of neutral lipids into lipid droplets prevent lipotoxicity. The light microscopy study of *L. starkeyi* cells supplemented with serine demonstrated that the formation of such lipid droplets was enhanced during lipid accumulation. These findings suggest that the production, storage and mobilisation of lipids within serine supplemented cells are adapted to cellular requirements, promoting a cancerous phenotype.

In order to gain an insight into the potential impact that an altered metabolic state may give to meningioma, a liposomal study was developed. Supplementation of both phosphatidylserine-consisting liposomes, as well as tumour-derived liposomes, enhanced the cellular viability of the non-cancerous cell line, SVG, during exponential phase. The supplementation of meningioma-derived liposomes also increased the viability of the non-cancerous human fetal glial SVG cell line, similar to that observed with phosphatidylserine containing liposomal preparations. Therefore, the data suggest that in fact, the phospholipid (phosphatidylserine), rather than the fatty acid (DHA) plays a role in cellular viability.

It is concluded that the results gained from this study can be used clinically in the diagnosis and management of meningioma as well as other diseased cells displaying ectopic lipid accumulation. The observation that meningioma has an altered biochemistry may provide guidance when histologically grading meningioma tumours. For those tumours expressing the enzymes involved in serine biosynthesis, such as PKM2 and PHGDH, a targeted treatment therapy surrounding enzyme inhibitors can be examined. By targeting serine biosynthesis, the resources needed to enable a cancerous phenotype are depleted. Future research can examine such targeted therapies utilizing either the developed model organism, *L. starkeyi* or the conventional SVG and U87 cell lines.

Table of Contents

Abbreviation List

Abbreviation	Term/Phrase
22:6	Docosahexaenoic acid
3PHG	3-phosphoglycerate
AA	Arachidonic acid
ACAT	Acyl-CoA:cholesterol acyltransferase
ACC	Acetyl-CoA carboxylase
ACL	ATP citrate lyase
AGPAT	1-acylglycerol-3-phosphate-O-acyltransferase
A-KG	Alpha-ketoglutarate
AMP	Adenosine monophosphate
Asc1	Alanine-serine-cysteine-1
ASCT1	Alanine/Serine/Cysteine/Threonine Transporter 1
ATP	Adenosine triphosphate
BBB	Blood brain barrier
CAFs	Cancer associated fibroblasts
CCT	Phosphocholine cytidylyltransferase
CDP-DAG	Cytidine diphosphate diacylglycerol
CL	Cardiolipin
CLM	Carbon-limiting media
CNS	Central Nervous System
CoA	Coenzyme A
COX1	Cyclooxygenase-1
COX2	Cyclooxygenase-2
CPT1C	Carnitine palmitoyltransferase 1C
CT	Computerised tomography
DAG	Diacylglycerols
DESI-MS	Desorption electrospray ionization mass spectrometry

DGAT	Diacylglycerol Acyltransferases
DH_20	Distilled water
DHA	Docosahexaenoic acid
DHAP	Dihydroxyacetone phosphate
DMS	Dimethylsterols
DMSO	Dimethyl sulfoxide
DNA	Deoxyribonucleic acid
ELOVL	Elongation of very long chain fatty acids
EPA	Eicosapentaenoic acid
ER	Endoplasmic reticulum
ERR-alpha	Estrogen-related receptor alpha
FADS	Fatty acid desaturases
FASN	Fatty acid synthase
FFA	Free fatty acids
FV	Fat vacuole
G-3-P	Glycerol-3-phosphate
GA	Golgi apparatus
GLUT3	Glucose transporter-3
GLUT1	Glucose transporter-1
GPAT	Glycerol 3-phosphate acyltransferases
HMGCR	Hydroxymethylglutaryl-CoA receptor
HMGCS	Hydroxymethylglutaryl-CoA synthase
ICDH	Isocitrate dehydrogenase
L. starkeyi	*Lipomyces Starkeyi*
LD	Lipid droplet
LPA	Lysophosphatidic acids
LPC	Lysophotidylcholine
LPC-DHA	Lysophophatidylcholine-docohexanoic acid
MAG	Monoacylcerols
MAGL	Monoacylglycerol lipase
ME	Malic enzyme

mL	Millilitres
mM	Millimetres
MMS	Monomethylsterols
MRI	Magnetic Resonance Imaging
MRS	Magnetic resonance spectroscopy
MT	Mitochondria
NADP	Nicotinamide adenine dinucleotide phosphate reduced
NADPH	Nicotinamide adenine dinucleotide phosphate
NLM	Nitrogen-limiting media
NM	Nanometers
OD	Optical density
PA	Phosphatidic acid
PC	Phosphatidylcholine
PDH	Pyruvate dehydrogenase
PE	Phosphatidylethanolamine
PET	Positron emission tomography
PEX	Peroxisome
PG	Phosphatidylglycerol
PGE2	Prostaglandin E2
PGH2	Prostaglandin H2
PHGDH	Phosphoglycerate dehydrogenase
PI	Phosphatidylinositol
PIPx	Phosphatidylinositol phosphate
PKC	Protein kinase C
PL	Phospholipid
PPAP	Phosphate phosphohydrolase
PS	Phosphatidylserine
PSS1	Phosphatidylserine synthase-1
PSS2	Phosphatidylserine synthase-2
R. gracilis	*Ramaria gracilis*
RPM	Revolutions per minute

S	Sterols
S1P	Sphingosine-1-phosphate
SCD	Stearoyl-CoA desaturase
SE	Sterol esters
SHMT1/2	Serine hydroxymethyltransferase 1 and 2
SPH	Sphingosine-1-phosphate
SPHK	Sphingosine kinase
SREBP-1	Sterol receptor element-binding protein-1
TAG	Triacylglycerides
TCA	Tricarboxylic acid
WHO	World Health Organisation
YEPD	Yeast extract peptone dextrose

List of Figures

7.2	A parsimonious tree summarising the phylogenetic relationship between Lipomycetaceae (Kurtzman et al., 2007).	218
7.3	Photographic visualisation via light microscopy of the immunohistochemistry antibody expression profiles associated with serine biosynthetic and glycolytic pathways in the tissue sections belongings to patient 1, a grade I meningioma patient (n=1).	219
7.4	Photographic visualisation via light microscopy of the immunohistochemistry antibody expression profiles associated with serine biosynthetic and glycolytic pathways in the tissue sections belongings to patient 88, a grade I meningioma patient (n=1).	220
7.5	Photographic visualisation via light microscopy of the immunohistochemistry antibody expression profiles associated with serine biosynthetic and glycolytic pathways in the tissue sections belongings to patient 91, a grade I meningioma patient (n=1).	221
7.6	Photographic visualisation via light microscopy of the immunohistochemistry antibody expression profiles associated with serine biosynthetic and glycolytic pathways in the tissue sections belongings to patient 95, a grade I meningioma patient (n=1).	222
7.7	Photographic visualisation via light microscopy of the immunohistochemistry antibody expression profiles associated with serine biosynthetic and glycolytic pathways in the tissue sections belongings to patient 99, a grade I meningioma patient (n=1).	223
7.8	Photographic visualisation via light microscopy of immunohistochemistry antibody expression profiles associated with serine and glycolytic pathways in patient 118 tissue sections, a grade I meningioma patient (n=1).	224

7.9	Photographic visualisation via light microscopy of the immunohistochemistry antibody expression profiles associated with serine biosynthetic and glycolytic pathways in the tissue sections belongings to patient 145, a grade I meningioma patient (n=1).	225
7.10	Photographic visualisation via light microscopy of the immunohistochemistry antibody expression profiles associated with serine biosynthetic and glycolytic pathways in the tissue sections belongings to patient 36, a grade I meningioma patient (n=1).	226
7.11	Photographic visualisation via light microscopy of the immunohistochemistry antibody expression profiles associated with serine biosynthetic and glycolytic pathways in the tissue sections belongings to patient 395, a grade II meningioma patient (n=1).	227
7.12	Photographic visualisation via light microscopy of the immunohistochemistry antibody expression profiles associated with serine biosynthetic and glycolytic pathways in the tissue sections belongings to patient 457, a grade II meningioma patient (n=1).	228
7.13	Photographic visualisation via light microscopy of the immunohistochemistry antibody expression profiles associated with serine biosynthetic and glycolytic pathways in the tissue sections belongings to patient 677, a grade II meningioma patient (n=1).	229
7.14	Photographic visualisation via light microscopy of the immunohistochemistry antibody expression profiles associated with serine biosynthetic and glycolytic pathways in the tissue sections belongings to patient 708, a grade II meningioma patient (n=1).	230

7.15	Photographic visualisation via light microscopy of the immunohistochemistry antibody expression profiles associated with serine biosynthetic and glycolytic pathways in the tissue sections belongings to patient 286, a grade II meningioma patient (n=1).	231
7.16	Photographic visualisation via light microscopy of the immunohistochemistry antibody expression profiles associated with serine biosynthetic and glycolytic pathways in the tissue sections belongings to patient 198, a grade II meningioma patient (n=1).	232
7.17	Photographic visualisation via light microscopy of the immunohistochemistry antibody expression profiles associated with serine biosynthetic and glycolytic pathways in the tissue sections belongings to patient 143, a grade II meningioma patient (n=1).	233
7.18	Photographic visualisation via light microscopy of the immunohistochemistry antibody expression profiles associated with serine biosynthetic and glycolytic pathways in the tissue sections belongings to patient 392, a grade II meningioma patient (n=1).	234

List of Tables

Chapter One

Lipid metabolism reprogramming in cancer

1.1 INTRODUCTION

Cancer cases are expected to triple per annum by 2030 to 26 million diagnosed cases coupled with 17 million deaths (Thun et al., 2010). Demographic changes in the increasing ageing population are one of the many factors accounting for this ever-increasing statistic on cancer diagnosis. The risk of cancer development is heightened with several associated risk factors surrounding an adoption of unhealthy lifestyle choices i.e. smoking, poor diet and reduced physical activity. One cancer type, which often embodies relatively rare, but serious health-associated risks, is those that are in the central nervous system (CNS). According to the World Health Organisation (WHO) there are a multitude of brain tumour types (>125) which can be histopathologically assessed (Eberlin et al., 2013). Under the umbrella of brain and spinal cord tumours, gliomas and meningiomas are the most common diagnosed per year (Taylor et al., 2009).

1.1.1 Meningioma

Meningioma is the most common primary intracranial tumour diagnosed in the adult population; accounting for 13-26% of all CNS tumours (Alexiou et al., 2010; Eberlin et al., 2013). Interestingly, Harvey Cushing first described it in 1915 and at that time arachnoidal cap cells were believed to be the point of origin of the meningeal brain tumour. Cushing further defined the tumour in 1922 with the term 'meningioma', which has retained its global acceptance until the present day. The cells, previously referred to as the arachnoidal cap cells, are now known as the non-neuroepithelial progenitor cells which cover the brain and spinal cord.

The work by Cushing and Bailey (1915) in the meningioma classification laid the foundation in the WHO classification of the disease. This included a histopathological classification system with four subclasses of meningioma, consisting of: meningiothelial, fibroblastic, angioblastic and osteoblastic. Remarkably, even with the recent scientific advances, the histopathological basis for

meningioma diagnosis, reported by the WHO in 2007, remains like that originally described by Cushing and Percival (1915).

1.1.2 Current Epidemiology of Meningioma

The WHO classification is used clinically to diagnose meningioma tumours. In 2012 alone, an estimated 57,000 new cases of brain and other CNS tumours in Europe were diagnosed. Europe wide occurrence of brain and other CNS tumours was reviewed in a seven-year EUROCARE-5 study (Visser et al., 2015). From this study, an observed gender-bias was displayed in the diagnosis of CNS tumours with many cases being diagnosed in males (57%) as opposed to females (43%). Interestingly, the proportion of CNS cases diagnosed which originating from the United Kingdom accounted for over a third of the total diagnosed cases in Europe in this seven-year period. Disappointingly, UK and Ireland was ranked at the bottom of the survival rates in comparison to other European countries.

The five year prognosis of individuals with benign meningioma is high with 80% of individuals diagnosed reaching this period (Taylor et al., 2009). A marked difference between meningioma and glioma is the five-year survival rate. Those individuals who are diagnosed with meningioma have a higher chance of reaching the five-year survival (70-95%) as opposed to those diagnosed with glioma (<3%) (Sehmer et al., 2014) demonstrating the marked difference in the aggressive nature of these tumours.

A ten-thousand patient case-control study of UK residents on meningioma diagnosis demonstrated an incidence rate of 5.30 per 100,000 persons (between 1996 and 2008). Similar incidence rates were demonstrated in a review by Sehmer et al. (2014) on glioma diagnoses between 2006 and 2010; 7.10 per 100,000 persons. Within the meningioma diagnosis cohort, the incidence rate in women was shown to be twofold higher compared to males, with the incidence rate of women being 7.19 compared to 3.05 found in males per 100,000. This study suggests a meningioma

female gender basis in diagnoses. Interestingly, this is opposite to that reported by the EUROCARE-5 study (Visser et al., 2015). However, to keep in mind, the EUROCARE-5 study gathered information from a variety of cancer types including liver, pancreas etc., not just meningioma. Therefore, this supports the postulation that meningioma risk can be related to the individuals' gender especially that of women. Incidence rates of meningioma is shown to increase with age; indifferent of gender, peaking in individuals ranging from 70-80 in years. However, a study by Nielsen et al. (2009) demonstrated a link between medical advances including the use of computerised tomography (CT) scanning and oligodendroglioma incidence rates (a glioma variant). From 1943 to 2002, diagnoses in Denmark nearly doubled to 0.45 cases/100,000 persons presumably through improved diagnostic techniques.

1.1.2.1 Tumour Anatomy

The anatomy of a tumour can be observed using recent medical advances, including that of CT. Meningioma can reside in various locations within the brain and spinal cord. This is important as the origin of tumour site aids not only meningioma classification, but also the appropriate treatment avenue available. Furthermore, the tumour location is also an important factor clinically when considering if surgery is a viable option; the associated risk of tumour removal can be too great if the tumour is too deep. Illustrations of the most common locations of meningioma in the brain are shown in Figures 1.1 and 1.2.
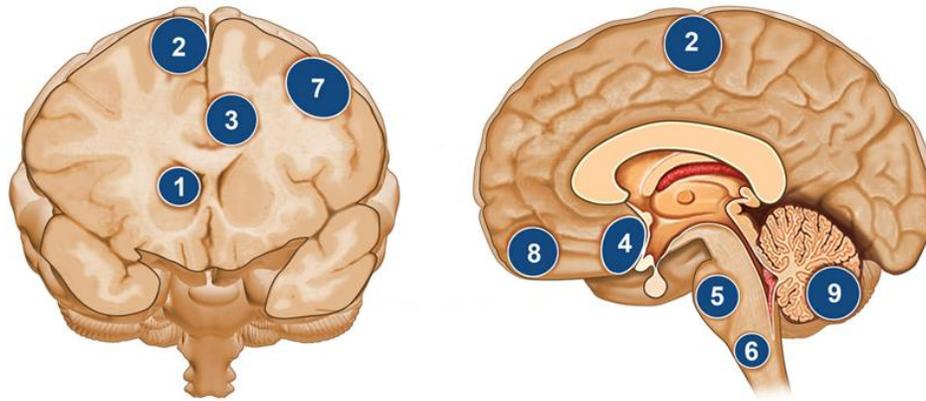
Figure 1.1: Diagrams showing the common locations of Meningioma in the Coronal and Sagittal planes (taken from The Mount Sinai Hospital, 2017). **Legend:** 1. Intraventricular, 2. Parasagittal, 3. Falcine, 4. Suprasellar, 5. Clivus, 6. Foramen Magnum, 7. Convexity, 8. Olfactory Groove and 9. Cerebellar.
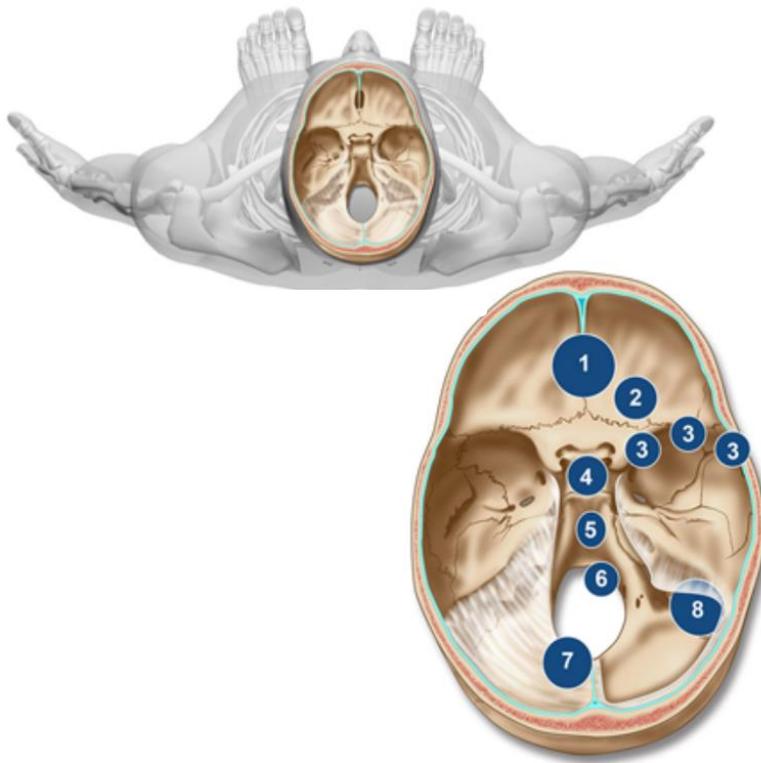
Figure 1.2: Diagrams showing common locations of Meningioma in the Skull Base planes Locations (taken from The Mount Sinai Hospital, 2017). **Legend:** 1. Paranasal/ Olfactory, 2. Optic Sheath, 3. Sphenoid Wing, 4. Suprasellar, 5. Clivus, 6. Foramen Magnum, 7. Tentorial and 8. Posterior Fossa.

Although meningioma tumours can occur at any point along the meninges, some areas are more common than others, namely the Falx and Parasagittal regions (refer to Figure 1.1 and 1.2). The majority of meningioma's are located intracranially (90%) in the supratentorial compartment; along the dural venous sinuses in the cerebral convexity; parasagittal and in the spheroid wing regions (Cea-Soriano et al., 2012). These supratentorial tumours account for approximately 20% of the total intracranial tumours diagnosed (Cea-Soriano et al., 2012). Other locations where meningioma tumours can be found include the optic nerve sheath, choroid plexus and the cerebellopontine angle. Therefore, the position of the meningioma tumour can provide an indication of its type during diagnosis.

1.1.2.2 Recent imaging and histological markers aiding diagnosis

Brain tumour detection via modern imaging techniques display the position of the meningioma tumours. The use of such medical advances, as opposed to the interpretation of tumour symptomatology alone, have enabled earlier detection and diagnosis of meningioma. Often, meningioma patients display wide-ranging location-related symptoms, including seizures, impaired vision, headaches, anosmia and mental changes. Consequently, a postponement of diagnosis can occur, due to a misdiagnosis (Nakasu et al., 1987).

The result of either misdiagnosis or undetected symptomology of meningioma is highlighted with the number of cases diagnosed post-death, during autopsy. A review by Nakasu et al. (1987) of autopsies between 1950 to 1982, highlighted a meningioma incidence rate of 1-2% with a 3:1 female to male ratio. Increasingly, the unexpected meningioma findings during autopsy demonstrated a trend between age and the tumour size and older the individual the larger the tumour. Similar observations were described in a study by Sugiyama et al. (1996), whereby the main meningioma histological variant observed was psammomatous. The observation of psammomatous meningiomas being found during autopsy may be as a result of their reduced nature of proliferation compared to other meningioma variants. Hence, due to psammomatous meningiomas reduced growth rate, associated symptomology

due to the tumour may not have occurred. Therefore, the postulation from both studies as to why these meningioma tumours have gone undetected until autopsy may be due to the specific tumour variant which delays meningioma associated symptomology in addition to recent medical advances i.e. CT not being utilised pre-death.

The use of current imaging techniques would be important if an individual was to have a recent onset of seizures or had focal neurological signs. Novel imaging techniques which can aid meningioma diagnosis include magnetic resonance imaging (MRI) (Cea-Soriano et al., 2012). Accurate diagnosis of meningioma is achieved by a MRI scanner, as the characteristic meningioma features are displayed to the clinician. Such markers of the tumour in plain radiographs include hyperostosis, increased vascular markings and psammomatous calcifications. The benefit of such imaging techniques such as CT and MRI scans, is the ability to detect the tumour before the symptoms are present. This is especially important for highly aggressive tumours whereby symptoms can be presented at a late stage of malignancy where treatment is limited. By detecting the tumour earlier via imaging, a better prognosis can be achieved as treatment intervention occurs earlier. Once the mass is identified, a biopsy is taken which will enable the tumour classification to be identified which will in turn direct the anti-tumour therapies available.

1.1.2.3 World Health Organisation Grading System

The WHO tumour grading objectives have been constant since its existence (Scheithauer, 2009) to categorise and establish the grading of human neoplasms; such as meningioma (Louis et al., 2007).   In each new published classification edition to aid accurate tumour diagnosis the WHO included new advances in the field. Such examples of the incorporation of recent medical advances include the immunohistochemistry introduction in diagnostic pathology including the signs and symptoms alongside prognosis and predictive factors being taken into account when classifying the tumour (Louis et al., 2016; Louis et al., 2007).

The most recent 2016 WHO classification was an updated version of the 2007 edition, the details can be found in the review of CNS classification by Louis et al. (2016). In brief, the molecular alterations previously used as prognostic markers have now been incorporated in the diagnostic classification, the review by Louis (2006) details the spectrum of malignant glioma in terms of genetic alterations. Interestingly, meningioma did not undergo re-classification in this sense, only glioma. Hence, the 2016 WHO edition has significantly updated the classification codes including integrating molecular parameters with microscopy. Interestingly, the observation of a tumour having invasive characteristics will override the previously diagnosed atypical meningioma, which is currently classified via the 2007 WHO edition via several histological characteristics (Louis et al., 2016). However, unlike glioma which had molecular parameters considered in the new 2016 WHO edition, meningioma did not. Currently, meningioma is diagnosed and classified into three Grades (I-III) per the WHO grading system as summarised in Table 1.1.

Table 1.1: Meningioma classifications in terms of grade (I-III) based on histomorphological features, according to the 2007 WHO diagnostic criteria.

WHO Grade	Histomorphological Features					
I	Predominant histological variant - Meningothelial - Fibrous - Transitional - Psammomatous - Secretory - Microcystic - Angiomatous - Lymphoplasmacyte-rich - Metaplastic					
II	Any Grade I histologic variant with brain invasion	OR	Atypial by elevated mitoses (4-19 mitoses/10 high powered fields)	OR	≤3 atypical features including: - Hypercellularity - 'Sheet-like' growth - Spontaneous necrosis - Small cell change	OR	Predominant histologic variant - Clear cell - Chordoid
III	Frank anaplasia (Sarcoma-, carcinoma-, or Melanoma-like histology)	OR	Anaplasia by elevated mitoses (≥20 mitoses/10 high powered fields)	OR	Predominant histologic variant - Rhabdoid - Papillary		

On the premise of the 2007 WHO classification as shown in Table 1.1, benign (grade I) meningioma was the predominant grade diagnosed (80%); depending on its location this can be cured via surgical resection (Riemenschneider et al., 2006). Meningioma tumours which display more aggressive clinical features are classified as grade II. This variant only accounts for 15-20% of diagnosed meningioma cases. However, in circumstances where infiltrating malignant behaviours are displayed, diagnoses of grade III (malignant) occur (1-3%).

1.1.2.4 Histological classification

When reviewing histological meningioma sections distinctive histological findings are customary due to the cellular origination of meningioma, the arachnoidal cap cells. This is in-part due to arachnoidal cap cells metabolically-active subgroup which is responsible for cerebrospinal fluid reabsorption. The position of these arachnoidal cap cells are perfect for venous blood flow exposure hence cerebrospinal fluid reabsorption. A full review on the function and structure of the arachnoidal villi was done by Pollay (2010). With the basis of arachnoidal cap cells function in mind, the WHO histological classification of meningioma is imperative to enable accurate diagnosis in terms of grade and histological variance (Table 1.1).

Within the three grades (I-III) of meningioma, there are 11 histologic subtypes (Backer-Grondahl et al., 2012). Clinically, these histomorphological features of meningioma (Table 1.1) can be diagnosed using a light microscope. Images of meningioma tissue sections of various grades and histomorphological features that were described in Table 1 are illustrated in Figure 1.3.

1. Histology of WHO grade I meningioma
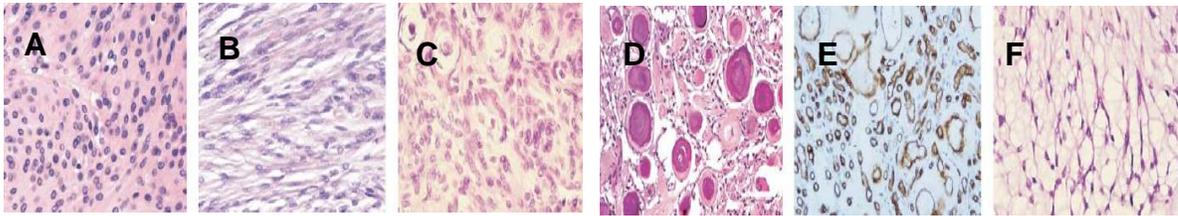
2. Histology of WHO grade II meningioma (Atypical)
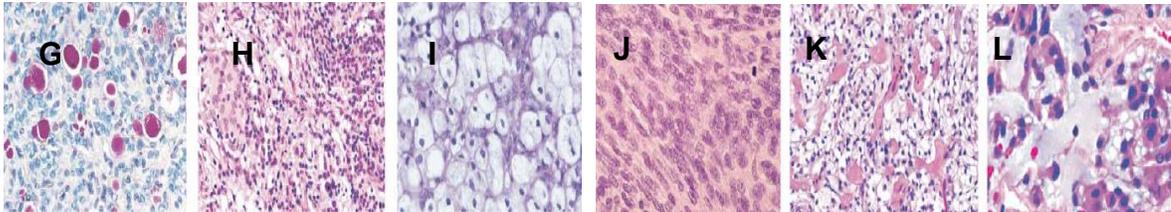
3. Histology of WHO grade III meningioma (Anaplastic and malignant)
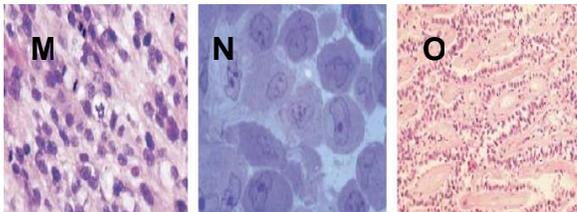
Figure 1.3: Samples of photographs showing the histomorphological features of (1) grade I meningioma, (2) grade II meningioma and (3) grade III meningioma in accordance with the WHO classification (2007). These features aid diagnosis and thereafter, grade classification which in turn gives an indication of the tumours behavior adapted from Riemenschneider et al. (2006).

Legend: Grade I, meningioma variants (Adapted from Riemenschneider et al., 2006): meningiothelial (A), fibrous (B), transitional (C), psammomatous (D), angiomatous (E), microcystic (F), secretory (G), lymphoplasmacyte-rich (H) and metaplastic (I). Grade II, atypical variants (Adapted from Riemenschneider et al., 2006): atypical meningioma with increased mitotic activity (J), clear-cell with glycogen-rich cytoplasm (K) and choroid showing chordoma-like growth in myxoid matrix (L). Grade III, anaplastic (malignant) variants (Adapted from Riemenschneider et al., 2006): anaplastic meningioma with cellular anaplasia and mitotic figures (M), rhabdoid meningioma with large tumour cells with eccentric nuclei (N) and papillary meningioma showing a pseudopapillary growth pattern (O).

The histomorphological features of meningioma as depicted in Figure 1.3, are clinically used in the process of diagnosing and predicting the biological behaviour of the neoplasm. On closer inspection from the neoplasm sections (Figure 1.3), three histological growth patterns have been concluded, namely; meningiothelial, fibroblastic and transitional. In accordance with several other factors stated in the WHO classification, the meningioma grade can be determined using the tumour location and histological growth pattern. This in turn, aids the appropriate treatment avenues for the diagnosed tumour grade. The appropriate treatment avenue for a meningioma tumour is dependent primarily on its location, as this determines the likelihood of surgical viability. Unfortunately, even with aggressive intervention, to date, effective treatments for malignant meningiomas are still unavailable.

1.1.2.5 Tumour grade as a prognostic factor

In combination with WHO classification, other factors are taken into consideration in predicting the response to a particularly therapy. These factors which determine the likelihood of therapy outcome include the individual's clinical history, their age, neurological performance alongside the tumour location and size and the presence of neoplastic mutations (genetic). To enable an accurate diagnosis of tumour type, grade and histological variance, a pre-work up is carried out whereby the tissue sections are examined histologically in terms of morphology and the presence of progesterone, oestrogen and invasiveness marker (Ki67) receptors. Going forward, the tumour progression, before-, during- and after treatment can then be measured using the same observations of receptor presence alongside tumour size which together provide an indication of therapy outcome.

1.1.3 Risk Factors

The aetiology of meningioma is generally unknown. However, there have been suggestions of a relationship between increasing age and exposure to other risk factors upon meningioma development (Alexiou et al., 2010). These risk factors include, but not limited to; ionising radiation, gender (female: male, 2:1 basis), genetic mutations and pre-existing medical conditions such as diabetes and

previous cancer history. These risk factors are summarised in detailed reviews by Barnholtz-Sloan and Kruchko (2007) and Riemenschneider et al. (2006).

1.1.4 Treatment

Standard level of care treatments for meningioma considers all aspects already ascertained and they include; but not limited to: the neoplasm site of origin, its' size and growth rate, the medical history of patient alongside their age and any neurological symptomologies due to neoplasm and, the histopathological biopsy profiles (if any have been taken in previous surgery) to aid determination of grade classification. Available treatment avenues for meningioma currently involve surgery, radiotherapy, stereotactic radiotherapy, hormonal therapy, chemotherapy and antiangiogenic therapy (Alexiou et al., 2010).

1.1.4.1 Surgery and Preoperative meningioma embolization

After initial diagnosis of meningioma, patients generally opt for surgical removal of the tumour. This is due to surgery being the standard therapeutic option, as excision alone cures the clear majority of meningioma cases. This reflects upon the recent neurosurgery advances i.e. micro-neurosurgery and image-guided surgery where the tumour removal can be more completed enabling lower reoccurrence rates (Alexiou et al., 2010). As discussed by Alexiou et al. (2010), the rate of tumour reoccurrence is observed to be higher when the surgery for resection is poor, however the option for surgery is dependent on tumour locality. In 1957, Simpson proposed the evaluation of the surgical reception in terms of grade to establish the likelihood of a tumour reoccurring. The proposed tumour resection quality scheme is described in Table 1.2.

Table 1.2: The proposed method of assessing tumour resection quality, via the Simpson Grade classification scheme grading from stage 1-5.

Stage	Resection Quality
1	Complete excision extending to the dura and bone.
2	Complete excision alongside dural attachment coagulation.
3	Solid tumour complete excision but insufficient excision of dura and bone and dural attachment coagulation.
4	Incomplete resection thus macroscopic tumour residue visible
5<	Biopsy only.

Staging of Simpson grade (1-5) corresponds with resection quality, as shown in Table 1.2. This has been proven to be an invaluable clinical asset in predicting meningioma reoccurrence after surgical resection. A clinical study demonstrated a correlation in meningioma grade I patients whereby a reduced reoccurrence rate was observed in those individuals which had a lower a Simpson grade (Saito et al., 2012). To reduce further the reoccurrence of meningioma, other therapeutic treatment avenues need to be available. By gaining a better understanding of the biochemical processes of the cancerous cells in relation to its behaviour, individualised treatment avenues can be sought.

There has been a plethora of studies examining brain tumours, as far back as the 19th century with Cushing and Percival Bailey to the present day. At this time, Otto Warburg described cancer to be an altered energy state of metabolism (Warburg, 1956). Interestingly, this has only recently been recognised in the cancer classification list (Hanahan and Weinberg, 2011).

1.2 IS CANCER A METABOLIC DISEASE?

Work pioneered by Otto Warburg as far back as the 1920s, recognized that tumour cells exhibited an altered state of metabolism, for which he won a Nobel prize in 1931 for Medicine (Warburg, 1925; Warburg, 1956). However, cancer is still to an extent viewed as a proliferative disease, which is often observed to be uncontrollable. Fueling the sustainability of this uncontrollable proliferation requires intermediary metabolites including proteins, nucleic acids and lipids such that the biochemical pathways ensuring growth are maintained.

1.2.1 Warburg and Crabtree effect

The observation that cancerous cells have altered metabolism was denoted nearly a century ago by Otto Warburg, terming these the Warburg and Crabtree effect. Warburg suggested that mitochondrial metabolism was suppressed in cancerous cells (Warburg, 1956). The mitochondria are often referred to as the 'power-house' of the cell due to the role they play in cellular processes and energy metabolism.

Several studies have demonstrated Otto Warburg's theory. These include the observation that cancerous cells display a decreased respiration in parallel with a heightened lactate production, proposing that the adenosine triphosphate (ATP) supply is dependent upon fermentative metabolism. Furthermore, the increased cellular proliferation of the cancerous cells was in line with reduced energy yield. Subsequently, the suppression of oxidative metabolism with oxygen presence occurs with such, the glycolysis is aerobic in nature hence termed the "Warburg effect" (Diaz-Ruiz et al., 2011; Zhou et al., 2010).

Energy demands of the cancerous cells are enabled by the result of the 'Warburg effect' long term on metabolic reprogramming (Zhou et al., 2010). Hence, the proliferative nature of the cancerous cells will continue. However, the specific

advantages the cancer cells ascertain by undergoing these metabolic alterations are unidentified. Several theories have been proposed and they include: 1) proliferation being supported in hypoxia and 2) apoptosis is prevented via the reduction of oxidative metabolism.   These metabolic alterations are advantageous for the cancerous cells to survive especially in in such conditions as hypoxia where nutrients required for proliferation maybe limited.   Opposing this purely 'glycolytic' cancerous cell view is the growing body of evidence of cancer cell lines possessing functional mitochondria. By possessing such, this would suggest that these cancerous cells are able to obtain their ATP via oxidative phosphorylation. Interestingly, some cancerous cells have been shown to reversibly switch between fermentative and oxidative metabolism depending on the tumours environment i.e. glucose status aiding their survival and ability to proliferate.

Cancerous cells can metabolically adapt to their environment. This is referred to as the 'Crabtree effect' whereby respiration and oxidative phosphorylation are suppressed by glucose. These short-term reversible switches occur between glycolysis and oxidative phosphorylation. The possibility of an intra-neoplasm metabolic switch in relation to the tumour environment i.e. oxygen availability etc. was recently displayed with reports of cancerous cells of differing subpopulations mutually co-existing: one subtype producing lactate (Warburg, 1956), whereas the other was utilizing lactate (Kennedy and Dewhirst, 2010). Hence, demonstrating the hypoxia conditions cancerous cells reside in, result in the production of lactate. This is contrary to those oxygen-rich cancerous cells, which have the capacity to take up lactate as its' preferred energy source. Similar results have been found in the study of cancerous breast cells by Park et al. (2016), whereby the deprivation of glucose did not affect the proliferative nature of the cells, as the preferred energy source was that of lactate not glucose. Interestingly, a link was found between lactate preference and the expression of ERRα (estrogen-related receptor alpha). With this in mind, cancerous cells' energy metabolism has been investigated as a possible anti-tumour therapy. One of the many anti-tumour therapy avenues researched surround energy metabolism, especially that of lipids, as these have been shown to be altered in many diseases including that of cancer.

1.2.2 Lipid metabolism

The process of nutrient-derived carbons being converted to fatty acids is referred to as lipid synthesis. Once thought as just an energy source, fatty acids have proven to be active molecules with roles ranging from; protein synthesis regulation, signal transduction and the involvement in membrane fluidity thus permeability. These fatty acids act as lipid mediators regulating both metabolic pathways and responses to inflammation. In many cancerous tissues, lipid biosynthesis is described as 'reactivated'; illustrating an example of disease lipid dysregulation (Coller, 2014; DeBerardinis et al., 2008b). An overview of the pathways involved in lipid metabolism is represented in Figure 1.4 below.
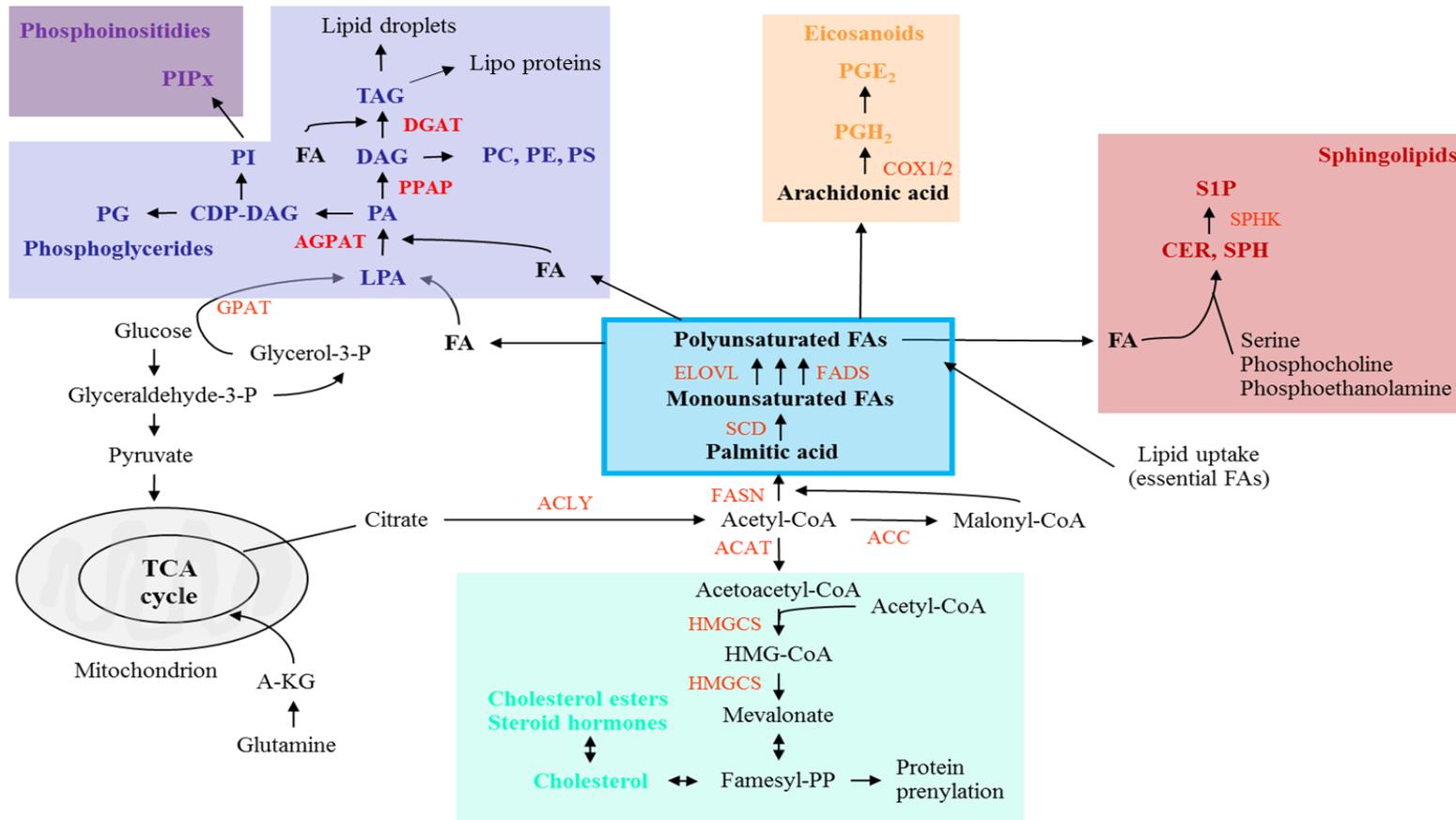
Figure 1.4: Flow diagram showing an overview of lipid biosynthesis pathways and their cross-talk. The fundamental precursor for all lipid classes (fatty acids, cholesterol, sphingolipids etc.) is the small molecule, acetyl-CoA which arises from the tricarboxylic acid (TCA) cycle (Adapted from Baenke et al., 2013; and Yamashita and Nikawa, 1997). **Legend:** triacylglycerides (TAGs) and diacylglycerols (DAGs).

The main precursor of all the lipid classes is a small two carbon unit called acetyl-CoA (Figure 1.4). Lipid classes are defined and based on their components, including: cholesterol and cholesterol esters, glycerol including triacylglycerides, diacylglycerols and monoacylcerols, eicosanoids, and sphingolipids. These lipid classes all have specific roles in proliferation, signalling and structural support. Full detailed reviews on lipid biosynthesis can be found in Zweytick et al. (2000) and Yamashita and Nikawa (1997).

1.3 FATTY ACIDS: CENTRAL LIPID

Lipids make up a large proportion of biological matter. From this, fatty acids are the main embodiment. This is good on several fronts since: 1) as they provide an invaluable energy source where excesses are stored for later use; 2) cellular membranes are mainly comprised of phospholipids which in turn are made from fatty acids and, 3) as they are involved in prostaglandin production which are involved in the inflammatory process. Fundamentally, fatty acids are carboxylic acids, varying in carbon length from 2-36 forming either a saturated or unsaturated structure. Their RCOOH structure is comprised of a methyl end, hydrocarbon chain and finally a carboxylic terminus, as shown below.

Figure 1.5: Diagram showing the structural formula of a fatty acid including the hydrocarbon backbone, a methyl end and a carboxylic terminus. The example illustrated is that of palmitic acid (sixteen carbons with no double bonds, 16:0).

Figure 1.5 shows the structural formula of a fatty acid within eukaryotes, there are several fatty acid types each serving a specific role and some examples of their structures are shown in Figure 1.6.
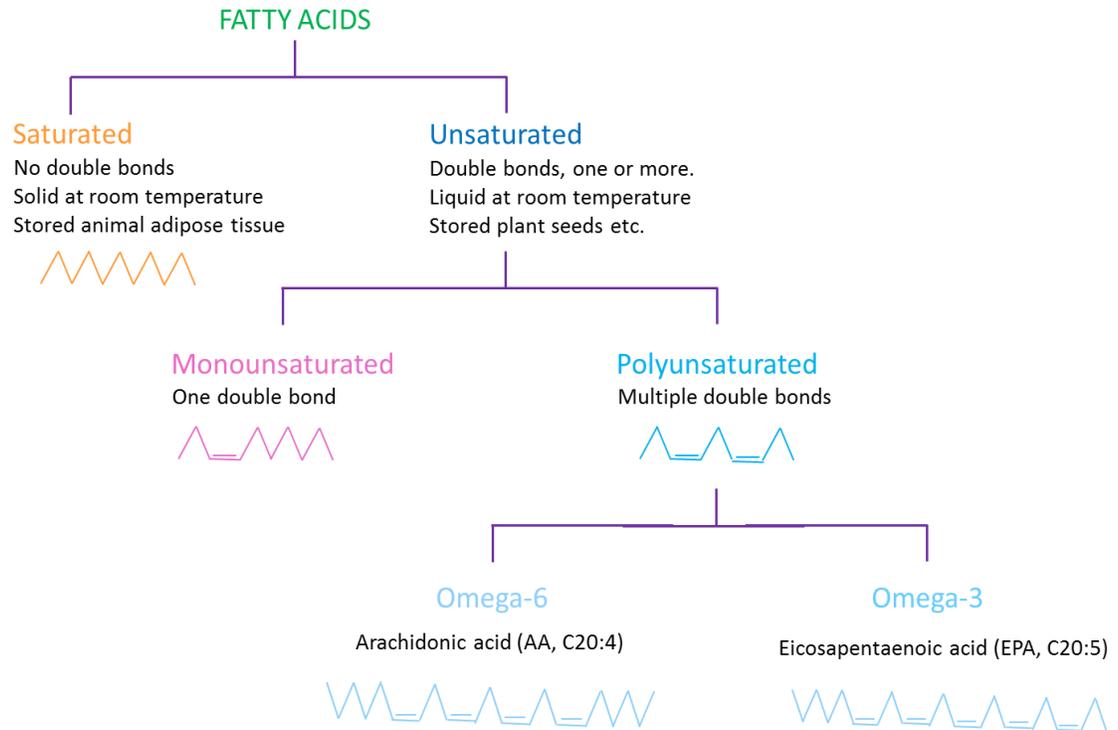
Figure 1.6: Flow chart showing a wide variety of eukaryotic fatty acids exist, many of which are illustrated above. The nomenclature of fatty acids are dependent on their structural characteristics, which in turn affects a range of; physical, chemical and biological properties. Double bond presence within the hydrocarbon chain (C=C), classifies these fatty acids as unsaturated, unlike saturated fatty acids which contain no double bonds. The number of these double bonds, further defines them as; monounsaturated (one double bond present) or polyunsaturated (> than one double bone present) fatty acids. Within the polyunsaturated pool, the position at the methyl terminal (ω:n) of the double bond, further classifies these either as omega-3 (ω:n-3) or omega-6 (ω:n-6) fatty acids. Figure drawn by hand.

As illustrated in Figure 1.6, the fatty acid structure alone can be used in the identification of their fatty acid subtype. For example, monounsaturated fatty acids, have one double bond whilst polyunsaturated fatty acids like, arachidonic acid have four (more than one). In most eukaryotic cells, fatty acids are stored as triacylglycerides, the conversion of which is shown below.
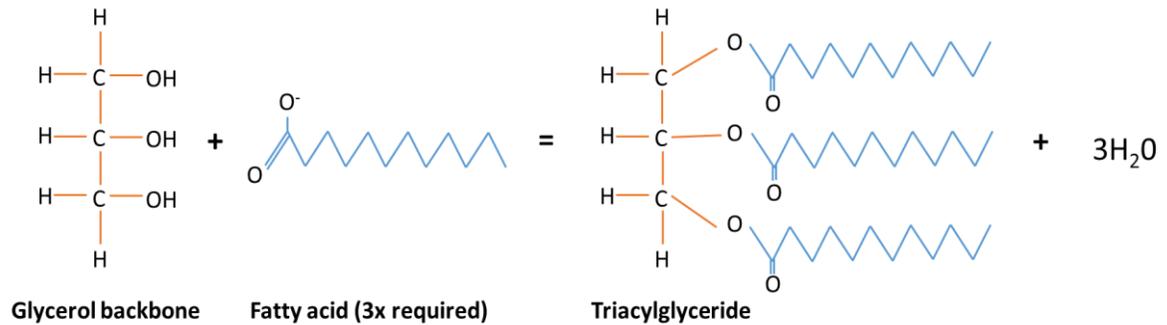
Figure 1.7: Diagrams of chemical structures, which provide energy in eukaryotic cells. The highly energy-rich triacylglyceride molecules provide stored energy and essential fatty acids via lipolysis in times of requirement such as membrane biosynthesis. Triacylglycerides are produced when fatty acids are esterified to a glycerol backbone and these fatty acids may be of differing lengths and saturation (Adapted from, Santos and Schulze, 2012 and Yen et al., 2008a).

After each successive fatty acid addition to the glycerol backbone, the final step is catalyzed via diacylglycerol acyltransferases (DGAT) which aid the conversion from diacylglycerols to triacylglycerides (Yen et al., 2008b). Once triacylglycerides are produced, this neutral lipid serves as cellular storage molecule that is highly enriched with ATP and essential fatty acids required for cellular events including membrane biosynthesis. However, due to the hydrophobic nature of triacylglycerides, they are stored in the core of a lipid droplet (LD) alongside sterol esters (Walther and Farese Jr, 2009). Therefore, to utilize these lipids, several organelles and key enzymes need to be orchestrated.

1.3.1 Lipid droplets

In the environmentally changing landscape of nutrient availability, the ability of a cell to store energy would be advantageous. A summary of the LDs' anatomy and their alliances with other organelles, which enable such storage of lipids in a cell is illustrated in Figure 1.8.
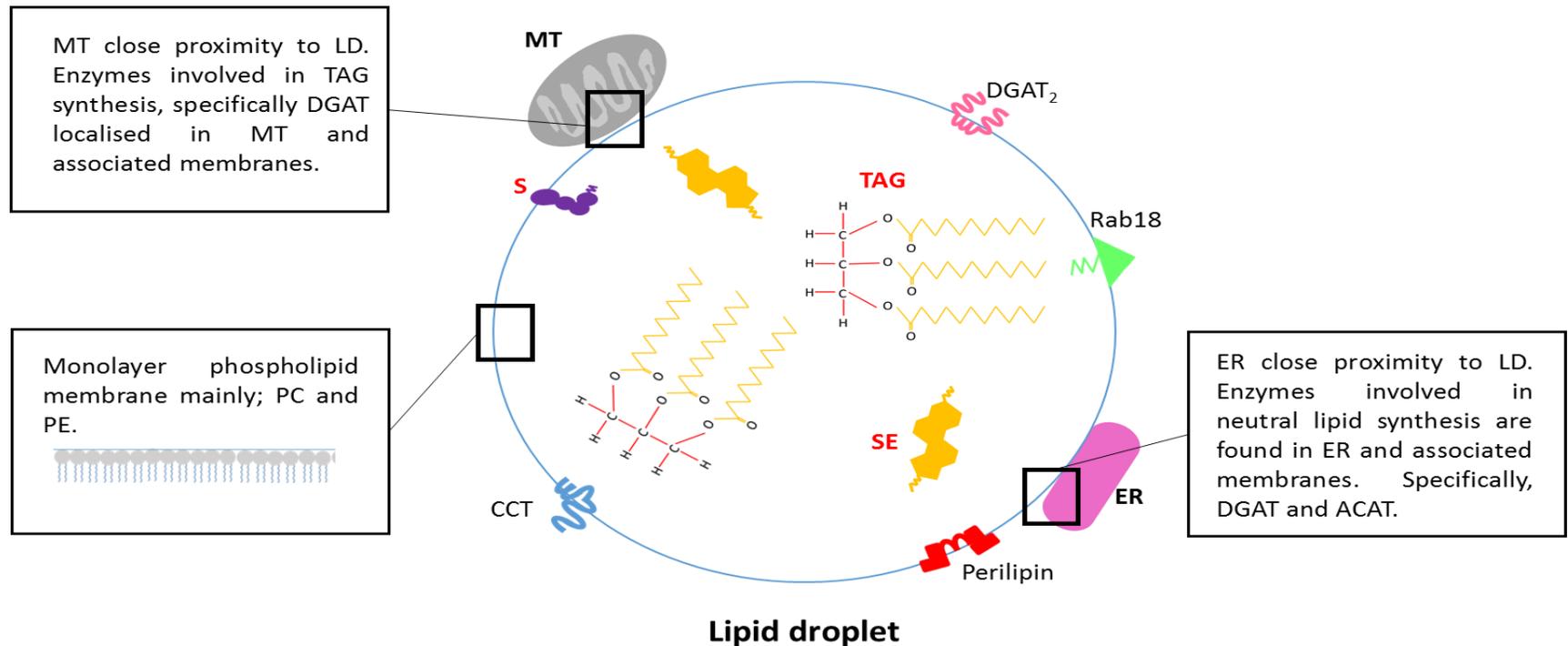
Figure 1.8: Diagram showing the anatomy and LD interactions with the mitochondria (MT) and endoplasmic reticulum (ET) provides an insight into its role as a high-energy storage organelle preventing lipotoxicity. Neutral lipids are stored within the core of the LD; sterol esters (SEs) and TAG are surrounded by a phospholipid monolayer consisting of; phosphatidylcholine (PC), phosphatidylethanolamine (PE) with minor sterol (S) traces. LD size is paralleled with neutral lipid storage and mobilization; close proximity with other organelles enriched with enzymes within membranes aids such a process. Proteins are targeted to the LD, including; Phosphocholine cytidylyltransferase (CCT), perilipin, Rab18 and Diacylglycerol O-Acyltransferase 2 (DGAT2) (Adapted from Farese and Walther, 2009 and Walther and Farese Jr, 2009).

As depicted in Figure 1.8, the alliance of several cellular organelles enable the efficient storage of lipid within LDs. The benefit of grouping such lipids into a separate cellular organelle is to 'buffer' the free lipid cytoplasmic content which would usually become lipotoxic when levels become raised (Walther and Farese Jr, 2009). When the cell requires these stored lipid resources with the LDs, lipolysis is initiated whereby several lipases and LD proteins act in unison to mobilize the required lipids Thiele and Spandl (2008). An overview of triacylglyceride lipolysis is shown in Figure 1.9 where energy is released subsequently.

Figure 1.9: Chemical structures depicts lipolysis of triacylglycerides to produce (1)
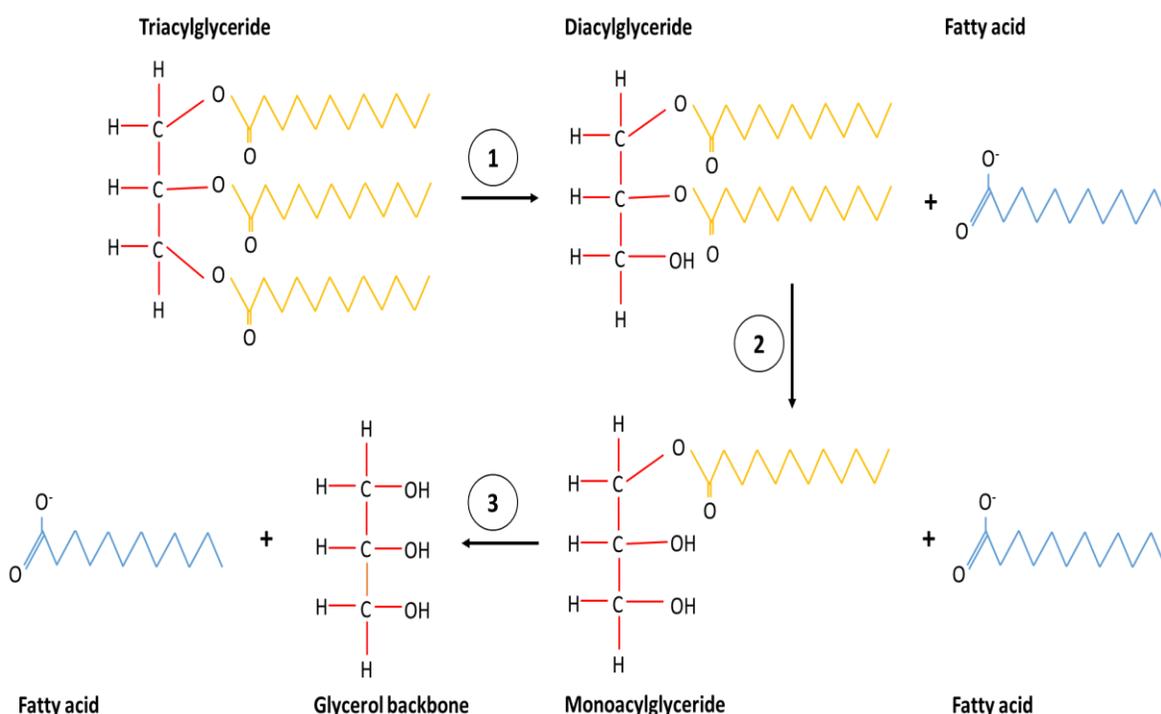
diacylglycerides then (2) monoacylglycerides, at each one of these stages fatty acids are released. The mobilization of these fatty acids enables membrane biosynthesis and other cellular processes. The diagram is adapted from Yen et al. (2008b).

In cancerous cells, the number of LDs are higher in comparison to non-cancerous cells (Accioly et al., 2008). Alterations in lipases have been associated in cancer, for example monoacylglycerides lipase (MAGL) has been observed to be overexpressed in cancerous cells, resulting in the mobilization of neutral lipids to enable energy production (Beller et al., 2010). Therefore, it can be suggested that

if this was a continuous state alongside the increased fatty acid production triacylglyceride would be accumulated in LD. Subsequently, the observed number of LDs in cancerous cells may be a sign of the cancerous cells adaptation to the raised cytosolic lipid content: mobilization demand.

Until recently, the role LDs play within the nervous system was quite sparse. It has been suggested however, that LD formation and neurodegeneration are paralleled. A study on *Drosophila* by Liu et al. (2015) demonstrated the knock-on effect of neuronal mitochondrial dysfunction and reactive oxygen species upon glia. The study demonstrated how glia with dysfunctional mitochondria increase their ability of storing neutral lipids within LDs. Furthermore, the onset of the neurodegeneration was shown to be paralleled with such lipid accumulation. Promisingly though a reduction of such lipid accumulation delayed the onset of neurodegeneration, therefore providing an insight into future treatment options focused upon lipid metabolism.

1.4 CANCERS ALTERED LIPID LANDSCAPE

As previously outlined, alterations in lipid metabolism have been observed in cancer. This dysregulation of lipid metabolism has been linked with chemo-resistance in many types of cancer, including; breast, cervical and colon (see Zhao et al. 2013 for review).

1.4.1 Altered metabolism: at a glance

One area of altered lipid metabolism that has gained research interest is that of fatty acids. In cancerous cells, carbon is diverted away from the production of energy to supply fatty acid metabolism (Currie et al., 2013). The observed increase in fatty acid metabolism provides supply into several fundamental processes which enable

membrane biosynthesis thus proliferation. In addition to this, the production of phospholipids is affected by the altered state of fatty acid metabolism.

1.4.1.1 Fatty acids

To examine fatty acid production within cancerous cells, some studies have looked at a transcriptional level. Studies by Li et al. (2014b) on hepatocellular carcinoma displayed the relationship upon the three-year survival rate of patients who showed an expression of Sterol Receptor Binding Protein-1 (SREBP-1). The study demonstrated the paralleled relationship of SREBP-1 expression with increasing tumour size, aggressiveness (grade) and the observation of metastasis. This transcription factor regulates the synthesis of cholesterol, fatty acids and phospholipids. Therefore, the overexpression of SREBP-1 within a cancerous cell will enable the required lipid source for the tumour to thrive in terms of growth and resistance to its microenvironment.

Interestingly, cancerous cells have the capability to generate fatty acids *de novo*, unlike non-cancerous cells which source their fatty acids exogenously (Currie et al., 2013). Further studies however, have demonstrated this may not be the case in all cancer types. Recent research on ovarian tumours have shown adipocytes near the tumour provide fatty acids to the cancerous cells via the lipid chaperone, fatty acid binding protein 4 (FABP4) (Nieman et al., 2011). Another point that the study by Zaugg et al. (2011) examined was the influence the cells accessibility to the produced fatty acids. Those tumour cells expressing carnitine palmitoyltransferase 1C (*CPT1C*) brain isoform had the ability to transport fatty acids across the mitochondrial membrane. This transportation of fatty acids to the mitochondria aided the oxidation of fatty acids therefore ATP generation needed for cellular processes. The overexpression of carnitine palmitoyltransferase 1C (*CPT1C*) has also shown to increase the cellular resistance to both glucose deprivation and hypoxia conditions. This demonstrates that fatty acid mobilization aids tumour resistance to environmental stressors i.e. oxygen and nutrient availability.

1.4.1.2 How lipid microenvironment relates to cancer progression

Cellular processes are dependent upon lipid availability to function. Such processes are tightly regulated by preventing lipotoxicity and membrane dysfunction. An example of which is the SREBP family, often described as master regulators of lipid homeostasis by targeting fatty acid and cholesterol biosynthesis (Camargo et al., 2012; Horton et al., 2002). The link between cancer progression and the presence of lipids surrounding the tumours microenvironment are summarized in Figure 1.10.
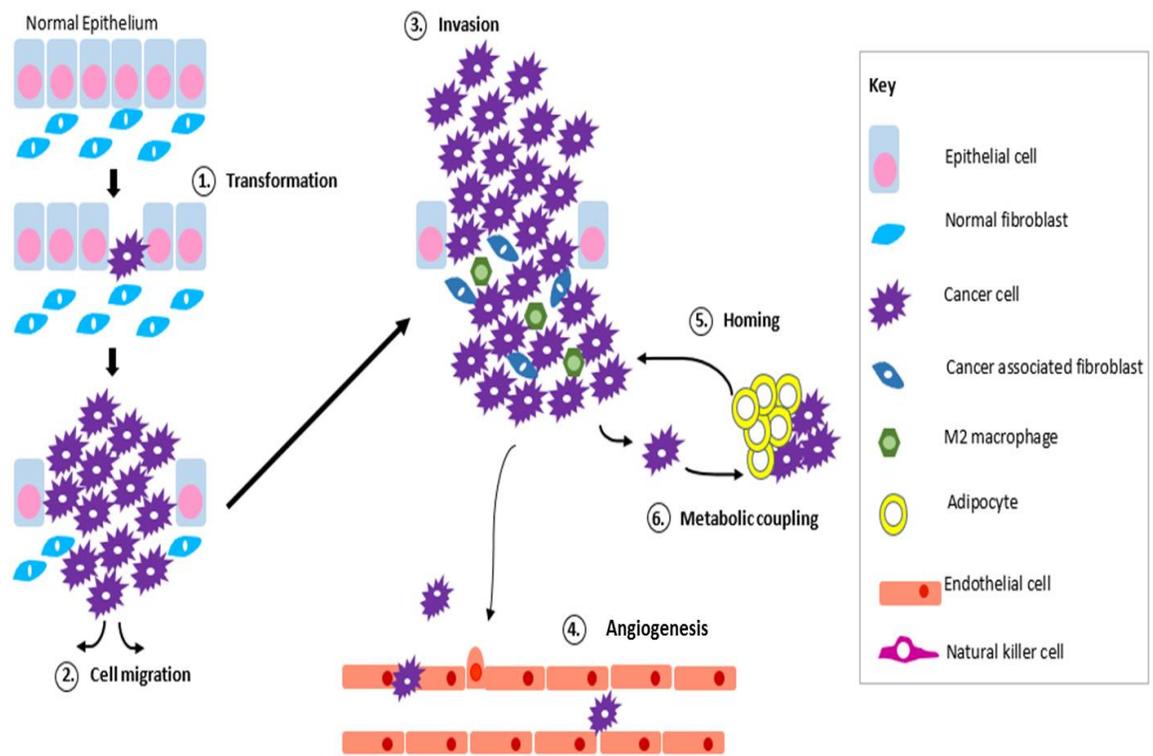
Figure 1.10: Diagrams showing how the normal epithelium can be used to demonstrate the influence lipid presence in the microenvironment of tumour may have upon cancer progression (stages 1-5). During transformation (1), fatty acids and triacylglycerides are released due to SREBP and mevalonate activation. Lipases overexpression exaggerates fatty acid release, which in turn aids migration (2) via the production of protumourigenic signalling molecule(s). Migration (3) is propagated by increased fatty acid synthetase expression with Wnt pathway involvement. Presence of certain fatty acids aid angiogenesis (4). Adipocytes release cytokines, which aid homing (5). Lipolysis in adipocytes produce a desirable, high energy-dense product, lipids. In ovarian cancerous cell, these lipids are observed to be chaperoned to them (5) (Adapted from Baenke et al., 2013). See text for detailed studies.

In tumour microenvironments, disease progression has been shown to be influenced by lipid presence. This is important to consider when considering previous findings

of altered lipid profiles in brain tumours (Eberlin et al., 2013; Hill, 2011). Using epithelial cancer development as a platform, the presence of lipids upon the stages of disease progression including the following: 1) transformation, 2) cell migration, 3) invasion, 4) angiogenesis, 5) homing and 6) metabolic coupling are summarized in Figure 1.10.

The breakdown of normal epithelial tissue during cellular migration and invasion are highlighted as part of Hanahan and Weinberg (2011) classification of cancer (Figure 1.09, Stage 1 and 2). Cellular transformation is promoted by the dysregulation of the mevalonate pathway, which is responsible for cholesterol and isoprenoids production as shown in mice by Clendening et al. (2010) (Figure 1.10, Stage 1). The growth of epithelial cells was observed to be induced by the rate-limiting enzyme, hydroxymethylglutaryl-CoA receptor (HMGCR), during the stage of transformation (Figure 1.10, Stage 1). Therefore, disruptions to the architectural tissue occurred leading to the activation of both SREBP and the mevalonate pathway. This leads to the release of both fatty acids and triacylglycerides into the microenvironment of the tumour.

The release of fatty acids has been associated with the promotion of migration (Figure 1.10, Stage 2). Studies by Nomura et al. (2010) highlighted overexpression of the monoglyceride-lipase in several human cancer cells and primary tumours including ovarian, melanoma and breast. With this overexpression, monoacylglycerols are hydrolyzed releasing free fatty acids into the tumour's microenvironment. This release of free fatty acids into the tumour microenvironment results in the release of additional protumourigenic signalling molecules including; diacylglycerols, lysophosphatidic acids (LPAs) and prostaglandins (Baenke et al., 2013). As such, initiation of cancerous cell migration occurs (Figure 1.10, Stage 2).

Stromal cells aid neoplasm progression by a specialised group within the fibroblasts known as the cancer associated fibroblasts (CAFs) which aid such cellular invasiveness (Kuzet and Gaggioli, 2016). Studies by Santolla et al. (2012) revealed

the lipid exchange with tumour stroma. The increased expression of fatty acid synthetase (FASN) subsequently led to the migration and invasion (Figure 1.10, Stage 3). Similarly, studies by Wang et al. (2016) found that FASN regulates colorectal cancer invasion and migration via the Wnt pathway which is involved in the cellular polarity (Komiya, 2006). Furthermore, FASN expression has been correlated with the malignancy of prostate cancer in a recent study by Hamada et al. (2014) (Figure 1.10, Stage 3). Therefore, demonstrating the paramount importance fatty acids in the lipid microenvironment in regards to cancer progression.

Angiogenesis (Figure 1.10, Stage 4) is an essential process in maintaining the tumours' supply of nutrients and oxygen. Moreover, it too has been shown be can affected by lipid presence. Work by Seguin et al. (2012) on B16-F10 melanomas demonstrated that synthesis of fatty acids led to tumour-induced angiogenesis via the utilisation of orlistat, a FASN inhibitor. Because of angiogenesis, the tumour then has an optimal environment with a resource of oxygen and nutrients whilst at the same time; such waste products i.e. lactate can be retrieved.

Furthermore, adipocytes within the tumours microenvironment can encourage homing of cancerous cells to the bone (Figure 1.10, Stage 5) via the release of cytokines (Baenke et al., 2013). Studies have linked disease progression and altered lipid metabolism with this cytokine release. Research by Nieman et al. (2011) found co-culturing adipocyte-ovarian cancerous cells led to the transfer of lipids from the adipocytes to the ovarian cells, which in turn supported their growth. Observations of adipocytes lipolysis to transfer such lipids were observed. In this case, adipocytes can be viewed as a lipid source providing energy for the ovarian cells (Figure 1.10, Stage 6).

With the increasing knowledge that lipid presence within the tumours' microenvironment effects disease progression and initiation, coupled with Warburg's

observations of metabolic re-programming in cancer, research surrounding cancers lipid biochemistry is ever increasing.

1.5 BRAIN LIPID ALTERATIONS

After adipose tissue, the brain is the most enriched lipid organ of which 50% dry weight is accountable (Mitchell and Hatch, 2011). Taking this into consideration for this study, the phospholipid profile as described by Hill (2011) may provide great clinical insight into a range of disorders including neurodegenerative diseases. Further to this, mammalian cells have been estimated to contain >9600 phospholipid species (Yetukuri et al., 2008). These phospholipid species not only serve in a role securing the integrity of biological membranes, but also they act in several biological systems including as precursors for second messengers.

1.5.1 Altered lipid brain tumour profiles

Because of multidisciplinary approaches, characterization of modern analytical applications has been developed. Desorption electrospray ionization mass spectrometry (DESI-MS) is one of these technologies which have shown promising results. Using this application, glioma and meningioma tumours have been classified from non-cancerous tissue based on type and grade. Interestingly, the component which aided the differentiation of such tissues was in fact a lipid specifically phospholipids (Eberlin et al., 2013).

Similar research on lipid profiles have been carried out at the University of Central Lancashire on meningioma. A study by Hill (2011) examined the phospholipid relative distributions including their particular molecular species. In comparison to other areas of the brain, meningioma grade II tissues were shown to have an altered phospholipid profile. An overview is illustrated in Figure 1.11.
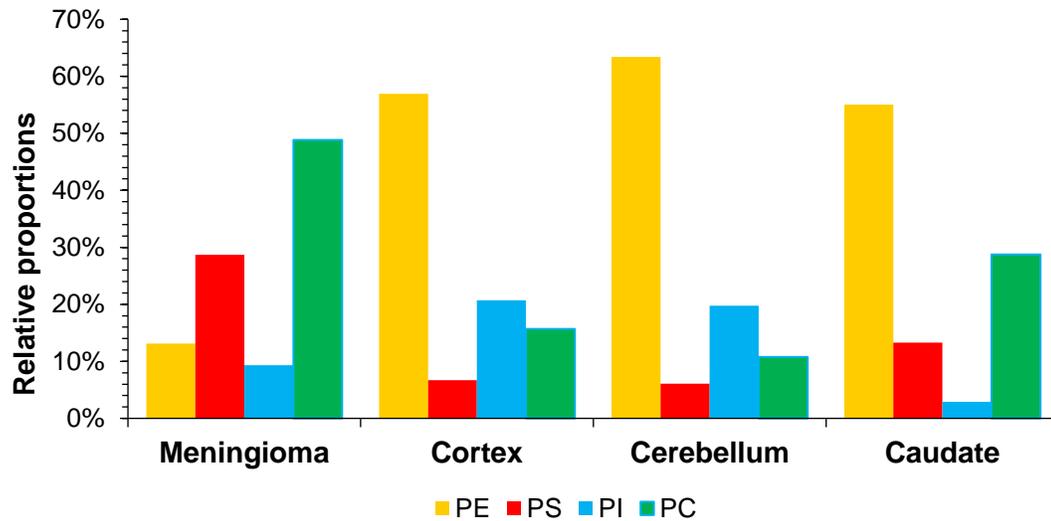
Figure 1.11: Bar chart showing meningioma grade II tissue phospholipid profile of, PE, phosphatidylserine (PS), phosphatidylinositol (PI) and PC in comparison to other areas of the brain. Meningioma grade II tissue displayed an altered phospholipid profile compared to other areas of the brain; increased proportions of PS and PC with a paralleled reduction in PE and PI (Adapted from Murphy et al., 2000 and Yao et al., 2000).

In contrast to other areas of the brain, meningioma grade II tissue had an overriding presence of PC (49%) when compared to other areas of the brain which was reported to be led by PE (>50%). Hill (2011) observed the relative proportions of PS to be triple that, when compared to other areas of the brain. Enrichment of docosahexaenoic acid (DHA) within PS was also observed to be elevated via Liquid Chromatography Mass Spectrometry (LCMS) analysis. Hence, research displayed two biological molecules of interest within the meningioma grade II tissue namely, DHA and serine (Hill, 2011).

1.5.1.1 Phospholipids

Basic architecture of eukaryotic membranes are lipid bilayers of which, the main components are phospholipids, cholesterol and glycolipids. The amphiphilic nature of phospholipids helps the formation of such bilayers in aqueous environments. Within eukaryotes, lipids are either in a bilayer form such as the plasma membrane or in a monolayer fashion like that observed in cellular LDs. Alterations in membrane phospholipid composition can hinder its ability to function, as the fluidity and plasticity of the membrane are dependent on the nature of the phospholipids present within the membrane. In relation to their role in the membrane, phospholipids serve as structural components protecting and isolating the cell from the external environment, in addition to isolating the intracellular organelles from the cytoplasmic domains of the cell (Zweytick et al., 2000; Vance and Vance, 2008; Musille et al., 2013). In this section, several areas are covered in relation to phospholipids including their structure, type, function and their relation to this study. Detailed reviews will be noted in each sub-subsection.

1.5.1.2 Structure

Architecturally, lipids contain a phosphorus, polar a non-polar portion. As demonstrated in Figure 1.12, a phospholipid molecule comprises of two hydrophilic tails linked via an alcohol group with a hydrophobic head group (Musille et al., 2013).
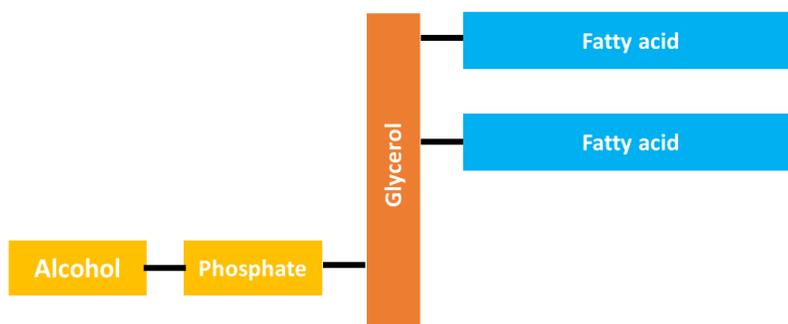
Figure 1.12: A simplified overview of phospholipid structure.

The alcohol, which the phospholipid has as a backbone, whether a glycerol or sphingosine, further categorizes these phospholipids as glycerophospholipids and sphingomyelins, respectively. Within eukaryotes, those phospholipids with a glycerol backbone make up most the phospholipid cellular makeup. An umbrella of phospholipids exist due to head group variation. The proportions of phospholipid variety is of interest to this study, as previous research by Hill (2011), Eberlin et al. (2013) have shown phospholipids to be altered within cancerous tissue. To investigate the impact of possible alterations in phospholipids in this study upon the behavior of meningioma, it is necessary to first consider the membrane lipid metabolism in eukaryotic cells.

1.5.1.3 Phospholipid membrane biosynthesis

In eukaryotic cells, membrane phospholipid synthesis is carried out in a few of the cellular organelles including that of the endoplasmic reticulum and the golgi apparatus. Full details of phospholipid metabolism can be found in detailed reviews by Lagace and Ridgway (2013); Hagen et al., (2010) and Hapala et al., (2011). An overview of phospholipid metabolism is illustrated in Figure 1.13.
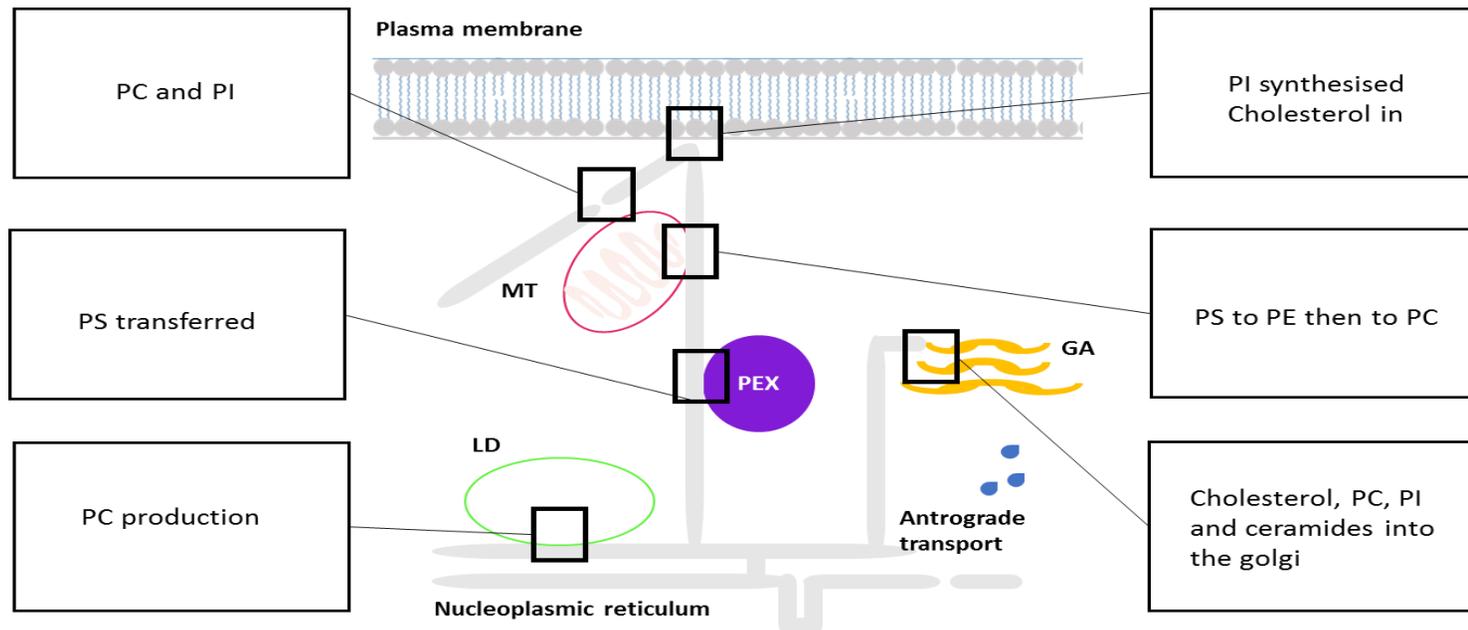
Figure 1.13: Diagram to show how the originating organelle determines the phospholipid synthesized. The close proximity of the membranes of those organelles involved in the lipid transport and biosynthetic pathways within the cell; endoplasmic reticulum (ET, colored grey), golgi apparatus (GR), MT, peroxisome (PEX) and the LD aid this process. In the ER, the CDP-choline pathway aids PC synthesis, whilst CDP-DAG helps PI production. PS is moved across the ER to the PEX. In the LD interface, PC is produced and stored as a main component of the LD phospholipid monolayer via CDP-choline synthesis. Whereas at the interface of the ER and the plasma membrane, PI is produced with choline being transferred into the ER. The PC, PS and PE interconversions are demonstrated at the MT and ER membrane interface. In contract to the golgi apparatus, in which cholesterol, PC and PI enter from the ER (Adapted fro Lagace and Ridgway, 2013 and Fagone and Jackowski, 2009).

As shown in Figure 1.13, the phospholipid type produced is dependent upon the originating organelle where it is synthesized. For example, specialized phospholipids such as plasmalogens are only synthesized in the PEXs whereas phosphoglycerate and cardiolipin are synthesized in the mitochondria of the cell. The proximity of organelles within the cell involved in phospholipid biosynthesis aid the variety and mobilization of phospholipids within the cell. Some of these organelles, specifically the endoplasmic reticulum have been associated with cancer.

1.5.1.4 Link between cancer and endoplasmic reticulum?

Studies have suggested a link between endoplasmic reticulum stress and cancer via the unfolded protein response involving phosphatidylcholine (Lagace and Ridgway, 2013) (see Table 1.4). The unfolded protein response is initiated when the glucose-regulated proteins (GRP) become activated with the presence of cellular stress. Such cellular stresses include changes in Ca^{2+}, nutrient levels and protein synthesis. The unfolded protein response aims to restore normal cellular function in several ways including inhibition of protein translation, degradation of misfolded protein and increasing protein folding. However, if this is not achieved, apoptosis is initiated.

Interestingly, increased GRP-78 expression has been observed in glioblastoma in accordance with poor rates of patient survival (Lee et al., 2008). The presence of endoplasmic reticulum stress within cells has been shown to result in an altered lipid metabolism. For example, SREBP is observed to be activated leading to cholesterol and triacylglyceride synthesis (Werstuck et al., 2001). Hence, the unfolded protein response which is initiated due to endoplasmic reticulum stress has become a therapeutic target especially due to its role in phospholipid biosynthesis (Wang et al., 2014).

1.5.1.5 Phospholipid remodeling

Due to the pivotal role phospholipids play in cellular function, a re-modelling system exists enabling a plethora of phospholipid molecular species to be motion (Yamashita et al., 2014). Phospholipid function (Table 1.3) is not only determined by head group, but also by the fatty acid chains which are esterified to the positions sn-1 and sn-2. These fatty acids are usually 16-24 carbons in length, both in saturated and unsaturated variants (Isaac et al., 2006). In mammalian systems to date, there have been over 100 phospholipid species identified; dependent on cell type and tissue (Yamashita and Nikawa, 1997).

The phospholipid remodelling system enables molecular species of variation in each phospholipid category. In brief, the phospholipid *de novo* remodelling pathways of the glycerophospholipids variant share a common intermediate with triacylglyceride synthesis; namely, glycerol-3-phosphate precursor (G-3-P) and phosphatidic acid (PA). Therefore, due to the common PA precursor, the molecular species of newly synthesized phospholipids will be a reflection this. A summary of the key physiological roles of major phospholipids is shown in Table 1.3.

Table 1.3: Overview of phospholipid characteristics including net charge and summarized functions.

Phospholipid	Net charge (pH 7)	Functions
PC	0	Neurons of the cholinergic nature use choline in the PC component as a precursor in their neurotransmitter acetylcholine synthesis (Blusztajn et al., 1987). Involved in the unfolded protein response in the endoplasmic reticulum; essential for secretion and expansions of the membrane (Lagace and Ridgway, 2013).
PE	0	Aids membrane fusion but negatively impacts the curvature of the membrane (Haque et al., 2001)
PG	-1	With the aid of Cardiolipin synthase 1, PG and CDP-DAG are condensated, producing Cardiolipin (Morita and Terada, 2015).
PI	-1	Precursor of the second messengers involved in the transmission of neural messages (Lodish H, 2000).
PS	-1	Neuronal survival and differentiation promoted with PS interaction which is located in the cytoplasmic leaflet of the plasma membrane (Kim et al., 2014). PS extracellular exposure involved in apoptosis cascade (Hampton et al., 1996).
SM	-2	Coupled with cholesterol, aids the lipid raft structural stability, which are responsible for signal transduction, protein transport and sorting membrane components (Kolter and Sandhoff, 2006; Gulati et al., 2010; Goñi and Alonso, 2006).
CL	0	Makes up one fifth of the mitochondrial inner leaflet phospholipids. Cardiolipin plays a role in maintaining optimal conditions such that he enzymes involved in energy metabolism can function (Morita and Terada, 2015).

From Table 1.3, the major phospholipids are shown to play differing roles within the mammalian system. For example, PC aids the cell to expand its membrane (Lagace and Ridgway, 2013), whereas PE is involved with the ability of membranes to fuse (Haque et al., 2001). Both of these would be beneficial to proliferating cells such as cancerous cells. When considering these factors with previous observations that show an altered energy metabolism and lipid profiles within cancerous tissue, the role of phospholipids and their possible connection to a cancerous phenotype is the subject of this study.

1.5.1.6 PC, PE and PS interconversion

The noted enrichment (13-15%) of the major acidic phospholipid PS in the human cerebral cortex, is pertinent to this study. An overview of the inter-conversion is depicted in Figure 1.14.
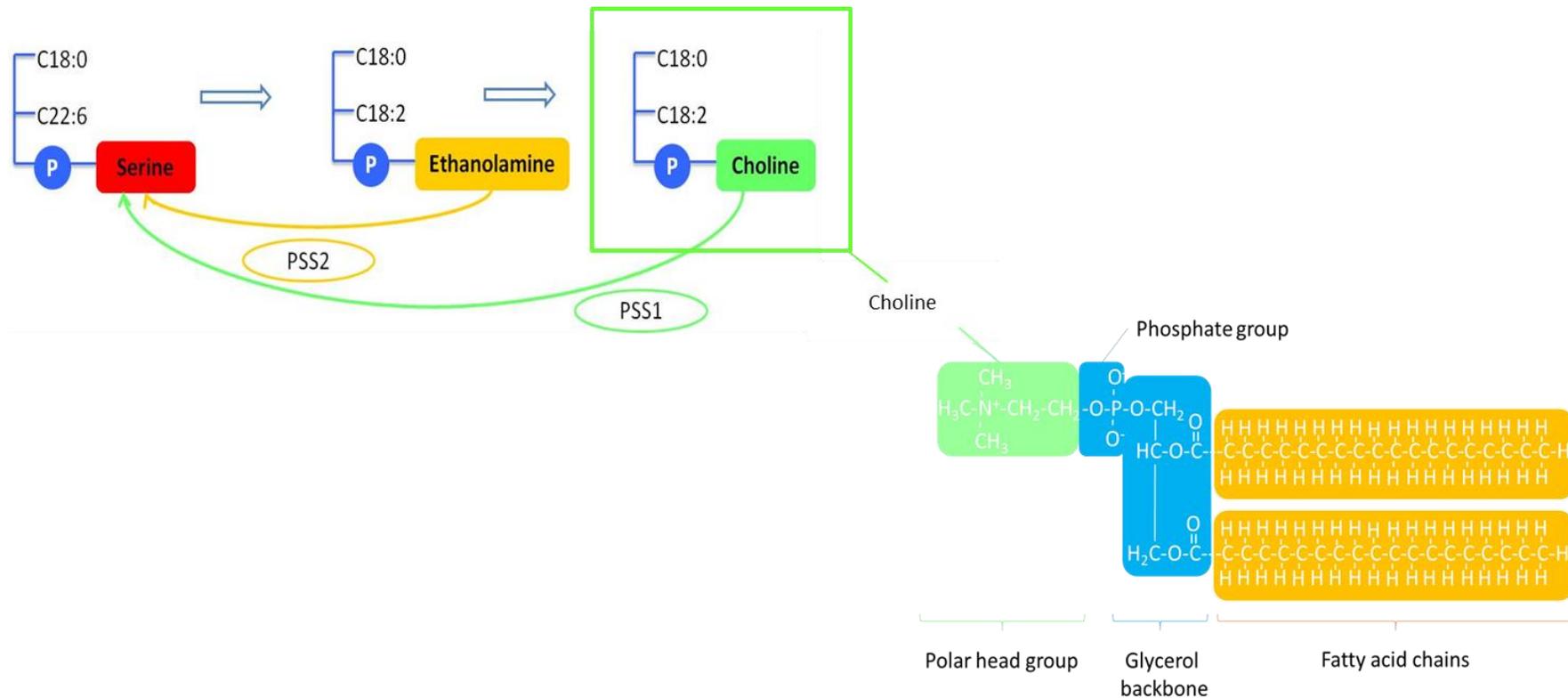
.**Figure 1.14:** Flow diagram shows enrichment of PS, PC and PE in the brain in particular reference to mitochondria and microsome regions which have high levels of PS, PC and PE. These regions are especially important in disease states, as they are involved in energy metabolism. Their inter-class interconversions, as depicted above, are catalyzed via the enzymes PSS1 and PSS2. The fatty acid chain saturation type is determined by the locality of the molecular species, usually the sn-2 fatty acid is esterified by an unsaturated fatty acid (contains double bonds) whereas the sn-1 contains a saturated fatty acid. **Legend:** P – phosphate head group and PSS - phosphatidylserine synthases 1 and 2, respectively.

In the brain, PS synthesis is a Ca^{2+}-dependent head-group exchange process located in the endoplasmic reticulum. During this inter-conversion reaction, the head group of the substrate phospholipid namely, PS or PE is replaced with serine. This process of head group exchange is catalyzed by PSS I and II, respectively (Figure 1.14). Enrichment of these enzymes that enable such phospholipid interconversion are heightened on the membranes associated with the mitochondria and endoplasmic reticulum. This phospholipid inter-conversion allows the conservation of molecular species within each phospholipid class (Musille et al., 2013).

It has also been hypothesized that the PSS1 enzyme shown in figure 1.14 may be responsible for the enrichment of polyunsaturated PS within the CNS. However, to supply such unsaturated fatty acids in this exchange, a polyunsaturated PC synthesized from a three-step methylation PE process is needed to produce a polyunsaturated PS. This three-step process, producing polyunsaturated PC, is known as the PE N-methyl transferase reaction. Studies have suggested that neuronal levels of this reaction are however low, therefore the only other tissue capable of producing such output is that of the liver. Therefore, demonstrating that to meet the supply-demand of PS biosynthesis in the brain, the best substrates are in fact PE and PC.

1.5.1.6 Choline

Studies by Usenius et al. (1994) on brain tumours' displayed a cholinergic phenotype different to that observed in non-cancerous tissue. The cholinergic specific phenotype can be detected using non-invasive procedures such as magnetic resonance spectroscopy (MRS) and positron emission tomography (PET) which can examine levels of choline containing compounds. Compared to the non-cancerous tissue, brain tumours were shown to display an increased abundance of PC and total choline-containing compounds by 50% and 85%, respectively. The intricacy of the cholinergic profile was brought back to the forefront with the work of Glunde et al. (2011) whereby several key enzymes involved in choline production were shown to

be overexpressed. These studies alongside those previously discussed demonstrate the clinical relevance lipid metabolism can play in cancerous tissue. Therefore, to understand the implications of such altered lipid metabolism, the regulations and profiles of the brain need to be discussed.

1.6 BRAIN ENRICHMENT OF PS CONTAINING 22:6

Throughout life, the human brain maintains PS levels within a range of 13-14%. Within the gray matter, the abundance of the 'neuroprotective' agent DHA (also referred to as 22:6), is raised in both PS and PE phospholipids by 29.9% and 27.4%, respectively. The abundance of DHA within PS and PE are ten-fold higher when compared with the levels of PC within the gray matter which have DHA enrichment (Calder, 2016). A possible theory for this specific DHA enrichment to PS and PC includes either 1) the aided interconversion of a 22:6 molecular species containing PE resulting in DHA enriched PS or 2) the mitochondrial PS decarboxylase reaction converts the PE containing 22:6 phospholipids into 22:6 containing PS.

The importance of lipid composition is further highlighted with the characteristics of the blood-brain barrier (BBB). The unaided as opposed to the aided movement substances raise important questions into their role of the lipids in the brain which have aided movement. Both serine and DHA have essential roles in brain development, yet one has facilitated transport across the BBB but the other has not. Similarly, the abundance of PS DHA enrichment within brain fractions are shown to increase with age, specifically in the microsomal and mitochondrial locations by a third (Norris et al., 2015).

1.7 THE POLYUNSATURED FATTY ACID, DHA.

DHA is an important omega-3 polyunsaturated fatty acid. Due to the chain length of DHA, 22 carbons consisting of 6 double bonds (see Figure 1.15), this makes it the longest polyunsaturated fatty acid in biological systems.

Figure 1.15: Chemical structure of DHA, also referred to as 22:6 due to the number of carbons (22) and there being six double bonds in its structure which also gives its nomenclature of a polyunsaturated fatty acid with their locality in relation to the methyl end (ω:n-6). Image drawn by hand.

The concentration of DHA is thought to enable brain development, cellular survival and neuroinflammation regulation (Domenichiello et al., 2015; Wang et al., 2016). Research by Sidhu et al. (2016) displayed that DHA is involved in ageing. This research was built on their previous findings, which showed that the polyunsaturated fatty acid was involved in synaptogenesis and neurite outgrowth.

1.7.1 Enrichment of DHA within membranes

DHA is embedded in eukaryotic cell membranes on the sn-2 position of PS and PE (Isaac et al., 2006). However, a 'perfect fit' for those membranes enriched with DHA is prevented due to the steric restrictions associated with the structural double-bonds present. This presence within the membranes of a polyunsaturated fatty acid can affect the properties underpinning the structural integrity of the membrane, including: acyl-chain order (fluidity), stage behavior, fusion, flip-flop, elastic compressibility and permeability. As previously discussed, human DHA enrichment is high due to its neuroprotective role, for example in the brain DHA is accountable for half of the neurons' plasma membrane weight. To maintain essential neurocognitive function,

the brain requires 2.4-3.8mg/day of DHA. DHA is not only enriched in the brain, but also the retina from which over 60% of polyunsaturated fatty acids found are that of DHA (Kim, 2008). With such high demand of DHA in the body, dietary sources are exploited i.e. fish and krill oil as *de novo* DHA synthesis in mammals does not occur (Domenichiello et al., 2015). Having said that, DHA can be synthesized from its precursor, α-linolenic acid, within the body.

1.7.1.1 Liver: α-linolenic acid precursor of DHA synthesis

In terms of meeting the supply-demand of DHA within the body, the conversion of α-linolenic acid to DHA only accounts for <1% of the required DHA needed to maintain functional cognition (Domenichiello et al., 2015). Hence, debates as to whether this conversion is solely adequate for cognitive function has been fought. An overview of the conversion between α-linolenic acid and DHA found in the liver is illustrated in Figure 1.16.
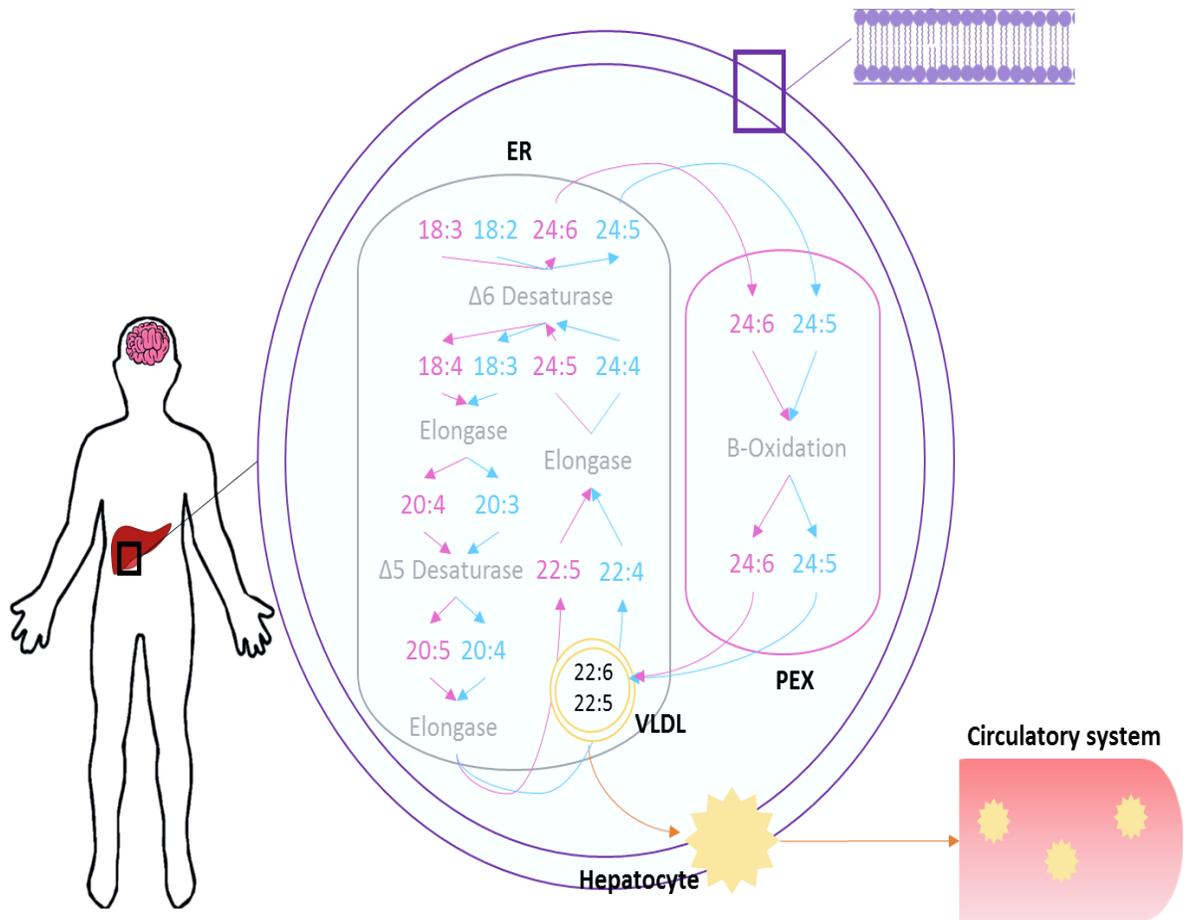
Figure 1.16: Diagrams showing the essential omega-3 polyunsaturated fatty acid, DHA, is essential for a range of cognitive functions. Much of the DHA is accountable from dietary sources within the body. However, in the liver via sequential steps of: desaturation and elongation in the ET followed by; β-oxidation in the PEX, DHA can be synthesized by α-linolenic acid (18:3). Enzymes, which are used in the process, include elongases and desaturases (see depiction for details). After production, DHA is packaged into a very low-density lipoprotein in the ET to be circulated systemically, an example of a possible destination may be the brain if the DHA is to be released and bound to albumin (Adapted from, Domenichiello et al., 2015).

Synthesis of polyunsaturated fatty acids, like DHA, occurs in the liver from α-linolenic acid. As show in Figure 1.16, the enzymes which aid the conversion from α-linolenic acid to DHA include the elongases and desaturases. In comparison to other organs such as the heart and brain, the expressions of such elongases and desaturases enzymes within the liver are much greater suggesting an organ specific role. Initially, in the endoplasmic reticulum the rate-limiting process of α-linolenic acid desaturation occurs aided by Δ6-desaturase forming 18:4n-3. DHA is produced via elongation and desaturation steps shown in Figure 1.16 followed by the movement of 24:6n-3 into the peroxisome from the endoplasmic reticulum, where it is then β-oxidized. DHA is then transported back into the endoplasmic reticulum where it goes on to be esterified and packaged into lipoproteins. These packaged DHA-lipoproteins are then secreted into the blood.

In the circulatory system, DHA can be present in either it un-esterified form bound to albumin, or esterified variant as a phospholipid, cholesteryl esters or triacylglycerides. To enter the brain, DHA must cross the BBB, the rate of which is determined by the amount previously consumed by the brain therefore requiring replacement.

1.8 BLOOD-BRAIN BARRIER (BBB)

To enable optimum conditions for neuronal function as per discussed by Campos-Bedolla et al. (2014), the BBB regulates the selective transport of molecules into the CNS. A dysfunctional blood-brain barrier is often observed in neurological diseases such as Alzheimer's disease. In such diseases, observations of substance transport deregulation occur due to the BBB breakdown. Consequently, the optimum conditions previously regulated by the BBB, which enable cognitive and neuronal function, are hindered.

In 2014, an orphaned transporter was observed to play an important physiological role in the normal formation and upkeep of the BBB. This was found to be solely expressed on the endothelium of the blood-brain barrier (Ben-Zvi et al., 2014). In the same year, DHA was observed to have facilitated movement across the blood-brain barrier via this same transporter, which is now referred to as Msfd2a (Nguyen et al., 2014).

1.8.1 DHA, facilitated movement across blood-brain barrier

Due to the essential neuronal function DHA plays, it can either be obtained via dietary sources or synthesized from α-linolenic acid in the body. However, DHA enriched in the brain is mainly sourced from the diet. DHA movement across the BBB is enabled by the Mfsd2a transporter (Campos-Bedolla et al., 2014). However, fatty acids with a 14-carbon or shorter side chain cannot be transported across the BBB by this Mfsd2a transporter (Nguyen et al., 2014). Studies by Nguyen (2014) demonstrated that the loss of this Msf2da transporter reduced the proportion of lysophophatidylcholine-DHA found in mice brains by 90%.

Recent studies have shown conflicting evidence as to whether DHA is solely delivered to the BBB or whether it is coupled with lysophophatidylcholine. However, the main consensus is that the affinity of DHA to the Mfsd2a transporter is greater when it is packaged with lysophosphatidylcholine in the lysophophatidylcholine-DHA complex (Subbaiah et al., 2016). The proposed DHA mechanism of crossing the BBB is illustrated in Figure 1.17**.**
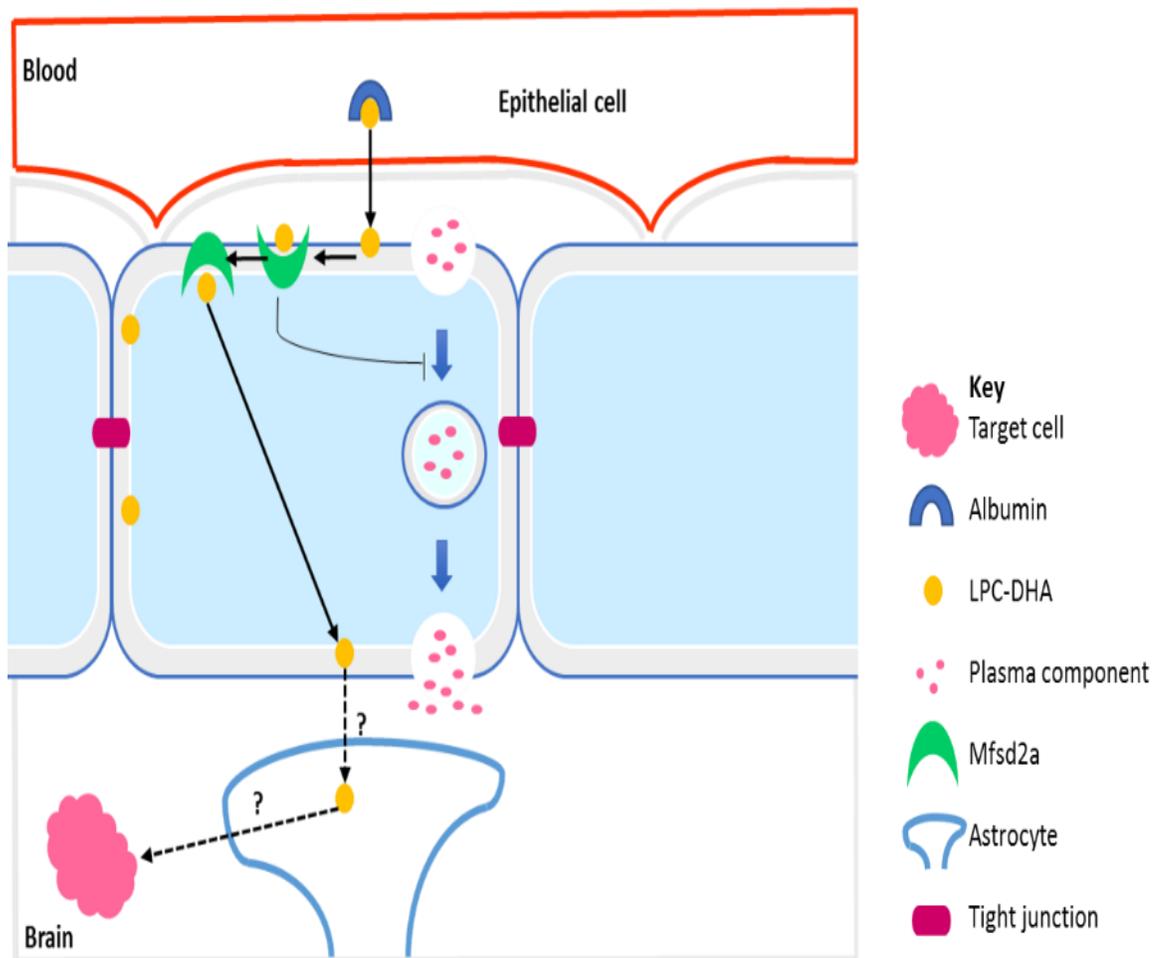
Figure 1.17: Diagram showing the facilitated transport of DHA across the BBB. The lysophotidylcholine, which is bound to albumin, releases the lysophosphatidylcholine-DHA complex once it reaches the BBB. The lysophosphatidylcholine-DHA complex then crosses the BBB by the Mfsd2a transporter to the astrocytes (Taken from Subbaiah et al., 2016).

To enable the facilitated movement of DHA to the BBB, as shown in Figure 1.17, albumin only releases the carrier of DHA upon reaching its destination. The carrier, lysophophatidylcholine, is coupled with DHA forming a lysophophatidylcholine-DHA albumin complex. This lysophophatidylcholine-DHA complex detaches from albumin and is absorbed in the outer lipid leaflet of the endothelial cell membrane (depicted in Figure 1.17) upon arriving at the BBB. The Mfsd2a transporter then binds to the LPC-DHA complex, transferring the complex to the inner lipid leaflet.

It is interesting to note that, targets of DHA in the brain are still under investigation. However, DHA usually resides in PS as 1-steroyl-2-docosahexaenoyl-PS (18:0, 22:6-PS) (Kim and Edsall, 1999). Studies have shown that neuronal cells with phospholipid DHA incorporation have inhibited release of such polyunsaturated fatty acids which is in contrast to astroglia (Garcia and Kim, 1997). This provides insight into the neuronal development which requires DHA maintained enrichment to prevent enzymatic oxygenation (Sawazaki et al., 1994). This therefore, illustrates that in fact the transport protein, Mfsd2a, plays a dual role in not only the integrity of the BBB but also the facilitated transport of the neuroprotective polyunsaturated fatty acid, DHA to the brain. Interestingly, deletion of the Mfsd2a transporter has been shown to result in the breakdown of the blood-brain, which in turn demonstrated it pivotal role in maintaining cognitive function thus, survival (Chow and Gu, 2015).

1.9 DHA'S RELATIONSHIP WITH CANCER

In clinical trials, omega-3 polyunsaturated fatty acids such as DHA have shown protective effects upon prostate and colon cancers (Lee et al., 2014). The ratio of omega-3/omega-6 presence upon tumour development has long been the object of cancer biology investigations. Tumour growth has also been observed to be heightened with altered omega presence. Similarly, the presence of omega-6 fatty acids compared to omega-3 fatty acids are increased in cancerous tissue. This therefore implies that there is a paralleled relationship between, the tumour omega fatty acid profile and tumour growth rate.

Investigations to examine the effect of unbalanced dietary omega-6 and -3 fatty acids across a variety of cultures upon disease have been studied. In Western culture, the ratio of dietary omega fatty acids which is omega-6 in nature, is higher with 10-20:1 compared to other cultures with 1-2:1. This finding that western culture has an

altered omega-3: omega-6 fatty acid profile provides scope for future research, as this alteration was positivity correlated with disease prevalence. In comparison to the Western culture, the Japanese population have a traditional diet which is naturally sourced in omega-3 fatty acids (such as DHA). This heightened omega-3 diet has been shown to decrease cancer development risk specifically in colon, prostate, kidneys and the breast.

The effect of dietary omega fatty acids upon the incidence rate of cancer has been recently displayed in Japan. Traditionally, the food culture in Japan has been towards the omega-3 fatty acids as opposed to omega-6 fatty acids. However, with recent adoption of an omega-3 fatty acid Western diet, the incidence of cancer has steadily increased. Whether this increased incidence rate if because of raising population obesity is under speculation. In one study by Park et al. (2010) mice obesity, both genetically and dietary induced, were shown to be positively correlated with hepatocellular carcinoma development. Therefore, it may be speculated that reduced DHA intake, positively effects the development of cancer due to its involvement in inflammation, apoptosis and oxidative stress, especially when it is esterified to lipids such as PS.

1.10 L-SERINE, THE PRECURSOR OF PS

L-serine is an essential amino acid which is involved in several key processes some of which involve the production of L-serine-derived lipids, including that of PS (Tabatabaie et al., 2010; Damseh et al., 2015). L-serine has a functional capacity of the CNS by aiding stages of development and cognitive function (Damseh et al., 2015; Tabatabaie et al., 2010). Dysfunctional uptake or biosynthesis of L-serine has been observed in several developmental diseases. Research carried out by Damseh et al. (2015) presented three recessive mutations encoding the alanine, serine and cysteine transporter (ASCT1) which were paralleled with cognitive

impairment and hypo-myelination. Similar results have been described by de Koning et al. (2000) on the inborn error of serine metabolism.

The machinery required for serine biosynthesis in the CNS is localized only within the astrocytes and radial glia (Yamasaki et al., 2001). This is an important point to consider, as in contrast to DHA, which has facilitated movement across the BBB, L-serine has poor permeability across the BBB (Damseh et al., 2015). Instead, the CNS availability of L-serine is provided by the ability of astrocytes to shuttle pre-formed L-serine by transporters (Kim et al., 2014). A summary of the shuttling of L-serine from the astrocytes is shown in Figure 1.18.
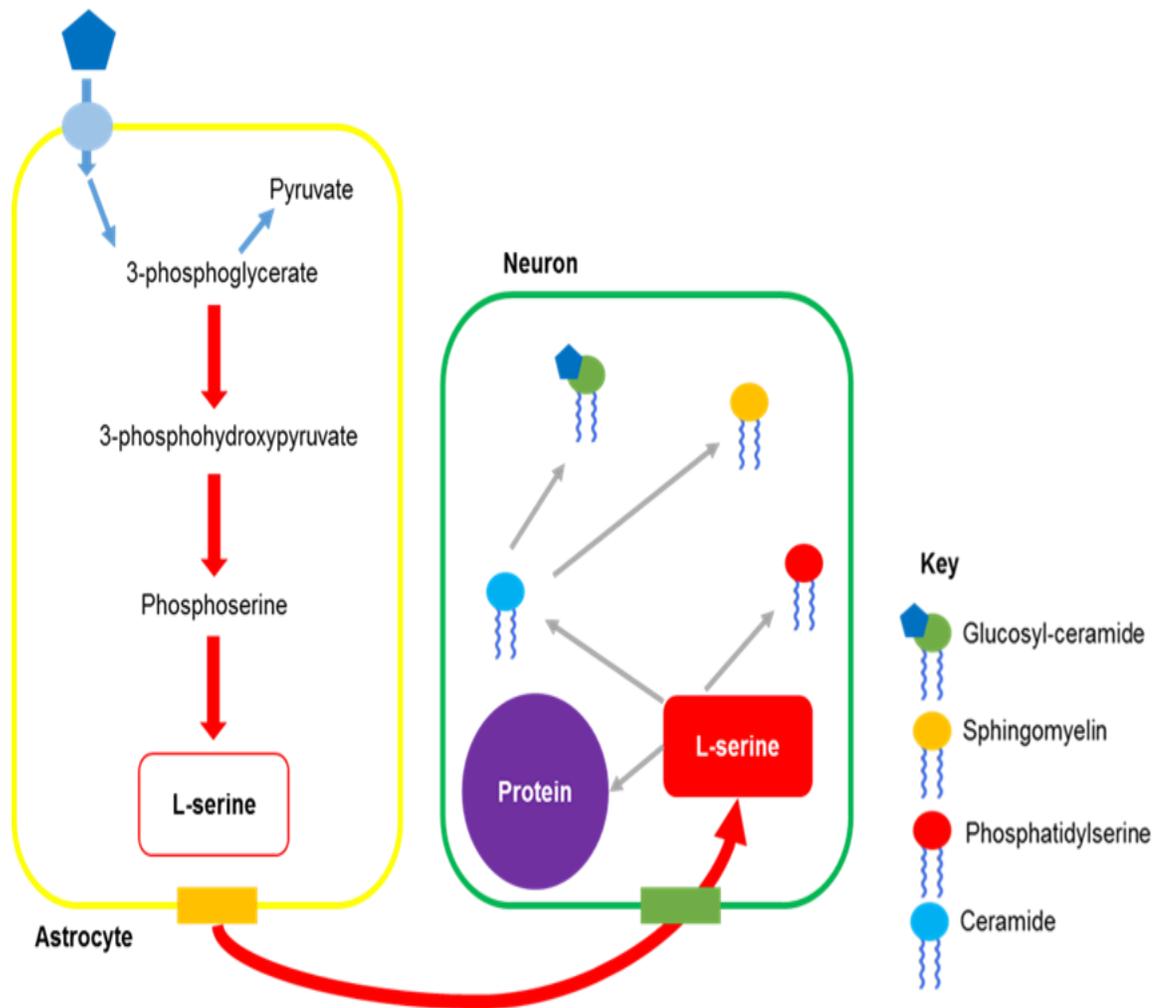
Figure 1.18: Flow diagram showing that neurones do not possess the rate-limiting enzyme for L-serine synthesis, phosphoglycerate dehydrogenase (PHGDH). The L-serine shuttle from the astrocyte to the neurons aids L-serine derived lipids to be synthesized. The glucose is taken up from the cerebra via the glucose transporter-1 (GLUT1) astrocyte transporter; glycolytic diversion aids L-serine production. Once produced, the Na+ dependent ASCT1 releases L-serine for the Alanine-serine-cysteine-1 (Asc1) neuron transporter to take up (Na$^+$ dependent). (Adapted from Hirabayashi and Furuya, 2008).

As depicted in Figure 1.18, the diversion of 3-phosphoglycerate (3-PHG) from the glycolytic pathway, enables the conversion of serine via a same three-step-process. Once synthesized, serine is released into the extracellular fluid by the specialized astrocyte Na^+-dependent ASCT1 transporter. Importantly, ASCT1 are proportionate to that of PHGDH suggesting that, astrocytes release L-serine to replenish neighboring neurones. The serine depleted neurones become replenished when they uptake serine either from the extracellular fluid or the cerebral circulation. This uptake of serine is facilitated by the neurone-specific transporter, Na^+-dependent ASC1 (Hirabayashi and Furuya, 2008). Interestingly, exogenous L-serine presence stimulates PS and PE enrichment in neuronal membranes suggesting a mechanism of membrane regulation with serine presence.

1.10.1 Serine's relationship with cancer

The key enzyme involved in serine biosynthesis is PHGDH. The gene for PHGDH is localized on chromosome 1p. It has received a lot of attention surrounding its relationship between serine and cancer progression (Sun et al., 2015; Amelio et al., 2014a). This enzyme aids the glycolytic diversion in the cell, such that the demand for L-serine is met. Therefore, it can be said that as glycolysis diversion itself aids L-serine synthesis, glucose itself can be deemed a precursor of L-serine lipids (Hirabayashi and Furuya, 2008).

In brain tumours, such as meningioma, increased expressions of glucose transporters such as glucose transporter-3 (GLUT 3) are observed. Such increased GLUT3 expression in tumours aids the flux through glycolysis and subsequently the production of L-serine via PHGDH. The presence of L-serine itself has been implicated in the orchestration of metabolic re-programming in a range of mammalian tumours (Sun et al., 2015).

The glycolytic diversion observed in cancerous cells can also lead to glycine biosynthesis (Hirabayashi and Furuya, 2008; Sun et al., 2015). Studies by Labuschagne et al. (2014) was built on the work of Arends et al., (1995) which displayed how serine and glycine could irreversibly interconvert via L-serine hydroxymethyl transferase. The work by Labuschagne et al. (2014) of cancerous cells undertaking one carbon metabolism suggested that in fact serine was the key player over glycine. The cancerous cells preference of serine over glycine was shown in them selectively consuming serine. Therefore, supporting the suggestion that in fact, some cancerous cells are supported by serine presence solely in one carbon metabolism.

1.11 THE RELATIONSHIP BETWEEN DHA AND PS

In several mammalian systems, a unique relationship between DHA and PS has been shown. Dietary DHA supplementation has been known to modulate cellular PS concentrations; of relevance to this study, glial cells have already displayed this phenomenon (Kim and Choi, 2010; Garcia and Kim, 1997). It is therefore plausible to suggest, that the specific phospholipid profile observed by Hill (2011) may be because of DHA's relationship with PS. An overview of the effect of key PS-dependent pathways upon neuronal survival and differentiation are illustrated with coupled DHA presence in Figure 1.19 (Kim et al., 2010; Kim, 2008; Steelman et al., 2011).
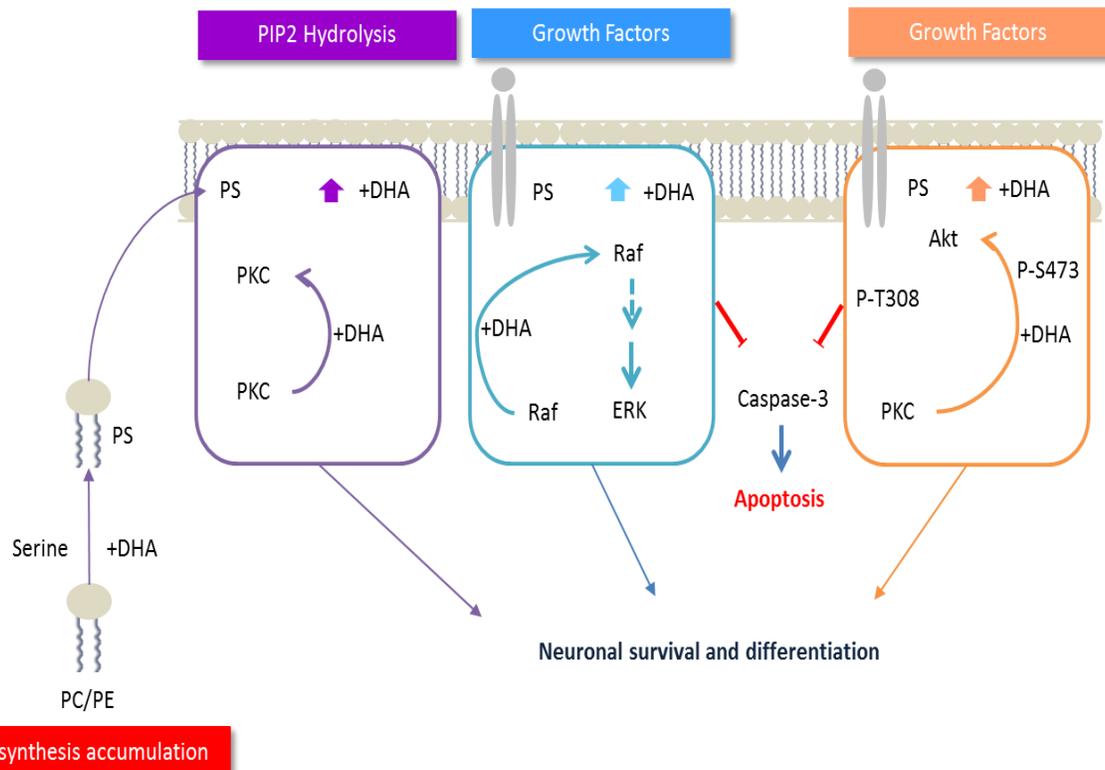
Figure 1.19: Diagram showing DHA induced synthesis and plasma membrane localization of PS. DHA enriched PS localized on the cytoplasmic side of the plasma membrane gather forming anionic micro-domains, crucial for signal transduction proteins, leading to neuroprotection (Image adapted from Kim et al., 2010; Kim, 2008).

Studies have demonstrated PS to be pivotal in key CNS signalling pathways. Furthermore, DHA enriched PS has also been shown to be highly localized in the inner leaflet of the plasma membrane. Unlike other signalling molecules producing active products for the end effect, as an inner anion domain member of the plasma membrane, PS acts as binding/activation site for cytosolic proteins involved in neuronal signalling. The fundamental molecular characteristics of PS aid this protein interaction, because of which neuronal signalling is activated via electrostatic interactions or Ca^{2+} bridges. Hence, the previous research on meningioma tissue comprising of an altered phospholipid profile of heightened PS with DHA enrichment will be of interest in terms of the effect upon cellular events shown in Figure 1.19 in this study.

1.12 YEAST AS A MODEL ORGANISM

For a cell to be classified as cancerous, alterations have to occur in cellular processes including induction of senescence and apoptosis prevention as defined by Hanahan and Weinberg (2011). Interestingly, similarity between phospholipid membrane profiles amongst three differing domains of life e.g. archaea, bacteria and eukaryotic cells has suggested an evolutionary conservation as discussed by Lombard et al. (2012). Additionally, lipidomic studies within fungi (yeast) have shown similar lipid accumulation characteristics when compared to cancerous eukaryotic cells. Detailed reviews can be found by Natter and Kohlwein (2013) and Diaz-Ruiz et al. (2009). Therefore, a paradigmic organism including that of yeast can be utilised in this study to determine the effect of DHA and/or serine upon cellular processes.

A yeast paradigm has several 'good model features' including its unicellular nature, which not only permits higher cultivation turn-over in comparison to a mammalian model, but it also provides cost effective experimental outlines. One limitation to consider however, is the unicellular nature of the yeast species as opposed to the multi-cellular nature of mammalian systems. Nevertheless, in regards to this study, this can be viewed as an advantage, as the mammalian system complexities are stripped away. With such ability to strip away these system complexities in the yeast paradigm, the effect upon cellular processes can be examined in further detail.

In many human diseases, ectopic lipid accumulation has been recognised and hence, the model organism must be able to accrue lipids. From the 1600 known yeast species, only 50-160 have been identified to accumulate lipids at the level to be classified as oleaginous in type; at least 20% of their dry weight (Sitepu et al., 2014; Calvey et al., 2016). Typically, yeasts of oleaginous nature are found in the following genera including but not restricted to Rhizopus, Trichospron, Lipomyces and Yarrowia (Beopoulos et al., 2011). For this study, the oleaginous yeast, *Lipomyces starkeyi* (*L. starkeyi*), was utilised as the paradigmic model. Oleaginous yeasts like *L. starkeyi* have a growth cycle consisting of a lag-, log-,

diauxic- and stationary phase. Figure 1.20 (A and B) summarises the growth cycle of a typical oleaginous yeast, *Rhodotorula gracilis,* alongside a depiction of the effect media nutrient status has upon lipid accumulation.

A) An example of a growth phase profile exhibited by yeast (adapted from Herman, 2002).
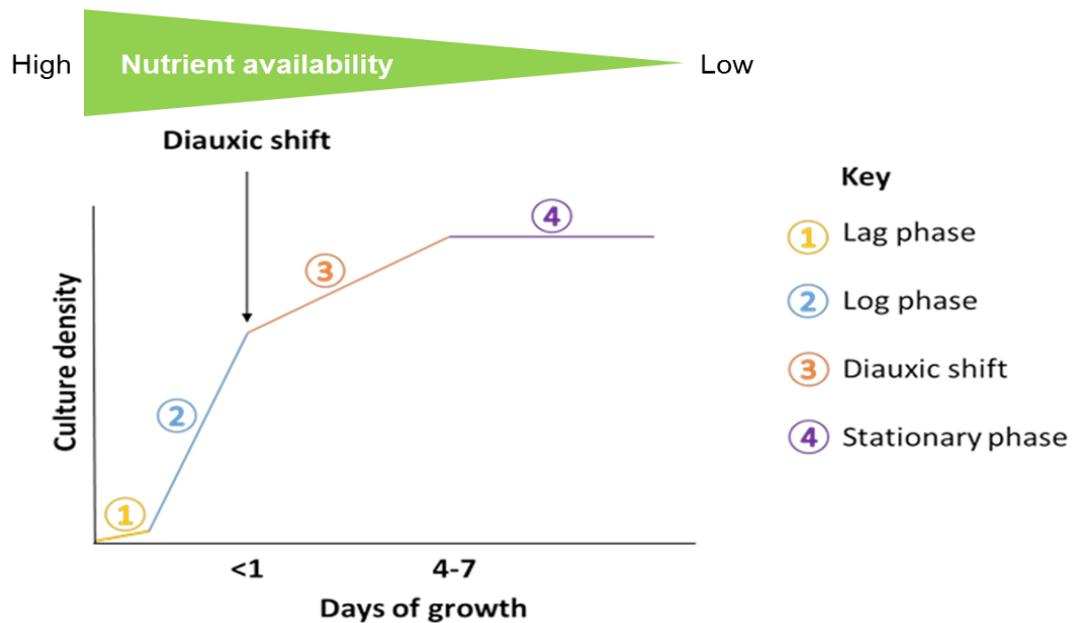
B) Effect of media type upon *Ramaria gracilis* (*R. gracilis*) lipid accumulation during stationary phase (adapted from Rolph et al. 1989).
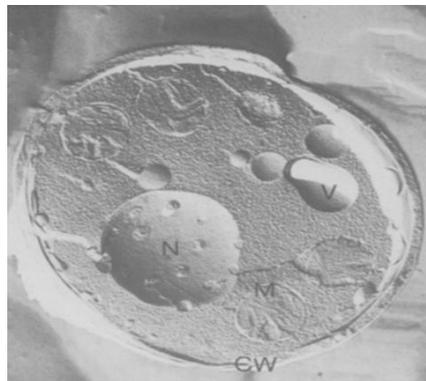
i) Carbon-limiting media   ii) Nitrogen-limiting media
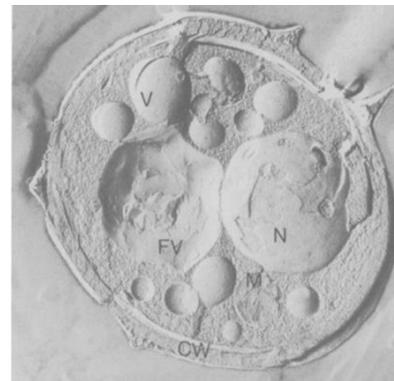
Key: Scales have been corrected such that compared directly, was originally 1.5cm: 500 nm and 2 cm: 500 nm respectively.

Figure 1.20: Growth curve shows the relationship between growth profile (A) and photographs displaying lipid accumulation (B) in yeast. With increasing culture density during log-phase (2) nutritional sources were reduced as a result. Thus, to re-supply the energy reserves a respiratory mode were promoted (3) but consequently this slows the growth rate. After these sources were exhausted true stationary phase (4) is reached. During such phase, lipid accumulation is observed (B) in the fat vacuole (FV).

During log-phase (G_1) demand for nutrients are high and this is to fulfil cellular process requirements such as proliferation (Figure 1.20, A). However, with increasing cellular community, the nutritional sources within the media become depleted. To replenish the nutrient source required for cellular processes, activation of a respiratory mode of energy production is promoted, short-term. Because of nutritional depletion, transcriptional rates reduce by 3.5 fold leading to the rate of proliferation to reduce (Choder, 1991). After the diauxic-shift (Figure 1.20, A. 3) energy sources are provided via the by-products of fermentation (ethanol). Therefore, only after this energy supply via fermentation is exhausted, the true stationary phase is reached.

Entry into the 'non-resting state' termed stationary phase is regulated by the Ras and Tor signal transduction pathways which become activated with nutrient media reductions in nitrogen, phosphorus and carbon. During stationary phase, lipid accumulation of neutral lipids occurs in a fat vacuole. Lipid accumulation during this growth phase is demonstrated in the freeze-fracture electron micrographs of *R. gracilis* (Figure 1.20, B). Cultivation of *R. gracilis* in nitrogen-limiting media (NLM) (Figure 1.20, B. ii) increased *de novo* lipid accumulation within the mono-fat vacuole in comparison to the carbon-limited *R. gracilis* culture (Rolph et al., 1989). Within the fat vacuole, the main lipid class stored include the neutral lipids, triacylglyceride followed by a small portion of sterol esters.

The main metabolic activities in oleaginous yeast are re-tailored during nitrogen limitation towards lipid accumulation. Under the same conditions of nutrient limitations, similar alterations towards lipid accumulations have been observed in cancer. In *L. starkeyi* once the stationary phase of growth is reached, such intracellular stores of lipids reach >65% in comparison to its dry cellular weight. The key modulators involved in lipid metabolism in oleaginous yeast like *L. starkeyi* are summarised in Figure 1.21, both with and without nutrient availability.
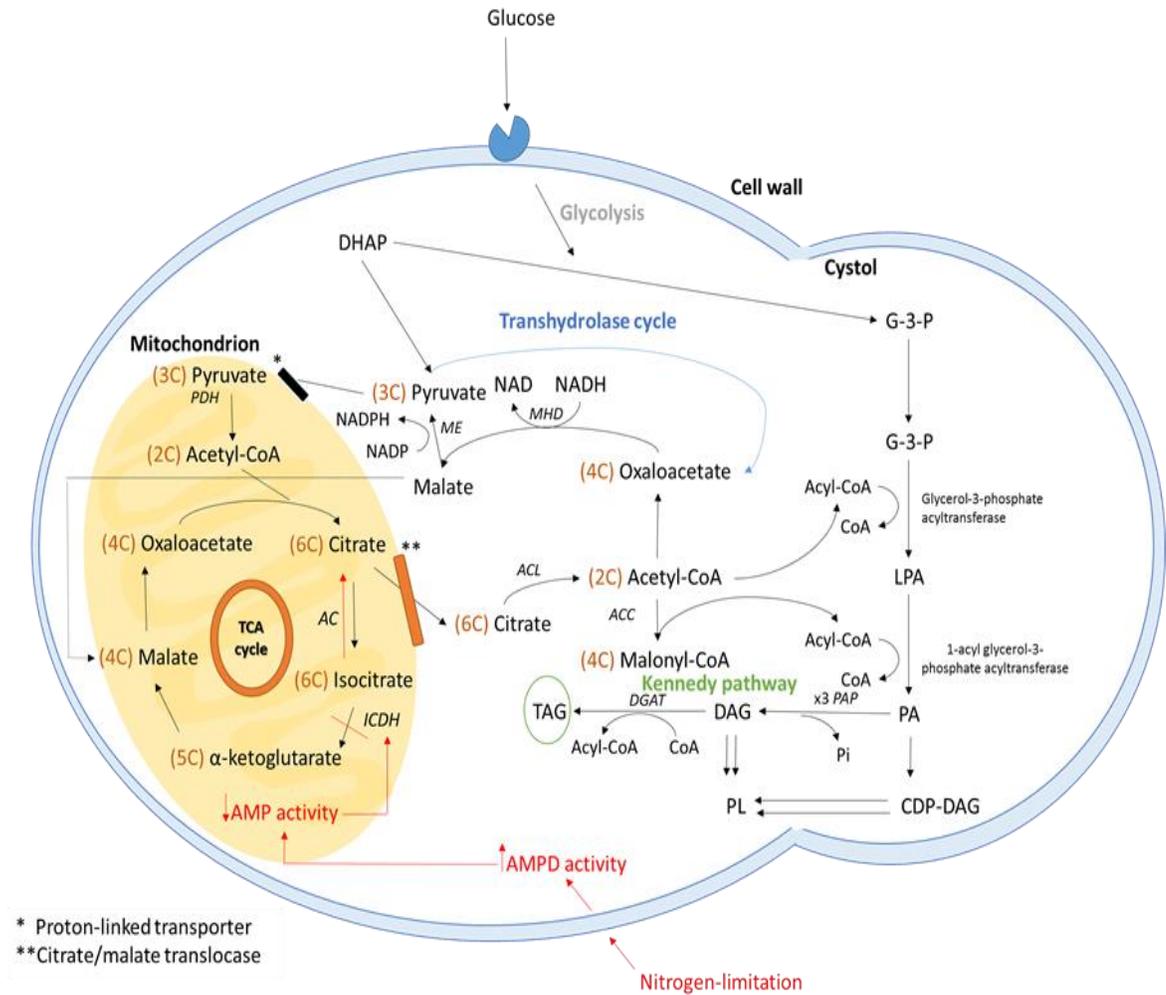
Figure 1.21: Diagram showing the metabolic pathways re-tailored in oleaginous yeast in response to nutrient depletion (highlighted in red) leading to lipogenesis. With nitrogen depletion, adenosine monophosphate deaminase (AMPD) is activated which in turn causes citrate to be translocated via the citrate/malate translocase from the mitochondria to the cystol which is utilised in the Kennedy pathway for neutral lipid production (Adapted from Patel et al., 2016).

The ability to accumulate lipids under nitrogen limitation in oleaginous yeasts as opposed to non-oleaginous yeasts is accountable to the conserved mechanism of ammonia scavenging, as demonstrated in Figure 1.21. The activity and/or activation

of AMPD increases with nitrogen depletion. This in turn reduces mitochondrial AMP levels. Due to the functional dependence of isocitrate dehydrogenase (ICDH) on AMP, a number of knock-on effects occur with the reduction of mitochondrial adenosine monophosphate (AMP) levels including 1) the conversion of isocitrate to α-ketoglutarate is suppressed, and 2) an altered balance between oxygen consumption and carbon dioxide output is observed. Because of the metabolic retailoring, the citrate/malate translocase aids the transfer of cytosolic malate for mitochondrial citrate. Once in the cystol, citrate is then cleaved with acetyl-CoA and oxaloacetate via ATP citrate lyase (ACL), which is then converted to malonyl-CoA via acetyl-CoA carboxylase (ACC). As a result, lipid accumulation via the Kennedy pathway can be promoted, leading to triacylglyceride production. Interestingly, non-oleaginous yeasts are void of ACL which gives rise to their lipid accumulation limitations. More recently, this ACL gene was transferred from *L. starkeyi* into the baker's yeast *Saccharomyces cerevisiae*. Because of ACL insertion into the non-oleaginous yeast, the production of fatty acids increased; demonstrating the central role ACL plays within lipid production.

During nitrogen limitation, oleaginous yeast increases their triacylglyceride pool within their lipid bodies (see Figure 1.21, B.ii). Such production of the neutral lipid is brought about via the Kennedy pathway (Figure 1.21) which initiates from PA. The source of PA, G-3-P or dihydroxyacetone phosphate (DHAP) is dependent on whether the culture was sourced with nitrogen or not (Figure 1.21). In order to produce the neutral lipids, PA is firstly dephosphorylated and this requires three phosphatidate phosphatase (PAP) isoenzymes (Figure 1.21). After which the acetyl-CoA then binds to the diacylglycerol backbone via DGAT resulting in triacylglyceride formation. Generally, during nitrogen-limitation oleaginous yeasts store lipid in their lipid vacuoles, particularly in the TAG and FFA form – as observed in tumour cells. Industries now utilise these aspects of oleaginous yeasts, specifically lipid accumulation in terms of biodiesel applications. The conserved re-tailoring of lipid production in oleaginous yeast like that in tumour cells makes *L. starkeyi* an attractive paradigm for the research presented in this study.

1.13 RESEARCH AIMS

1.13.1 Working hypothesis

Both DHA and L-serine are involved in the development and progression of brain cancer.

1.13.2 Main aims

This novel research was developed to identify whether meningioma displays an altered lipid biochemistry and whether this was related to metabolic reprogramming. Previous studies have shown that meningioma displays an altered lipid profile in the form of an increased abundance of DHA-enriched phosphatidylserine. This study attempted to provide an insight into the impact of such lipid alterations upon the cancerous phenotype displayed in meningioma. In order to achieve the aims, the study focused on three main objectives:

1. Are the cellular processes surrounding cancer affected by DHA and/or serine presence?
2. Are the altered lipid profiles displayed within grade II meningioma related to a serine-derived metabolic flux?
3. Do the altered lipid profile shown in meningioma grade II tissues, support cancer progression via an increased cellular viability?

1.13.3 Scope of study

Firstly, in order to establish whether the presence of phosphatidylserine enriched with DHA promotes a cancerous phenotype, a lipid-accruing model organism was developed. Second, to monitor the impact of such DHA and/or serine presence, the model organism, *Lipomyces starkeyi*, was supplemented with these biological agents during lag phase.

The initial focus or phase of this research investigated the possibility that DHA and/or serine supplementation influenced cellular processes including proliferation, lipid accumulation, cellular metabolism and *de novo* lipid biosynthesis. By monitoring the *L. starkeyi* cells during their growth cycle, the impact of such DHA and/or serine presence upon growth phase transition could be established. With many cancers being observed to have an altered lipid biochemistry, the model organism was then subjected to a radiolabel study examining whether DHA and/or serine presence alone could influence lipid biosynthesis. Once lipids were synthesised in cancerous cells, they were often stored in lipid droplets in the form of triacylglycerides and sterol esters. In diseased cells, multiple lipid droplets were observed, aiding lipid mobilisation during times of membrane biosynthesis. Hence, to ascertain whether the presence of the two biological agents, L-serine and DHA, were affected, the number and size of the lipid droplets within a cell, a preliminary assessment via light microscopy during the lipid-accruing stage were carried out.

The second phase of the research was deciphered to examine if the increased abundance of phosphatidylserine, a serine-derived lipid, within meningioma tissues was related to metabolic reprogramming. An immunohistochemistry study was carried out in grade I and grade II meningioma tissues, examining whether glycolysis was diverted to serine biosynthesis. The staining profile of p53, PKM2, fascin and PHGDH was of interest in this part of the study.

Finally, in order to investigate whether the altered phospholipid profile in meningioma played a role in tumourigenesis, a cellular viability study using SVG and U87 cell lines was developed. The focus of this preliminary study involved the preparation of liposomes derived from grade I and grade II meningioma tissues as well as PC: PS. These liposomal preparations were then supplemented into log phase SVG and U87 cultures. The effect of upon phospholipid alterations with non-cancerous and cancerous cells could then be determined using a Presto Blue cellular viability reagent. The results of the studies are presented in Chapter 2, 3 and 4.

Chapter Two

Biochemistry inter-play of DHA and L-serine via an oleaginous paradigm, *Lipomyces starkeyi*.

2.1 Materials and Methodology

2.1.1 MATERIALS

Media used for yeast inoculation and culturing for experiments include: Yeast extract peptone dextrose (YEPD) and NLM. YEPD composition includes; glucose (20%, w/v), yeast extract (10%, w/v) and peptone (10%, w/v). Addition of agar (2%, w/v) to YEPD enables the maintenance of *L. starkeyi,* which was sub-cultured quarterly. NLM as per denoted by Rolph (1989) comprises of monopotassium phosphate (0.7%, w/v), disodium hydrogen phosphate (0.2%, w/v), magnesium sulphate heptahydrate (0.15%, w/v), calcium chloride dehydrate (0.01%, w/v), ferric chloride hexahydrate (0.008%, w/v), zinc sulphate heptahydrate (0.0001%, w/v), yeast extract (0.15%, w/v), ammonium chloride (0.05%, w/v) and glucose (3%, w/v).

2.1.2 METHODOLOGY

2.1.2.1 Strain and culture conditions

The yeast strain, *L. starkeyi* (2710) was obtained via the National Collection of Yeast Cultures. The yeast strain was stored in cryopreservation plus media and stored at -80ºC for preservation. A Rich (YEPD) media starter culture of *L. starkeyi* was achieved by an inoculation of a single colony from a rich medium (YEPD) agar plate into YEPD media. The starter YEPD *L. starkeyi* culture was then stored in an orbital shaker at; 30ºC and at 2000 revolutions per minute (492 x g) of 180 overnight.

Lipid accumulation was promoted during stationary phase whether the conditions were nitrogen- limiting. To initiate a culture for experimental examination, the initial YEPD starter culture would have a proportion of the cells centrifuged at 2000 rpm (492 x g) for a duration of 2 minutes. After centrifugation, the supernatant was discarded leaving the pellet to then be re-suspended in NLM overnight; following which an experiment could be initiated in NLM cultures.

2.1.2.2 Cellular Viability: DHA, L-serine and co-supplementation

The determination of DHA and/or L-serine supplementation upon *L. starkeyi* NLM cultures was achieved by a viability study carried out on a 96-well plate. This was performed with a media-, culture-, and a culture with varying concentrations of DHA and/or L-serine lanes. The effect of the solvents, dimethyl sulfoxide (DMSO) and/or water was also examined to determine if these solvents had an effect upon cellular viability. These plates were left in a static incubator at 30°C for 48 hours and subjectively examined for growth.

2.1.2.3 Supplementation of DHA, L-serine and co-supplementation

In order to determine the effect of DHA (91 nM) and L-serine (95 mM) upon lipid synthesis, *L. starkeyi* cultures were cultured in NLM (pH 6.0) and supplemented during the initial inoculation phase.

2.1.2.4 Lipid biosynthesis from [^{14}C] Acetate: Uptake

The rate of the metabolic carbon flux was determined by the examined of [^{14}C] acetate (55.2 mCi/ mmol) administration to either DHA (91 nM) and/or serine (95 mM) supplemented *L. starkeyi* NLM cultures. A time course over a 45-minute period examined the rate of [^{14}C] acetate uptake via the presence remaining in the media (NLM). Per time point, a 1 ml culture sample was removed and centrifuged at 2000 rpm (492 x g). From which, a NLM (100 µl) sample was added to 5 ml scintillant (EcoScint) whereby the presence of radiolabel was quantified via scintillation counting over a 1-minute period.

In order to determine the impact of DHA and/or L-serine supplementation upon the uptake of radiolabelled acetate in *L. starkeyi*, the DPM values ascertained from the scintillation was corrected for cell number, specifically 10. By doing so, the DPM values from each culture could be compared to determine if DHA and/or L-serine affected radiolabelled acetate uptake.

2.1.2.5 Lipid biosynthesis from [^{14}C] Acetate: Lipid *De Novo* synthesis

To determine the effects upon *de novo* lipid synthesis, with DHA and/or L-serine co-administration on *L. starkeyi* NLM cultures, a lipid extractions was performed. Cultures were centrifuged at 2000 rpm (492 x g), the pellet was then re-suspended in NLM (1 ml) and reconstituted in pre-heated methanol (70°C) for a period of 30 minutes. After cooling to room temperature, the extract was added to chloroform (4 ml) and 5% sodium chloride (2 ml, w/v). The overall mixture was then vortexed three times and left to stand until two phases formed. The bottom phase was kept and aliquoted into a new vial which was then blown down under nitrogen gas (40°C) to achieve complete dryness.

2.1.2.6 Thin-layer Chromatography

Lipid extracts were re-dissolved in chloroform, then spotted via the use of capillary tubes onto the pre-activated 25 mm thick silica gel G plates alongside the standards of; phosphatidylcholine, tristearin, stearic acid, lanosterol and ergosterol. The solvent system comprised of hexane/diethylether/glacial acetic acid (80:20:2 (v/v)). After development, lipid bands were visualized using iodine vapour and scraped into scintillation vials containing 5 ml of scintillant (EcoScint). Quantification of [^{14}C] radiolabel presence was performed via scintillation counting over a 1-minute period.

2.1.2.7 Statistical analysis

All data were analysed using SPSS programme. Data were expressed as mean ± standard deviation (SD). Test and control data were compared using ANOVA and student t-test, a value of $p < 0.05$ was taken as significant. Most experiments were repeated at least 3 times (n=3).

2.2 Results

2.2.1 Effect upon NLM cultured *L. starkeyi* viability, with DHA and/or L-serine supplementation

From previous research (Hill, 2011), two biological molecules stood out as having the potential to act as regulators namely, L-serine and DHA, on culture growth. To establish the *L. starkeyi* viability with DHA and/or L-serine supplementation, a 96-well plate viability plate was utilized. From this, the working concentrations of 91 nM of DHA and 95 mM of L-serine were proposed.

2.2.2 Effect upon NLM cultured *L. starkeyi* growth profile with DHA and/or serine supplementation

The effect of DHA and/or L-serine upon growth profile was ascertained by the paradigmic *L. starkeyi* cells being supplemented with such biological molecules during lag-phase. The cultivating media employed in this study were nitrogen-limited, which promote lipid accumulation in the paradigmic oleaginous yeast during the stationary phase of growth, similar to that observed in cancerous cells. A depiction of the full time course of growth profile demonstrated by *L. starkeyi* are illustrated in Figure 2.1 whereby, the effect upon maximal cell number and growth phase transition are examined with supplementation of DHA and/or serine.
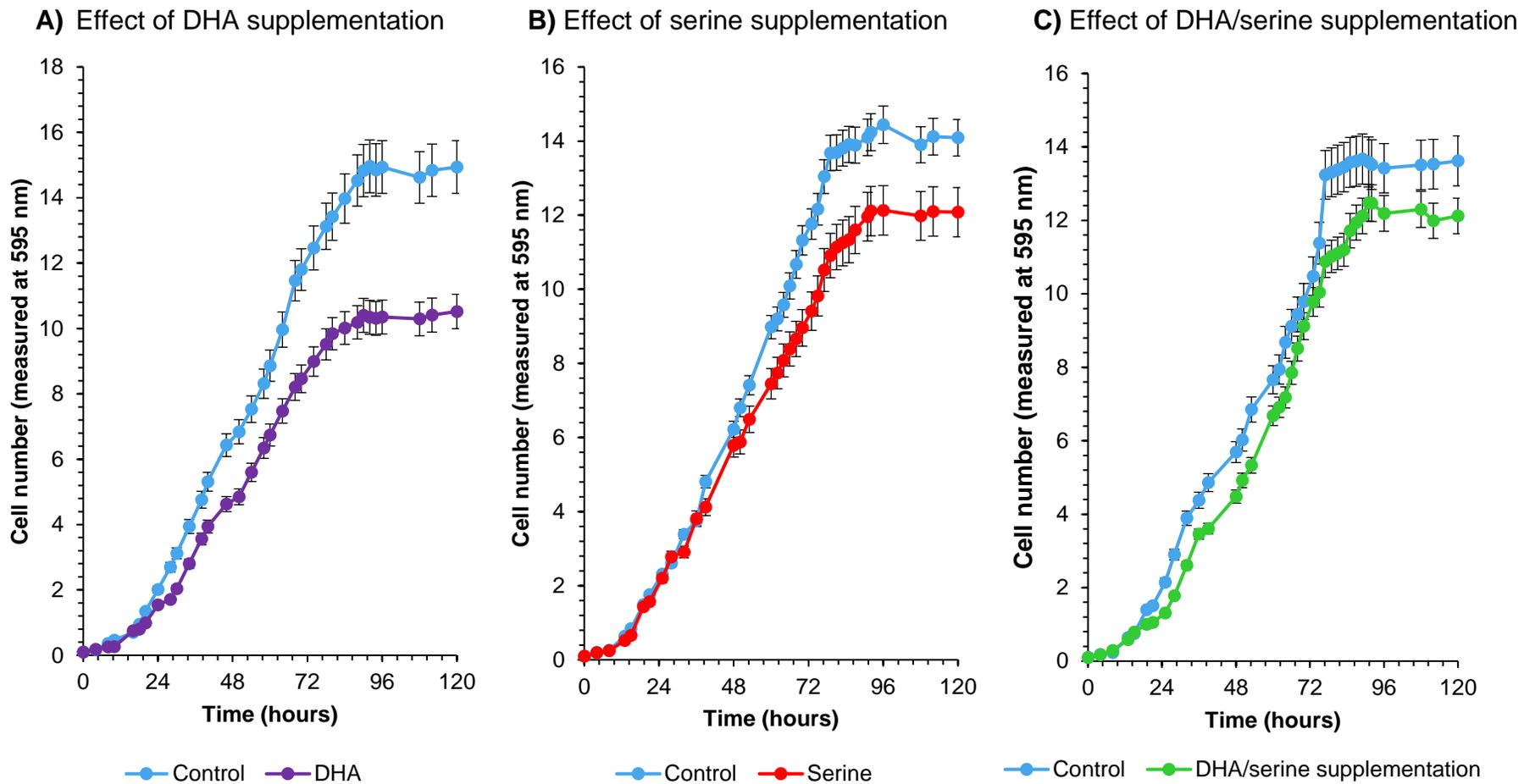
Figure 2.1: Full time course growth profile of NLM cultured *L. starkeyi*, examining the effect supplementation of DHA (A), L-serine (B) and co-administration of both (C). **Growth conditions:** orbital setting; 30°C, 180 rpm and, NLM media pH being 6.0. **Control solvents:** DMSO (0.0003%) and/or dH_2O (20%). Data presented in A, B and C are Data are mean ± SD, n=3.

As displayed in Figure 2.1, *L. starkeyi* cultured in NLM did not affect the full growth curve characteristics of the yeast paradigm, namely the lag-, exponential- and stationary- growth phases from being displayed. Lag-phased supplementation with DHA to NLM *L. starkeyi* cultures did not affect the transition and timing between each growth phase, nor the full growth curve profile from being displayed (Figure 2.1, A). Similar to that presented with *L. starkeyi* DHA supplemented cells, serine supplementation during lag-phase (Figure 2.1, B) did not affect the full growth curve characteristics of *L. starkeyi* from being achieved nor the timing between each growth phase, compared to the un-supplemented counterpart. Like previous growth profiles displayed in Figure 2.1 co-supplementation of DHA and L-serine to lag-phased *L. starkeyi* cells did not alter the growth profile of the yeast including the timing between growth phases (Figure 2.1, C).

To characterise the effects of these biological molecules in the paradigmic model, the effect upon proliferation has been examined and results are outlined in Figure 2.2.

Hypothesis

Null hypothesis: There is no relationship between the rate of log-phased growth of *L. starkeyi* supplemented with either DHA and/or L-serine.

Alternative hypothesis: There is a relationship between the rate of log-phased growth of *L. starkeyi* supplemented with either DHA and/or L-serine.
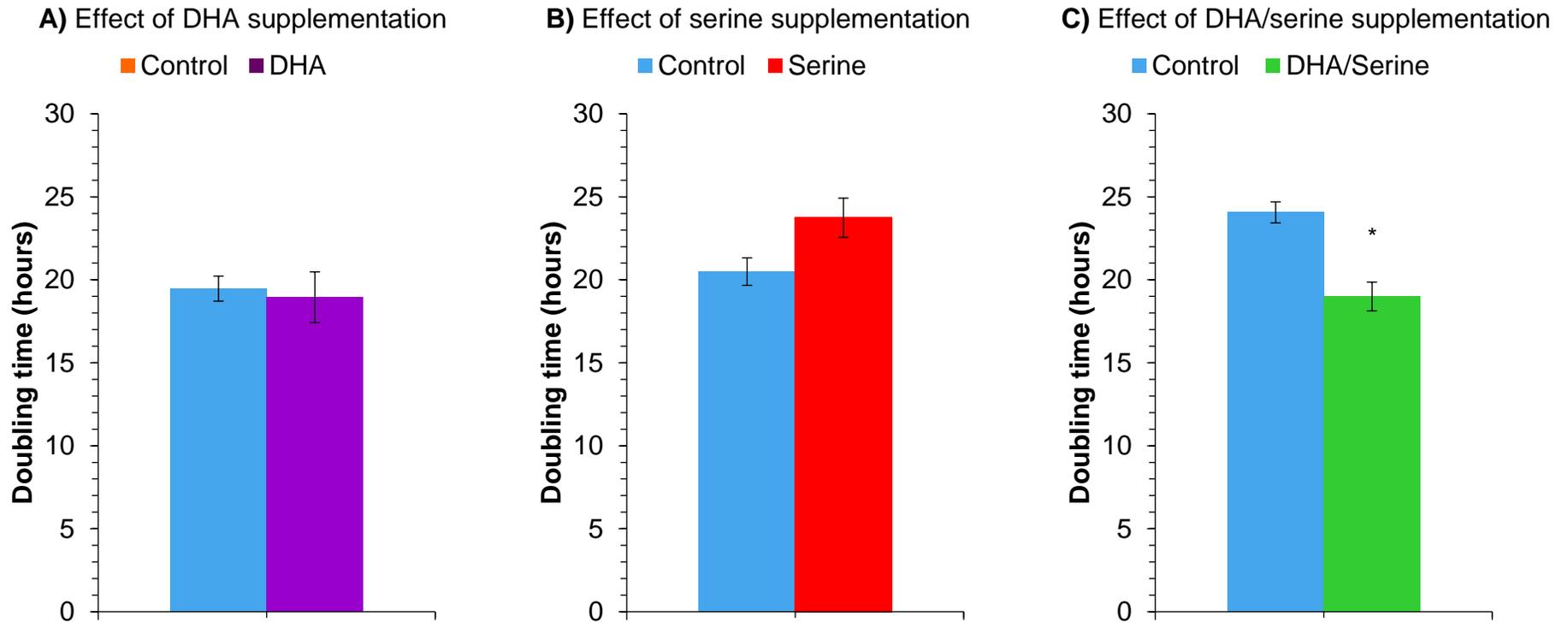
Figure 2.2: Bar chart showing the full time course growth profile of NLM cultured *L. starkeyi*, examining the effect supplementation of DHA (A), L-serine (B) and co-administration of both (C) has upon the rate of exponential growth. **Growth conditions:** orbital setting; 30°C, 180 rpm and, NLM media pH being 6.0. **Control solvents:** DMSO (0.0003%) and/or dH$_2$0 (20%). Data are mean ± SD, n=3; a one-tailed t-test statistical analysis compared the control with supplemented cultures; p<0.05 showed significance.

As shown in Figure 2.2, the presence of DHA and/or serine upon the proliferative nature of *L. starkeyi* is displayed. In comparison to the un-supplemented counterpart, the doubling time of *L. starkeyi* was reduced with DHA supplementation (Figure 2.2, A). However, the effect of DHA upon doubling time was not considered quite significant; the one-tailed t-test displayed a P value of 0.0746 (t = 2.289 with 2 degrees of freedom). Interestingly, serine supplemented *L. starkeyi* cells also displayed a slight reduction in the doubling time during log-phase, similar to that displayed in DHA supplemented cultures (Figure 2.2, A and B). Likewise, to the effect of DHA supplementation, serine presence was not considered significant in the one-tailed t-test upon doubling time; P value of 0.2607 (t = 0.7709 with 2 degrees of freedom). As shown in Figure 2.2 (C) co-administration of DHA and L-serine to *L. starkeyi* cultures, reduced the doubling rate by 25% which was considered to be significant in the one-tailed t-test; P value of 0.0189 (t = 4.996 with 2 degrees of freedom).

Furthermore, by a one-way ANOVA, the effect upon *L. starkeyi* doubling rate was deemed significant (p<0.0004) between those cells supplemented with serine and those co-administered with DHA and serine (Figure 2.2, B and C). Therefore, the null hypothesis previously stated can be rejected and instead the alternative hypothesis can be accepted. The maximal optical density reached during stationary phase can also display the effects of DHA and/or seine supplementation upon the growth cycle. These results are summarised in Figure 2.3.

Hypothesis

Null hypothesis: There is no relationship between the maximal growth achieved of *L. starkeyi* supplemented with either DHA and/or L-serine.

Alternative hypothesis: There is a relationship between the maximal growth achieved of *L. starkeyi* supplemented with either DHA and/or L-serine.

A) Effect of DHA supplementation

B) Effect of serine supplementation

C) Effect of DHA/serine supplementation
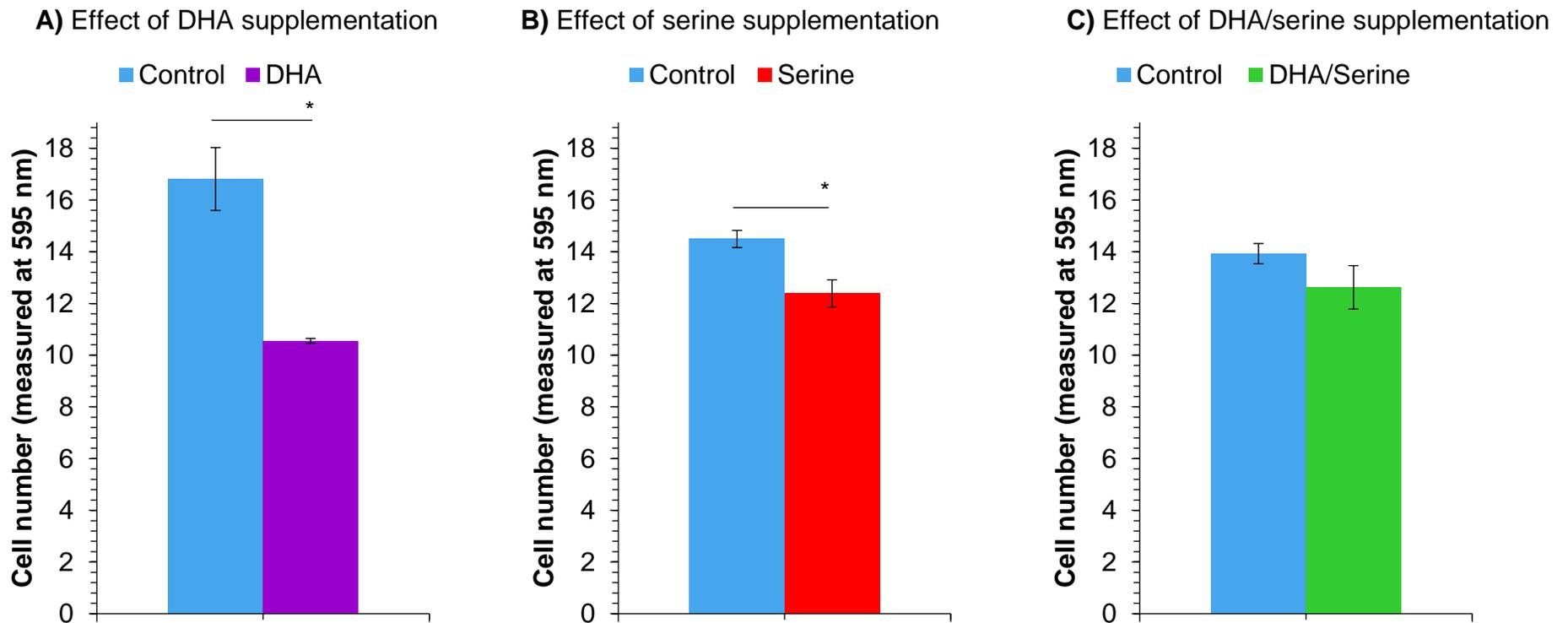
Figure 2.3: Bar chart showing the full time course growth profile of NLM cultured *L. starkeyi*, examining the effect supplementation of DHA (A), L-serine (B) and co-administration of both (C) has upon the maximal growth reached in stationary phase. **Growth conditions:** orbital setting; $30^{\circ}C$, 180 rpm and, NLM media pH being 6.0. **Control solvents:** DMSO (0.0003%) and/or dH_2O (20%). Data are mean ± SD, n=3; a one-tailed t-test statistical analysis compared the control with supplemented cultures; $p < 0.05$ showed significance.

The effect upon maximal optical density reached in stationary phased *L. starkeyi* cultures with/without DHA and/or serine supplementation are shown in Figure 2.3. Those stationary phased *L. starkeyi* cultures supplemented with DHA had an observed 30% reduction in maximal optimal density, compared to those un-supplemented cells (Figure 2.3, A). In the one-tailed t-test, the effect upon maximal optical density of stationary phased *L. starkeyi* cultures was deemed significant with DHA supplementation; P value is 0.0001, considered extremely significant (t = 61.218 with 2 degrees of freedom).   Similar to the effect shown in DHA supplemented cultures, those cultures supplemented with serine showed a 14% reduction in maximal optical density (Figure 2.3, B).   The effect serine supplementation had upon the maximal optical density achieved in the stationary phased *L. starkeyi* cultures was deemed significant in the one-tailed t-test; P value is 0.0130 (t = 6.080 with 2 degrees of freedom). The reduction in maximal optical density of the *L. starkeyi* cultures was also observed in those supplemented with both DHA and serine (Figure 2.3, C), like that previously observed in both the DHA supplemented and serine supplemented cultures (Figure 2.3, A-B). The effect upon *L. starkeyi* maximal optical density reached during stationary phase with dual supplementation of DHA and serine was also considered significant; one-tailed t-test displayed a P value of 0.0407 (t = 3.289 with 2 degrees of freedom).

To examine whether the supplementation type influenced the maximal optical density achieved in stationary phased, an ANOVA was carried out. The comparisons between groups demonstrated specific within group differences, $F_{(5, 12)} = 27.526$, $P < 0.001$. The post hoc tukey analysis displayed a between group significance on the effect of maximal optical density achieved between those *L. starkeyi* cultures supplemented with: 1) DHA and serine supplemented cultures ($p < 0.05$) and 2) DHA and dual supplementation of DHA and serine ($p < 0.01$).   Therefore, the null hypothesis can be rejected and the alternative hypothesis accepted.

Overall, the presence of DHA and/or serine in the paradigmic model was shown to affect the proliferative nature, but also the maximal cell number achieved in

stationary phased cultures. Importantly, the timings of growth phase transition during the growth curve was unaffected by DHA and/or serine presence (Figure 2.1) therefore future work on the metabolic and lipid profiles would utilize the following time points: 48 hours (early exponential), 72 hours (mid-exponential), 96 hours (early stationary) and 120 hours (stationary phase). These time points represent the same distinct phases of culture growth in all supplementation types.

2.2.3 Lipid vacuole accumulation in NLM cultured *L. starkeyi* cells

Oleaginous yeast, like *L. starkeyi* accumulate lipids once nutrient sources in the medium are exhausted. Hence, a NLM was used to aid such promotion once a stationary phase of growth was reached (Figure 2.1, A-C). Neutral lipids are those observed to be altered in many disease states. In *L. starkeyi* cells these neutral lipids are stored in lipid vacuoles, which account for up to 65% of their cellular body.

To examine the potential effect upon cellular incorporation and accumulation of lipids, morphological examination of *L. starkeyi* stationary-phased cells cultured in NLM was carried out. The morphological examination of LD presence in cultures supplemented with DHA and/or serine will provide an insight as to whether these biological molecules are involved in cellular lipid metabolism. Such effects upon lipid metabolism are observed in many cancer types and is described to be a key alteration by Hanahan and Weinberg (2011). Determination of lipid accumulation in *L. starkeyi* was achieved via light microscopy alongside the utilisation of Image J software. As such, the effect of DHA, serine and co- supplementation of both upon cellular area and the proportion of which is taken up by the lipid vacuole(s) was determined. Data collected from the stationary phased *L. starkeyi* cells are summarised in Figure 2.4, A-C.

Hypothesis

Null hypothesis: There is no relationship between the proportion of cellular space taken up by LD in *L. starkeyi* supplemented with either DHA and/or L-serine.

<u>Alternative hypothesis:</u> There is a relationship between the proportion of cellular space taken up by LD in *L. starkeyi* supplemented with either DHA and/or L-serine.

A) Morphology of stationary-phased, *L. starkeyi* cells via light microscopy (X40 magnification).

10μm

Control A   Control B   DHA   Control C   Serine   Control D   DHA/Serine
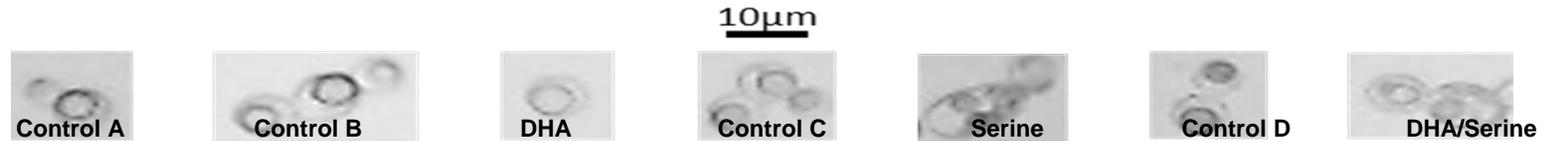
B) Area of stationary-phased *L. starkeyi* cells cultured in NLM with various supplementation types.
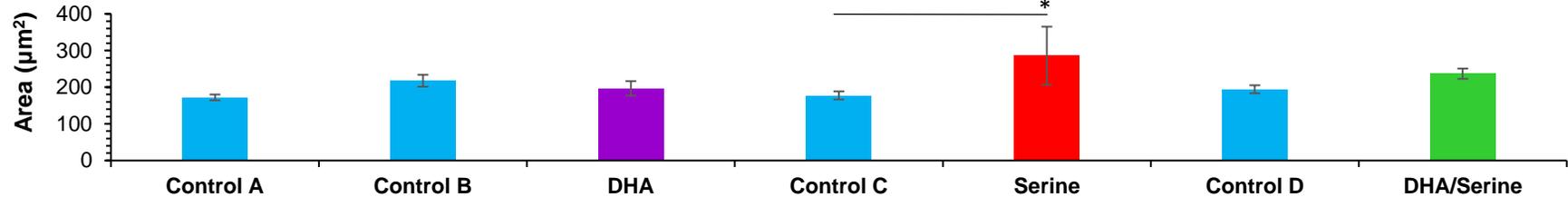
C) Lipid droplet proportion to cell area, of stationary-phased *L. starkeyi* in NLM, with various supplementation.
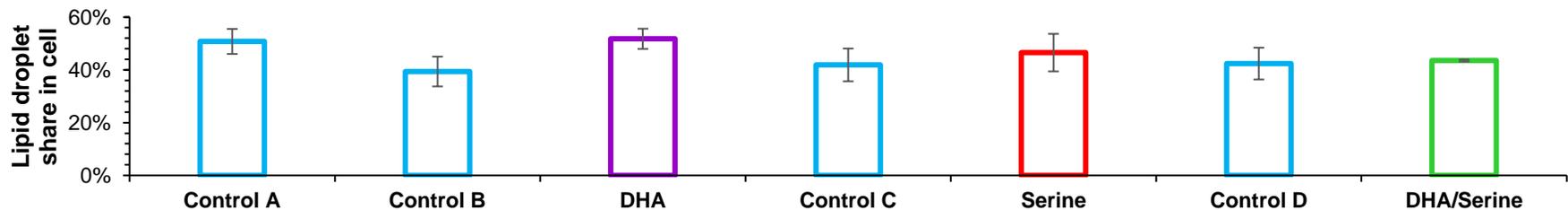
Figure 2.4: **A)** Morphological effects DHA and/or serine supplementation has upon stationary-phased *L. starkeyi* cells cultured in NLM. **B and C)** Histogram showing the effect DHA and/or serine supplementation upon the area (B) of stationary-phased *L. starkeyi* cells cultured in NLM and (C) the proportion of the cell which is taken up by the LDs. **Growth conditions:** orbital setting; 30°C, 180 rpm and, NLM (pH 6.0). **Control solvents:** A) NLM only, B) DMSO (0.0003%), C) dH_2O (20%) and D) DMSO and dH_2O (0.0003% and 20%, respectively). All data are mean ± SD, n=3; an ANOVA statistical analysis compared the control with supplemented cultures; p<0.05 showed significance.

Lipid body development in oleaginous yeast, like *L. starkeyi*, is the dominant feature during the stationary phase of growth. Microscopy images, shown in Figure 2.4 (A) illustrate *L. starkeyi* cellular accruement of lipids during this growth phase. Lipids, especially neutral in type are stored in LDs, as displayed in Figure 2.4 (A). These LDs appear to take up over half of the internal area in all cultured cells, indifferent of supplementation type. Interestingly, supplementation of the two biological molecules, DHA and/or serine, had differing effects on the; number and cellular proportion the LDs displayed within the stationary-phased NLM cultured *L. starkeyi* cells (Figure 2.4, A and B).

Cells supplemented with DHA had a large mono-LD, similar to that displayed by the un-supplemented counterpart (Figure 2.4, A, Control B). Whilst serine supplemented *L. starkeyi* cultures were observed to have cells with increased number of LDs compared to their controlled mono-LD counterpart (Figure 2.4, A, Control C). In addition to increased number of LDs, cells supplemented with serine were observed to have LDs smaller in size compared to the larger mono-LD observed in the un-supplemented *L. starkeyi* cells. Interestingly, the dual supplemented NLM cultured *L. starkeyi* cells demonstrated multiple, smaller LDs in contrast to the control which contained a mono-LDs (Figure 2.4, A, Control D).

The effect upon the size of the cells with DHA and/or serine supplementation are summarised in Figure 2.4 (B). The cell area was shown to be affected by supplementation type; whether DHA and/or serine. The ANOVA statistical test highlighted specific within group differences in cell area, $F_{(6, 14)} = 1.579$, $P>0.05$. Specifically, those *L. starkeyi* cells supplemented with serine which showed an increased cellular area of 60% ($p<0.05$). Hence, the null hypothesis can be rejected and the alternative hypothesis accepted in terms of serine affecting stationary phase cell size.

To examine whether the supplementation type influenced the portion of the stationary phased *L. starkeyi* cells which were taken up by LDs, Image J software was utilised. The proportion of which the *L. starkeyi* stationary-phased cells were embodied by the LD(s) are summarised in Figure 2.4 (C). The proportion of which the cell was taken up by LD(s) with DHA/ serine presence, was not shown to be significant in the ANOVA statistical test; $F_{(6, 14)} = 1.578$, $p = 0.2253$. Therefore, the null hypothesis can be accepted and the alternative hypothesis rejected in terms of DHA and/or serine supplementation increasing the proportion of which the *L. starkeyi* cells are taken up by LD.

Overall, *L. starkeyi* exhibits a large mono-LD during stationary phase. Supplementation of DHA to *L. starkeyi* increases the occupancy within the cell of this vacuole by up to a third, but not significantly. Whilst, serine supplementation increases the number of LDs within the cell alongside significantly increasing its area by 61%, however the proportion of the cell occupied with LD(s) were not significantly affected.

2.2.4 Effect of the two biological molecules upon radio-labelled acetate uptake

To gain better insight into the effects upon cellular lipid metabolism with DHA and/or serine presence the cultured NLM *L. starkeyi* cells were incubated with radiolabelled acetate during exponential and stationary phases of growth. With such incubation, the uptake of acetate can be traced over time giving an indication of the cellular nutritional requirements. The acetate uptake profiles are depicted in Figure 2.5 – 2.7 with the mean rates of uptake displayed on the associated figures.

Hypothesis

Null hypothesis: There is no relationship between acetate uptake of exponential and stationary phased in *L. starkeyi* cells supplemented with either DHA and/or L-serine.

<u>Alternative hypothesis:</u> There is a relationship between acetate uptake of exponential and stationary phased in *L. starkeyi* cells supplemented with either DHA and/or L-serine.
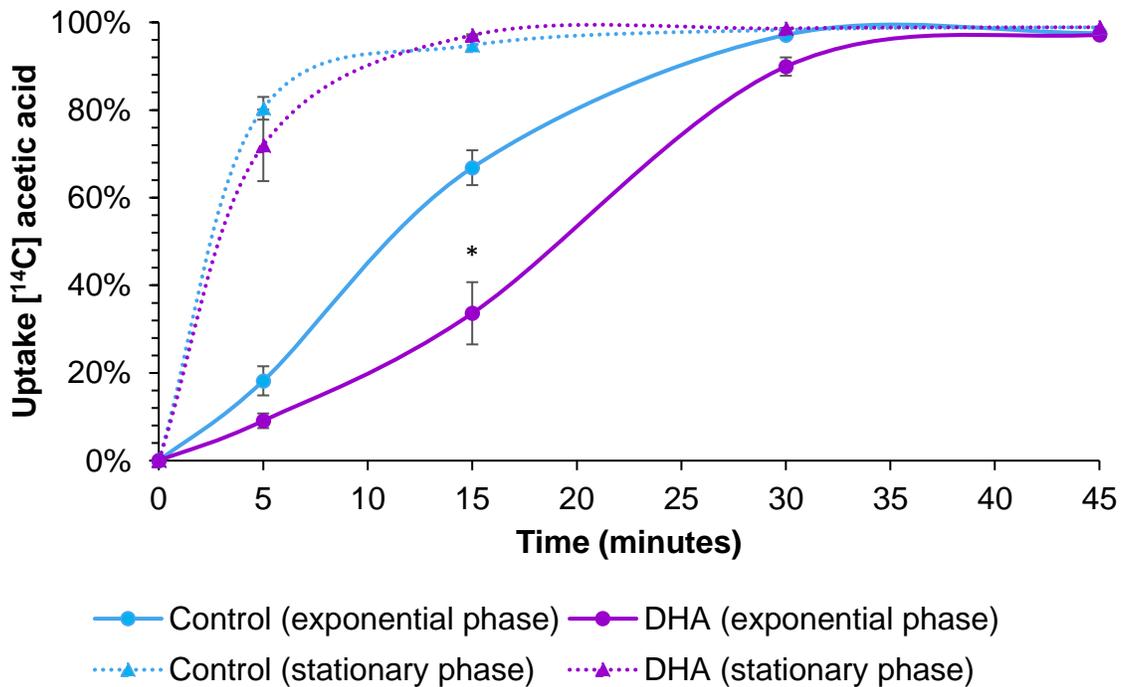
Figure 2.5: Initial [^{14}C] acetic acid uptake rates shown over a 45-minute period in *L. starkeyi* NLM cultures, during exponential and stationary growth phases; examining the effect of lag-phase supplementation of DHA. **Growth conditions:** orbital setting; 30°C, 180 rpm and, NLM media pH being 6.0. **Control solvents:** DMSO (0.0003%). Results have been corrected for an optical density of 10. All data are mean ± SD, n=3; an ANOVA statistical analysis compared the control with supplemented cultures; $p < 0.05$ showed significance.
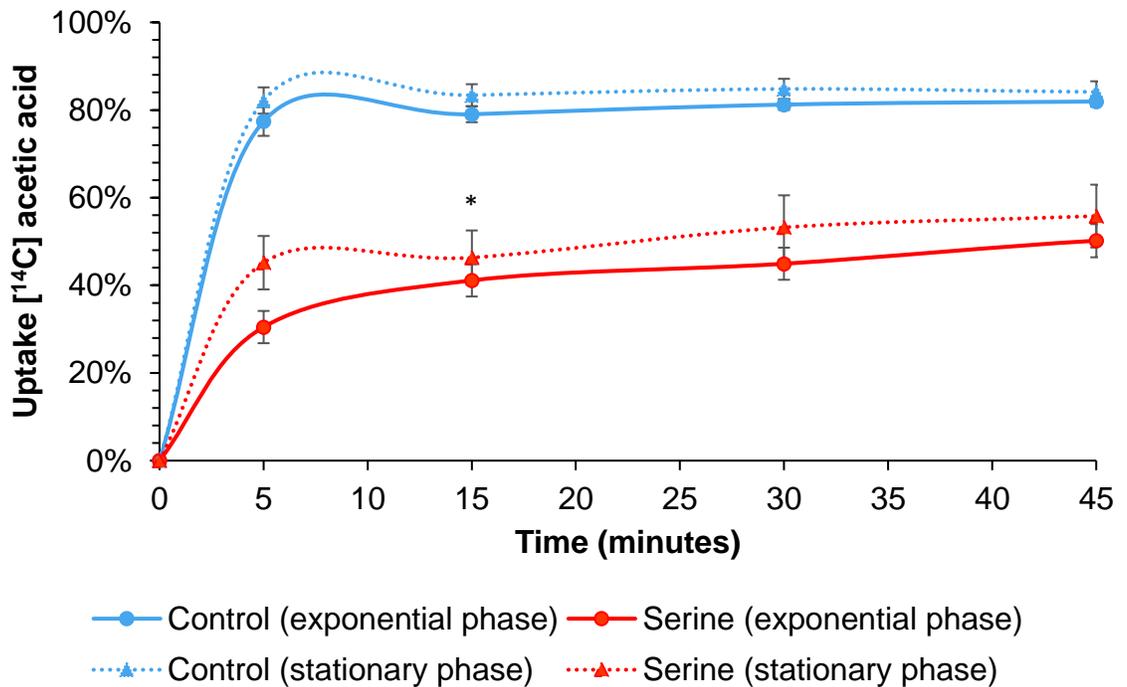
Figure 2.6: Initial [^{14}C] acetic acid uptake rates shown over a 45-minute period in *L. starkeyi* NLM cultures, during exponential and stationary growth phases; examining the effect of lag-phase supplementation of serine. **Growth conditions:** orbital setting; 30°C, 180 rpm and, NLM media pH being 6.0. **Control solvents:** dH$_2$0 (20%). Results have been corrected for an optical density of 10. All data are mean ± SD, n=3; an ANOVA statistical analysis compared the control with supplemented cultures; p<0.05 showed significance.
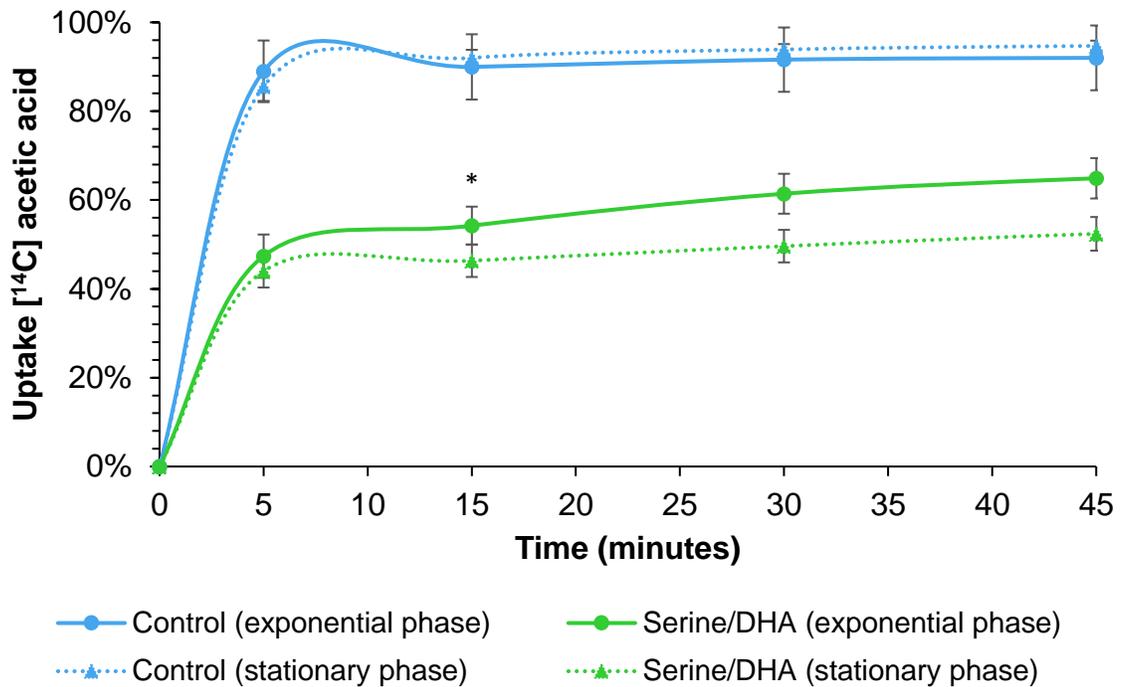
Figure 2.7: Initial [^{14}C] acetic acid uptake rates shown over a 45-minute period in *L. starkeyi* NLM cultures, during exponential and stationary growth phases; examining the effect of lag-phase supplementation of DHA and serine. **Growth conditions:** orbital setting; 30°C, 180 rpm and, NLM media pH being 6.0. **Control solvents:** co-administration of DMSO and dH$_2$0 (0.0003% and 20%, respectively). Results have been corrected for an optical density of 10. All data are mean ± SD, n=3; an ANOVA statistical analysis compared the control with supplemented cultures; $p < 0.05$ showed significance.

Figure 2.5- 2.7 summarises the radiolabelled acetate up taken from the NLM into the *L. starkeyi* cells in both phases of growth; exponential and stationary, respectively. The rate at which the radiolabelled acetate was up taken by the NLM cultured *L. starkeyi* cells from the media and the level which was reached over the time course was shown to be dependent on whether the cells were supplemented with DHA and/or serine.

To examine the effect of DHA supplementation upon the rate of radiolabel uptake, a repeated ANOVA was conducted between exponential and stationary phased *L. starkeyi* cells (Figure 2.5). The ANOVA statistical test highlighted specific within group differences in the maximum radiolabel up taken by the *L. starkeyi* cells over the time course, $F = (3, 2) = 1.507$, $p = 0.0017$ (Figure 2.5). In comparison to the un-supplemented counterpart during exponential growth phase (Figure 2.5), those NLM cultured *L. starkeyi* cells supplemented with DHA displayed a 50% reduced uptake of acetate ($p<0.05$). However, as cells transitioned to stationary phase, the maximal acetate taken up was unaffected with DHA presence in either growth phases examined (Figure 2.5).

To examine the effect of serine supplementation (Figure 2.6) upon the ability of NLM cultured *L. starkeyi* cells to uptake [^{14}C] acetic acid from the media a repeated ANOVA was conducted. The ANOVA statistical test displayed a specific within group difference on the ability of *L. starkeyi* cells to uptake acetic acid when supplemented with serine, $F = (3, 2) = 36.300$, $p = 0.0003$ (Figure 2.6). As depicted in Figure 2.6, during exponential growth phase the radiolabelled acetic acid up taken from the media by *L. starkeyi* serine supplementation cells were reduced by half in comparison to the un-supplemented counterpart ($p<0.01$). Furthermore, the growth phase transition from exponential through to stationary phase, displayed a slight increase in the [^{14}C] acetic acid up taken, however this was not significant. However, the retailoring of the [^{14}C] acetic acid previously demonstrated in the exponential growth phase was carried forward as the cells transitioned into stationary phase ($p<0.01$).

Supplementation with both biological molecules (Figure 2.7) produced an [^{14}C] acetic acid uptake profile like that displayed in those cells supplemented with serine solely (Figure 2.7, B). The repeated measures ANOVA examining the effect of DHA and serine co-supplementation upon the ability of *L. starkeyi* cells to uptake acetic acid demonstrated significant within group differences, $F = (3, 2) = 27.112$, $p = 0.0007$ (Figure 2.7).

As Figure 2.7 illustrates, NLM cultured *L. starkeyi* cells supplemented with DHA and serine displayed a reduced maximal [^{14}C] acetic acid uptake from the media; 32% and 55% during exponential ($p<0.01$) and stationary phases ($p<0.01$), respectively. This is paralleled to the profile displayed in *L. starkeyi* NLM cultured cells supplemented with serine solely (Figure 2.6). Interestingly, this retailoring of acetate uptake is not demonstrated in DHA supplemented *L. starkeyi* NLM cultured cells (Figure 2.5). Whereas *L. starkeyi* cultures supplemented with serine in some form, either solely or alongside DHA (Figure 2.6 and 2.7) demonstrated a preserved serine-dependent acetate-uptake effect on the ability of acetate to be up taken from the media into the *L. starkeyi* cells in both exponential and stationary growth phases.

In summary, radiolabelled acetic acid uptake from *L. starkeyi* NLM cultures in both exponential and stationary phases of growth was shown to be hindered by the supplementation of serine not DHA, affecting the maximal acetate up taken from the media.

2.2.5 Effect of the two biological molecules upon *de novo* lipid synthesis

In addition to the lipid accumulation observed in many diseased states, the neutral lipid profile within these tissues have been displayed to be altered. The retailoring of these neutral lipids via alterations in the *de novo* lipid synthesis pathways have been understood to aid the characteristics of these diseases. In order to ascertain the effect of the two biological molecules upon *de novo* lipid synthesis, those *L. starkeyi* cells previously supplemented with DHA and/or serine and incubated with

radiolabelled [^{14}C] acetic acid were extracted for lipids which were then separated via TLC and quantified via the [^{14}C] acetic acid presence within each neutral lipid band. A summary of the effect DHA supplementation had upon the *de novo* neutral lipid profile, during exponential and stationary phased NLM cultured *L. starkeyi* cells production of neutral lipids is depicted in Figure 2.8.

<u>Hypothesis</u>

<u>Null hypothesis:</u> There is no relationship between neutral lipid *de novo* synthesis in exponential and stationary phased in *L. starkeyi* cells supplemented with DHA.

<u>Alternative hypothesis:</u> There is a relationship between neutral lipid *de novo* synthesis in exponential and stationary phased in *L. starkeyi* cells supplemented with DHA.
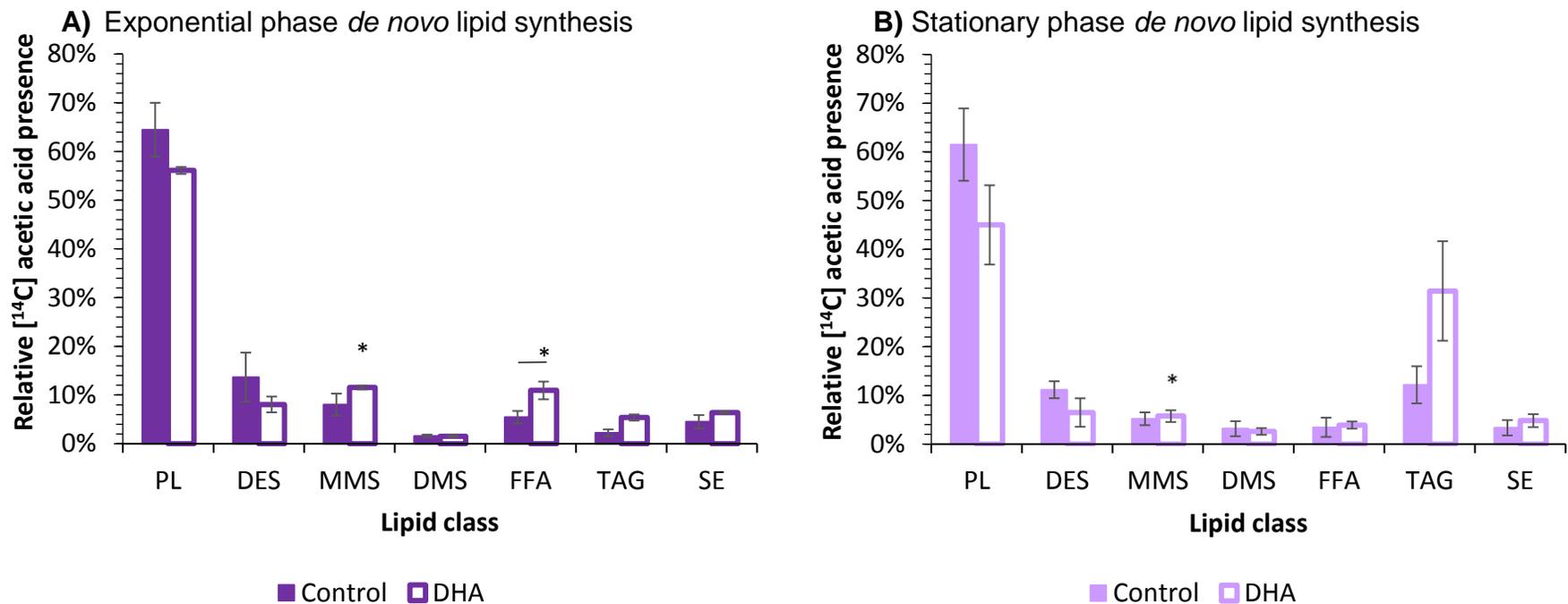
Figure 2.8: Bar charts showing the effect of DHA supplementation upon *de novo* lipid synthesis during exponential (A) and stationary (B) phased *L. starkeyi* cells via [^{14}C] acetic acid incubation over a 45-minute period. A lipid extraction followed by a TLC enables visualization thus quantification of radiolabel presence by scintillation counting of various lipid pools by scraping these bands. **Key:** PL (phospholipid), DES (desmethyl-sterols), MMS (monomethyl-sterols), DMS (dimethyl-sterols), FFA, TAG and SE. All data are mean ± SD, n=3; an ANOVA statistical analysis compared the control with supplemented cultures; $p < 0.05$ showed significance. Statistical analysis showed the lipid class synthesised to be growth phase specific, particularly the MMS proportion; $F = (27, 83)$, $p < 0.0001$. The post hoc turkey test displayed that DHA supplementation increased the *de novo* synthesis of FFA during exponential phase ($p < 0.05$).

As displayed in Figure 2.8, the most abundant lipid class, with over 65% of radiolabelled presence was that of the phospholipids, independent of growth phase. On closer examination, there is a growth-phase specific trend with those *L. starkeyi* cells supplemented with DHA in comparison to the un-supplemented counterpart. During the exponential growth phase (Figure 2.8, A), DHA supplemented NLM cultured *L. starkeyi* cells had an increased incorporation of [^{14}C] acetic acid the following lipid pools; MMS, FFA and TAGs and SE by 70%. On closer examination, this was constituted mainly by the doubling of FFA and TAG *de novo* synthesis with DHA supplementation in comparison to the non-supplementation *L. starkeyi* culture. However, with this supplementation, the proportion of phospholipids were reduced by 13%, DES by 40% and DMS by 4%.

As the *L. starkeyi* cells transitioned from exponential to stationary phase, the newly synthesized phospholipid pool reduced slightly by 5%, but this is still the overriding lipid pool of abundance with over 60% of total radiolabel presence (Figure 2.8, B). *De novo* lipid pool rearrangement with growth phase transition can also be observed in the un-supplemented culture with the reduction in the following lipid pools; DES, MMS, FFA and SE by approximating 27%. This is in contrast to the quadrupled *de novo* synthesis of DMS and TAG with growth phase. It is worthy to note, that TAG radiolabel presence increased 5.5-fold with transition into to stationary phase alone.

As Figure 2.8 demonstrated, those cells supplemented with DHA displayed this lipid pool rearrangement with growth phase transition however, to a greater extreme. Once DHA supplemented cells transitioned into stationary phase, the phospholipid pool reduced greatly by 20%; like the un-supplemented culture this is the dominant lipid pool of radiolabel presence (Figure 2.8, B). When compared to the exponential phase those cells supplemented DHA, unlike the un-supplemented control, displayed a 47% reduction in *de novo* synthesis in the following lipid pools; DES, MMS and FFA. This contrasts with, DMS and TAG lipid pools which increased 3.2-fold with stationary phase transition. Additionally, whilst TAG presence increased 4.5-fold in the un-supplemented cultures with transition from an exponential to a

stationary phase of growth, DHA supplementation enhanced this further to a 12-fold increase in TAG *de novo* synthesis, which equates to a 3-fold increase when compared to the non-supplemented stationary phase culture.

Overall, DHA supplementation was shown to influence *de novo* lipid synthesis in NLM cultured *L. starkeyi* cells. Hence, the previously stated null hypothesis can be rejected and the alternative hypothesis accepted. To determine if serine presence within the culture can also influence *de novo* lipid synthesis, NLM cultured *L. starkeyi* cells were supplemented with radiolabelled acetate over a time course, then the neutral lipids were measured for radiolabel presence.

Hypothesis

Null hypothesis: There is no relationship between neutral lipid *de novo* synthesis in exponential and stationary phased in *L. starkeyi* cells supplemented with L-serine.

Alternative hypothesis: There is a relationship between neutral lipid *de novo* synthesis in exponential and stationary phased in *L. starkeyi* cells supplemented with L-serine.
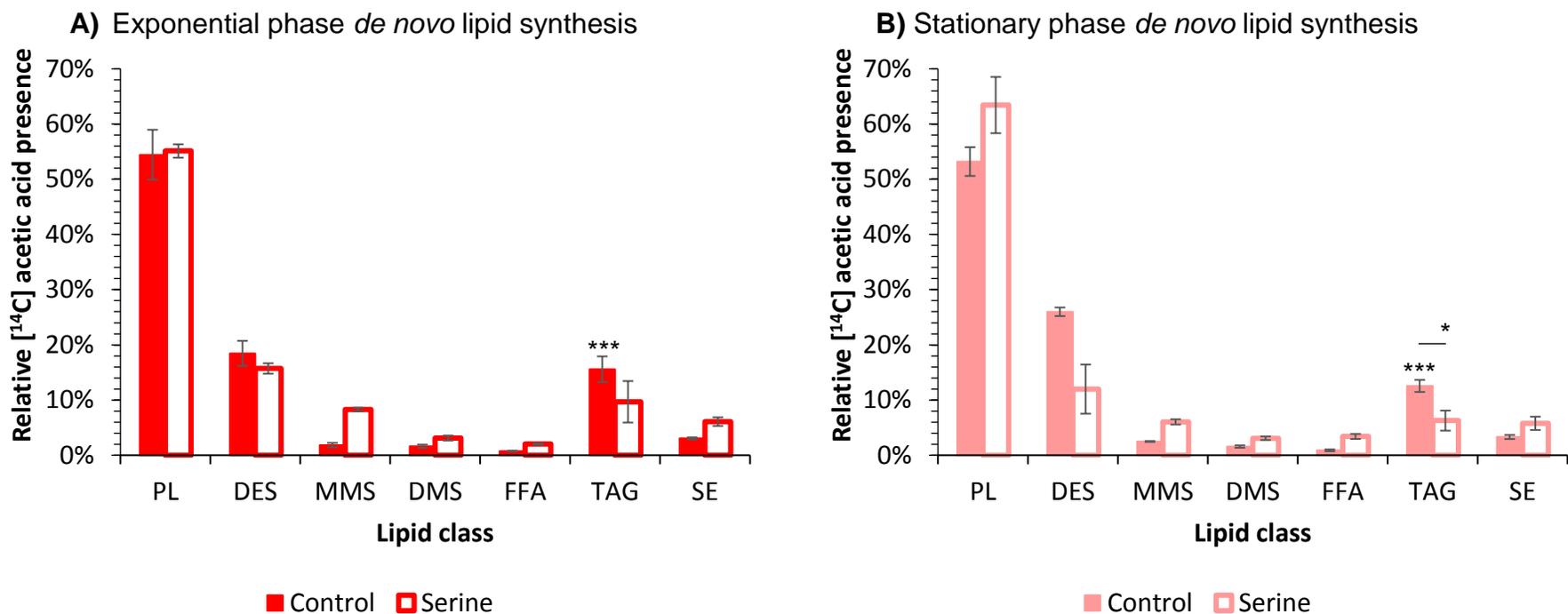
Figure 2.9. The effect upon *de novo* lipid synthesis during exponential (A) and stationary (B) phase NLM cultured *L. starkeyi* cells with serine supplementation via [^{14}C] acetic acid incubation over a 45-minute period. A lipid extraction followed by a Thin-layer chromatogram enables visualization thus quantification of radiolabel presence by scintillation counting of various lipid pools by scraping these bands. **Key:** PL (phospholipid), DES (desmethyl-sterols), MMS (monomethyl-sterols), DMS (dimethyl-sterols) FFA, TAG and SE. All data are mean ± SD, n=3; an ANOVA statistical analysis compared the control with supplemented cultures; $p < 0.05$ showed significance. Statistical analysis showed the lipid class synthesised to be growth phase specific, particularly the TAG proportion; $F = (27, 83)$, $p < 0.0001$. The post hoc turkey test displayed that serine supplementation decreased the *de novo* synthesis of TAG during stationary phase ($p < 0.05$).

Resembling cells supplemented with DHA (Figure 2.8, A-B) the effect upon lipid *de novo* synthesis is shown in Figure 2.9 examining the effect L-serine supplementation has on NLM cultured *L. starkeyi* cells. The most abundant lipid class as shown in Figure 2.9 with over 50% of the [^{14}C] acetic acid presence was that of the phospholipids, independent of growth phase. In-depth growth-phase examination however reveals specific trends with serine supplementation in comparison to the un-supplemented counterpart (Figure 2.9, A-B). As displayed in Figure 2.9 the [^{14}C] acetic acid presence within the lipid pools changed in *L. starkeyi* cultures with the transition from exponential through to stationary phase. In the un-supplemented NLM cultured *L. starkeyi* cells, a *de novo* lipid synthesis reduction with growth phase transition was observed in the following lipid pools; PL, DMS and TAG. This reduction of [^{14}C] acetic acid presence with the non-supplemented culture entry into stationary phase was paralleled with a 9% increase in *de novo* lipid synthesis of the remaining lipid pools (Figure 2.9, A-B).

During the exponential growth phase, serine supplemented NLM cultured *L. starkeyi* cells had increased incorporation of [^{14}C] acetic acid the following lipid pools; MMS, DMS, FFA and SE approximating 2.7-fold (Figure 2.9, A). However, as displayed in Figure 2.8 (A), serine supplemented cells had a reduced [^{14}C] acetic acid presence within the DES and TAG pools by 25%. This trend in radiolabel presence was unlike that displayed with DHA supplementation (Figure 2.8, A) whereby *de novo* TAG synthesis is doubled compared to the non-supplemented counterpart; contrary to the 38% reduction observed with serine supplementation (Figure 2.9, A). However, the presence of [^{14}C] acetic acid in both SE and FFA lipid pools are increased in cultures supplemented with serine (Figure 2.9, A) and DHA (Figure 2.8, A).

Growth phase transition from exponential to stationary phase, as depicted in Figure 2.9 alters the [^{14}C] acetic acid presence within the lipid pools. Transition into stationary phase (B), increases phospholipid *de novo* synthesis by 15% that is unlike both the un-supplemented counterpart. This is in part, due to the coupled reduction of [^{14}C] acetic acid in the following lipid classes; DES, MMS, DMS, TAG and SE

approximately to 23%. To make note of is the proportion of FFA within the stationary phased *L. starkeyi* cells, which increased 1.5-fold compared to the exponential phase of growth. Examining the [^{14}C] acetic acid profile of stationary phased *L. starkeyi* cells further in comparison to the un-supplemented counterpart, those cells supplemented with serine display a 51% reduction in the *de novo* synthesis of DES and TAG lipids during stationary phase whereas the remaining lipid pools are increased by a third (Figure 2.9, B)

Overall, serine supplementation (Figure 2.9) appears to affect *de novo* lipid synthesis differently than DHA supplementation (Figure 2.8). As displayed in Figure 2.8 *de novo* synthesis of TAG was reduced with serine supplementation in both growth phases examined in contrast to DHA supplementation (Figure 2.8), however SEs were increased (Figure 2.8, A-B). Therefore, the previously stated null hypothesis can be rejected and the alternative hypothesis accepted. The effect of co-administered serine and DHA supplementation upon NLM cultured *L. starkeyi* cells de *novo* lipid synthesis during exponential and stationary phases are depicted in Figure 2.10.

A) Exponential phase *de novo* lipid synthesis

B) Stationary phase *de novo* lipid synthesis
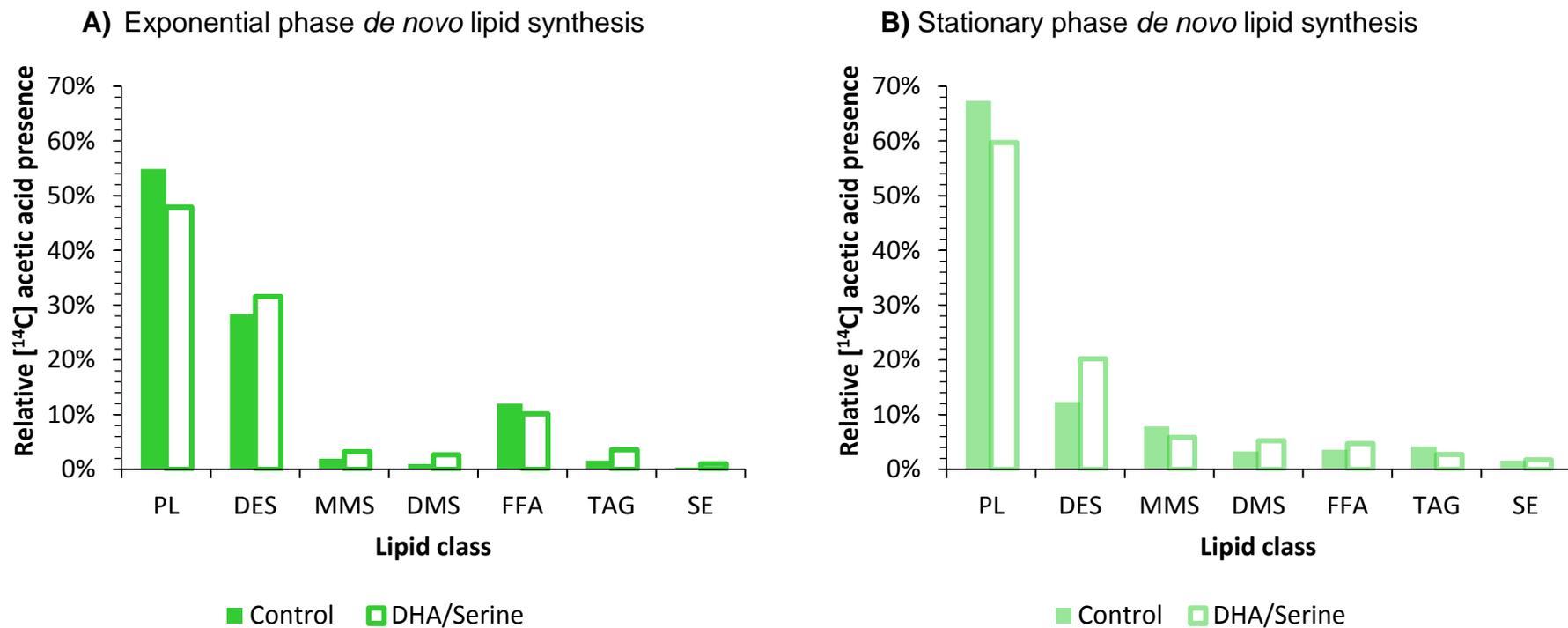
Figure 2.10: Bar charts showing the preliminary examination of the effect upon *de novo* lipid synthesis during exponential (A) and stationary (B) phased *L. starkeyi* cells upon serine and DHA supplementation via [^{14}C] acetic acid incubation over a 45-minute period. A lipid extraction followed by a Thin-layer chromatogram enabled visualization. Quantification of radiolabel presence was determined via scintillation counting of lipid pools. **Key:** PL (phospholipid), DES (desmethyl-sterols), MMS (monomethyl-sterols), DMS (dimethyl-sterols), FFA, TAG and SE. Data obtained from n=1.

The preliminary study into the effect of both biological molecules of interest, DHA and serine, upon *L. starkeyi de novo* lipid synthesis has demonstrated a morphed profile previously displayed in those cultures individually supplemented with DHA (Figure 2.8) and serine (Figure 2.9). Like previous *de novo* lipid synthesis profiles, the most abundant class as shown in Figure 2.10 is that of phospholipids. The abundance of the phospholipid lipid pool is independent of whether the *L. starkeyi* culture was incubated with [^{14}C] acetic acid during exponential (Figure 2.10, A) or in a stationary (Figure 2.10, B) growth phase; with over 50% [^{14}C] acetic acid presence.

DHA and serine co-supplementation reproduced the growth-phase specific trend previously encountered with individual DHA and serine supplemented cultures in comparison to their un-supplemented counterparts. As displayed in Figure 2.10, during exponential phase (A) in the un-supplemented culture, heightened *de novo* lipid synthesis included the; phospholipids, DES and FFA lipid pools which accounted for over 95% of the total [^{14}C] acetic acid presence. In contrast with co-supplemented DHA/serine *L. starkeyi* culture which these same lipid classes displayed a 7% total reduction. On closer view of the effect of dual supplementation of DHA/serine in comparison to the un-supplemented culture, the following lipid pools demonstrated an increased [^{14}C] acetic acid presence; DES (10%), TAG (2-fold) and SE (tripled) during exponential phase hence *de novo* synthesis.

With growth cycle progression, from exponential to stationary phase alterations in *de novo* lipid synthesis is apparent (Figure 2.10, A-B). The most abundant lipid class in the control culture with [^{14}C] acetic acid presence, the phospholipids, gained 15% abundance with growth phase transition from exponential to stationary phase. On closer view, other lipid classes which have increased radiolabel presence include; phospholipids, DES, TAG and FFA which together have quadrupled in their *de novo* synthesis. Interestingly, with DHA/serine co-supplementation these same lipid classes increase by half in comparison. However, when comparing their radiolabelled presence during the exponential- (Figure 2.10, A) to that of stationary phase (Figure 2.10, B), these lipid pools are

double that displayed in the un-supplemented counterpart. Lipid classes, which have in fact reduced their de novo synthesis with growth phase transition, include DES and FFA, which between exponential and stationary phase in the un-supplemented cultures loose ~61% of their [^{14}C] acetic acid presence. However, with serine and DHA co-supplementation the reduction from the exponential profile is only 40%. When directly comparing the stationary cultures (un-supplemented vs DHA and serine co-administered) there is a 60% increase in the presence of these lipid classes.

Comparison of the individually supplemented DHA (Figure 2.8) or serine (Figure 2.9) *L. starkeyi* cultures to the dual administered DHA and serine culture (Figure 2.10) has illustrated some similarities in their *de novo* lipid synthesis profiles of *L. starkeyi* during exponential and stationary phases of growth. To name a few, the reduced phospholipid presence observed in both phases is also displayed with DHA supplementation (Figure 2.8). Furthermore, the limited TAG increase with transition into stationary phase is displayed with serine supplementation (Figure 2.9).

Overall, the proportion of *de novo* lipid synthesis is NLM cultured *L. starkeyi* cells during exponential and stationary growth phases is dominated by the acyl lipids. The supplementation of the biological molecules of interest (Figure 2.10, A-C), DHA and/or serine, re-tailored the *de novo* synthesis of acyl lipids, sterols and SEs within the *L. starkeyi* cultures resulting in an increased isoprenoid presence compared to the control cultures.

2.3 Discussion

The main findings from this chapter suggest that serine, rather than DHA influences cellular processes. Serine supplementation resulted in the altered uptake of radiolabelled acetate in *L. starkeyi*. In addition, with serine supplementation, lipid accruement during stationary phase was altered. *L. starkeyi* supplemented with serine accrued lipids in multiple, rather than mono lipid droplets. Data from this chapter, suggest that the presence of serine can enhance the availability of neutral lipids needed for energy generation and cellular membrane biosynthesis. Such requirements are essential components of a cancerous phenotype.

2.3.1 OLEAGINICITY: MODEL ORGANISM

In many human diseases, like cancer, ectopic lipid accumulation is observed in the lipid body (Coller, 2014; DeBerardinis et al., 2008b; DeBerardinis et al., 2008a; DeBerardinis and Chandel, 2016). The ability to accumulate lipids has been conserved thru evolution in higher eukaryotes, including fungi. Results gained by Peregrin-Alvarez et al. (2009) have demonstrated to fulfil life, the enzymes involved in amino acid, energy, carbohydrate and lipid metabolism are required. However, some yeast strains specifically those, which are of non-oleaginous in type do not have the capacity to accrue lipids. An example of which is the Baker's yeast, *S. cerevisiae*, which is often used as a genetic model in various studies (Mager and Winderickx, 2005). To model the lipid accumulation observed in diseased cells, the paradigmic model organism, *L. starkeyi*, was cultured in NLM. The abundance of *L. starkeyi* lipid accumulation during stationary phase was shown in Figure 2.4. Light microscopy images of the stationary phased, nitrogen limited *L. starkeyi* cells demonstrated the yeasts capability to accrue lipids via the large mono-lipid body, which it houses. The high proportions of the cell, shown in Figure 2.4 (A), which is taken up by the lipid body demonstrates the *L. starkeyi* strain's oleaginicity; the dry cell of which has been reported to be >65%. *L. starkeyi's* mono-lipid body will be storing the neutral lipids, triacylglycerides and sterol esters, surrounded by a phospholipid membrane also housing sterols.

The lipid accumulation observed in *L. starkeyi* in Figure 2.4 (A) is because of the nutrient exhaustion exhibited on the cells during stationary phase. Nutrient exhaustion is because of the cellular processes taking place during the log phase of growth. Such processes requiring nutrient input from the media include, proliferation and protein and nucleic acid synthesis. Hence, with increasing *L. starkeyi* cellular density with growth curve progression, levels of nutrients in the media reduce, specifically nitrogen which was already limited in the NLM media. Due to nutrient exhaustion, protein and nucleic acid synthesis in *L. starkeyi* halts which is similar to that observed in mammalian cells. Subsequently, metabolic retailing as per described in Figure 1.21 is promoted leading the lipid accumulation observed in Figure 2.4.

The metabolic retailoring responsible for the lipid accumulation observed in *L. starkeyi* as opposed to a non-oleaginous yeast stems from their taxonomic hierarchy. *L. starkeyi* is one out of 1000 known ascomycete yeasts and is part of the Lipomycetaceae family. A parsimonious tree (Appendix 2) illustrates the genetic divergence between Lipomycetaceae members, of which *L. starkeyi* belongs (Kurtzman et al., 2007). The genetic divergence between *L. starkeyi* and *S. cerevisiae* is great, hence explaining why during stationary phase *S. cerevisiae,* divert the excess carbon into the production of polysaccharides (glycogen, glucan and mannan) whilst *L. starkeyi* produces and subsequently stores intracellular lipids in a lipid body. In mammalian cells, during diseased states, cells accumulate lipids, hence an oleaginous yeast is better biochemically suited to study the effect of lipid accumulation with DHA and/or L-serine supplementation.

2.3.1.1 Oleaginous vs non-oleaginous yeasts: energy metabolism

One of the major differences between the yeast strains, *L. starkeyi and S. cerevisiae*, is their energy metabolism preference. Growth in high glucose environments would be observed in Crabtree positive yeasts like *S. cerevisiae*. Crabtree positive yeasts aerobically ferment alcohol when sugar is in excess. Whereas non-fermentative yeasts, like *L. starkeyi,* under nutrient exhaustion lead

to be metabolic retailoring via increased AMP-activated protein kinase (AMPK) resulting in the accruement of lipids once the stationary phase of growth is. The enzymatic differences between the two types of yeasts, Crabtree positive and negative, provide reasoning for this. Many studies have used the lipid accumulating benefits of oleaginous yeast, like *L. starkeyi*, to increase the lipid production in non-oleaginous yeasts like *S. cerevisiae* by genetically improving the strain. In disease states, like cancer, lipolysis is described to be 'reactivated'. As a result, the products of which including, triglycerides and phospholipids are increased and subsequently result in the traits of a cancerous cell becoming enabled, as per described by Hanahan and Weinberg (2011) (Beloribi-Djefaflia et al., 2016). These neutral lipids are housed in a lipid body within *L. starkeyi*, which during nitrogen limitation over half of the cell was shown to be taken up by (Figure 2.4, A-C).

Considering the focus of the research in addition to the details above, the lipid enzymatic capabilities of the model needs to be taken into account. One of the lipids increased during diseased states is the neutral lipid, triacylglyceride, for which the rate-limiting step involves the ACC enzyme. The study by Wang et al. (2016) demonstrated how the expression of ACC from *L. starkeyi* improved the oleaginicity of *S. cerevisiae*, not only via the lipid content (24%) but also the productivity of which it was made (22%). Other studies have demonstrated other key enzymes (ACL) which are involved in triacylglyceride production to be void in non-oleaginous yeast strains like *S. cerevisiae* but present in oleaginous yeasts like, *L. starkeyi*. However, due to the easy genetic manipulation of the *S. cerevisiae* strain, metabolic engineering of the ACL gene has been shown to increase the fatty acid synthesis within this model (Tang, 2013).

Considering all factors, *L. starkeyi* was therefore used as the model organism, examining the effect of the two biological molecules surrounding cellular events leading to lipid accumulation, as opposed to the Bakers yeast, *S. cerevisiae*.

2.3.2 INFLUENCE OF DHA SUPPLEMENTATION

Several studies on the human diet, have shown to reduce the risk of cancer, including colon, when the ratio of polyunsaturated fatty acids are higher in ω-6 compared to the ω-3.

2.3.2.1 Effect on growth

The 22 carbon, six-double bonded biological molecule, DHA has been shown in several studies to inhibit not only cancer cellular proliferation but also induce cell death (Song and Kim, 2016). From the results shown in Figure 2.03, *L. starkeyi* cells supplemented with DHA (90 nM) resulted in a reduction in the overall culture density by a third. This is in line with previous findings with concentrations between 10-100 mM (Fasano et al., 2012; Abdi et al., 2014). In this study, *L. starkeyi* cells were exposed to a much lower concentration of 90 nM as higher concentrations induced premature senescence, which made the determination of culture growth impossible. This may suggest that in fact, those *L. starkeyi* cells supplemented with DHA had an increased demand for nutrients from the culture media. This in turn would lead to the premature limitation of nutrients in the media which would cause activation of several upstream signalling pathways including mTOR and Raf. Because of signalling pathway activation, premature entry into stationary phase would occur. Subsequently, a reduction in cellular density would be demonstrated, as was in Figure 2.4 (A).

Conversely, DHA has been shown to promote apoptosis in mammalian cells (Abdi et al; 2014) which may account for the reduction in cell number witnessed in our experiments. However, under osmostress the viability of those cells supplemented with DHA was increased. This increased cellular viability under stress, suggests a thicker cell wall during stationary phase with DHA supplementation.

2.3.2.2 Effect on lipid accruement

In disease states, such as neurodegeneration and cancer lipid accumulation is observed to be altered. Studies have focused their attention on the storage unit of these neutral lipids, the LD. Within these units, the neutral lipids, triacylglyceride and sterol esters, are stored awaiting mobilisation. As demonstrated in Figure 2.4, DHA supplementation had no effect on cell size (A) but the proportion of which was taken up by the LD (B) was increased by a third compared to the un-supplemented counterpart. The influence DHA has upon lipid droplet formation has been documented in several studies (Tremblay et al., 2016). One factor to consider would be whether the *L. starkeyi* cells supplemented with DHA had an altered phospholipid nomenclature, which would therefore impact on the intrinsic curvature of the LD, which in turn would increase its area within the cell. A study by Shi et al. (2013) has shown that the size of the LD can be regulated via stearoyl-CoA desaturase (SCD) which is also found in *L. starkeyi*. As a key conversion enzyme for mono-desaturation of fatty acids, SCD1 regulates lipogenesis providing lipids required for rapid proliferation and cellular structure observed in cancer cells. This would result in the reduction in lipid mobility once triacylglyceride and sterol esters are stored in the LD.

The effect of DHA supplementation upon *de novo* lipid synthesis was gained with the incubation and quantification of radiolabelled acetate within *L. starkeyi* exponential and stationary phased cultures.

2.3.2.3 Effect on lipid metabolism

The results of this study have shown that un-supplemented stationary phased cultures were able to take up radiolabelled acetate at a faster rate than their exponential phase counterparts (Figure 2.4). Once taken up by the cells, acetate, in the form of acetyl-CoA, was used as a precursor for both isoprenoid and acyl lipid biosynthesis, hence the labelling of the sterol and combined acyl lipid (phospholipids and triglyceride) pools, respectively. Approximately, 75% of labelled carbon were shown to accumulate in the acyl lipid pool whilst the

remaining 25% was utilized for isoprenoid synthesis. Consequently, it may be postulated that for every four acetate molecules converted to acetyl-CoA, three of these molecules are used to support acyl lipid synthesis. This feature has been shown to be independent of the growth phase, whether exponential or stationary. In addition, the biosynthesis of triglycerides relative to that of phospholipids increased as the cells moved into a more quiescent period (stationary phase). Furthermore, those *L. starkeyi* cells supplemented with DHA had a raised triglyceride: PL ratio, which increased further with stationary phase entry, compared to the control. These results are in line with the studies of Rolph et al (1989) on lipid accumulation in another oleaginous yeast, *R. gracilis*. Therefore, the depiction of a larger mono-LD in Figure 2.4 (A) in those cells supplemented with DHA support this raised *de novo* production of triglyceride during stationary phase (Figure 2.8, B). This raised neutral lipid production observed with DHA supplementation demonstrated an increased flux through the Kennedy pathway (Figure 1.21).

The rate at which the radiolabelled acetate was taken from the NLM media by those cells supplemented with DHA had little effect on the rate at which it was up-taken in proliferating cells, whilst stationary-phase cells exhibited a slight decrease (Figure 2.5-2.7, A). However, despite the reduced rate of uptake, more of the radiolabel accumulated in the form of triglycerides in the DHA treated cells (Figure 2.8). Also, to note, the increased amount of radiolabelled sterol ester upon DHA treatment (Figure 2.8). However, at this stage it is impossible to determine the biosynthetic origins of the enhanced production of sterol esters.

2.3.3 INFLUENCE OF SERINE SUPPLEMENTATION

2.3.3.1 Effect of growth

As relatively little is known about the uptake of serine by *L. starkeyi*, it was decided to use as high a concentration as possible for the serine supplementation studies. Consequently, *L. starkeyi* cultures were grown in media supplemented with 91 mM serine. The use of such a high serine concentrations would provide a serine concentration, which could mimic the transfer of L-serine from the astrocytic producers to the glial cells of the brain (see Chapter 1). Another issue which needed to be addressed was also the fact that the yeast paradigm was also surrounded by a cell wall, whose thickness would increase as the cultures aged. As with DHA supplementation, serine supplementation had little effect on the timing of growth phase transitions but did reduce the final cell density reached by 14%.

2.3.3.2 Effect on lipid accruement

Those cells supplemented with serine exhibited an altered number of LDs within those cells, which reached stationary phase (Figure 2.4). The yeast paradigm, *L. starkeyi*, accumulates lipids in a mono-LD; however, serine supplementation resulted in the formation of several LDs (Figure 2.4). Observations of several LDs have been reported in diseased cells. It has been postulated that the budding off from the endoplasmic reticulum into the cystol is altered in these states. In addition to the multi-LD occupancy within the stationary phased serine supplemented *L. starkeyi* cells, the size of these cells were also increased by 61% (Figure 2.4, B). This like those cells supplemented with DHA, may suggest an altered phospholipid nomenclature of the phospholipid membranes, resulting in an increased cell size due to the impact upon intrinsic curvature of the membranes. Likewise, the increase in cell size could also be explained by the cellular response to prevent lipotoxicity due to the raised LD occupancy observed.

2.3.3.3 Effect on lipid metabolism

Similar to the effect of DHA supplementation, serine supplemented *L. starkeyi* cells showed an increase in the amount of radiolabelled acetate which was taken up in stationary phase compared to exponential phase (Figure 2.5, B). Approximately, 90% of labelled carbon was shown to accumulate in the acyl lipid pool whilst the remaining 10% was utilized for isoprenoid synthesis. Consequently, it may be postulated that for every ten acetate molecules converted to acetyl-CoA, one of these molecules are used to support acyl lipid synthesis. This feature has yet to be shown to be independent of the growth phase, but is the same for incubation with serine from exponential and stationary phases. The biosynthesis of phospholipids relative to that of triacylglycerides was interestingly increased during stationary phase in comparison to the exponential cells. This may, in part, be due to the proportion of the cell which is taken up by the LDs. However, as the levels of triacylglycerides and sterol esters are relatively unchanged upon stationary phase entry, this is unlikely. Therefore, the increased proportion of PL to TAG is more likely to be because of the mobilisation of the phospholipids surrounding the LDs in aid of supporting the demands for membrane biosynthesis. This is further evidenced with the increased cell size observed in cells supplemented with serine during stationary phase in Figure 2.4.

In comparison to DHA supplementation which had little effect upon rate of radiolabelled uptake, serine supplementation reduced uptake in both proliferating and stationary *L. starkeyi* cells by half (Figure 2.5, B). Furthermore, the ratio of triacylglyceride: phospholipid *de novo* synthesis during stationary phase was also greater in those DHA treated cells. However, as previously stated, at this stage it is impossible to determine the biosynthetic origins the enhanced production of sterol esters.

2.3.4 INFLUENCE OF SERINE AND DHA SUPPLEMENTATION

2.3.4.1 Effect of growth

With the relationship between DHA and L-serine being well documented, the effect of dual supplementation to *L. starkeyi* during lag phase was examined. As with DHA and serine supplementation, co-supplementation had little effect on the timing of growth phase transitions but the culture density was slightly reduced by 8%.

2.3.4.2 Effect on lipid accruement

Those cells supplemented with both DHA and serine exhibited an altered number of LDs within those cells, which reached stationary phase (Figure 2.4), similar to that observed in those cells solely supplemented with serine. The yeast paradigm, *L. starkeyi*, accumulates lipids in a mono-LD; however, co-supplementation resulted in the formation of several smaller LDs (Figure 2.4). The observation of several smaller LDs was also shown in those cells supplemented with serine alone. In addition to the multi-LD occupancy within the stationary phased *L. starkeyi* cells, the size of the *L. starkeyi* cells were also increased by 22% (Figure 2.4). This like those cells supplemented with DHA, either demonstrated an altered phospholipid nomenclature, which results in a larger cell due to the affected intrinsic curvature. However, unlike those cells supplemented with DHA or serine solely, the proportion of which the stationary phased cells which were taken up by the LDs were unaffected. This therefore suggests that the LDs have either been mobilised for their phospholipids for membrane biosynthesis, which would explain the larger cell size.

These LDs function within the *L. starkeyi* cells is to store the neutral lipids, triacylglycerides and sterol esters. Hence, to see the effect of supplementation of both serine and DHA upon *de novo* lipid synthesis, exponential and stationary phased cells were incubated with radiolabelled acetate.

2.3.4.3 Effect on lipid metabolism

As the effect observed with serine supplementation, dual supplementation to *L. starkeyi* showed an increase in radiolabelled acetate uptake with the transition of the oleaginous *L. starkeyi* from late exponential to stationary phase (Figure 2.6). Approximately, 90% of labelled carbon were shown to accumulate in the acyl lipid pool whilst the remaining 10% were utilized for isoprenoid synthesis, like that demonstrated with serine supplementation alone. Consequently, it may be postulated that for every ten acetate molecules converted to acetyl-CoA, one of these molecules are used to support acyl lipid synthesis. This feature has yet to be shown to be independent of the growth phase, but is the same for incubation with serine/DHA from exponential and stationary phases. The biosynthesis of phospholipids relative to that of triacylglycerides was interestingly increased during stationary phase in comparison to the exponential cells. This may in part be due to the proportion of the cell, which is taken up by the LDs, as it requires a mono-phospholipid bilayer. However, as the levels of triacylglyceride and sterol esters are relatively unchanged with stationary phase entry from exponential phase this is unlikely. Therefore, the increased proportion of phospholipid to triacylglycerides are more likely to be as a result of the mobilisation of the phospholipids surrounding the LDs for membrane biosynthesis. This is further evidenced with the increased cell size observed in cells supplemented with both serine and DHA during stationary phase in Figure 2.4.

In comparison to those cells supplemented with DHA, those cells supplemented with both DHA and serine exhibited an altered upon of radiolabelled uptake. Similar to that observed in serine-supplemented cells, those *L. starkeyi* cells supplemented with both DHA/serine had a reduced uptake by half in both proliferating and stationary phases (Figure 2.7, C). Furthermore, the ratio of triacylglyceride: phospholipid *de novo* synthesis during stationary phase was lower compared to the profile shown in DHA treated cells (Figure 2.8 and 2.9, B).

2.4 CONCLUSION

In conclusion, the results of the study have shown that it is possible to employ a yeast model to study phospholipid synthesis using radiolabelled ^{14}C- acetate uptake mechanism. The data further show that DHA and/or serine presence within cells can alter metabolic pathways including lipid biosynthesis and lipid droplet formation, both are associated with a cancerous phenotype.

Chapter 3

Serine-directed metabolic flux, an immunohistochemical study of meningioma

3.1 INTRODUCTION

One of the many key features of cancer is ectopic lipid synthesis, which can be modulated by a variety of factors including the amino acid, serine. This non-essential amino acid has been implicated to be the orchestrator of the metabolic reprogramming observed in many cancerous cells to sustain their growth and proliferation (Tsun and Possemato, 2015). The ability of cancerous cells to enable their survival is their ability to generate lipids, nucleic acids and proteins (Amelio et al., 2014b). An overview of the serine biosynthetic pathway observed during tumourigenesis is depicted in figure 3.1.
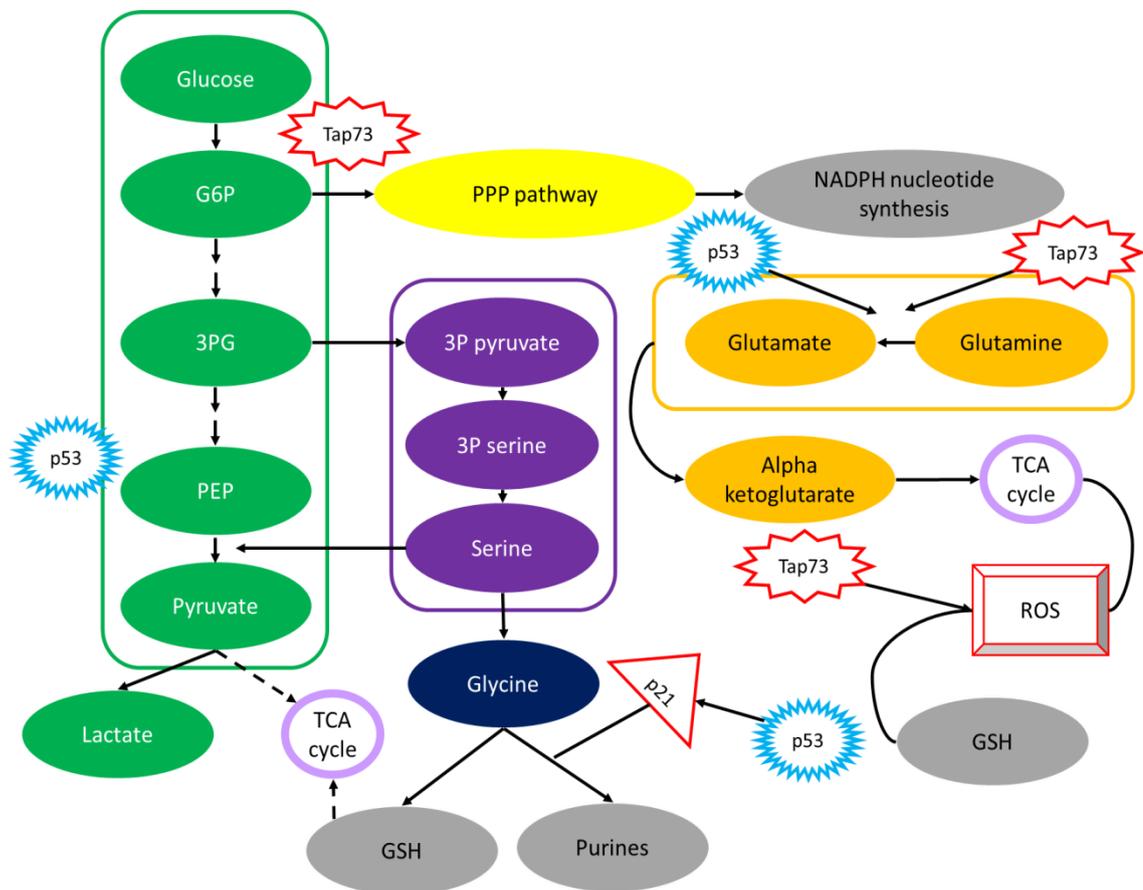
Figure 3.1: Diagram showing how glycolysis is diverted during *de novo* serine biosynthesis in cancerous cells to fulfil the cellular demands. There are several enzymatic reactions leading up to serine biosynthesis: 1) 3P pyruvate a glycolytic intermediate would be converted to the serine precursory, 3P serine, by PHGDH and nicotinamide adenine dinucleotide (NAD). After which 2) a PSTA1 and 3) a PSPH reaction converts 3P serine into serine (Adapted from Amelio et al., 2014a). **Legend:** 3-phosphoglycerate (3P pyruvate), 3-phosphohydroxypyruvate (3P serine), transamination reaction (PSTA1) and phosphate ester hydrolysis (PSPH).

In cancerous cells the serine biosynthesis, shown in Figure 3.1, is central to the metabolic reprogramming which enables the sustained demand for cellular nutrients including amino acids, lipids and nucleic acids. Serine acts a precursor for such cellular nutrients and hence, the diversion from glycolysis to serine biosynthesis provides such sources. The enzyme profile of key enzymes surrounding serine biosynthesis within cancerous tissues are tabulated in table 3.1.

Table 3.1: Table showing key serine-biosynthetic enzymes associated with cancer prevalence.

Enzymes	Cancer types	References
PKM2	Solid tumours	(Zhu et al., 2016)
PHGDH	Colorectal and gastric cancer	(Jia et al., 2016; Xian et al., 2016)
p53	Colorectal adenocarcinoma	(Akshatha et al., 2016)

Legend: pyruvate kinase isoform 2 (PKM2) and phosphoglycerate dehydrogenase (PHGDH).

Studies shown in Table 3.1 examined the key enzymes involved in serine biosynthesis. By doing so, it is possible to show a paralleled relationship between the levels of enzyme expression and patient prognosis. A review by Zhu et al. (2016) on the rate-limiting glycolytic enzyme, PKM2, whose activity is vital for metabolic reprogramming observed in cancer was found to be correlated with patient prognosis. The review examined 27 studies, with 4,796 cases, from which the paralleled relationship between increased PKM2 expression and poor prognosis was ascertained.

Another enzyme, which is believed to be involved in the remodelling of cancer metabolism is PHGDH and it has been associated with several tumours including melanoma and breast cancer. A study by Jia et al. (2016) on colorectal cancer found that the expression of PHGDH was related to the individuals prognosis.

Hence, current data suggests a correlation between the metabolic reprogramming of glycolysis to *de novo* serine biosynthesis and reduced cancer prognosis. Enzymes involved in this metabolic reprogramming have several roles and therefore, mutations or altered expressions of these enzymes can result in tumourigenesis. Subsequently, research has focused on the possible treatment avenues, which may lie within the serine biosynthetic pathway investigating whether the effects of the enzymes themselves can be hindered to reduce cellular growth and proliferation. A summary of studies which have demonstrated the use of enzyme inhibitors in a cancerous model to aid prognosis is shown in table 3.2.

Table 3.2. A summary of possible treatment avenues for altered serine-biosynthesis via enzyme inhibitors.

Enzyme	Potential treatment	References
PKM2	Compound 3 Small interfering RNA (siRNA) 156	(Vander Heiden et al., 2010; Goldberg and Sharp, 2012)
PHGDH	Allosteric inhibitors CBR-5884	(Wang et al., 2017; Mullarky et al., 2016)
p53	Small molecules such as *CP-31398*	(Wang and Sun, 2010)

PKM2 expression in cancerous cells enables aerobic glycolysis and therefore it is an ideal target for inhibition for treatment. Initial studies developing potential PKM2 inhibitors by Vander Heiden et al. (2010) and Goldberg and Sharp (2012), have shown increased rates of cancerous cell death due to the loss of growth signalling and decreased viability. Furthermore, the PHGDH treatments showed specific tumour site action due to the serine metabolic reprogramming not to be found in non-cancerous cells (Wang et al., 2017, Mullarky et al., 2016). Clinically,

these findings are promising, as those cancers which show a heightened serine biosynthetic profile can also be treated in future with other treatments which will reduce chemo-resistance and reduce the availability of such resources to the cancer including; lipids, nucleic acids and amino acids. Therefore, taking into consideration previous findings (Chapter 2), this part of the study was designed to uncover evidence of whether serine biosynthesis is activated within meningioma.

3.2 MATERIALS AND METHOD

In this study, the paraffin embedded, formalin fixed tissue blocked of surgical specimens were retrospectively evaluated. These contained 16 cases of Meningioma, 8 of Grade I and II, from the files of Royal Preston Hospital (RPH). All patients had given their consent prior to this study. Clinical data including Simpson Grades of sections were also provided from RPH. Hematoxylin and eosin (H&E) slides from the paraffin blocks were reviewed by Pathologists and graded per the 2007 WHO Graded system. See Appendix 3 and appendix 4 for the ethical approval and histological characteristics of the meningioma tissue sections.

3.2.1 Materials list

Patient samples from grade I and grade II meningioma (8 patients per grade) were used to measure serine biosynthesis. Enzyme presence was achieved by immunohistochemistry. Reagents used for the experiments included: histoclear, ethanol, hydrogen peroxide, methanol, phosphate-buffered saline (PBS), diluted blocking serum, primary antibodies (p53, PKM2, PHGDH and fascin), diluted biotinylated secondary antibody, VECTASTAIN *Elite ABC* Reagent, diaminobenidine (DAB), peroxidase substrate solution, hematoxylin and eosin.

3.3 METHODOLOGY

3.3.1 Immunohistochemical staining

Representative blocks of paraffin-embedded tissues were selected and cut at 4-6µm. The slides were de-paraffinised in histoclear, rehydrated through an alcohol series and subsequently hydrated in tap water for a period of 5 minutes. After treating with 3% hydrogen peroxide (H_2O_2) in methanol for 10 minutes, sections were washed in phosphate-buffered saline (PBS) buffer for 5 minutes followed by a 20-minute incubation of diluted normal blocking serum, which was then blotted and followed, by a 30-minute incubation of primary antibody diluted in PBS buffer. Primary antibodies used in this study were purchased from Abcam and of Anti-rabbit origin. Based on recommendations from Abcam, the following dilutions of antibody (in diluent) were used the study: p53 1:8000, PKM2 1:50,

Fascin 1:250 and PHGDH 1:40. After incubation in primary antibody, slides were then washed for 5 minutes in PBS buffer and incubated for 30 minutes with diluted biotinylated secondary antibody. After this time, this was rinsed off with PBS and further incubated with VECTASTAIN *Elite ABC* Reagent for a period of 30 minutes. The slides were then rinsed again with PBS buffer (5 minutes), then incubated with diaminobenidine (DAB) containing peroxidase substrate solution (6 minutes) and finally rinsed with tap water. Slides were then counterstained with H&E; then cleared and mounted. Immunohistochemical evaluation was achieved by the utilization of Image J software.

3.3.2 Statistical analysis

All data were analysed using SPSS programme. Data were expressed as mean ± standard deviation (SD). Test and control data were compared using a one way and two way ANOVA, a value of $p < 0.05$ was taken as significant. Most experiments were repeated at least 3 times (n=3).

3.4 RESULTS

Out of the 16 meningiomas, 8 were Grade I and 8 were Grade II. Regarding histological characteristics, the meningioma consisted of microcystic (n=1), meningothelial (n=4), transitional (n=2), atypical (n=5), choroid (n=1), benign (n=1) and not stated (n=2). In Grade I meningioma samples, there is a 1:7 male to female ratio in comparison to Grade II with a 3:5 split.

In the current study, the meningioma tissues were evaluated for the expression of several key enzymes involved in the tumourigenic phenotype during metabolic reprogramming namely; p53, PKM2, fascin and PHGDH. The positive expression of PKM2 and PHGDH would indicate a metabolic swift from glycolysis to serine biosynthesis. The association of such antibody expressions via IHC evaluation was correlated per meningioma grade (I and II) as well as histological variance. The expression profiles of each antibody was measured in the immunohistochemical study, Figures 3.2 and 3.3 demonstrate the staining of such antibodies in the meningioma tissues. The full photographic visualization of all the tumour sections stained are shown in Appendices 5- 20.

X10 magnification   X40 magnification   X10 magnification   X40 magnification

X10 magnification   X40 magnification   X10 magnification   X40 magnification
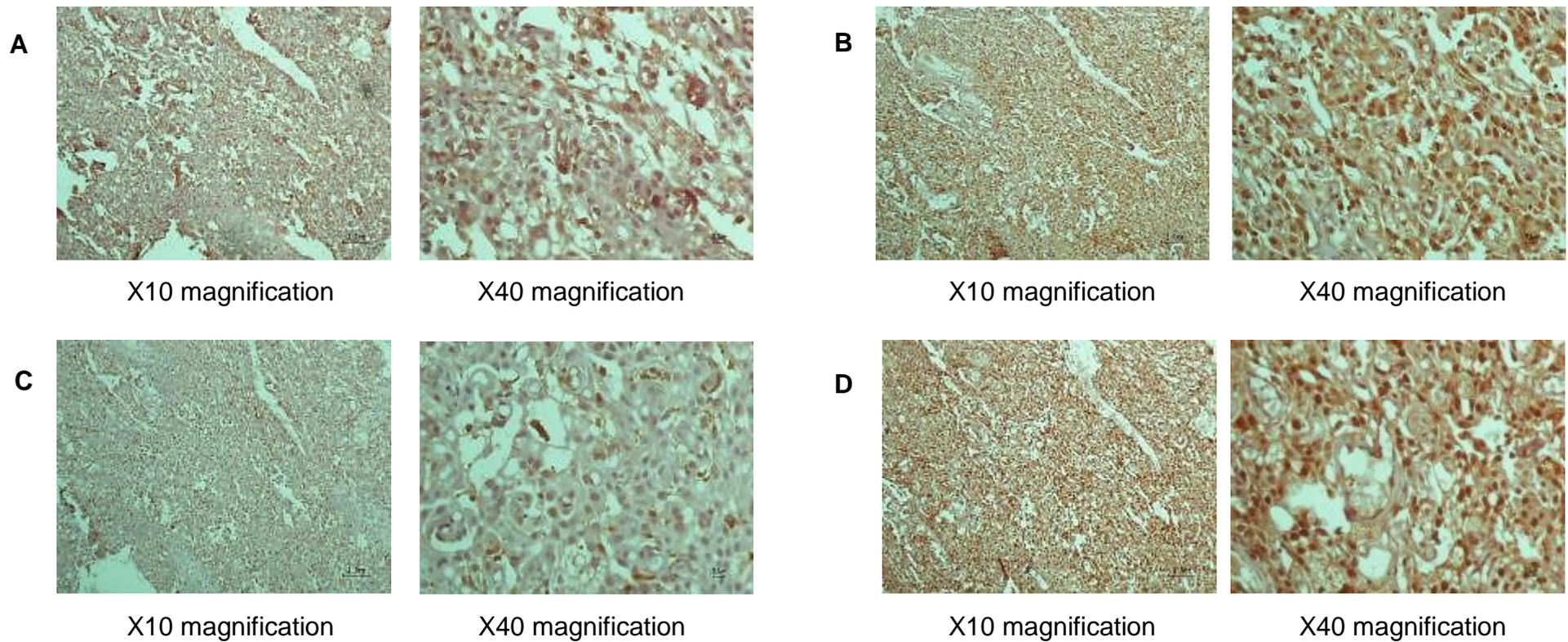
Figure 3.2: Photographic visualisation via light microscopy of the immunohistochemistry antibody expression profiles associated with serine biosynthetic and glycolytic pathways in the tissue sections belongings to patient 1, a grade I meningioma patient (n=1). Antibodies of stained for include; p53 (A), PKM2 (B), Fascin (C) and PHGDH (D). Incubation with DAB (6 minutes) enables the antibody presence, appears brown. H&E counterstain followed DAB incubation, appearing blue in color allowing indication of cellular bodies.

To determine the antibody expressions within meningioma, all patient sets were collated indifferent of grade and variance. The expression profile was determined using Image J software. A summary of the results are shown in Figure 3.3.

Hypothesis

Null Hypothesis: There cannot be a serine-directed metabolic flux profile displayed in the meningioma grade I and grade II tissues.

Hypothesis: There can be a serine-directed metabolic flux profile displayed in the meningioma grade I and grade II tissues.

A) Meningioma antibody expression profiles of p53, PKM2, fascin and PHGDH.
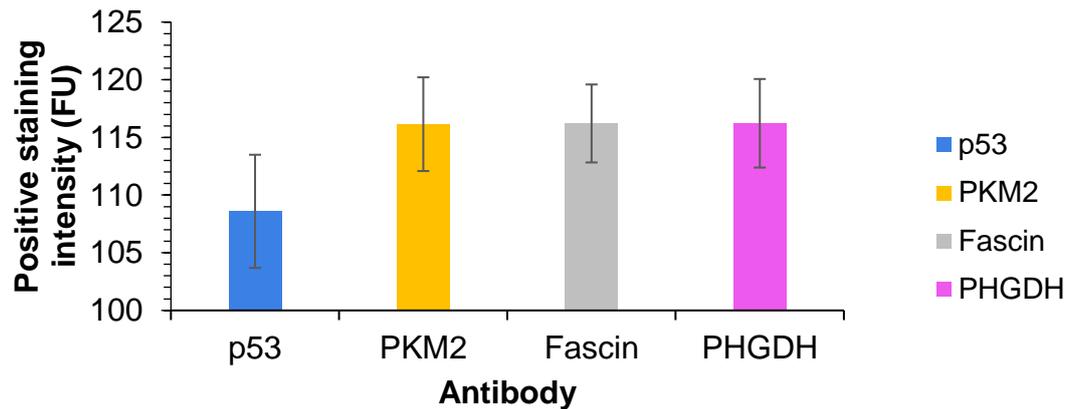
B) Meningioma cellular abundance of p53, PKM2 and fascin PHGDH.
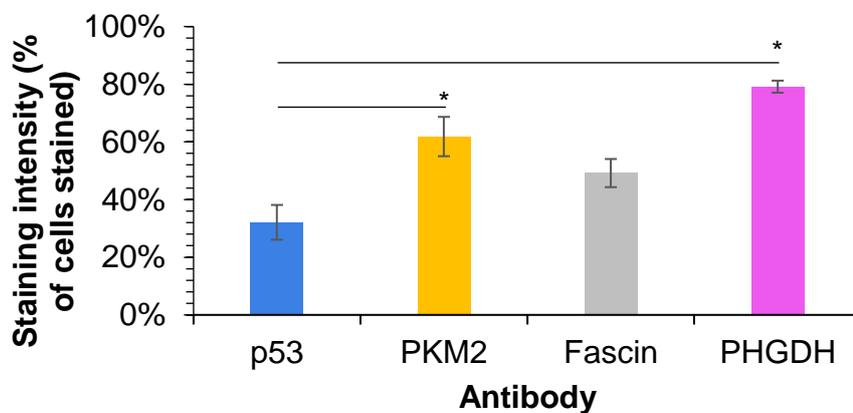
C) Meningioma antibody expression profile of p53, PKM2 and fascin PHGDH.
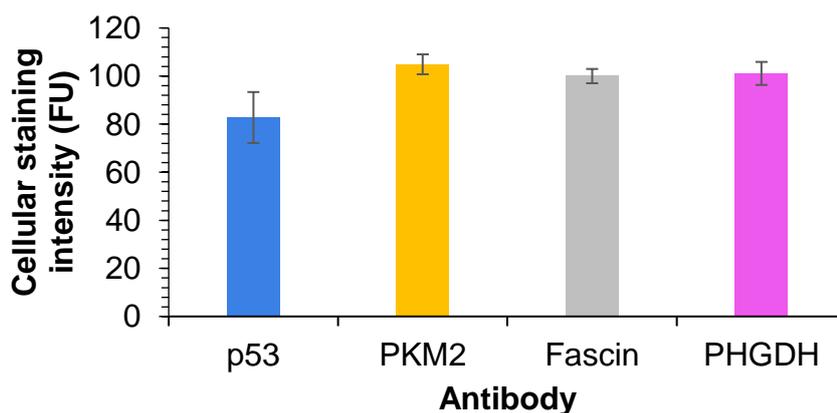
Figure 3.3: Bar charts showing a summary of the immunohistochemistry antibody expression profiles in the meningioma tissues using light microscopy (x40 magnification). Expression profiles shown for: positive expression (A), abundance of positivity within the cellular bodies (B) and the intensity of the cellular body positive expression (C). All data are mean ± SD, n=16; an ANOVA statistical analysis compared enzyme expressions within the meningioma tissue sections; $p < 0.05$ showed significance. **Legend:** fluorescent unit (FU).

The immunohistochemistry profiles shown in Figure 3.3 of the meningioma sections demonstrate the positive presence of all the enzymes examined including p53, PKM2, fascin and PHGDH. To establish whether meningioma tissue sections can be classified further using expression profiles surrounding serine biosynthesis, a methodological optimization using Image J software was carried out. Firstly, the positive stain intensity of the tissue sections was viewed and subsequently examined at x40 magnification using the Image J software (Figure 3.3, A). By doing so, an area of the tissue section was analyzed positive staining of p53, PKM2, fascin and PHGDH by using the software. A one-way ANOVA between the antibody groups was conducted to compare their staining intensity within all the meningioma patients, irrespective of grade. However, there was no significant effect between the antibodies examined, $F = (3, 50) = 0.7349$, $p = 0.5362$.

To gain a better insight and understanding into staining location within the meningioma tissue sections, they were then examined for the abundance of antibody presence within cellular bodies (Figure 3.3, B). A one-way ANOVA analysis was carried out to compare if the positive cellular abundance was antibody specific. The statistical test showed a significant difference between the antibodies measured and their cellular abundance, $F = (3, 50) = 7.450$, $p = 0.0003$. Specifically, between the high abundance of PKM2 ($p<0.01$) and PHGDH ($p<0.001$) compared to that of p53 within the cellular bodies.

By using the Image J software, these cellular bodies were then examined for their staining intensity of the antibodies examined. However, as shown in Figure 3.3 (C), there was not a significant difference between the intensity of the antibody profile within the cellular bodies of the meningioma tissue sections, $F = (3, 50) = 1.979$, $p = 1.291$.

To gain a better insight into whether the *de novo* serine biosynthesis via glycolysis diversion is altered in meningioma, the antibody profiles previously collated

together in Figure 3.3 have been examined per grade of meningioma and summarized in Figure 3.4 (A-C).

Hypothesis

<u>Null Hypothesis:</u> There cannot be a serine-directed metabolic flux profile displayed in meningioma grade I tissues and meningioma grade II tissues.

<u>Hypothesis:</u> There can be a serine-directed metabolic flux profile in both meningioma grade I tissues and meningioma grade II tissues.

A) Meningioma antibody expression profile of p53, PKM2, fascin and PHGDH.
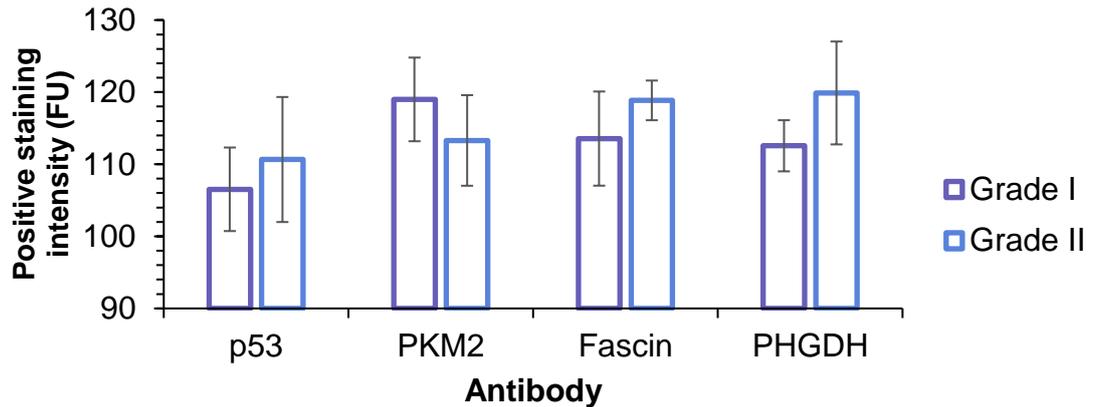
B) Meningioma antibody expression profile, on both x10 and x40 magnifications, examining p53, PKM2, fascin and PHGDH.
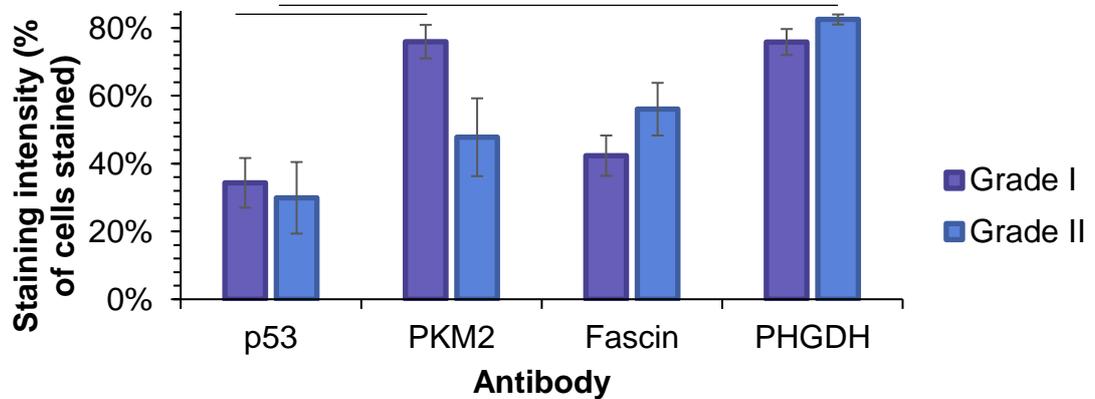
C) Meningioma antibody expression profile, on both x10 and x40 magnifications, examining p53, PKM2, fascin and PHGDH.
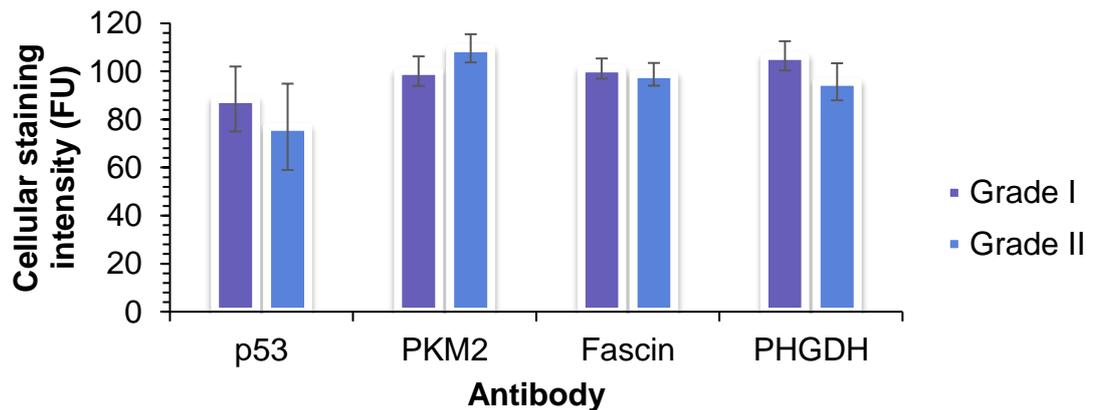
Figure 3.4: Bar charts showing a comparison of the immunohistochemistry antibody expression profiles of meningioma grade I and II tissues. Expression profiles shown for: positive expression (A), abundance of positivity within the cellular bodies (B) and the intensity of the cellular body positive expression (C). All data are mean ± SD, n=8; an ANOVA statistical analysis compared the control with supplemented cultures; $p < 0.05$ showed significance. **Legend:** fluorescent unit (FU).

To establish whether meningioma tissue sections of differing grades can be classified further using expression profiles surrounding serine biosynthesis, sections were analysed per grade (Figure 3.4). Firstly, the positive stain intensity of meningioma grade I and II tissue sections were viewed and subsequently examined at x40 magnification using the Image J software (Figure 3.4, A). A two-way ANOVA between the antibody groups was conducted in comparison to meningioma grade, however, there was no significant ($p > 0.05$) effect between these groups.

To gain insight into the staining location within grade I and II meningioma tissue sections, samples were then examined for their antibody abundance within cellular bodies (Figure 3.4, B). A two-way ANOVA analysis was carried out to compare if the positive cellular abundance was antibody and grade specific. The statistical test showed a significant difference between the grade of meningioma and the cellular abundance of antibodies measured; $F = (7, 46) = 4.573$, $p = 0.0006$. There was a significant increase in the abundance of PKM2 ($p < 0.05$) in comparison to p53 in grade I meningioma tissue sections. Whereas, in grade II meningioma tissue sections, there was a significant increase between the abundance of cellular body abundance of PHGDH staining compared to PKM2 ($p < 0.05$).

By using the Image J software these cellular bodies were then examined for their staining intensity of the antibodies examined. However, as shown in Figure 3.4 (C), there was not a significant difference ($p > 0.05$) between the intensity of the antibody profile within the cellular bodies of grade I and II meningioma tissue sections. From the data displayed in Figure 3.4, the null hypothesis can be rejected and the alternative hypothesis accepted. To examine if there is a correlation between meningioma histological grade and glycolytic diversion to support *de novo* serine biosynthesis, the enzyme profiles of p53, PKM2, fascin and PHGDH were collated and summarized in Figure 3.5.

Hypothesis

Hypothesis: There can be different serine-directed metabolic flux profiles displayed in the various histological meningioma variants.

Null Hypothesis: There cannot be different serine-directed metabolic flux profiles displayed in the various histological meningioma variants.
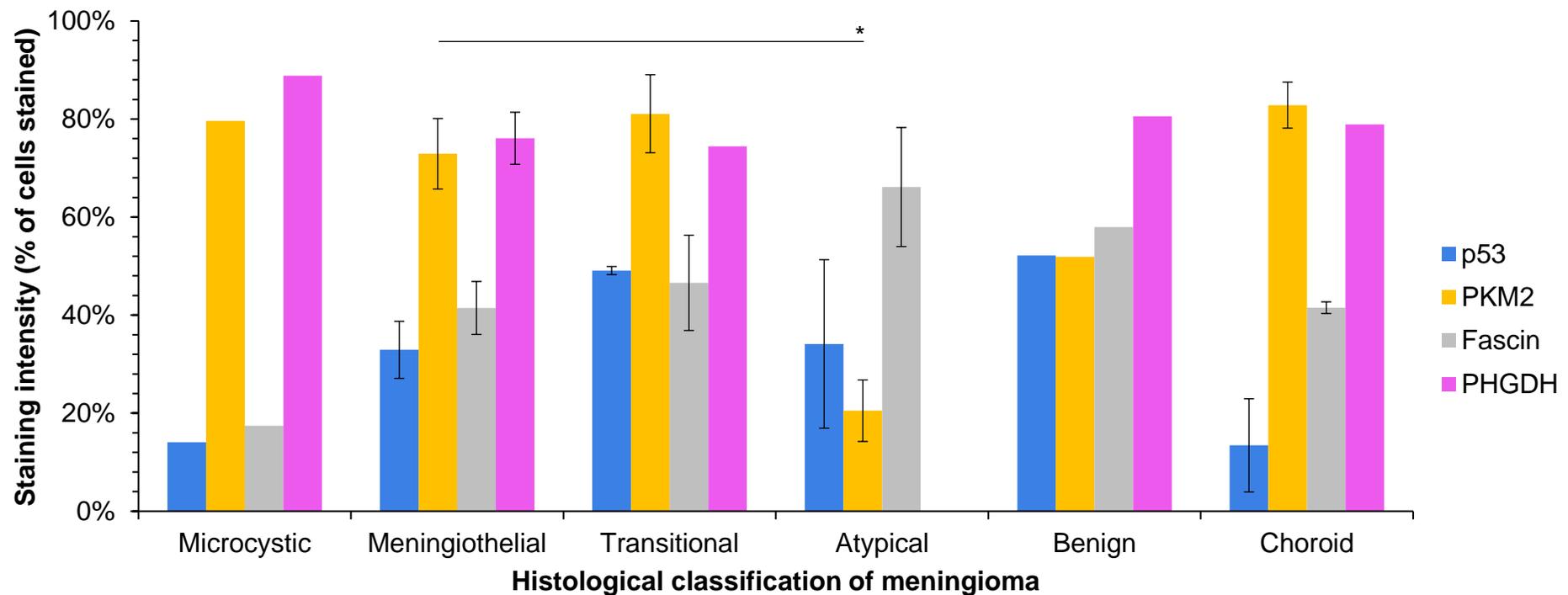
Figure 3.5: Bar charts showing a comparison of the immunohistochemistry antibody expression profiles of meningioma tissues of various histological variance namely; microcystic (n=1), meningiothelial (n=4), transitional (n=2), atypical (n=5), benign (n=1) and choroid (1). Expression profiles shown for the abundance of positivity within the cellular bodies. All data are mean ± SD an ANOVA statistical analysis compared the expressions of p53, PKM2, PHGDH and fascin; p<0.05 showed significance.

From the 16 meningioma tissues examined, the histological variants included microcystic (n=1), meningothelial (n=4), transitional (n=2), atypical (n=5), choroid (n=1), benign (n=1) and not stated (n=2). Figure 3.5 summarizes the immunohistochemical profile of p53, PKM2, fascin and PHGDH across these meningioma variants in grade I and grade II meningioma. The expression of p53 was shown in all of the meningioma variants apart from patients 99, 286 and 395 which were of varying histological variance; meningothelial, choroid and atypical.

From Figure 3.5, an immunohistochemistry profile specific to meningioma variants are demonstrated. For example, the expression profiles of microcystic, meningothelial, transitional and choroid meningioma variants show the same overall trend in the abundance of positivity; increased PKM2 and PHGDH compared to that of p53 and fascin expression. However, in the atypical and benign variants of meningioma, the relationship between the antibodies are different to the other histological variants displayed.

Taking a closer look at the expression profiles displayed in Figure 3.5, there is a strong positive correlation shown between the expressions of PKM2 and PHGDH in the following meningioma variants; microcystic, meningiothelial, transitional and choroid. Interestingly, benign and atypical meningioma variants demonstrated a reduction in PKM2 expression compared to the other variants examined.

In order to establish whether meningioma tissue sections of differing histological variance can be classified further using expression profiles surrounding serine biosynthesis, a two-way ANOVA test between the antibody groups was conducted in comparison to the histological variant. However, due to the sample set, only a statistical analyse between atypical and meningiothelial meningioma tissue sections were carried out. The two-way ANOVA analysis showed a significant difference between the histological variant of meningioma and the cellular abundance of antibodies measured; $F = (5, 23) = 3.515$, $p = 0.0266$. There was a significant increase in the abundance of PKM2 ($p<0.05$) within

meningiothelial tissue sections as opposed to PKM2 within atypical. From the data displayed in Figure 3.5, the null hypothesis can be rejected and the alternative hypothesis accepted.

3.5 DISCUSSION

Metabolic reprogramming is a recognized hallmark in tumourigenesis (Hanahan and Weinberg, 2011). The ability of a cell to produce lipids, nucleic acids and proteins is thought to be the limiting factor in the ability of cancerous cells to proliferate. Despite the numerous studies of the fundamental hallmark of metabolic reprogramming in tumours, such metabolic alterations have not yet been confirmed in meningioma. Since PHGDH diverts glycolysis to produce serine via the *de novo* serine biosynthetic pathway, it may act as an initiator of serine production in meningioma tumours. Serine biosynthesis in tumours is essential for the production of lipids, secondary messengers and proteins; aiding cellular survival (Amelio et al., 2014b). The expressions of several key enzymes involved in tumourigenesis and serine biosynthesis namely, PKM2, p53, fascin as well as PHGDH were determined in meningioma grade I and grade II tissues to see if there was a histological correlation with histological grade and/or variant.

In this Immunohistochemical study, the expression of PHGDH was high in meningioma and indifferent of grade and variant examined (Figures 3.2-3.5). The meningioma patients with the highest PHGDH expression tended to have grade I (Figure 3.4). Moreover, this study demonstrated that the high levels of PHGDH were associated with the positive expression of PKM2, fascin and p53 in tissue matched meningioma sections (Figure 3.2-3.5). Additionally, there was a positive correlation between the PHGDH and PKM2 expression profiles; indifferent of grade and variant type.

3.5.1 Diversion of glycolysis to serine biosynthesis

Several studies have associated the levels of PHGDH expression found in tumours with the promotion of serine biosynthesis (Possemato et al., 2011; Locasale et al., 2011). A recent study by Liu et al. (2015) using isotope labelling provided an insight into the influence PHGDH upon colorectal cancer in terms of cellular metabolic flux from glycolysis towards serine biosynthesis. Hence, demonstrating the importance of PHGDH within cancerous cells for serine

biosynthesis. Within meningioma, PHGDH expression was found within grade I and grade II tissue sections; 75% and 82%, respectively (Figure 3.4).

3.5.2 Tumourigenesis aided by heightened PHGDH expression

The positive expression of PHGDH in grade I and II meningioma, might not only be linked with just *de novo* serine biosynthesis since other studies have implicated PHGDH expression with several other cancerous attributes. In a study by Liu et al. (2015), there was a paralleled relationship between the cancerous cell protein levels and PHGDH expression. Furthermore, there have been positive correlations between those breast cancers, which are ER-negative displaying heightened PHGDH expression. There have also been studies showing the association of malignant transformation in those tumours with PHGDH expression, due to the maintenance of an anchorage-dependent fashion of their proliferation Liu et al. (2015). Therefore, the positive expression observed in the grade I and II meningioma tissue sections may also be associated with other tumourigenic factors including protein synthesis, endoplasmic reticulum status of the tumour and an indicator of malignant transformation. This may be an indicator of tumour transformation in the grade I meningioma tissues which showed an increased PHGDH expression compared to grade II (Figure 3.4).

3.5.3 Relationship between glycolysis and serine biosynthesis

The diversion of glycolytic intermediates into the *de novo* serine biosynthesis pathway via PHGDH has been displayed in this study (Figures 3.2-3.5). To fully appreciate the relationship of the diversion from glycolysis to serine production, the glycolytic flux was also examined via the expression of PKM2. In this Immunohistochemical study, the positive expression of PKM2 was shown in 100% of the meningioma tissue sections examined varying from 7% positive presence to 92% presence. From Figure 3.4 the expression of PKM2 was shown to be indicative of grade and an indicator of histological variance (Figure 3.4). The meningioma patients with the highest PKM2 expression tended to have meningioma grade I (Figure 3.5). The comparison of PKM2 expression and histological variant demonstrated the meningiothelial, transitional and choroid tissues to contain over 70% positivity over the tissue section compared with

atypical meningiomas which only displayed 20% tissue section positivity for PKM2 (Figure 3.4). Moreover, this study demonstrated a paralleled relationship between PKM2 and PHGDH expression in the meningioma tissues specifically; meningiothelial, transitional and choroid variants (Figure 3.5). These data suggest a possible synergistic relationship between glycolytic flux and *de novo* serine biosynthesis within these meningioma tissues.

3.5.4 Relationship between glycolytic flux and *de novo* serine biosynthesis

One avenue, which might explain the increased expression of PKM2 in the meningioma tissues examined, may be due to their proliferating cancerous nature. Studies have shown that the M2 isoform of pyruvate kinase is expressed in proliferating cells (Dong et al., 2016). It is thought that this switch to the M2 isoform from the M1 pyruvate kinase isoform is initiated during transformation. Therefore, alongside the PHGDH expression demonstrated in the meningioma tissues, the heightened PKM2 presence may also be indicative of tumour transformation.

The switch between the pyruvate kinase isoforms can affect the rate of enzymatic activity in glycolysis. For example, the M2 isoform has a lower conversion rate of phosphoenolpyruvic acid (PEP) to pyruvate compared to the M1 isoform. Hence, it can be postulated that in PKM2 positive meningioma, tissues have a reduced conversion rate of PEP to pyruvate. Because of the reduced flux to pyruvate, glycolytic intermediates may build-up as shown in Figure 3.1. From other studies, it has been shown that these intermediates are diverted into other pathways including the pentose phosphate pathway (PPP) and serine biosynthesis. Therefore, the observation of positive correlations of PKM2 and PHGDH expressions in the meningiothelial, transitional and choroid meningioma variants may be indicative to the build-up of glycolytic intermediates because of the switch to the M2 pyruvate kinase isoform. The expression of PKM2 rather than PKM1 may then lead to the diversion of glycolytic intermediates into the *de novo* serine biosynthesis pathway, which is enabled by the rate-limiting enzyme PHGDH for which the meningioma tissues have shown positive expression.

3.5.5 Serine presence alone can regulate PKM2 activity

Another avenue to consider is the ability of serine presence alone to allosterically regulate PKM2 activity (Chaneton et al., 2012). Such studies have shown that with serine availability, PKM2 activity is facilitated, whereas during states of serine depletion, PKM2 activity is reduced. This mechanism of allosteric regulation therefore suggests that the meningioma tissues could contain high levels of the non-essential amino acid which in turn enables aerobic glycolysis and lactate production, both of which are vital for cell growth and survival. It has also been shown that the nutrient status of the cell, including that of serine, can affect tumour suppressors, including p53.

3.5.6 p53 response to serine

Studies are highlighting the implication of tumour suppressors regulating cellular metabolism, therefore p53 expression was examined across the meningioma grade I and grade II tissue sections. Alongside its role as a tumour suppressor, p53 has been implicated in several cellular processes, which occur in both non-cancerous and cancerous cells including stress responses associated with hypoxic conditions and DNA damage (Pflaum et al., 2014). Furthermore, studies have associated the cellular status of serine cellular to the activation of the cellular stress response, which is aided by p53. In one study, p53 was shown to respond to serine starvation by enabling the cellular antioxidant capacity therefore aiding cellular viability and proliferation (Maddocks et al., 2013).

In this study, p53 expression was found to be indicative of meningioma histological variance, especially between meningiothelial, transitional and choroid variants that displayed positivity of 33%, 49% and 14%, respectively (Figure 3.5). This therefore suggests, in terms of serine status, that meningioma tissues have metabolically adapted to counteract reactive oxygen species produced under such metabolic stress as serine depletion. The notion of cancerous cells protecting themselves from such metabolic stress fits in with observations of the Warburg effect, which would avoid metabolic reactive oxygen species (ROS) from

being produced. Therefore, with the presence of p53 in 80% of the meningioma tissues examined, it would appear that the implication of tumour suppressor involvement with metabolic stress due to serine depletion may be indicated as the non-essential amino acid plays an important role in cellular processes within these tissues. To assess the proliferative nature as well as nutrient supply into the tumour, the enzyme expression profiles of fascin were undertaken in the meningioma tissues.

3.5.7 Promotion of angiogenesis aids serine supplies

Meningioma by nature is a tumour with good blood supply. To gather the proliferative nature of the tumour in addition to its exposure to a blood supply would provide insight into the cellular status and nutrient availability. Fascin expression has been previously shown to promote cancer progression in breast and pancreatic cancer (Xing et al., 2011; Li et al., 2014a). The expression of fascin within meningioma was indicative of the histological variance of the tissue; especially between the transition, meningiothelial and choroid variants (Figure 3.2-3.5). Hence, fascin expression may be used as an indicative marker of meningioma histological variance, which in turn, related to the tumours progression.

3.6 CONCLUSION

In conclusion, the result of this chapter of the thesis has clearly demonstrated the presence of enzymes involved in the diversion of glycolysis to serine biosynthesis.

Chapter 4

Preliminary study into the effect of tumour-derived liposomes upon cellular viability

4.1 INTRODUCTION

One highly researched area of drug-delivery now surrounds the blood-brain barrier (BBB). As previously, discussed in Chapter 1, the blood-brain barrier is tightly regulated in the body ensuring that the conditions for optimum neuronal function are maintained in the brain. However, in brain pathologies, including that of Alzheimer's disease, the BBB is observed to be dysfunctional (Chakraborty et al., 2017; Zenaro et al., 2016). The dysfunctional BBB observed in Alzheimer's disease leads to the entry of substances, which were previously prevented access. Due to the observed increase of undesirable substances crossing the BBB, non-optimum conditions for neuronal functions are met. Because of the dysfunctional control of substances crossing the BBB, inflammatory responses are activated which lead to neuronal damage.

The inaccessibility of drug-delivery into the brain, via the blood brain barrier, has somewhat hindered therapeutic advances. To overcome such inaccessibility to the brain, research has focused on novel treatment avenues with the aim of crossing the BBB. This idea of specific drug-delivery was described as far back as the 1900s by Paul Ehrlich (Tavano and Muzzalupo, 2016). Since then, several studies have used an array of therapeutic delivery models however, due to their rapid clearance and toxicity these therapeutic avenues were without success (Spencer and Verma, 2007; Banks, 2009). Subsequently, a new delivery models that can cross the BBB are still sought. One potential avenue is the utilization of lipids, specifically that of phospholipids, which have several appealing characteristics for the foundation of a drug-delivery model.

4.1.1 Drug-delivery system: model concepts

The design and production of an efficient therapeutic delivery system is based on the foundations that the drug-delivery system can do the following by: 1) increase drug bioavailability; 2) control and maintain the delivery to the site of action and 3) avoid non-diseased tissues (Sun et al., 2017). Several carrier systems currently researched include the utilization of phospholipids. One of the desirable

traits of phospholipids is their biocompatibility in the mammalian system making them an ideal drug-delivery system (Isaac et al., 2006; Yamashita et al., 2014).

4.1.2 Liposomes

In 1965, Alec Bangham described the use of phospholipids in a drug-delivery system referring to them as liposomes (Deamer, 2010). The advantage of using phospholipids in a drug-delivery model is that the mammalian biological membranes mainly consist of phospholipids. Liposomes are structurally like biological membranes as they are comprised of phospholipids in either a mono- or bilayer arrangement. One of the main advantages of using phospholipids in a drug-delivery system is their amphiphilic nature in aqueous environments, resulting in the formation of spherical shells. The desired drug can then be carried either within the spherical shells' aqueous core and/or within the phospholipid layer itself (Calandra et al. 2015).

The liposome drug-delivery model has demonstrated several positive attributes they include: (a) prolonged blood circulation therefore drug bioavailability to the specific site of action, (b) tumour site accumulation observed aiding specific drug-delivery to cancerous cell, (c) ligands enable site-specific recognition to the cancerous cells' surface providing a therapeutic dose of the drug and, (d) the ability of the liposomes to entry the cancerous cells via peptide channels enables drug-delivery.

4.1.3 Liposomes as an anti-tumour therapy

During disease states, both the size of the pores and the permeability of the blood-brain barrier are observed to be increased in line with enhanced vasculature permeability (Azzi et al., 2013). The increased permeability has been postulated to be related to the angiogenic switch in many solid tumours, including that of glioma (Ribatti, 2014; Xu et al., 2016). As a result of this increased permeability, the observed range of pore size diameter are increased to ranges between 100- 780 nm in solid tumours (Wang et al., 2011). Studies using drug-encapsulated liposomes of a diameter ranging between 60- 500 nm have shown

an accumulation of these liposomes at the tumour site (Bozzuto and Molinari, 2015). Subsequently, the drug is delivered to the tumour cells more specifically aided their effectiveness.

Once the liposome has reached the site of action, it then has to interact with the cell to release the drug for the end result i.e. anti-proliferative effect. There are several ways a drug-encapsulated liposome can bind onto the cell surface they include receptors activation, electrostatic interaction, incorporation of the drugs via endocytosis and, incorporation of the liposomal membrane into the cellular membrane facilitating the drug into the cell. The ability of the drug in the liposome to interact with the cell is because of the presence of lipases, which degrade the membrane of the liposomes allowing the release of the drug into the extracellular fluid. In this way, not only does it prevent clumping of cells due to the repulsion of cellular charge and drugs, but also the uptake of the drug via receptors into the cells (Bozzuto and Molinari, 2015).

4.1.4 Other applications

The amphiphilic nature of phospholipids has also given rise to other model systems including the use of blood cells specifically; erythrocytes as a potential drug-delivery carrier system. Generally, blood cells have several appealing advantages as a model drug-delivery system these include; long circulation, natural adhesion and targeted release. However, even taking these advantages on board, the storage and mass production required of such blood cells would potentially hinder such a concept. Many studies have used blood cells to investigate the potential use of these as a drug-delivery system (see Sun et al. 2017 for a detailed review). By using the amphiphilic nature of the phospholipids, a variety of drug classes have been encapsulated into these erythrocyte-based carriers including, but not restricted to; anti-cancer agents, anti-inflammatory agents, anti-infective agents, cardiovascular agents and immunosuppressive agents (Jin and Jiang, 2002; Staedtke et al., 2010; Alanazi et al., 2011; Harisa et al., 2012; Biagiotti et al., 2011).

The utilization of erythrocytes has also been expedited more recently in other research avenues. A review by McNeil and Steinhardt (2003) described the ability of the erythrocyte membrane to re-form. Researchers use this ability of the erythrocyte membrane to, repair after disruption (haemolysis) to produce ghost cells. After which, these ghost cells can be adapted to act as a circulatory 'sponge' absorbing specific pore-forming toxins from the circulation. These are now known as nanosponges (Hu et al., 2013). One study by Chhabria and Beeton (2016) employed this concept using ovine erythrocytes as a model system which would absorb the pore-forming toxin, streptolysin-O, which is observed in individuals suffering from sepsis.

Therefore, with such combinations, there are potential phospholipid-based drug-delivery systems exist, with varying combinations of head group and molecular species (saturated and unsaturated). Therefore, the characteristic of the liposomes produced can reflect the properties of the phospholipids themselves (Calandra et al. 2015). Furthermore, phospholipids used in formulations can either be gathered from natural or synthetic sources from a research perspective, naturally sourced phospholipids are lower in cost. Due to the desirable characteristics phosphatidylcholine possess, many carrier systems use this as their structural foundation (Li et al., 2015).

Over the past few years, the focus of cancer therapy research has aimed to minimize the associated side effects of anti-tumour drugs i.e. chemotherapy alongside increasing its' clinical therapeutic index. Due to chemotherapies focus on high proliferating cells, a low specificity to the tumour site is often observed. Subsequently, higher chemotherapy doses are required across multiple sessions leading to multiple adverse side effects. Therefore, a more specific drug-delivery system, a magic bullet, to the designated tumour site has been sought. In this study therefore the aim was to investigate whether the lipid profile of a cell can support its cellular viability as per shown in cancerous cells.

4.2 MATERIALS AND METHODOLOGY

4.2.1 Materials

Cells used in this part of the study include U87-MG and SVGp12. Media used for cell line maintenance and growth curve initiation was Eagle's Minimum Essential Medium (EMEM) (Lonza). Additional supplementations as per cell line, as recommended by ECACC and ATCC comprised of; Fetal Bovine Serum (FBS) (10%, w/v), L-glutamine (2 mM), sodium pyruvate (1 mM) and non-essential amino acids (1%, w/v). The basal EMEM was stored at 4°C and replaced every 3 months. Other constituents include PBS and trypsin. See Appendices 3 and 4 for the ethical approval and histological characteristics of the meningioma tissue sections.

4.3 METHODOLOGY

4.3.1 Cell line: Description

The effect of exogenous lipids of varying type and origin upon viability was determined via the utilization of U87-MG and SVGp12 commercial cell lines namely; human glioblastoma astrocytoma epithelial grade IV and human non-tumourigenic, respectively. U87-MG cells are fibroblastic-like cells, which are bipolar in morphology; elongated and bipolar in shape. Contrary to SVGp12, an epithelial-like cell line that is polygonal in morphology. Both were purchased from ECACC and ATCC (UK) with no evidence of infectious viruses present. Cryopreservation of both, are aliquoted and stored in the protective agent, DMSO, in liquid nitrogen; allowing for continual cultured cells to be maintained.

4.3.2 Culture environment

Physiological and physiochemical environment for U87-MG and SVGp12 cell propagation during these studies included EMEM pH of 7.4 with incubator conditions of 37°C and 5% carbon dioxide in air. As both were anchorage-dependent, sub-culturing for growth curves etc. was performed using solid surfaces i.e. T75 flasks etc.

4.3.3 Thawing frozen cells

The frozen aliquots of both U87-MG and SVGp12 cell lines were thawed in a pre-warmed water bath (37°C) and placed in a T75 flask with EMEM (37°C). After 24 hours the media were renewed and DMSO was removed from the cryopreservation media.

4.3.4 Sub-culturing

Sub-culturing aided the space provided in the solid surface, in order to allow adequate nutrient uptake for proliferation. Passaging was performed for both cell lines during log-phase growth. EMEM was removed such that the monolayer of cells could be washed with PBS solution (37°C). Cells were then exposed to trypsin (x1, 37°C) and kept in the incubator (37°C and 5% carbon dioxide in air) for 2-3 minutes. Cellular de-attachment quantity was then visualized under the light microscope (magnification, x40) before the neutralization step of EMEM was initiated (2:1 EMEM to x1 trypsin-EDTA). The cells were then divided (i.e. 1 in 4) into fresh EMEM media (37°C) and kept in the 37°C and 5% carbon dioxide in air incubator in order to generate growth curves (Figure 4.1).
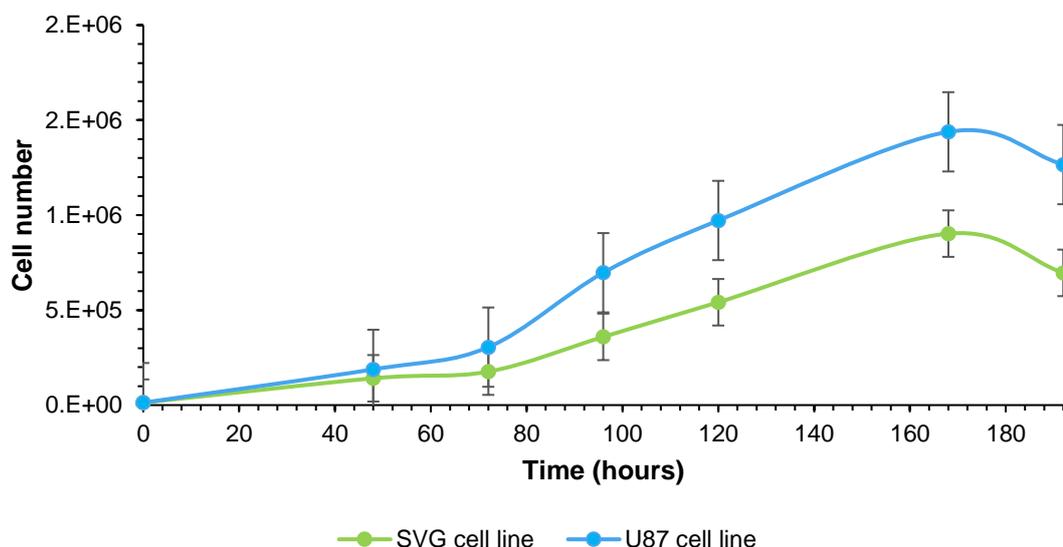
Figure 4.1: Time course graph showing the growth curves of SVG and U87 cell line. **Culture conditions:** cells were kept in a 37°C and 5% carbon dioxide in air incubator. All data are mean ± SD, n=3.

4.3.5 Cell quantification

Cellular quantification of both cell lines were performed in a 1 in 2 dilution of a subculture sample with Trypan Blue. Cells were counted and visualized under a light microscope with a haemocytometer.

4.3.6 Growth curve determination

The U87-MG and SVGp12 cell line growth profile was performed over a 5-day period in a 96 well plate kept in an incubator (37°C and 5% carbon dioxide in air); rate of growth determination. Cells were seeded using (cells/per well); 500, 1000, 2000, 2500, 5000 and 10,000 over this period of time examining affect seeding density on growth to determine optimum. Per 24 hours, cell viability was performed via PrestoBlue assay (see following section).

4.3.7 PrestoBlue: Cell Viability Assay

PrestoBlue Cell Viability Reagent (Thermo Fisher Scientific) was used in the growth profile determination of U87-MG and SVGp12. Varied seeding densities over the 5-day period, as described above was examined to take into consideration the linearity of such an assay in addition to the cell line growth profile. As recommended by Molecular probes by life technologies, each 90 µl well which contained EMEM and cells of a particular seeding density was incubated with PrestoBlue (10 µl) for 10 minutes in an incubator (37°C and 5% carbon dioxide in air). After which, the 96 well plate was bottom-read for fluorescence (535 nm excitation and 612 nm emission).

4.3.8 Tissue lipid extraction

In order to determine the effects upon cellular viability of SVG and U87 cell lines, lipid extractions were performed with various meningioma and glioma tissue of various grade and histological variance (see Appendix 3). The mammalian tissue (75 mg) was reconstituted in pre-heated methanol (70°C) for a period of 30

minutes. After cooling to room temperature, the extract was added to chloroform (4 ml) and 20% sodium chloride (2 ml, w/v). The overall mixture was then vortexed three times and left to stand until two phases formed. The bottom phase was kept and aliquoted into a new vial, which was then blown down under nitrogen gas (40°C) to achieve complete dryness. After which, the lipid film was then reconstituted in 1 ml bovine serum albumin (BSA) buffer (pH 7.4) where the liposomal preparation continued.

4.3.9 Liposomal preparation

After the reconstitution of the sample in BSA buffer (pH 7.4, 1 ml), the sample was subjected to sonication (37°C) and freezing cycles over a period of 90 minutes. To make sure the vesicles were uniform in size, they were then serially extruded through a 400 nm to a 100 nm polycarbonate membrane.

4.3.10 Statistical analysis

All data were analysed using SPSS programme. Data were expressed as mean ± standard deviation (SD). Test and control data were compared using a one way and two way ANOVA, a value of $p < 0.05$ was taken as significant. Most experiments were repeated at least 3 times (n=3).

4.4 RESULTS

To establish whether the tumours lipid composition effects its viability and therefore drug resistance and disease progression, the effect upon U87 and SVG cellular viability was ascertained with various tumour-derived and PC: PS liposomes being supplemented during log-phase growth. Hence, in order to determine the effect upon cellular viability the PrestoBlue cellular viability reagent was utilised. A depiction of the effect upon U87 and SVG cellular viability with various tumour-derived liposomal supplementations after 12-hours incubation are shown in Figure 4.2.

Hypothesis

Null hypothesis: There is no relationship between cellular viability of U87 and SVG cell lines supplemented with tumour-derived liposomes.

Alternative hypothesis: There is a relationship between cellular viability of U87 and SVG cell lines supplemented with tumour-derived liposomes.
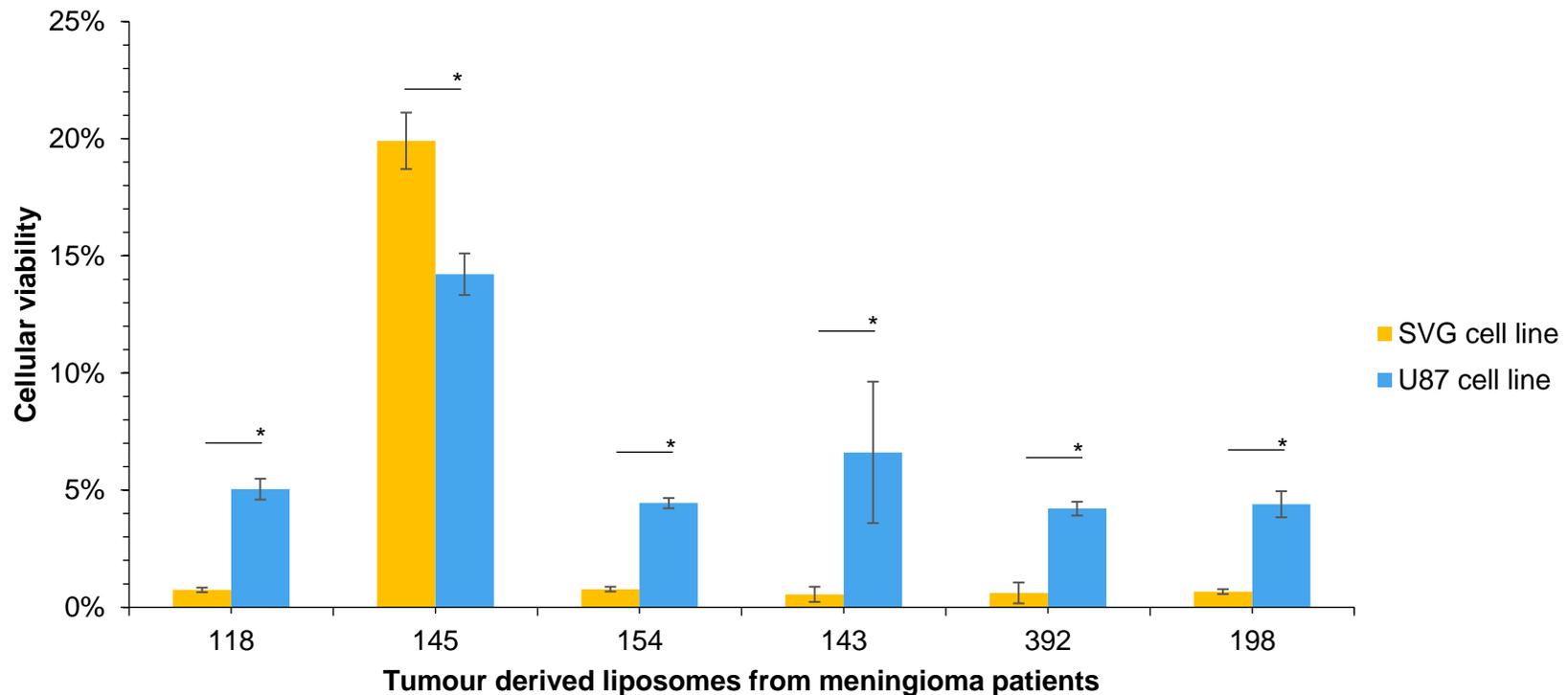
Figure 4.2: Bar chart showing the utilization of a cultured SVG and U87 model system to examine the effect tumour derived lipids upon cellular viability. Tumour derived lipids (from patients 118, 145, 154, 143, 392 and 198) were made into liposomes and supplemented to SVG and U87 cells during log-phase. After 12 hours of liposomal supplementation, PrestoBlue reagent enabled the effect of the tumour-derived liposomal supplementation upon SVG and U87 cellular viability. **Culture conditions:** cells were kept in a 37°C and 5% carbon dioxide in an air incubator. All data are mean ± SD an ANOVA statistical analysis compared the control cell line (SVG) to the cancerous cell line (U87); $p < 0.05$ showed significance.

From figure 4.2, the effect upon cellular viability with the supplementation of tumour-derived liposomes displayed a significant effect on the U87 and SVG cell line depending on the originating patient sample; ANOVA statistical test; $F_{(11, 3)} = 173.83$, $p < 0.001$. From Figure 4.2, 5 out of the 6 liposomal preparations showed a significant increase in the viability of the log-phased U87 cells ($p < 0.001$) compared to the control cell line, SVG. The liposomal preparation which significantly enhanced the cellular viability of the SVG cell line by a third ($p < 0.001$) as opposed to the SVG cell line, originated from a meningioma grade I patient (145).

From previous research by Hill (2011), it was observed that meningioma grade II had an increased abundance of PS with enriched DHA. To examine the effect of PS upon cellular viability, a range of PC: PS liposomes were prepared and supplemented in the log-phased U87 and SVG cultures. The results of the affect PC: PS derived liposomes upon log-phased SVG and U87 cellular viability is shown in Figure 4.3.

Hypothesis:

Null Hypothesis: There would be no difference in U87 and SVG cellular viability with various PC: PS-derived liposomal supplementations.

Alternative Hypothesis: There would be a difference in U87 and SVG cellular viability with various PC: PS -derived liposomal supplementations.
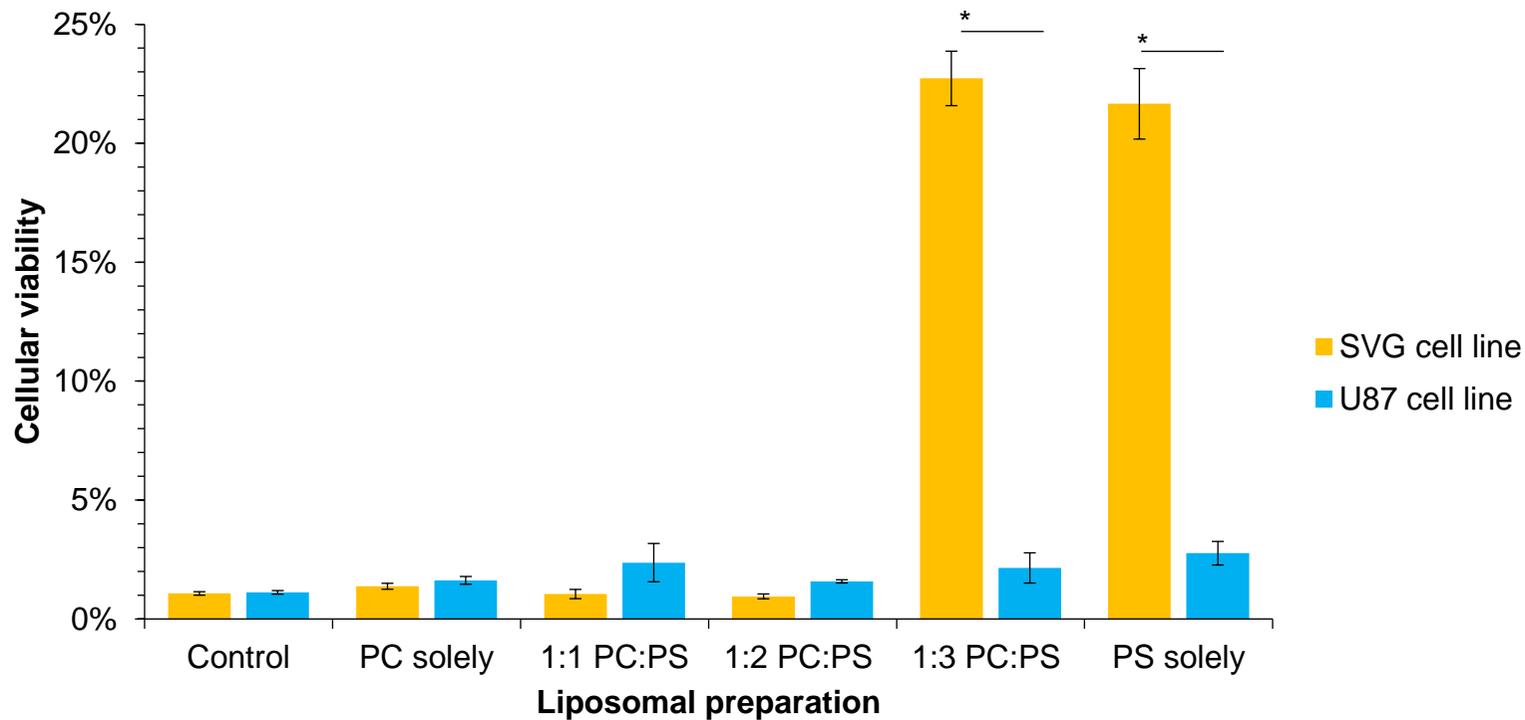
Figure 4.3: Bar chart showing the utilization of a cultured SVG and U87 model system to examine the effect of log-phase supplementation of PC:PS liposomes of various concentrations upon cellular viability. PrestoBlue reagent enabled the effect of the liposomal supplementation upon SVG and U87 viability to be determined, after the 12 hours of liposomal supplementation. **Culture conditions:** cells were kept in a 37°C and 5% carbon dioxide in air incubator. All data are mean ± SD an ANOVA statistical analysis compared the control cell line (SVG) to the cancerous cell line (U87); $p < 0.05$ showed significance.

From figure 4.3, the effect upon cellular viability was aided by the liposomal supplementation of various PC and PS content. The repeated measures ANOVA determined that the cellular viability was significantly affected by the liposomal preparation which was supplemented to the cell lines; $F_{(11, 3)} = 576.39$, $p < 0.001$. As shown in Figure 4.3, as the ratio of PS in the liposomal preparation increases, the greater the increase in SVG viability during log phase ($p<0.001$). The cellular viability of the SVG cell line, increased as the proportion of PS within the liposomal preparation increased ($p<0.001$).

Overall, the results show how the cellular viability can be affected with liposomal supplementation. Interestingly, the tumour-derived liposomes positively affected the cellular viability greater in the SVG and U87 cell lines, compared to the manufactured PC: PS liposomes.

4.5 DISCUSSION

In order to gain an insight and an understanding into the potential affect an altered membrane composition may give cancerous and non-cancerous cells in terms of cellular viability; liposomes of various origin were prepared. The scientific reasoning behind this has been shown in previous research by Sleight and Pagano (1985) whereby lipid-rich media led to an altered cellular lipid biochemistry, suggesting that the membrane composition may be transformed.

4.5.1 Liposomal preparation and supplementation

There were several parameters to consider during this preliminary study including: the particle size, particle shape and surface charge which can all affect the liposomal interaction with the cell surface of the U87 and SVG cells. Due to the amphiphilic nature of phospholipids they produce differing liposomal shapes when they are comprised of particular lipids; cylinder (PS/PC), cone (PE/ cholesterol) and inverted cone (sphingomyelin) (Peetla et al., 2013). The various liposomal shapes are due to the differing phospholipid head size and tail present in the membrane. To enable liposomal uniformity, a method of serial extrusion from a 400 nm to a 100 nm polycarbonate membrane was implemented. As a result, the stability of particle size was maintained at 37°C during the study. This is of benefit, as studies have shown that liposomal phospholipids can be incorporated into the nuclear membrane, mitochondria and the golgi apparatus at 37°C using a fluorescence probe (Sleight and Pagano, 1985).

Membrane biosynthesis in cancer cells is upregulated as a result of the increased rate of fatty acid biosynthesis (Currie et al., 2013). The upregulation of fatty acid biosynthesis enables the cancerous cell to proliferative at a faster rate (Rashid et al., 1997). Studies by Spector et al. (1980) demonstrated how mammalian cells in culture have the capacity to uptake lipids from the culture medium which in turn was observed to alter the lipid biochemistry of the cell. Hence, in this preliminary study, liposomes were supplemented during the log phase of the SVG and U87

cellular growth where the chances of uptake by the nutrient-demanding cells would be greatest.

4.5.2 Liposomal supplementation and cellular viability

The phospholipid bilayer of mammalian cells houses not only phospholipids but also receptors, transporter and membrane-bound enzymes (Spector and Yorek, 1985). Lipids are classed as primary and secondary messengers (van Meer et al., 2008). Therefore, any changes in phospholipid cellular membrane composition may affect cellular biological properties. During this preliminary study, cellular viability was shown to be affected by liposomal supplementation (Figure 4.2 and 4.3). This may be due to the lipid membrane composition alteration of the U87 and the SVG cells by the incorporation of the liposomal phospholipids and/or by the cell death mechanisms being altered as a result of the treatment.

Cultured cells have previously been supplemented with lipids, which have resulted in a cellular membrane profile alteration. Spector and Yorek (1985) discussed studies which had utilized cells in culture and which upon serum supplemented, the cellular membrane displayed a differing PUFA cellular membrane content compared to those cells which had no serum supplementation in the medium. Other studies have also postulated the idea of modifying cellular phospholipid membranes by the observations of 20-30% of the unilamellar vesicle-derived phospholipids remaining in the cellular membrane (Spector and Yorek, 1985). Therefore, in this preliminary study, it can be suggested that some of the phospholipids from the liposomal preparations, whether from the tissue or from the synthetic formulations were incorporated into the U87 and SVG cell phospholipid membranes. Subsequently, properties associated with the fluid mosaic model could have been affected leading to the increased cellular viability observed as a result.

4.5.3 Membrane fluidity, ratios of omegas and cellular viability

Alongside the observation the present results have shown that the lipid composition could be modified with serum enriched PUFA. Another consideration was examined further, as per discussed by Liu et al. (1994), whereby the ratio of the omegas upon membrane composition was determined. Subsequently, it was shown that differing omega -3 and -6 ratios, affected the efficiency of the membrane transporters due to altered membrane fluidity. Thus highlighting, as the ratio of phospholipid chain length increases alongside the proportion of those unsaturated the membrane fluidity increases (Spector and Yorek, 1985). The fluidity of the plasma membranes has been used as a prognostic factor in lung carcinoma patients, whereby those with increased plasma membrane fluidity have a poorer prognosis (Sok et al., 2002). Therefore, the differing effects of particular tumour-derived liposomes upon SVG and U87 cellular viability may be because of the differing tissue, U87, and SVG lipid profiles to start with; which in turn will affect the membrane fluidity differently.

Other studies have shown the importance of the ratio between omega-3 and polyunsaturated fatty acids surrounding the function of membrane receptors (Liu et al., 1994). Hence, it is very important to demonstrate how altered lipid composition may have on cellular mechanisms. The effect of modifications to the cellular membrane lipid composition are related to the resulting affect to the conformational changes which can, in turn affect the binding sites of the membrane receptors and transporters, and the active site of the enzymes. Subsequently, the tumour-derived liposomes may contain differing ratios of omega-3 and omega-6 fatty acids, which may result in differing alterations of the SVG and U87 membrane composition when incorporated into the cellular membranes during the log-phase.

4.5.4 Relationship between the mitochondria and cellular viability

Previous research, as far back as the 1980s, has shown phospholipid-derived liposomes residing in the mitochondrial membrane as well as other cellular organelles of the intact cells (Sleight and Pagano, 1985). Therefore, the affect shown to the U87 and SVG cellular viability (Figure 4.2 and 4.3) with various

liposomal supplementations may be as a result of an altered mitochondrial function due to an altered mitochondrial membrane composition. The mitochondria are involved in several roles surrounding; cellular energy generation, redox regulation, ROS production, Ca^{2+} buffering and apoptosis initiation (Wang and Youle, 2009). Involvement of the mitochondria in cancer was first described by Warburg (1956) with the observation that cancerous cells undertake aerobic glycolysis. Therefore, the altered U87 and SVG cellular viability shown with liposomal supplemented may occur as a result of an altered mitochondrial response to apoptosis.

In diseased states, such as in cancerous cells, dysfunction in the normal responses to stimulation which would normally result in cell death have been observed by drug resistance (Peetla et al., 2013). However, another explanation may also be involved as a result of mitochondrial adaptation to promote survival. This was noted in a study by Zhou et al. (2005) on brain mitochondria.

4.5.5 Considerations and limitations

Several considerations during the preliminary study of the effect supplementation of various lipid-derived liposomes upon cellular viability need to be addressed. Firstly, the research has detailed how cell lines have differing phospholipid membrane compositions. Hence, the cellular viability changes between SVG and U87 may occur as a result of the membrane fluidity between each cell line being affected differently due to the differences between the membrane compositions pre-supplementation. Furthermore, the effect of membrane composition modifications between the cell lines may affect the efficiency of the membrane proteins differently. For example, the effect of unsaturation levels between two differing cell lines affected receptor efficiency differently showing cell line differences to membrane compositions. Hence, the affect upon cellular viability between SVG and U87 will need more detailed analysis before any conclusions can be made.

4.6 CONCLUSION

During diseased states, cells are observed to have an altered phospholipid membrane composition. Previous research has highlighted the differential differences between cancerous and non-cancerous phospholipid membrane compositions (Eberlin et al., 2013). Subsequently, the altered phospholipid signature observed by Hill (2011) in meningioma grade II, may provide an insight into the effect an altered phospholipid membrane profile may have upon cellular events. One of the many hallmarks of cancer is the resistance to cell death including apoptosis. During this preliminary study to postulate whether the altered membrane composition observed in cancerous cells can promote hallmarks of cancer, cellular viability was shown to be affected with both meningioma and glioma tumour-derived and PC: PS liposomes. This would suggest that the phospholipids were incorporated into the cellular and mitochondrial membrane which in turn would affect the membrane fluidity, curvature and a number of downstream events, including cell death. However, the exact membrane phospholipid profile of each cell line pre- and post- liposomal supplementation is unknown. Additionally, the exact phospholipid profile of the tumour-derived liposomes are unknown. Hence, the effect upon membrane fluidity therefore membrane protein efficiency to function may affect each cell line differently.

Chapter 5

General Discussion

5.1 INTRODUCTION

Per year, out of the >125 brain tumour types diagnosed, gliomas and meningiomas are the most common (Eberlin et al., 2013; Taylor et al., 2009). However, advances in meningioma diagnosis and treatment have somewhat lacked behind that of glioma. This is reflected in the new 2016 WHO edition, which included several new considerations for diagnosing glioma, such as molecular parameters, but no such considerations were mentioned for meningioma (Louis et al., 2016). Studies into meningioma have displayed altered lipid profiles, specifically that of phospholipids and their associated molecular species (Hill, 2011).

The study by Hill (2011) of an altered phospholipid profile within meningioma highlighted a serine-derived lipid, PS to be enriched with a neuroprotective agent (DHA). In this study, using yeast as a model the potential influence of these molecules within meningioma has displayed that serine, rather than DHA may direct the metabolic reprogramming observed in cancerous cells (Chapter 2). The suggestion that meningioma has an altered state of metabolism, is in line with the work by Otto Warburg in the late 1920s (Warburg, 1925; Warburg, 1956).

At present, metabolic reprogramming is a recognized feature of tumourigenesis (Hanahan and Weinberg, 2011). The ability of cancerous cells to survive is limited to the production of lipids, nucleic acids and proteins. In cancerous cells, the sustained demand for such cellular nutrients has been shown to surround serine biosynthesis (Amelio et al., 2014b). Due to the observed role serine plays in cancer metabolic reprogramming, research into serine biosynthesis has come to the forefront. This discussion will now concentrate on the following parameters: (a) meningioma need for serine by metabolic reprogramming, (b) altered lipid biosynthesis and lipid droplet formation with serine presence and (c) the role lipids play in cellular viability.

5.2 MENINGIOMA'S NEED FOR SERINE

In this study the immunohistochemical study has demonstrated serine biosynthesis to be altered within meningioma tissue. In cancerous tissues, such serine biosynthesis is met by the diversion away from the glycolytic pathway. The flux through the glycolytic pathway is enabled by glucose availability. Therefore, glucose itself is described as the precursor of L-serine within these cancerous tissues (Hirabayashi and Furuya, 2008). The diversion observed from glycolysis to serine biosynthesis during tumourigenesis is a sequential, enzyme-regulated process. Several enzymes associated with serine biosynthesis have been shown to be expressed within those meningioma tissues examined, as per displayed in Figure 5.1.
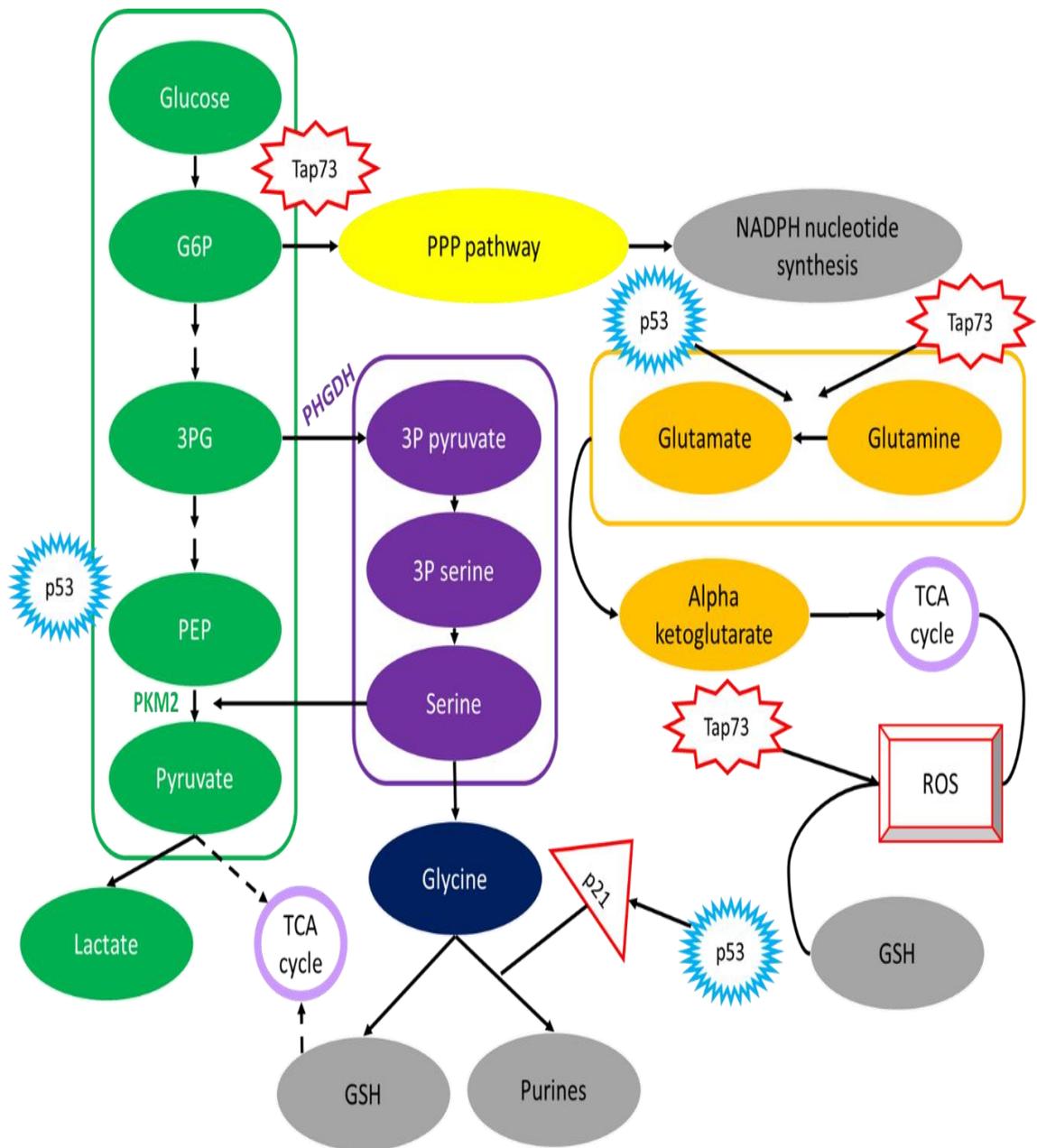
Figure 5.1: Flow diagram showing an immunohistochemical study using Image J software has shown a glycolytic diversion to serine biosynthesis within meningioma tissues. Such enzymes associated with serine biosynthesis showing positive expression within the meningioma cellular bodies include; PHGDH (79.15%), PKM2 (61.85%) and p53 (32.10%) (Adapted from Amelio et al., 2014a).

Legend: 3-phosphoglycerate (3P pyruvate), 3-phosphohydroxypyruvate (3P serine), transamination reaction (PSTA1) and phosphate ester hydrolysis (PSPH).

As shown in Figure 5.1, serine biosynthesis has been shown to be activated within meningioma. The key enzyme associated with serine biosynthesis is PHGDH, which catalyses the diversion from glycolysis to serine biosynthesis (Figure 5.1). Within the meningioma samples examined, over 80% of the cellular bodies displayed a positive PHGDH expression within the tissue (Figure 3.2, B). As shown in Figure 5.1, such strong PHGDH expression within these meningioma cellular bodies would result in the redirection of the metabolic flux from glycolysis to serine biosynthesis via the rate limiting step; 3P pyruvate to 3-phosphohydroxypyruvate. Similar PHGDH expression profiles have been demonstrated in several other cancers, including melanoma, breast and colorectal (Jai et al., 2016). One possible explanation, for the PHGDH expression is provided by the increased expression of the glucose transporter, found in brain tissues (Owen et al., 2002). Therefore, the glucose required for sustained flux through glycolysis would enable the continual production of L-serine via PHGDH.

Supporting this notion of meningioma metabolic reprogramming surrounding serine biosynthesis, is the expression of the PKM2 isoform within the cancerous tissues. Such expressions of PKM2, as opposed to PKM1, are indicative of proliferating transformed cells. Within meningioma, over 60% of the cellular bodies showed positivity for PKM2 (Figure 3.3, B). Several studies within solid tumours have also demonstrated an increase in the expression of PKM2 (Zhu et al., 2016). With the knowledge of serine acting as an allosteric regulator of PKM2, altered glycolytic flux enabling serine biosynthesis within meningioma is apparent. A summary of the allosteric regulation of PKM2 in cancerous tissues is shown in Figure 5.2.
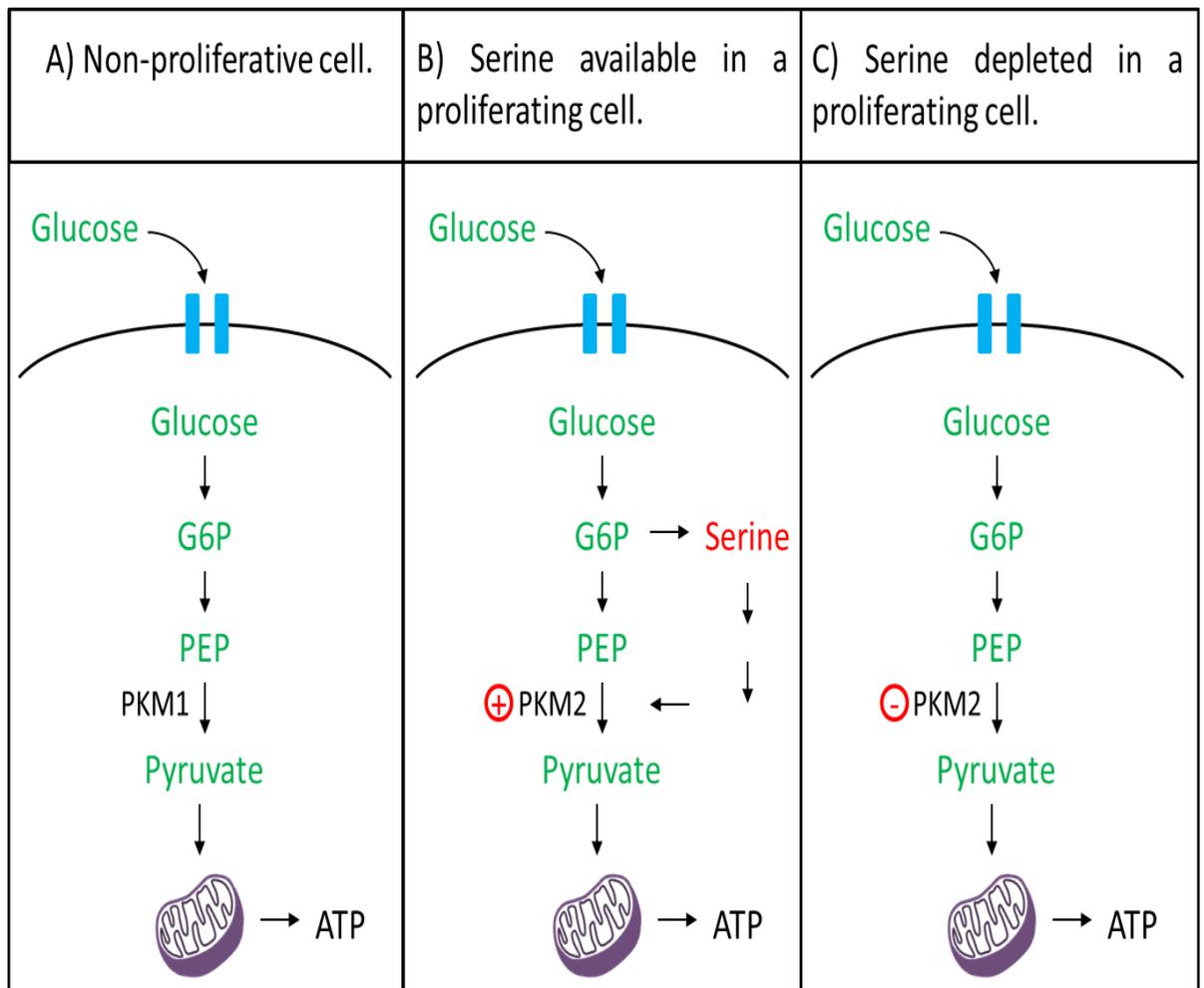
Figure 5.2: Flow pathways showing PKM2 expression within cancerous cells (B and C) as opposed to PKM1 (A) displays the presence of cancerous transformation. Such expressions of PKM2 and PHGDH have been demonstrated within meningioma. Therefore, demonstrating a serine-dependent PKM2 activation within meningioma (B and C). Suggesting that when serine stores are depleted within meningioma tissue, the catalytic rate of PKM2 will reduce, leading to the accumulation of upstream glycolytic intermediates. These intermediates will then be diverted from glycolysis to serine production via PHGDH (C). When serine stores are replenished, serine will then activate PKM2 activity; restoring the glycolytic flux (B). Thus highlighting, that the presence of serine can allosterically regulate the glycolytic flux, therefore the production of ATP.

As described in Figure 5.2, within tumours, serine presence alone can regulate PKM2 expression and therefore enhances the catalytic conversion rate of PEP to pyruvate. Such allosteric regulation within meningioma is displayed by the synergistic relationship between PKM2 and PHGDH expressions (see Chapter 3). This mechanism of allosteric regulation surrounding PKM2 and serine suggests that meningioma tissues must contain high levels of the non-essential amino acid, serine. Such levels of serine would then enable aerobic glycolysis and lactate production both of which are vital for cell growth and survival (Diaz-Ruiz and Zhou, 2011). Several cancerous phenotypical advances are promoted with such aerobic glycolysis including the upregulation of glycolysis to sustain cellular survival during intermittent hypoxia.

Within cancerous cells, the status of such nutrients like serine, have also been shown to be affected by the expression of tumour suppressors. Such tumour suppressors like p53 have been show to inhibit serine biosynthesis by targeting PHGDH (Ou et al., 2015). In human melanoma, over 80% of cases have been shown to retain their p53 expression. In such tissues, PHGDH activity is observed to be reduced resulting in serine depletion. Consequently, upon serine starvation, p53-mediated cell death was enhanced in response to Nutlin-3 treatment (Ou et al., 2015). However, those melanoma cells which demonstrated an overexpression in PHGDH inhibited the apoptotic response to such nutrient stress. Therefore, taking into consideration the overriding expression of PHGDH in correlation to p53 within the meningioma's examined in this study (Figure 3.3), it would suggest that serine biosynthesis is not suppressed and in fact, with serine depletions, the meningioma tumour would not be sensitive to p53-mediated cell death.

Subsequently, the altered serine biosynthetic pathway observed in meningioma would lead to the production of key molecules involved in cellular survival including lipids, secondary messengers and proteins (Amelio et al., 2014b). In order to identify the phenotypical advances, such tumours may gain with directed serine biosynthesis a study utilising a model organism was developed.

5.2.1 The influence of serine on metabolic reprogramming

In meningioma, in order to sustain such a cancerous phenotype, metabolic programming has to be altered (Tsun and Possemato, 2015). Such metabolic reprogramming surrounds lipid metabolism, specifically that of neutral lipids (Hanahan and Weinberg, 2011). These neutral lipids provide an energy source to the cells during nutrient depletion and hypoxia conditions. To support the notion that the observed serine biosynthesis within meningioma supports a cancerous phenotype, an oleaginous yeast model was established (see Chapter 2). The discussion will now detail the findings of this study.

An oleaginous yeast model, in the form of *L. starkeyi*, provided insight into the potential influence an increased serine presence may provide meningioma. With such capacity of yeast to uptake serine, the cellular events, which are recognised to be altered in a cancerous state were examined. A summary of the major findings are displayed in Figure 5.3.
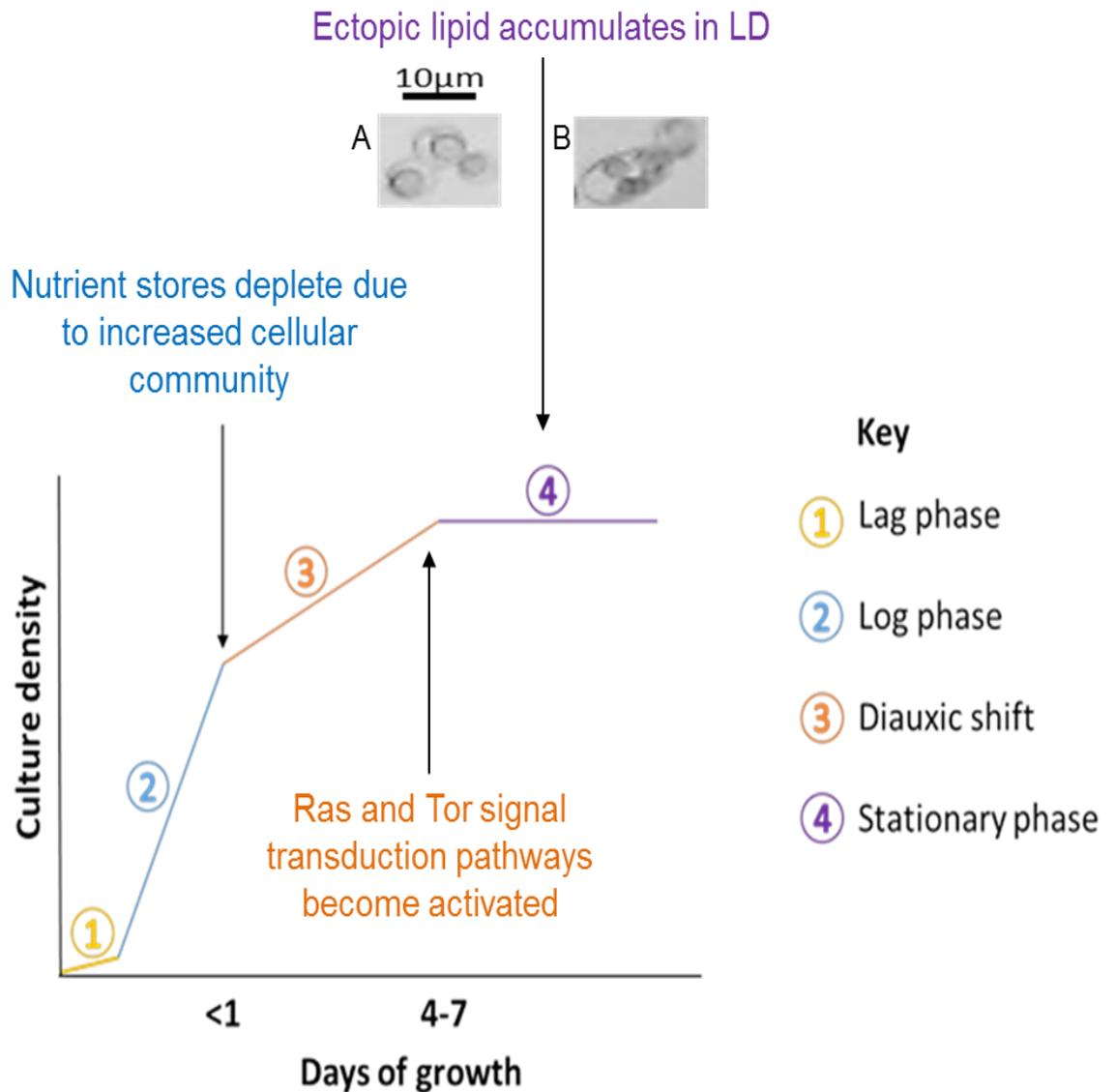
Figure 5.3: Growth curve showing that serine supplementation can alter lipid accruement during stationary phase (4, B) once cells have depleted nutritional resources during log phase (2). Consequently, Ras and Tor signal transduction pathways are activated (3) leading to ectopic lipid accumulation (4, A and B).

Like the CNS where serine is taken up by ASC transporters (Figure 1.18), yeasts also have the capability to uptake serine by transporters (Grenson and Hennaut, 1971). With serine being up taken as any other nutrient source in the media, alterations in the cellular characteristics of those supplemented were observed. Such alterations in cellular characteristics are pertinent to a cancerous phenotype in terms of proliferation, maximal cellular community and lipid storage (Figures

2.1- 2.4). To sustain proliferation, nutrients are required at an enhanced rate in cancerous cells. With serine presence, such increases in proliferation were observed (Figure 2.2, B) suggesting that serine presence within the cell affects cellular processing surrounding the cell cycle.

In response to the depleting sources of nutrients (nitrogen, phosphorus and carbon), the Ras and Tor signal transduction pathways are initiated (Figure 5.3). After such activation of Ras and Tor, to prevent lipotoxicity neutral lipids are then encapsulated into storage organelles known as LDs (Figure 5.3 and 5.4). The storage of neutral lipids within LDs is observed within many disease tissues, including cancer (Coller, 2014; DeBerardinis et al., 2008b; DeBerardinis et al., 2008a; DeBerardinis and Chandel, 2016).   Studies by Yen et al. (2008b) have described storage of neutral lipids in LDs to enable a source of energy for cellular events and a source of phospholipids, which are required for membrane biosynthesis. However, with serine presence, there is an uncharacteristic observation of multiple LDs per cell (Figure 5.3, A and B). The proposed mechanism of LD formation and LD mobilization is illustrated in Figure 5.4.
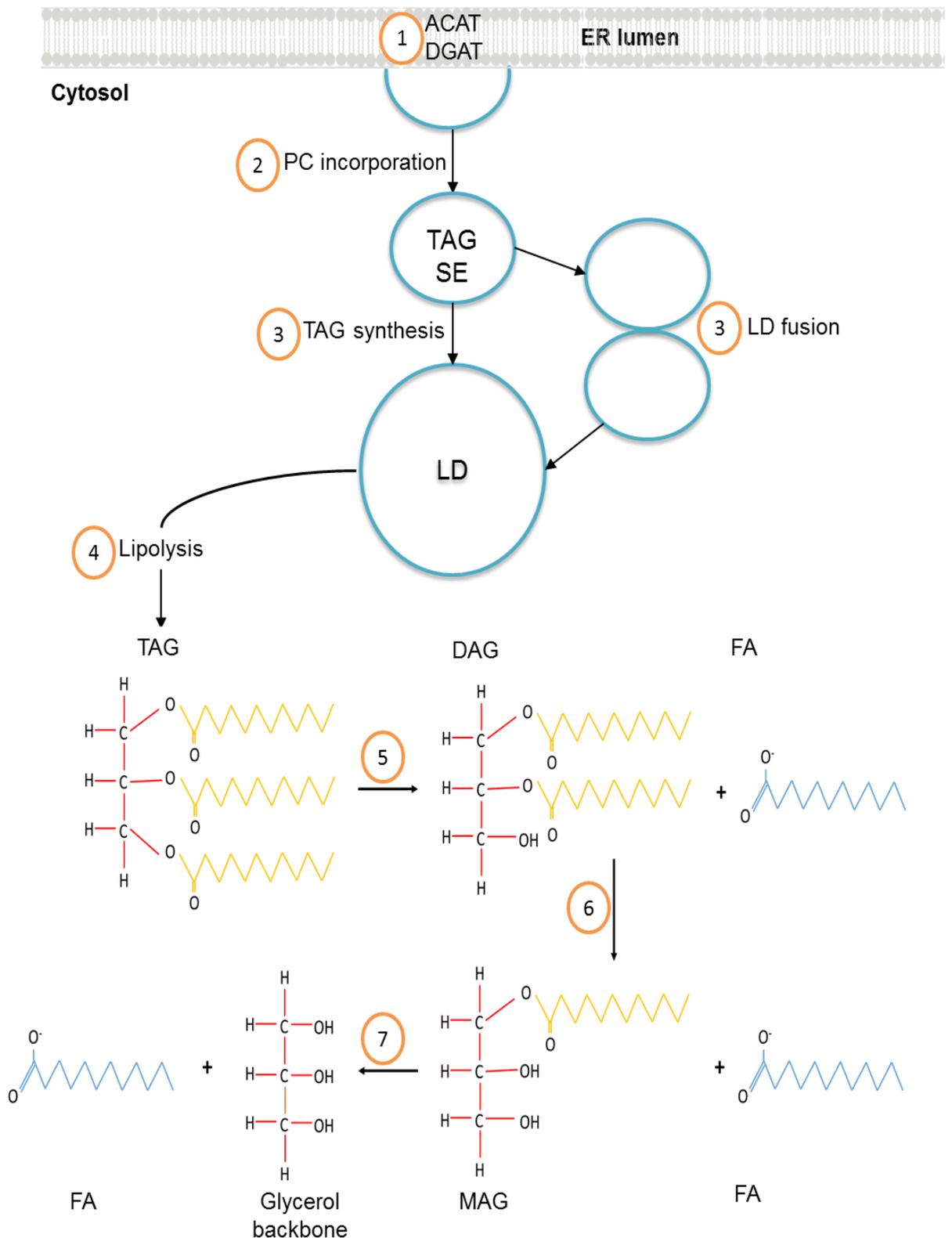
Figure 5.4: Flow diagram and chemical structures showing how the presence of serine alters the stages (1-7) of storage and mobilization of neutral lipids. The number of lipid droplets increase with serine presence, leading to an increased surface area to volume ratio, which the LD occupies within the cell. Hence, the mobilization of lipids via lipolysis may be enhanced (Images adapted from Thiele and Spandl, 2008 and Yen, 2008).

The observed increase in the number of smaller LDs within serine-enriched cells are in line with the observations that Accioly et al (2008) made when comparing cancerous to non-cancerous cells. LDs are produced by the endoplasmic reticulum (Figure 5.4, stage 1) when the cytosolic lipid content is raised. By incorporating these cytosolic lipids within a membrane bound compartment, lipotoxicity is prevented (Walther and Farese Jr, 2009). With serine presence, the observed alterations in LD formation may be due to an overexpression of lipases involved in lipolysis (Figure 5.4, stage 4). In cancerous tissue, the overexpression of lipases, such as MAGL, have been shown to produce increasing levels of free fatty acids after lipolysis (Beller et al., 2010). However, with serine presence, the expression of such lipases does not appear to be increased as *de novo* free fatty acid synthesis was not significantly increased (Figure 2.9).

Subsequently, the alterations in LD formation with serine presence may be a knock-on effect from cellular stress produced by presiding dysfunctional mitochondria as observed on *Drosophila* by Liu et al. (2015). As LD formation is an orchestration between the endoplasmic reticulum and mitochondria, such increases in cellular stress may impact on the size of LD, therefore, suggesting that serine presence may influence mitochondrial function. In either situation, due to the enhanced LD surface area to volume ratio, the mobilization of lipids via lipolysis would be increased (Figure 5.4, stage 4). A radiochemical study in this thesis (see chapter 2) provided insight into the effect serine presence may have upon *de novo* lipid synthesis. A summary of the metabolic pathways related to *de novo* lipid synthesis is illustrated in Figure 5.5.
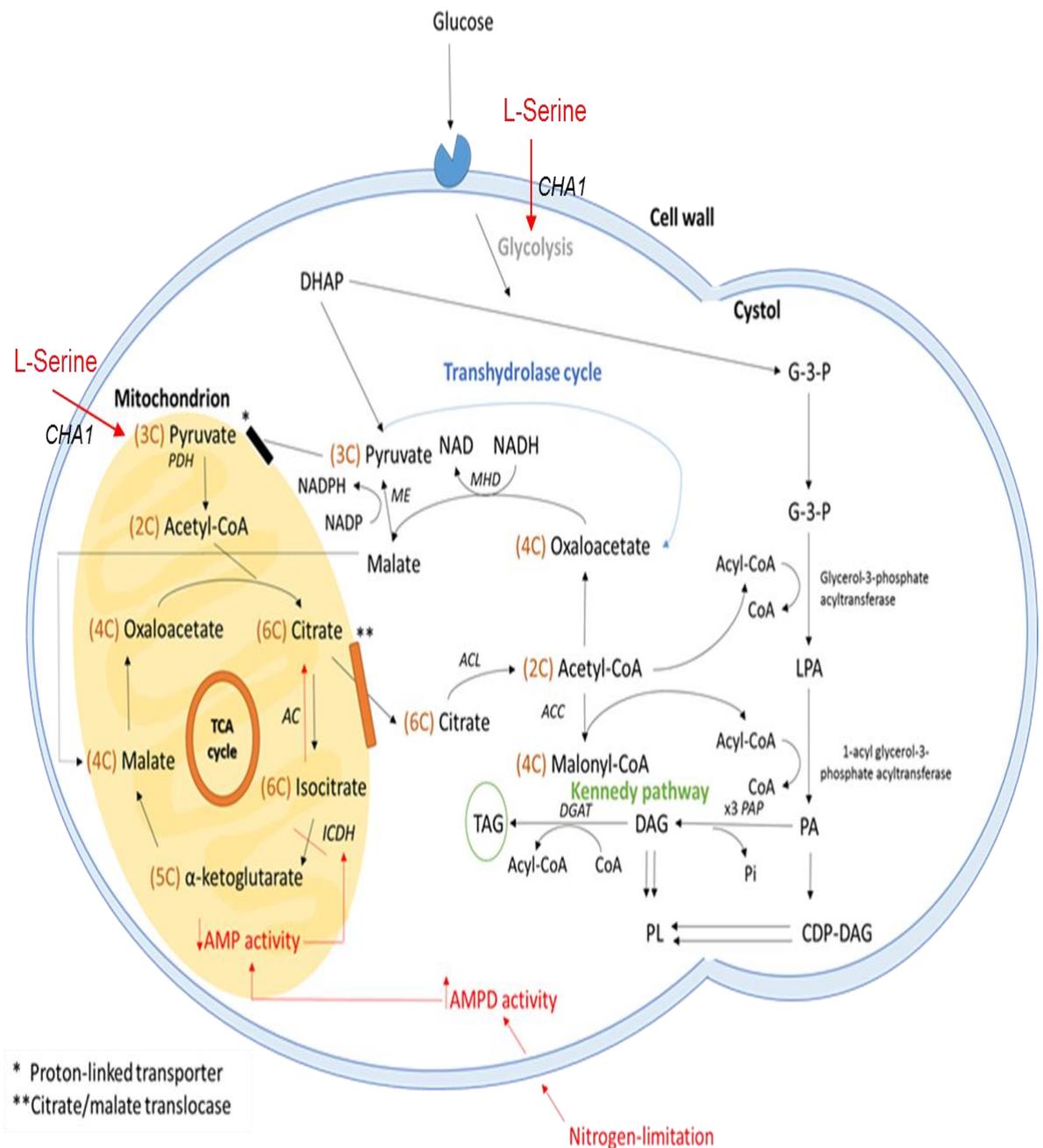
Figure 5.5: Biochemical diagram showing that with serine presence, metabolic re-tailoring surrounding *de novo* lipid synthesis and accumulation occurs in relation to nutrient depletion (highlighted in red). The conversion of serine to pyruvate by CHA1 also provides a flux to the Kennedy pathway enabling the production of triacylglycerides and phospholipids. The ratio of phospholipid: triacylglyceride *de novo* synthesis is increased with serine presence to house the multiple LDs within the cell (Image adapted from Herman, 2002).

With serine presence, an altered *de novo* synthesis of acyl lipids and isoprenoids were observed (Figure 2.9). From the current radiochemical study, it can be suggested that for every ten acetate molecules converted to acetyl-CoA, one of these molecules are used to support acyl lipid synthesis and the other 9 support isoprenoid synthesis. Such increases in isoprenoid synthesis reflect the requirement for membranes surrounding the multiple LDs (Figure 2.4). With stored energy in the form of multiple LDs within the cell, only half of the acetate was taken up by the cells (Figure 2.6). This demonstrates how serine presence alone can further re-tail metabolic pathways within a cancerous phenotype, enabling sources of energy and phospholipids to be abundant.

5.2.2 Serine's influence on cellular viability

One of the many derivatives of serine, is the phospholipid, phosphatidylserine which resides in the plasma membranes of the cell. In the study by Hill (2011), the phospholipid signature of meningioma was altered in comparison to other areas of the brain. Alterations were particularly noted within the phosphatidylserine portion, which was observed to be enriched with DHA. Previous studies have highlighted the beneficial relationship between phosphatidylserine and DHA within diseased cells, including neuronal survival and differentiation (Kim et al., 2010; Kim, 2008; Steelman et al., 2011). Considering that meningioma has been shown to promote serine biosynthesis, production of such serine-derived lipids like phosphatidylserine will be enhanced in such tissues which is in line with Hill (2011) observations.

Once produced, phospholipids are incorporated into a variety of cellular membranes. The phospholipid bilayer of mammalian cells houses not only phospholipids but also receptors, transporter and membrane-bound enzymes (Spector and Yorek, 1985). Lipids are classed as primary and secondary messengers (van Meer et al., 2008). Therefore, any changes in the composition of phospholipid cellular membranes may impede on cellular events.

One such organelle surrounded by a membrane, the mitochondria, play a central role in cellular events including; energy production, regulation of redox, the production of ROS, Ca^{2+} buffering and the initiation of apoptosis (Wang and Youle, 2009). Within the mitochondrial plasma membrane, several receptors and transporters reside. The function of such receptors and transporters can be easily influenced by alterations in the phospholipid composition of membrane (Liu et al., 1994). Hence, the notion that meningioma has a phospholipid signature different to other areas in the brain (Hill, 2011) may influence the cancerous phenotype observed.

5.2.3 U87 and SVG cell line study

Supplementation of PS liposomes increased the viability of the non-cancerous SVG cell line as well as the cancerous U87 cell line (Figure 4.2). Meningioma-derived liposomal preparations also increased cellular viability of both cell lines (Figure 4.2). Such liposomes have been shown to incorporate not only in the plasma membrane of cells but also within the; nuclear membranes, mitochondrial membranes and the golgi apparatus (Sleight and Pagano 1985). The observed liposomal incorporation within such membranes has been shown to alter their composition (Spector and Yorek, 1985). Incorporation of meningioma-derived lipids increased the viability of the non-cancerous SVG cell line like that observed with PS supplementation (Figures 4.2- 4.3). This observation suggests that in fact the phospholipid (PS), rather than the fatty acid (DHA), plays a role in cellular viability. This may be in part, due to the altered phospholipid composition of the cellular and organelle membranes. Such altered membrane composition will impact the fluidity and the entry and exit of substances into the cell.

5.3 CLINICAL IMPLICATIONS AND SPECULATIONS

The results gained from this study can be used clinically in the diagnosis and management of meningioma as well as other diseased cells displaying ectopic lipid accumulation. As previously discussed, meningioma is currently graded in

accordance with the WHO organization classification (Figure 1.3). The observation that serine biosynthesis is promoted within meningioma provides additional insight into the behaviour of the tumour in terms of proliferation and potential chemotherapy resistance. The observation that meningioma has an altered biochemistry, may provide guidance when histologically grading the tumours.

The requirement for serine biosynthesis within meningioma supports the observation that some cancerous cells have a preference to serine, rather than glycine, for one carbon metabolism (Labuschagne et al., 2014). Those tumours expressing enzymes involved in serine biosynthesis, such as PKM2 and PHGDH, can be targeted with treatment in the form of inhibitors. A review by Zhu et al. (2016) associated PKM2 expression with poor prognosis, however the effects of such PKM2 expression can be inhibited. Studies by Vander Heiden et al. (2010) and Goldberg and Sharp (2012) have shown that the flux through aerobic glycolysis can be reduced by targeting PKM2. Subsequently, the increased demand for energy in cancerous cells enabled by aerobic glycolysis would be hindered.

Another potential avenue for meningioma treatment would aim to prevent serine biosynthesis, therefore reducing serine-derived lipid production, which has been implicated with increased cellular viability as well as lipid accruement. To reduce serine biosynthesis, meningioma tissues exhibiting PHGDH expression can be targeted (Wang et al., 2017; Mullarky et al., 2016). By doing so, the observed correlation of PHGDH expression and prognosis in the study by Jia et al. (2016) would be reversed. The observation that PHGDH is expressed solely in cancerous cells aids the treatment to be tumour site specific (Wang et al., 2017; Mullarky et al., 2016). By hindering the capability of cancerous cells producing serine, the dysfunctional formation of LDs observed would also be hindered. Such LD alterations in breast, cervical and colon cancers have been correlated with increased chemotherapy resistance (Zhu, 2016). By targeting serine

biosynthesis, the resources needed to enable a cancerous phenotype are depleted.

5.4 CONCLUSION

Previous studies by Hill (2011) determined how meningioma tissues were enriched with the phospholipid, PS and the fatty acid, DHA. Within this thesis, the interaction between DHA and / or L-serine upon metabolic pathways have been examined. In Chapter 2, the oleaginous yeast *L. starkeyi* displayed how the metabolic reprogramming surrounding neutral lipid and lipid droplet formation were altered with L-serine presence. In Chapter 3, the immunohistochemical study illustrated a glycolytic diversion towards serine biosynthesis in both grade I and II meningioma. In Chapter 4, the phenotypical cellular viability of cancerous cells were enhanced with the supplementation of both PS and tumour-derived liposomes.

In conclusion, serine the non-essential amino acid has been implicated as an orchestrator of cancerous metabolic reprogramming in this study on meningioma. Meningioma has been shown to promote serine-directed metabolism, which in turn increases the abundance of serine-derived lipids promoting a cancerous phenotype. Such metabolic alterations have been implicated with poor prognosis in other types of cancer due to chemotherapy resistance. Hence, the implications surrounding such metabolic alterations can be considered clinically in terms of proliferation, response to treatment and subsequently prognosis.

5.5 SCOPE FOR FUTURE STUDIES

To take forward this present study on meningioma, the relationship between serine biosynthesis and the presentation of an altered state of metabolism can be explored further. To establish if serine can influence phospholipid profiles within cancerous cells, an analytical study can be carried out.   To analyse the

effect of serine, the model organism, *L. starkeyi*, can be supplemented with serine. During stationary phase, the phospholipid profile of such cells can then be analysed using high-performance liquid chromatography. Such methodologies exist (Pang et al., 2008) where the phospholipid as well as its assigned molecular species can be examined. This analytical study would provide an insight into the relationship between serine supplementation and the production of serine-derived lipids i.e. phosphatidylserine. Additionally, the relationship between phosphatidylserine and DHA during times of proliferation and lipid accumulation can be exploited. To gain an insight into the impact serine has upon glycolytic flux within cancerous cells, a study utilizing radiolabeled glucose can be performed upon those *L. starkeyi* cells supplemented with/without serine.

To determine whether the formation of lipid droplets in those cells supplemented with serine was related to a dysfunctional mitochondria and/or endoplasmic reticulum, a transmission electron microscopy study of *L. starkeyi* cells during stationary phase can be developed. Furthermore, the identification and semi-quantification of such lipid droplets can be achieved using fluorescent microscopy utilising Nile red as opposed to light microscopy.

To determine whether serine biosynthesis within meningioma can be reduced using enzyme inhibitors, a study using such treatments as supplements to the model organism, *L. starkeyi* and/or U87 and SVG cell lines can be optimized. By using enzyme assays to gain an insight into the flux through glycolysis and serine biosynthesis with such treatments, the clinical implications in terms of chemo resistance and cellular viability can be examined.

To determine if the metabolic reprogramming observed with the presence of L-serine is observed in other cancer types, the amino acids levels within cancerous tissues could be measured alongside their incorporation into phospholipids.

Chapter 6

Bibliography

Accioly, M. T., Pacheco, P., Maya-Monteiro, C. M., Carrossini, N., Robbs, B. K., Oliveira, S. S., Kaufmann, C., Morgado-Diaz, J. A., Bozza, P. T. & Viola, J. P. (2008). Lipid bodies are reservoirs of cyclooxygenase-2 and sites of prostaglandin-E2 synthesis in colon cancer cells. *Cancer Res,* 68**,** 1732-40.

Akshatha, C., Mysorekar, V., Arundhathi, S., Arul, P., Raj, A. & Shetty, S. (2016). Correlation of p53 Overexpression with the Clinicopathological Prognostic Factors in Colorectal Adenocarcinoma. *J Clin Diagn Res,* 10**,** Ec05-ec08.

Alanazi, F. K., Harisa Gel, D., Maqboul, A., Abdel-Hamid, M., Neau, S. H. & Alsarra, I. A. (2011). Biochemically altered human erythrocytes as a carrier for targeted delivery of primaquine: an in vitro study. *Arch Pharm Res,* 34**,** 563-71.

Alexiou, George A., Gogou, Pinelopi, Markoula, Sofia & Kyritsis, Athanasios P. (2010). Management of meningiomas. *Clin Neurology and Neurosurgery,* 112**,** 177-182.

Amelio, I., Markert, E. K., Rufini, A., Antonov, A. V., Sayan, B. S., Tucci, P., Agostini, M., Mineo, T. C., Levine, A. J. & Melino, G. (2014a). p73 regulates serine biosynthesis in cancer. *Oncogene,* 33**,** 5039-46.

Amelio, Ivano, Cutruzzolá, Francesca, Antonov, Alexey, Agostini, Massimiliano & Melino, Gerry. (2014b). Serine and glycine metabolism in cancer. *Trends in Biocheml Sciences,* 39**,** 191-198.

Azzi, S., Hebda, J. K. & Gavard, J. (2013). Vascular permeability and drug delivery in cancers. *Front Oncol,* 3**,** 211.

Backer-Grondahl, T., Moen, B. H. & Torp, S. H. (2012). The histopathological spectrum of human meningiomas. *Int J Clin Exp Pathol,* 5**,** 231-42.

Baenke, Franziska, Peck, Barrie, Miess, Heike & Schulze, Almut. (2013). Hooked on fat: the role of lipid synthesis in cancer metabolism and tumour development. *Disease Models and Mechanisms,* 6**,** 1353-1363.

Banks, William A. (2009). Characteristics of compounds that cross the blood-brain barrier. *BMC Neurology,* 9**,** S3-S3.

Barnholtz-Sloan, J. S. & Kruchko, C. (2007). Meningiomas: causes and risk factors. *Neurosurg Focus,* 23**,** E2.

Beller, Mathias, Thiel, Katharina, Thul, Peter J. & Jäckle, Herbert. (2010). Lipid droplets: A dynamic organelle moves into focus. *FEBS Letters,* 584**,** 2176-2182.

Beloribi-Djefaflia, S., Vasseur, S. & Guillaumond, F. (2016). Lipid metabolic reprogramming in cancer cells. *Onco,* 5**,** e189.

Ben-Zvi, A., Lacoste, B., Kur, E., Andreone, B. J., Mayshar, Y., Yan, H. & Gu, C. (2014). Mfsd2a is critical for the formation and function of the blood-brain barrier. *Nature,* 509**,** 507-11.

Beopoulos, Athanasios, Nicaud, Jean-Marc & Gaillardin, Claude (2011). An overview of lipid metabolism in yeasts and its impact on biotechnological processes. *Applied Micro and Biotec,* 90**,** 1193-1206.

Biagiotti, S., Rossi, L., Bianchi, M., Giacomini, E., Pierige, F., Serafini, G., Conaldi, P. G. & Magnani, M. (2011). Immunophilin-loaded erythrocytes

as a new delivery strategy for immunosuppressive drugs. *J Control Release,* 154**,** 306-13.

Blusztajn, J. K., Liscovitch, M., Mauron, C., Richardson, U. I. & Wurtman, R. J. (1987). Phosphatidylcholine as a precursor of choline for acetylcholine synthesis. *J Neural Transm Suppl,* 24**,** 247-59.

Bozzuto, G. & Molinari, A. (2015). Liposomes as nanomedical devices. *Int J Nanomedicine,* 10**,** 975-99.

Calvey, C. H., Su, Y. K., Willis, L. B., Mcgee, M. & Jeffries, T. W. (2016). Nitrogen limitation, oxygen limitation, and lipid accumulation in Lipomyces starkeyi. *Bioresour Technol,* 200**,** 780-8.

Camargo, N., Brouwers, J. F., Loos, M., Gutmann, D. H., Smit, A. B. & Verheijen, M. H. (2012). High-fat diet ameliorates neurological deficits caused by defective astrocyte lipid metabolism. *Faseb j,* 26**,** 4302-15.

Campos-Bedolla, Patricia, Walter, Fruzsina R., Veszelka, Szilvia & Deli, Mária A. (2014). Role of the Blood–Brain Barrier in the Nutrition of the Central Nervous System. *Archives of Medical Res,* 45**,** 610-638.

Cea-Soriano, Lucía, Blenk, Tilo, Wallander, Mari-Ann & Rodríguez, Luis A. García. (2012). Hormonal therapies and meningioma: Is there a link? *Cancer Epidemiology,* 36**,** 198-205.

Chakraborty, A., De Wit, N. M., Van Der Flier, W. M. & De Vries, H. E. (2017). The blood brain barrier in Alzheimer's disease. *Vascular Pharm,* 89**,** 12-18.

Chaneton, Barbara, Hillmann, Petra, Zheng, Liang, Martin, Agnes C. L., Maddocks, Oliver D. K., Chokkathukalam, Achuthanunni, Coyle, Joseph E., Jankevics, Andris, Holding, Finn P., Vousden, Karen H., Frezza, Christian, O/'Reilly, Marc & Gottlieb, Eyal. (2012). Serine is a natural ligand and allosteric activator of pyruvate kinase M2. *Nature,* 491**,** 458-462.

Chhabria, V. & Beeton, S. (2016). Development of nanosponges from erythrocyte ghosts for removal of streptolysin-O from mammalian blood. *Nanomedicine (Lond).*

Chow, Brian Wai & Gu, Chenghua. (2015). The Molecular Constituents of the Blood–Brain Barrier. *Trends in Neuro,* 38**,** 598-608.

Clendening, J. W., Pandyra, A., Boutros, P. C., El Ghamrasni, S., Khosravi, F., Trentin, G. A., Martirosyan, A., Hakem, A., Hakem, R., Jurisica, I. & Penn, L. Z. (2010). Dysregulation of the mevalonate pathway promotes transformation. *Proc Natl Acad Sci U S A,* 107**,** 15051-6.

Coller, Hilary A. (2014). Is Cancer a Metabolic Disease? *Am J Pathol,* 184**,** 4-17.

Currie, Erin, Schulze, Almut, Zechner, Rudolf, Walther, Tobias c & Farese Jr, Robert v. (2013). Cellular Fatty Acid Metabolism and Cancer. *Cell Metabolism,* 18**,** 153-161.

Damseh, N., Simonin, A., Jalas, C., Picoraro, J. A., Shaag, A., Cho, M. T., Yaacov, B., Neidich, J., Al-Ashhab, M., Juusola, J., Bale, S., Telegrafi, A., Retterer, K., Pappas, J. G., Moran, E., Cappell, J., Anyane Yeboa, K., Abu-Libdeh, B., Hediger, M. A., Chung, W. K., Elpeleg, O. & Edvardson, S. (2015). Mutations in SLC1A4, encoding the brain serine transporter, are

associated with developmental delay, microcephaly and hypomyelination. *J Med Genet,* 52**,** 541-7.

De Koning, T. J., Jaeken, J., Pineda, M., Van Maldergem, L., Poll-The, B. T. & Van Der Knaap, M. S. (2000). Hypomyelination and reversible white matter attenuation in 3-phosphoglycerate dehydrogenase deficiency. *Neuropediatrics,* 31**,** 287-92.

Deamer, David W. (2010). From "Banghasomes" to liposomes: A memoir of Alec Bangham, 1921–2010. *The FASEB Journal,* 24**,** 1308-1310.

Deberardinis, R. J. & Chandel, N. S. (2016). Fundamentals of cancer metabolism. *Sci Adv,* 2**,** e1600200.

Deberardinis, R. J., Lum, J. J., Hatzivassiliou, G. & Thompson, C. B. (2008a). The biology of cancer: metabolic reprogramming fuels cell growth and proliferation. *Cell Metab,* 7**,** 11-20.

Deberardinis, Ralph J., Sayed, Nabil, Ditsworth, Dara & Thompson, Craig B. (2008b). Brick by brick: metabolism and tumor cell growth. *Current Opinion in Genetics and Devel,* 18**,** 54-61.

Diaz-Ruiz, R., Rigoulet, M. & Devin, A. (2011). The Warburg and Crabtree effects: On the origin of cancer cell energy metabolism and of yeast glucose repression. *Biochim Biophys Acta,* 1807**,** 568-76.

Diaz-Ruiz, R., Uribe-Carvajal, S., Devin, A. & Rigoulet, M. (2009). Tumor cell energy metabolism and its common features with yeast metabolism. *Biochim Biophys Acta,* 1796**,** 252-65.

Domenichiello, A. F., Kitson, A. P. & Bazinet, R. P. (2015). Is docosahexaenoic acid synthesis from alpha-linolenic acid sufficient to supply the adult brain? *Prog Lipid Res,* 59**,** 54-66.

Dong, G., Mao, Q., Xia, W., Xu, Y., Wang, J., Xu, L. & Jiang, F. (2016). PKM2 and cancer: The function of PKM2 beyond glycolysis. *Oncol Lett,* 11**,** 1980-1986.

Eberlin, Livia S., Norton, Isaiah, Orringer, Daniel, Dunn, Ian F., Liu, Xiaohui, Ide, Jennifer L., Jarmusch, Alan K., Ligon, Keith L., Jolesz, Ferenc A., Golby, Alexandra J., Santagata, Sandro, Agar, Nathalie Y. R. & Cooks, R. Graham. (2013). Ambient mass spectrometry for the intraoperative molecular diagnosis of human brain tumors. *Proceedings of the National Academy of Sci,* 110**,** 1611-1616.

Fagone, P. & Jackowski, S. (2009). Membrane phospholipid synthesis and endoplasmic reticulum function. *J of Lipid Res,* 50**,** S311-S316.

Farese, R. V., Jr. & Walther, T. C. (2009). Lipid droplets finally get a little R-E-S-P-E-C-T. *Cell,* 139**,** 855-60.

Garcia, Martha C. & Kim, Hee-Yong. (1997). Mobilization of arachidonate and docosahexaenoate by stimulation of the 5-HT2A receptor in rat C6 glioma cells. *Brain Res,* 768**,** 43-48.

Glunde, K., Bhujwalla, Z. M. & Ronen, S. M. (2011). Choline metabolism in malignant transformation. *Nat Rev Cancer,* 11**,** 835-48.

Goldberg, M. S. & Sharp, P. A. (2012). Pyruvate kinase M2-specific siRNA induces apoptosis and tumor regression. *J Exp Med,* 209**,** 217-24.

Goñi, Félix M. & Alonso, Alicia. (2006). Biophysics of sphingolipids I. Membrane properties of sphingosine, ceramides and other simple sphingolipids. *Biochimica et Biophysica Acta (BBA) - Biomembranes,* 1758**,** 1902-1921.

Grenson, M. & Hennaut, C. (1971). Mutation affecting activity of several distinct amino acid transport systems in Saccharomyces cerevisiae. *J Bacteriol,* 105**,** 477-82.

Gulati, Sonia, Liu, Ying, Munkacsi, Andrew B., Wilcox, Lisa & Sturley, Stephen L. (2010). Sterols and sphingolipids: Dynamic duo or partners in crime? *Progress in Lipid Res,* 49**,** 353-365.

Hagen, Rachel M., Rodriguez-Cuenca, Sergio & Vidal-Puig, Antonio. (2010). An allostatic control of membrane lipid composition by SREBP1. *FEBS Letters,* 584**,** 2689-2698.

Hamada, S., Horiguchi, A., Kuroda, K., Ito, K., Asano, T., Miyai, K. & Iwaya, K. (2014). Elevated fatty acid synthase expression in prostate needle biopsy cores predicts upgraded Gleason score in radical prostatectomy specimens. *Prostate,* 74**,** 90-6.

Hampton, Mark B., Vanags, Daina M., Isabella Pörn-Ares, M. & Orrenius, Sten (1996). Involvement of extracellular calcium in phosphatidylserine exposure during apoptosis. *FEBS letters,* 399**,** 277-282.

Hanahan, Douglas & Weinberg, Robert. (2011). Hallmarks of Cancer: The Next Generation. *Cell,* 144**,** 646-674.

Hapala, Ivan, Marza, Esther & Ferreira, Thierry. (2011). Is fat so bad? Modulation of endoplasmic reticulum stress by lipid droplet formation. *Bio of the Cell,* 103**,** 271-285.

Haque, M. E., Mcintosh, T. J. & Lentz, B. R. (2001). Influence of lipid composition on physical properties and peg-mediated fusion of curved and uncurved model membrane vesicles: "nature's own" fusogenic lipid bilayer. *Biochem,* 40**,** 4340-8.

Harisa, G. I., Ibrahim, M. F. & Alanazi, F. K. (2012). Erythrocyte-mediated delivery of pravastatin: in vitro study of effect of hypotonic lysis on biochemical parameters and loading efficiency. *Arch Pharm Res,* 35**,** 1431-9.

Herman, Paul K. (2002). Stationary phase in yeast. *Current Opinion in Microbiology,* 5**,** 602-607.

Hill, Micheal. (2011). Building a Lipid Signature of Grade II Meningioma Tissue. University of Central Lancashire. Thesis.

Hirabayashi, Y. & Furuya, S. (2008). Roles of l-serine and sphingolipid synthesis in brain development and neuronal survival. *Prog Lipid Res,* 47**,** 188-203.

Horton, J. D., Goldstein, J. L. & Brown, M. S. (2002). SREBPs: activators of the complete program of cholesterol and fatty acid synthesis in the liver. *J Clin Invest,* 109**,** 1125-31.

Hu, Che-Ming J., Fang, Ronnie H., Copp, Jonathan, Luk, Brian T. & Zhang, Liangfang. (2013). A biomimetic nanosponge that absorbs pore-forming toxins. *Nat Nano,* 8**,** 336-340.

Isaac, G., Fredriksson, A., Danielsson, R., Eriksson, P. & Bergquist, J. (2006). Brain lipid composition in postnatal iron-induced motor behavior

alterations following chronic neuroleptic administration in mice. *Febs j,* 273**,** 2232-43.

Jia, Xiao-Qin, Zhang, Shu, Zhu, Hui-Jun, Wang, Wei, Zhu, Jin-Hong, Wang, Xu-Dong & Qiang, Jian-Feng. (2016). Increased Expression of PHGDH and Prognostic Significance in Colorectal Cancer. *Translational Oncology,* 9**,** 191-196.

Jin, Wenrui & Jiang, Lei. (2002). Study of uptake kinetics of vincristine for human erythrocytes by capillary zone electrophoresis with electrochemical detection. *Analytica Chimica Acta,* 461**,** 117-121.

Kennedy, K. M. & Dewhirst, M. W. (2010). Tumor metabolism of lactate: the influence and therapeutic potential for MCT and CD147 regulation. *Future Oncol,* 6**,** 127-48.

Kim, Eun Kyung & Choi, Eui-Ju (2010). Pathological roles of MAPK signaling pathways in human diseases. *Biochimica et Biophysica Acta (BBA) - Molecular Basis of Disease,* 1802**,** 396-405.

Kim, Hee-Yong. (2008). Biochemical and biological functions of docosahexaenoic acid in the nervous system: modulation by ethanol. *Chemistry and Physics of Lipids,* 153**,** 34-46.

Kim, Hee-Yong, Akbar, Mohammed & Kim, Yang-Suk. (2010). Phosphatidylserine-dependent neuroprotective signaling promoted by docosahexaenoic acid. *PLEFA,* 82**,** 165-172.

Kim, Hee-Yong & Edsall, Lisa. (1999). The role of docosahexaenoic acid (22:6n-3) in neuronal signaling. *Lipids,* 34**,** S249-S250.

Kim, Hee-Yong, Huang, Bill X. & Spector, Arthur A. (2014). Phosphatidylserine in the brain: Metabolism and function. *Progress in Lipid Res,* 56**,** 1-18.

Kolter, Thomas & Sandhoff, Konrad. (2006). Sphingolipid metabolism diseases. *Biochimica et Biophysica Acta (BBA) - Biomembranes,* 1758**,** 2057-2079.

Kuzet, Sanya-Eduarda & Gaggioli, Cedric. (2016). Fibroblast activation in cancer: when seed fertilizes soil. *Cell and Tissue Res***,** 1-13.

Labuschagne, Christiaan f, Van den broek, Niels j F., Mackay, Gillian m, Vousden, Karen h & Maddocks, Oliver d K. (2014). Serine, but Not Glycine, Supports One-Carbon Metabolism and Proliferation of Cancer Cells. *Cell Reports,* 7**,** 1248-1258.

Lagace, Thomas A. & Ridgway, Neale D. (2013). The role of phospholipids in the biological activity and structure of the endoplasmic reticulum. *BBA - Molecular Cell Research,* 1833**,** 2499-2510.

Lee, Eun Jeong, Yun, Un-Jung, Koo, Kyung Hee, Sung, Jee Young, Shim, Jaegal, Ye, Sang-Kyu, Hong, Kyeong-Man & Kim, Yong-Nyun. (2014). Down-regulation of lipid raft-associated onco-proteins via cholesterol-dependent lipid raft internalization in docosahexaenoic acid-induced apoptosis. *BBA - Molecular and Cell Biology of Lipids,* 1841**,** 190-203.

Lee, H. K., Xiang, C., Cazacu, S., Finniss, S., Kazimirsky, G., Lemke, N., Lehman, N. L., Rempel, S. A., Mikkelsen, T. & Brodie, C. (2008). GRP78 is overexpressed in glioblastomas and regulates glioma cell growth and apoptosis. *Neuro Oncol,* 10**,** 236-43.

Li, A., Morton, J. P., Ma, Y., Karim, S. A., Zhou, Y., Faller, W. J., Woodham, E. F., Morris, H. T., Stevenson, R. P., Juin, A., Jamieson, N. B., Mackay, C. J., Carter, C. R., Leung, H. Y., Yamashiro, S., Blyth, K., Sansom, O. J. & Machesky, L. M. (2014a). Fascin is regulated by slug, promotes progression of pancreatic cancer in mice, and is associated with patient outcomes. *Gastroenterology,* 146**,** 1386-96.e1-17.

Li, Chao, Yang, Wei, Zhang, Junli, Zheng, Xin, Yao, Yingmin, Tu, Kangsheng & Liu, Qingguang. (2014b). SREBP-1 Has a Prognostic Role and Contributes to Invasion and Metastasis in Human Hepatocellular Carcinoma. *International J of Molecular Sciences,* 15**,** 7124.

Li, Jing, Wang, Xuling, Zhang, Ting, Wang, Chunling, Huang, Zhenjun, Luo, Xiang & Deng, Yihui. (2015). A review on phospholipids and their main applications in drug delivery systems. *Asian Journal of Pharmaceutical Sciences,* 10**,** 81-98.

Liu, L., Zhang, K., Sandoval, H., Yamamoto, S., Jaiswal, M., Sanz, E., Li, Z., Hui, J., Graham, B. H., Quintana, A. & Bellen, H. J. (2015). Glial lipid droplets and ROS induced by mitochondrial defects promote neurodegeneration. *Cell,* 160**,** 177-90.

Liu, S., Baracos, V. E., Quinney, H. A. & Clandinin, M. T. (1994). Dietary omega-3 and polyunsaturated fatty acids modify fatty acyl composition and insulin binding in skeletal-muscle sarcolemma. *Biochem J,* 299 (Pt 3)**,** 831-7.

Locasale, Jason W., Grassian, Alexandra R., Melman, Tamar, Lyssiotis, Costas A., Mattaini, Katherine R., Bass, Adam J., Heffron, Gregory, Metallo, Christian M., Muranen, Taru, Sharfi, Hadar, Sasaki, Atsuo T., Anastasiou, Dimitrios, Mullarky, Edouard, Vokes, Natalie I., Sasaki, Mika, Beroukhim, Rameen, Stephanopoulos, Gregory, Ligon, Azra H., Meyerson, Matthew, Richardson, Andrea L., Chin, Lynda, Wagner, Gerhard, Asara, John M., Brugge, Joan S., Cantley, Lewis C. & Vander Heiden, Matthew G. (2011). Phosphoglycerate dehydrogenase diverts glycolytic flux and contributes to oncogenesis. *Nat Genet,* 43**,** 869-874.

Lodish H, Berk A, Zipursky Sl, Et Al. (2000). Second Messengers. *Molecular Cell Biology.* 4th ed. New York: W. H. Freeman.

Lombard, J., Lopez-Garcia, P. & Moreira, D. (2012). The early evolution of lipid membranes and the three domains of life. *Nat Rev Microbiol,* 10**,** 507-15.

Louis, D. N. (2006). Molecular pathology of malignant gliomas. *Annu Rev Pathol,* 1**,** 97-117.

Louis, David N., Perry, Arie, Reifenberger, Guido, Von Deimling, Andreas, Figarella-Branger, Dominique, Cavenee, Webster K., Ohgaki, Hiroko, Wiestler, Otmar D., Kleihues, Paul & Ellison, David W. (2016). The 2016 World Health Organization Classification of Tumors of the Central Nervous System: a summary. *Acta Neuropathologica,* 131**,** 803-820.

Louis, David, Ohgaki, Hiroko, Wiestler, Otmar, Cavenee, Webster, Burger, Peter, Jouvet, Anne, Scheithauer, Bernd & Kleihues, Paul. (2007). The 2007 WHO Classification of Tumours of the Central Nervous System. *Acta Neuropathologica,* 114**,** 97-109.

Maddocks, Oliver D. K., Berkers, Celia R., Mason, Susan M., Zheng, Liang, Blyth, Karen, Gottlieb, Eyal & Vousden, Karen H. (2013). Serine starvation

induces stress and p53-dependent metabolic remodelling in cancer cells. *Nature,* 493**,** 542-546.

Mager, W. H. & Winderickx, J. (2005). Yeast as a model for medical and medicinal research. *Trends Pharmacol Sci,* 26**,** 265-73.

Mcneil, P. L. & Steinhardt, R. A. (2003). Plasma membrane disruption: repair, prevention, adaptation. *Annu Rev Cell Dev Biol,* 19**,** 697-731.

Mitchell, Ryan W. & Hatch, Grant M. (2011). Fatty acid transport into the brain: Of fatty acid fables and lipid tails. *Prostaglandins, Leukotrienes and Essential Fatty Acids (PLEFA),* 85**,** 293-302.

Morita, S. Y. & Terada, T. (2015). Enzymatic measurement of phosphatidylglycerol and cardiolipin in cultured cells and mitochondria. *Sci Rep,* 5**,** 11737.

Mullarky, E., Lucki, N. C., Beheshti Zavareh, R., Anglin, J. L., Gomes, A. P., Nicolay, B. N., Wong, J. C., Christen, S., Takahashi, H., Singh, P. K., Blenis, J., Warren, J. D., Fendt, S. M., Asara, J. M., Denicola, G. M., Lyssiotis, C. A., Lairson, L. L. & Cantley, L. C. (2016). Identification of a small molecule inhibitor of 3-phosphoglycerate dehydrogenase to target serine biosynthesis in cancers. *Proc Natl Acad Sci U S A,* 113**,** 1778-83.

Musille, Paul M., Kohn, Jeffrey A. & Ortlund, Eric A. (2013). Phospholipid – Driven gene regulation. *FEBS letters,* 587**,** 1238-1246.

Nakasu, Satoshi, Hirano, Asao, Shimura, Toshiro & Llena, Josefina F. (1987). Incidental meningiomas in autopsy study. *Surgical Neurology,* 27**,** 319-322.

Natter, Klaus & Kohlwein, Sepp D. (2013). Yeast and cancer cells – common principles in lipid metabolism. *Biochimica et Biophysica Acta (BBA) - Molecular and Cell Biology of Lipids,* 1831**,** 314-326.

Nguyen, L. N., Ma, D., Shui, G., Wong, P., Cazenave-Gassiot, A., Zhang, X., Wenk, M. R., Goh, E. L. & Silver, D. L. (2014). Mfsd2a is a transporter for the essential omega-3 fatty acid docosahexaenoic acid. *Nature,* 509**,** 503-6.

Nielsen, Malene Schjønning, Christensen, Helle Collatz, Kosteljanetz, Michael & Johansen, Christoffer. (2009). Incidence of and survival from oligodendroglioma in Denmark, 1943–2002. *Neuro-Oncology,* 11**,** 311-317.

Nieman, K. M., Kenny, H. A., Penicka, C. V., Ladanyi, A., Buell-Gutbrod, R., Zillhardt, M. R., Romero, I. L., Carey, M. S., Mills, G. B., Hotamisligil, G. S., Yamada, S. D., Peter, M. E., Gwin, K. & Lengyel, E. (2011). Adipocytes promote ovarian cancer metastasis and provide energy for rapid tumor growth. *Nat Med,* 17**,** 1498-503.

Nomura, Daniel K., Long, Jonathan Z., Niessen, Sherry, Hoover, Heather S., Ng, Shu-Wing & Cravatt, Benjamin F. (2010). Monoacylglycerol Lipase Regulates a Fatty Acid Network that Promotes Cancer Pathogenesis. *Cell,* 140**,** 49-61.

Norris, Sarah E., Friedrich, Michael G., Mitchell, Todd W., Truscott, Roger J. W. & Else, Paul L. (2015). Human prefrontal cortex phospholipids containing docosahexaenoic acid increase during normal adult aging, whereas those

containing arachidonic acid decrease. *Neurobiology of Aging,* 36**,** 1659-1669.

Ou, Y., Wang, S. J., Jiang, L., Zheng, B. & Gu, W. (2015). p53 Protein-mediated regulation of phosphoglycerate dehydrogenase (PHGDH) is crucial for the apoptotic response upon serine starvation. *J Biol Chem,* 290**,** 457-66.

Pang, L. Q., Liang, Q. L., Wang, Y. M., Ping, L. & Luo, G. A. (2008). Simultaneous determination and quantification of seven major phospholipid classes in human blood using normal-phase liquid chromatography coupled with electrospray mass spectrometry and the application in diabetes nephropathy. *J Chromatogr B Analyt Technol Biomed Life Sci,* 869**,** 118-25.

Park, Eek Joong, Lee, Jun Hee, Yu, Guann-Yi, He, Guobin, Ali, Syed Raza, Holzer, Ryan G., Österreicher, Christoph H., Takahashi, Hiroyuki & Karin, Michael. (2010). Dietary and Genetic Obesity Promote Liver Inflammation and Tumorigenesis by Enhancing IL-6 and TNF Expression. *Cell,* 140**,** 197-208.

Park, Sunghee, Chang, Ching-Yi, Safi, Rachid, Liu, Xiaojing, Baldi, Robert, Jasper, Jeff s, Anderson, Grace r, Liu, Tingyu, Rathmell, Jeffrey c, Dewhirst, Mark w, Wood, Kris c, Locasale, Jason w & Mcdonnell, Donald p. (2016). ERRα-Regulated Lactate Metabolism Contributes to Resistance to Targeted Therapies in Breast Cancer. *Cell Reports,* 15**,** 323-335.

Patel, Alok, Arora, Neha, Sartaj, Km, Pruthi, Vikas & Pruthi, Parul A. (2016). Sustainable biodiesel production from oleaginous yeasts utilizing hydrolysates of various non-edible lignocellulosic biomasses. *Renewable and Sustainable Energy Reviews,* 62**,** 836-855.

Peetla, Chiranjeevi, Vijayaraghavalu, Sivakumar & Labhasetwar, Vinod (2013). Biophysics of cell membrane lipids in cancer drug resistance: Implications for drug transport and drug delivery with nanoparticles. *Advanced Drug Delivery Reviews,* 65**,** 1686-1698.

Peregrin-Alvarez, J. M., Sanford, C. & Parkinson, J. (2009). The conservation and evolutionary modularity of metabolism. *Genome Biol,* 10**,** R63.

Pflaum, J., Schlosser, S. & Muller, M. (2014). p53 Family and Cellular Stress Responses in Cancer. *Front Oncol,* 4**,** 285.

Pollay, M. (2010). The function and structure of the cerebrospinal fluid outflow system. *Cerebrospinal Fluid Res,* 7**,** 9.

Possemato, R., Marks, K. M., Shaul, Y. D., Pacold, M. E., Kim, D., Birsoy, K., Sethumadhavan, S., Woo, H. K., Jang, H. G., Jha, A. K., Chen, W. W., Barrett, F. G., Stransky, N., Tsun, Z. Y., Cowley, G. S., Barretina, J., Kalaany, N. Y., Hsu, P. P., Ottina, K., Chan, A. M., Yuan, B., Garraway, L. A., Root, D. E., Mino-Kenudson, M., Brachtel, E. F., Driggers, E. M. & Sabatini, D. M. (2011). Functional genomics reveal that the serine synthesis pathway is essential in breast cancer. *Nature,* 476**,** 346-50.

Rashid, A., Pizer, E. S., Moga, M., Milgraum, L. Z., Zahurak, M., Pasternack, G. R., Kuhajda, F. P. & Hamilton, S. R. (1997). Elevated expression of fatty acid synthase and fatty acid synthetic activity in colorectal neoplasia. *Am J Pathol,* 150**,** 201-8.

Ribatti, D. (2014). The discovery of angiogenic growth factors: the contribution of Italian scientists. *Vasc Cell,* 6**,** 8.

Riemenschneider, M. J., Perry, A. & Reifenberger, G. (2006). Histological classification and molecular genetics of meningiomas. *Lancet Neurol,* 5**,** 1045-54.

Rolph, Carole, Moreton, Rod & Harwood, John. (1989). Acyl lipid metabolism in the oleaginous yeast *Rhodotorula gracilis* (CBS 3043). *Lipids,* 24**,** 715-720.

Santolla, M. F., Lappano, R., De Marco, P., Pupo, M., Vivacqua, A., Sisci, D., Abonante, S., Iacopetta, D., Cappello, A. R., Dolce, V. & Maggiolini, M. (2012). G protein-coupled estrogen receptor mediates the up-regulation of fatty acid synthase induced by 17beta-estradiol in cancer cells and cancer-associated fibroblasts. *J Biol Chem,* 287**,** 43234-45.

Santos, C. R. & Schulze, A. (2012). Lipid metabolism in cancer. *Febs j,* 279**,** 2610-23.

Sawazaki, S., Salem, N., Jr. & Kim, H. Y. (1994). Lipoxygenation of docosahexaenoic acid by the rat pineal body. *J Neurochem,* 62**,** 2437-47.

Scheithauer, Bernd W. (2009). Development of the WHO Classification of Tumors of the Central Nervous System: A Historical Perspective. *Brain Pathology,* 19**,** 551-564.

Seguin, F., Carvalho, M. A., Bastos, D. C., Agostini, M., Zecchin, K. G., Alvarez-Flores, M. P., Chudzinski-Tavassi, A. M., Coletta, R. D. & Graner, E. (2012). The fatty acid synthase inhibitor orlistat reduces experimental metastases and angiogenesis in B16-F10 melanomas. *Br J Cancer,* 107**,** 977-87.

Sehmer, E. A., Hall, G. J., Greenberg, D. C., O'hara, C., Wallingford, S. C., Wright, K. A. & Green, A. C. (2014). Incidence of glioma in a northwestern region of England, 2006-2010. *Neuro Oncol,* 16**,** 971-4.

Shi, X., Li, J., Zou, X., Greggain, J., Rodkaer, S. V., Faergeman, N. J., Liang, B. & Watts, J. L. (2013). Regulation of lipid droplet size and phospholipid composition by stearoyl-CoA desaturase. *J Lipid Res,* 54**,** 2504-14.

Sidhu, Vishaldeep K., Huang, Bill X., Desai, Abhishek, Kevala, Karl & Kim, Hee-Yong. (2016). Role of DHA in aging-related changes in mouse brain synaptic plasma membrane proteome. *Neurobiology of Aging,* 41**,** 73-85.

Sitepu, I. R., Garay, L. A., Sestric, R., Levin, D., Block, D. E., German, J. B. & Boundy-Mills, K. L. (2014). Oleaginous yeasts for biodiesel: current and future trends in biology and production. *Biotechnol Adv,* 32**,** 1336-60.

Sleight, R. G. & Pagano, R. E. (1985). Transbilayer movement of a fluorescent phosphatidylethanolamine analogue across the plasma membranes of cultured mammalian cells. *J Biol Chem,* 260**,** 1146-54.

Sok, M., Sentjurc, M., Schara, M., Stare, J. & Rott, T. (2002). Cell membrane fluidity and prognosis of lung cancer. *Ann Thorac Surg,* 73**,** 1567-71.

Song, E. A. & Kim, H. (2016). Docosahexaenoic Acid Induces Oxidative DNA Damage and Apoptosis, and Enhances the Chemosensitivity of Cancer Cells. *Int J Mol Sci,* 17.

Spector, A. A., Mathur, S. N., Kaduce, T. L. & Hyman, B. T. (1980). Lipid nutrition and metabolism of cultured mammalian cells. *Prog Lipid Res,* 19**,** 155-86.

Spector, A. A. & Yorek, M. A. (1985). Membrane lipid composition and cellular function. *J Lipid Res,* 26**,** 1015-35.

Spencer, Brian J. & Verma, Inder M. (2007). Targeted delivery of proteins across the blood–brain barrier. *Proceedings of the National Academy of Sciences,* 104**,** 7594-7599.

Staedtke, V., Brahler, M., Muller, A., Georgieva, R., Bauer, S., Sternberg, N., Voigt, A., Lemke, A., Keck, C., Moschwitzer, J. & Baumler, H. (2010). In vitro inhibition of fungal activity by macrophage-mediated sequestration and release of encapsulated amphotericin B nanosupension in red blood cells. *Small,* 6**,** 96-103.

Steelman, L. S., Chappell, W. H., Abrams, S. L., Kempf, R. C., Long, J., Laidler, P., Mijatovic, S., Maksimovic-Ivanic, D., Stivala, F., Mazzarino, M. C., Donia, M., Fagone, P., Malaponte, G., Nicoletti, F., Libra, M., Milella, M., Tafuri, A., Bonati, A., Basecke, J., Cocco, L., Evangelisti, C., Martelli, A. M., Montalto, G., Cervello, M. & Mccubrey, J. A. (2011). Roles of the Raf/MEK/ERK and PI3K/PTEN/Akt/mTOR pathways in controlling growth and sensitivity to therapy-implications for cancer and aging. *Aging (Albany NY),* 3**,** 192-222.

Subbaiah, Papasani V., Dammanahalli, Karigowda J., Yang, Peng, Bi, Jian & O'donnell, J. Michael. (2016). Enhanced incorporation of dietary DHA into lymph phospholipids by altering its molecular carrier. *Biochimica et Biophysica Acta (BBA) - Molecular and Cell Biology of Lipids,* 1861**,** 723-729.

Sugiyama, Kazuhiko, Hirano, Asao, Llena, Josefina F., Uozumi, Tohru, Kurisu, Kaoru, Harada, Kunyu, Taniguchi, Eiji & Nishi, Tohru. (1996). Incidental Meningiomas in Autopsy Cases in Computed Tomography and Magnetic Resonance Imaging Era. *In:* NAGAI, M. (ed.) *Brain Tumor: Research and Therapy.* Tokyo: Springer Japan.

Sun, L., Song, L., Wan, Q., Wu, G., Li, X., Wang, Y., Wang, J., Liu, Z., Zhong, X., He, X., Shen, S., Pan, X., Li, A., Wang, Y., Gao, P., Tang, H. & Zhang, H. (2015). cMyc-mediated activation of serine biosynthesis pathway is critical for cancer progression under nutrient deprivation conditions. *Cell Res,* 25**,** 429-44.

Sun, Yanan, Su, Jing, Liu, Geyi, Chen, Jianjun, Zhang, Xiumei, Zhang, Ran, Jiang, Minhan & Qiu, Mingfeng. (2017). Advances of blood cell-based drug delivery systems. *J of Pharmaceutical Sciences,* 96**,** 115-128.

Tabatabaie, L., Klomp, L. W., Berger, R. & De Koning, T. J. (2010). l-Serine synthesis in the central nervous system: A review on serine deficiency disorders. *Mol Genetics and Metabolism,* 99**,** 256-262.

Tavano, Lorena & Muzzalupo, Rita. (2016). Multi-functional vesicles for cancer therapy: The ultimate magic bullet. *Colloids and Surfaces B: Biointerfaces,* 147**,** 161-171.

Taylor, Aliki J., Frobisher, Clare, Ellison, David W., Reulen, Raoul C., Winter, David L., Taylor, Roger E., Stiller, Charles A., Lancashire, Emma R., Tudor, Edward C.G., Baggott, Christina, May, Shaun & Hawkins, Mike M. (2009). Survival After Second Primary Neoplasms of the Brain or Spinal

Cord in Survivors of Childhood Cancer: Results From the British Childhood Cancer Survivor Study. *J of Clinical Oncology,* 27**,** 5781-5787.

Thiele, Christoph & Spandl, Johanna (2008). Cell biology of lipid droplets. *Current Opinion in Cell Biology,* 20**,** 378-385.

Thun, Michael J., Delancey, John Oliver, Center, Melissa M., Jemal, Ahmedin & Ward, Elizabeth M. (2010). The global burden of cancer: priorities for prevention. *Carcinogenesis,* 31**,** 100-110.

Tremblay, M. E., Zhang, I., Bisht, K., Savage, J. C., Lecours, C., Parent, M., Titorenko, V. & Maysinger, D. (2016). Remodeling of lipid bodies by docosahexaenoic acid in activated microglial cells. *J Neuroinflammation,* 13**,** 116.

Tsun, Zhi-Yang & Possemato, Richard. (2015). Amino acid management in cancer. *Seminars in Cell & Developmental Biology,* 43**,** 22-32.

Usenius, J. P., Vainio, P., Hernesniemi, J. & Kauppinen, R. A. (1994). Choline-containing compounds in human astrocytomas studied by 1H NMR spectroscopy in vivo and in vitro. *J Neurochem,* 63**,** 1538-43.

Van Meer, G., Voelker, D. R. & Feigenson, G. W. (2008). Membrane lipids: where they are and how they behave. *Nat Rev Mol Cell Biol,* 9**,** 112-24.

Vance, Dennis E. & Vance, Jean E. (2008). Chapter 8 - Phospholipid biosynthesis in eukaryotes. *In:* DENNIS, E. V. & JEAN, E. V. (eds.) *Biochem of Lipids, Lipoproteins and Membranes (Fifth Edition).* San Diego: Elsevier.

Vander Heiden, M. G., Christofk, H. R., Schuman, E., Subtelny, A. O., Sharfi, H., Harlow, E. E., Xian, J. & Cantley, L. C. (2010). Identification of small molecule inhibitors of pyruvate kinase M2. *Biochem Pharmacol,* 79**,** 1118-24.

Visser, Otto, Ardanaz, Eva, Botta, Laura, Sant, Milena, Tavilla, Andrea & Minicozzi, Pamela. (2015). Survival of adults with primary malignant brain tumours in Europe; Results of the EUROCARE-5 study. *European J of Cancer,* 51**,** 2231-2241.

Walther, Tobias C. & Farese Jr, Robert V. (2009). The life of lipid droplets. *Biochimica et Biophysica Acta (BBA) - Molecular and Cell Biology of Lipids,* 1791**,** 459-466.

Wang, C. & Youle, R. J. (2009). The role of mitochondria in apoptosis*. *Annu Rev Genet,* 43**,** 95-118.

Wang, J., Lu, Z., Gao, Y., Wientjes, M. G. & Au, J. L. (2011). Improving delivery and efficacy of nanomedicines in solid tumors: role of tumor priming. *Nanomedicine (Lond),* 6**,** 1605-20.

Wang, Jing-Zhang, Xiao, Ning, Zhang, Ying-Zhou, Zhao, Chao-Xian, Guo, Xin-Hua & Lu, Li-Min. (2016). Mfsd2a-based pharmacological strategies for drug delivery across the blood–brain barrier. *Pharmacological Res,* 104**,** 124-131.

Wang, Q., Liberti, M. V., Liu, P., Deng, X., Liu, Y., Locasale, J. W. & Lai, L. (2017). Rational Design of Selective Allosteric Inhibitors of PHGDH and Serine Synthesis with Anti-tumor Activity. *Cell Chem Biol,* 24**,** 55-65.

Wang, Wen-An, Groenendyk, Jody & Michalak, Marek (2014). Endoplasmic reticulum stress associated responses in cancer. *BBA - Molecular Cell Research,* 1843**,** 2143-2149.

Wang, Z. & Sun, Y. (2010). Targeting p53 for Novel Anticancer Therapy. *Transl Oncol,* 3**,** 1-12.

Warburg, O. (1956). On the origin of cancer cells. *Science,* 123**,** 309-14.

Warburg, O. (1925). Uber den Stoffwechsel der Carcinomzelle (About the metabolism of the carcinoma cell). *Klin Wochenschr Berl,* 4**,** 534-536.

Werstuck, G. H., Lentz, S. R., Dayal, S., Hossain, G. S., Sood, S. K., Shi, Y. Y., Zhou, J., Maeda, N., Krisans, S. K., Malinow, M. R. & Austin, R. C. (2001). Homocysteine-induced endoplasmic reticulum stress causes dysregulation of the cholesterol and triglyceride biosynthetic pathways. *J Clin Invest,* 107**,** 1263-73.

Xian, Y., Zhang, S., Wang, X., Qin, J., Wang, W. & Wu, H. (2016). Phosphoglycerate dehydrogenase is a novel predictor for poor prognosis in gastric cancer. *Onco Targets Ther,* 9**,** 5553-60.

Xing, P., Li, J. G., Jin, F., Zhao, T. T., Liu, Q., Dong, H. T. & Wei, X. L. (2011). Fascin, an actin-bundling protein, promotes breast cancer progression in vitro. *Cell Biochem Funct,* 29**,** 303-10.

Xu, R., Pisapia, D. & Greenfield, J. P. (2016). Malignant Transformation in Glioma Steered by an Angiogenic Switch: Defining a Role for Bone Marrow-Derived Cells. *Cureus,* 8**,** e471.

Yamasaki, M., Yamada, K., Furuya, S., Mitoma, J., Hirabayashi, Y. & Watanabe, M. (2001). 3-Phosphoglycerate dehydrogenase, a key enzyme for l-serine biosynthesis, is preferentially expressed in the radial glia/astrocyte lineage and olfactory ensheathing glia in the mouse brain. *J Neurosci,* 21**,** 7691-704.

Yamashita, A., Hayashi, Y., Nemoto-Sasaki, Y., Ito, M., Oka, S., Tanikawa, T., Waku, K. & Sugiura, T. (2014). Acyltransferases and transacylases that determine the fatty acid composition of glycerolipids and the metabolism of bioactive lipid mediators in mammalian cells and model organisms. *Prog Lipid Res,* 53**,** 18-81.

Yamashita, Satoshi & Nikawa, Jun-Ichi (1997). Phosphatidylserine synthase from yeast. *BBA - Lipids and Lipid Metabolism,* 1348**,** 228-235.

Yen, C. L. E., Stone, S. J., Koliwad, S., Harris, C. & Farese, R. V. (2008a). DGAT enzymes and triacylglycerol biosynthesis. *J Lipid Res,* 49.

Yen, C. L., Stone, S. J., Koliwad, S., Harris, C. & Farese, R. V., Jr. (2008b). Thematic review series: glycerolipids. DGAT enzymes and triacylglycerol biosynthesis. *J Lipid Res,* 49**,** 2283-301.

Yetukuri, Laxman, Ekroos, Kim, Vidal-Puig, Antonio & Oresic, Matej. (2008). Informatics and computational strategies for the study of lipids. *Molecular BioSystems,* 4**,** 121-127.

Zaugg, K., Yao, Y., Reilly, P. T., Kannan, K., Kiarash, R., Mason, J., Huang, P., Sawyer, S. K., Fuerth, B., Faubert, B., Kalliomaki, T., Elia, A., Luo, X., Nadeem, V., Bungard, D., Yalavarthi, S., Growney, J. D., Wakeham, A., Moolani, Y., Silvester, J., Ten, A. Y., Bakker, W., Tsuchihara, K., Berger,

S. L., Hill, R. P., Jones, R. G., Tsao, M., Robinson, M. O., Thompson, C. B., Pan, G. & Mak, T. W. (2011). Carnitine palmitoyltransferase 1C promotes cell survival and tumor growth under conditions of metabolic stress. *Genes Dev,* 25**,** 1041-51.

Zenaro, Elena, Piacentino, Gennj & Constantin, Gabriela. (2015). The blood-brain barrier in Alzheimer's disease. *Neuro of Disease.*

Zhou, P., Qian, L., Zhou, T. & Iadecola, C. (2005). Mitochondria are involved in the neurogenic neuroprotection conferred by stimulation of cerebellar fastigial nucleus. *J Neurochem,* 95**,** 221-9.

Zhou, Shengtao, Huang, Canhua & Wei, Yuquan. (2010). The metabolic switch and its regulation in cancer cells. *SCIENCE CHINA Life Sciences,* 53**,** 942-958.

Zhu, Haiyan, Luo, Hui, Zhu, Xuejie, Hu, Xiaoli, Zheng, Lihong & Zhu, Xueqiong. (2016). Pyruvate kinase M2 (PKM2) expression correlates with prognosis in solid cancers: a meta-analysis. *Oncotarget,* 8.

Zweytick, Dagmar, Athenstaedt, Karin & Daum, Günther. (2000). Intracellular lipid particles of eukaryotic cells. *Biochimica et Biophysica Acta (BBA) - Reviews on Biomembranes,* 1469**,** 101-120.

Chapter 7

Appendix

7.1 APPENDIX 1

The incidence of cancer has increased over the past few decades; Figure 7.1 shows the number of diagnoses of brain cancer in those individuals over the age of 90 in the UK.
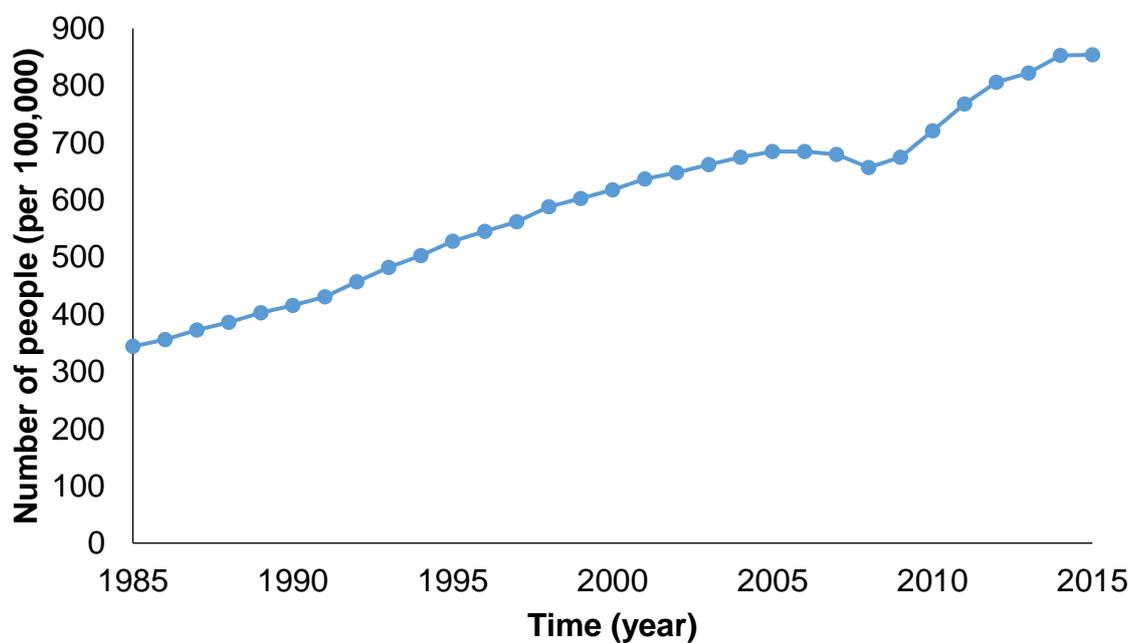

Figure 7.1: Graph showing how the number of people in the UK aged >90 (per 100,000) being diagnosed with brain cancer increasing from 1985 till 2015.

The phylogenetic relationship between this studies model organism, *L. starkeyi* and the well researched Baker's yeast, *S. cerevisiae*. Figure 7.2 shows the basis as to why the two yeasts accrue lipids differently.
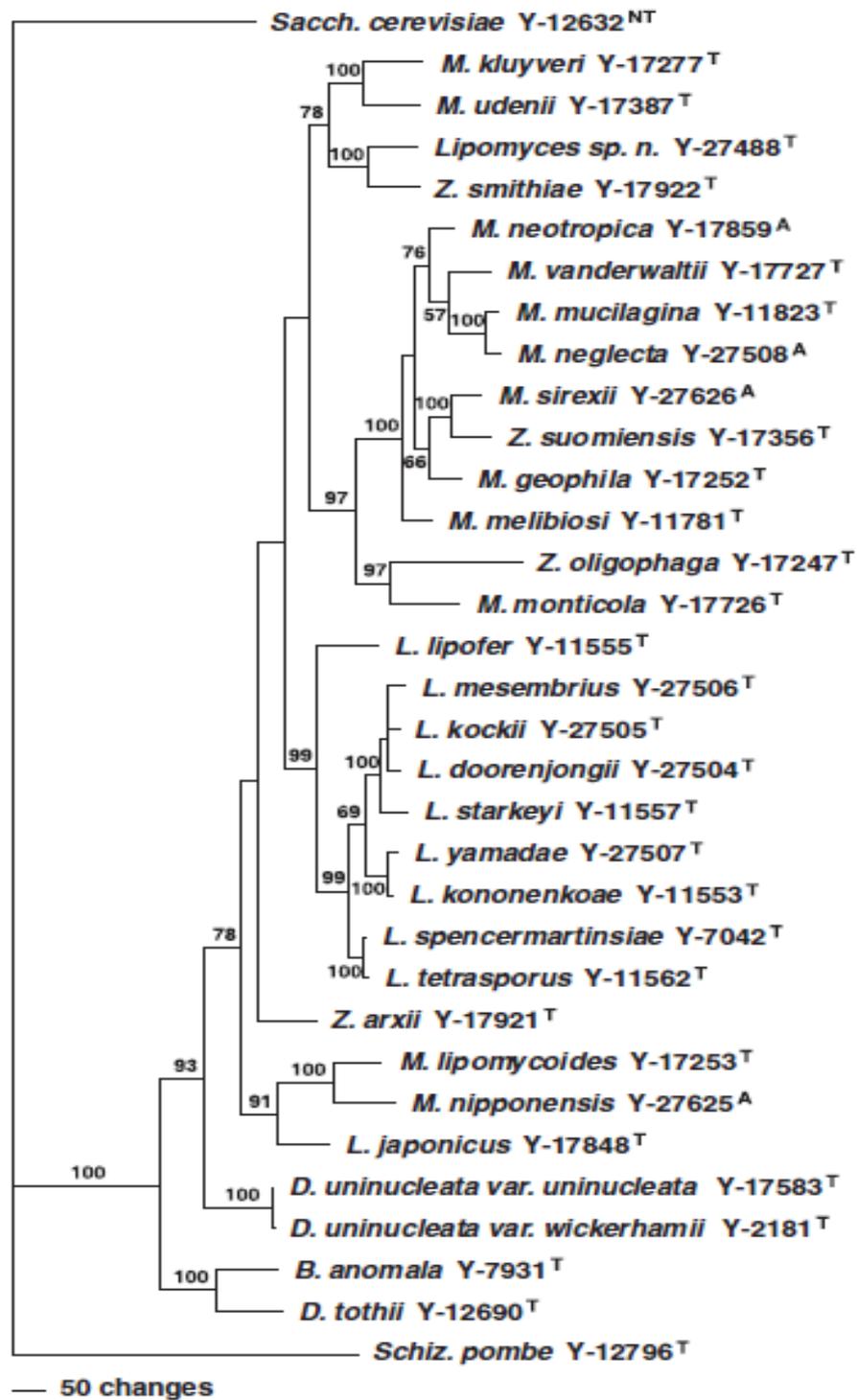

Figure 7: A parsimonious tree summarising the phylogenetic relationship between Lipomycetaceae (Kurtzman et al., 2007).

7.3 APPENDIX 3

Ethical approval for the thesis was gained from Brain Tumour North West in accordance with Royal Preston Hospital. The STEM reference number for this research was 121.

Application for clinical samples/data from the

Brain Tumour North West and

the Walton Research Tissue Banks

Applicant: Duration of Project: Till March 2016

Name: Hayley Hatchell

Address: UCLan

Preston

Lancashire

PR12HE

Tel: 01772201201

Email: hhatchell@uclan.ac.uk

Project Title: Tumour associated lipid signatures in Brain Tumours- Metabolic clues to reveal potential therapeutic targets.

Funding:

Is the funding for the project

b) internal (eg funded from a researchers laboratory or institutional budget)

If the project has been submitted as a grant application for external funding?   N/A

Was the application successful?   yes / no

Was the project externally peer-reviewed?   yes / no

External Funding body: N/A

Details of Funding: Total £N/A (staff N/A and consumables N/A)

Research Sponsor: N/A

Approvals:

Ethics Approval

Does the project have ethics approval?   yes

If yes, please supply reference number STEM121 and date of approval

The Tissue Bank has generic ethical approval to supply tissue/data for projects conducted by internal applicants, without the need for further ethics approval. External researchers wishing to use tissue or data supplied by the bank need to apply to REC for individual ethical approval.

Research Governance

a) Are the applicants employed by NHS establishment(s)?   no

b) Does the project involve research activity using the anonymised samples/data in an NHS establishment?   no

If yes to a or b, the project may require research governance approval and applicants should consult the Research Governance Manager at their hospital

Co-applicants: Name   N/A   Affiliation   N/A

Outline of Project

Title:

Tumour associated lipid signatures in Brain Tumours- Metabolic clues to reveal potential therapeutic targets.

Introduction

A preliminary study involving human meningioma tissue revealed unusually high levels of phosphatidylserine (PS) enriched with Docosahexaenoic acid (DHA) compared to other areas of the Brain. In order to study this phenomenon further in terms of cellular proliferation, metabolism and apoptosis, we have developed an oleaginous yeast paradigm.

Tissue Required – *Please indicate whether you require paraffin embedded tissue, fresh frozen tissue, cellular component of blood, plasma or serum and how many samples you require.*

Please indicate if all samples are required at the start of the project or if further applications for samples will be made in the light of initial findings.

We will be initially looking at 4 anti-bodies and one control per antibody.

- Tissue sections: Meningioma of various grades
  Glioma of various grades

  GBM

- Tissue samples (vials):   Meningioma Grade II (frozen)
  (as many as we can get from original study as not enough left to do all aspects of research)

  Glioma

If possible, please can we have matched samples such that we can compare/contrast the results of lipid profile and immunohistochemistry work between Glioma and Meningioma. Require if possible ten samples of each Glioma type which can be matched to the meningioma patient set. Frozen samples will be used for lipid extraction(s) analysing the phospholipid signature,

methyl esters, cholesterol status alongside future investigation into glycolytic flux via enzyme assays etc.

Please also provide a brief lay summary (maximum 200 words)

Examine the expression of several key markers which can possibly further characterise Glioma and Meningioma grades which will further aid diagnosis and avenues for future therapeutic targets.

For further information please contact:

BTNW Tissue Bank: Prof T Dawson email: Timothy.Dawson@lthtr.nhs.uk

Walton Research Tissue Bank: Dr C Walker email: carol.walker@thewaltoncentre.nhs.uk

Please email completed applications to:

BTNW Tissue Bank: Prof T Dawson email: Timothy.Dawson@lthtr.nhs.uk

Walton Research Tissue Bank: Dr C Walker email: carol.walker@thewaltoncentre.nhs.uk

Or to both for joint applications to both banks

Date Application Received	12/05/2015
Application Number	1505
Project Title	Tumour associated lipid signatures in Brain Tumours- Metabolic clues to reveal potential therapeutic targets.
Date sent to BTNW/WRTB Review Panel	12/05/15
Names of Reviewers	Prof T P Dawson Dr J E Alder Mr G Hall

Decision of BTNW/WRTB Committees	Approve Date: 18/06/2015

7.4 APPENDIX 4

Table 7.1 shows the meningioma tissue sections used in Chapter 3 and 4.

Table 7.1: Histological classifications of meningioma tissue sections provided by Royal Preston Hospital.

| BTNW	Sex	Type	Grade	PR status	ER status	Ki67
1	F	Microcystic	I	5% +ve	Cytoplasmic blushing	1-2%
36	M	Meningothelial	I	Patchy weak/mod 30-40% +ve	-ve	<5%
88	F	Meningothelial	I	>90% +ve	-ve	1-2%
91	F	Meningothelial	I	>90% +ve	-ve	Not stated
95	F	Not stated	I	30-40% +ve	-ve	Not stated
99	F	Not stated	I	-ve	-ve	5-8%
118	F	Transitional	I	Mod/strong >60% +ve	Occ weak +ve	Not stated
145	F	Transitional	I	50% +ve	Not stated	5-10%
143	F	Atypical	II	Weak, scant	-ve	5%
198	F	Atypical	II	5% +ve	-ve	20%
286	F	Choroid	II	Strong >75% +ve	Not stated	~5-8%
392	F	Atypical	II	+ve	-ve	15%
395	F	Atypical	II	75% +ve	Not stated	15%
457	M	Meningothelial	II	Most cells strongly +ve	-ve	10%
677	M	Atypical	II	50%	-ve	7%
708	M	Benign	II	25%	-ve	<1%
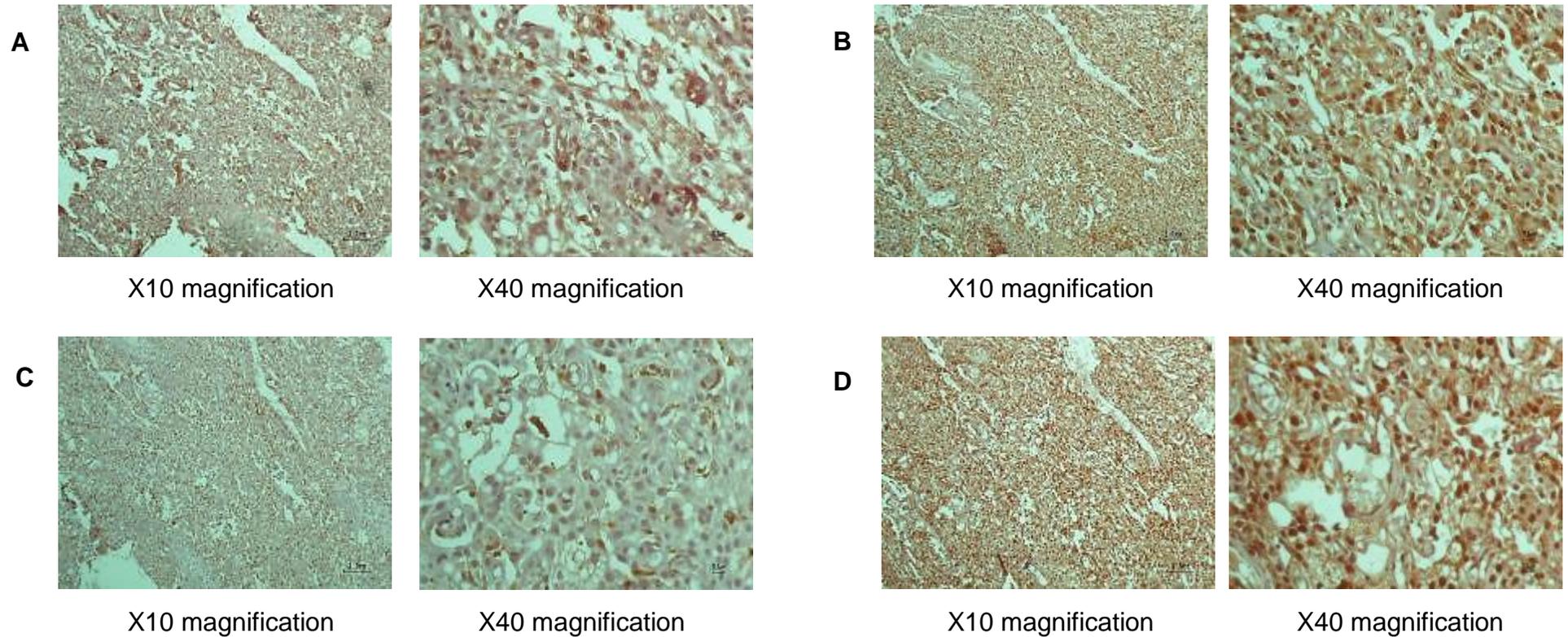
Figure 7.3: Photographic visualisation via light microscopy of the immunohistochemistry antibody expression profiles associated with serine biosynthetic and glycolytic pathways in the tissue sections belongings to patient 1, a grade I meningioma patient (n=1). Antibodies of interest include; p53 (A), PKM2 (B), Fascin (C) and PHGDH (D). Incubation with DAB (6 minutes) enables antibody presence, appears brown. H&E counterstain followed DAB incubation, appearing blue in color allowing indication of cellular bodies.

A

X10 magnification   X40 magnification

B

X10 magnification   X40 magnification

C

X10 magnification   X40 magnification
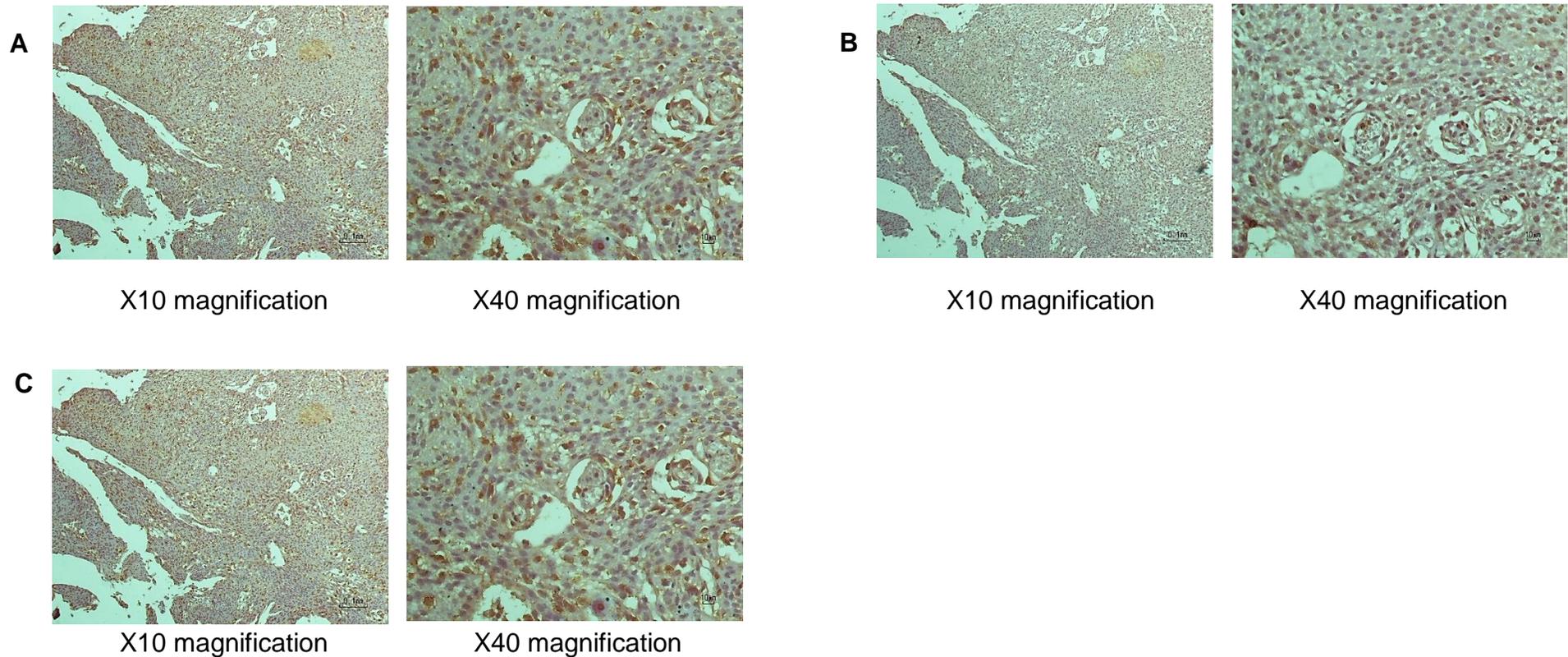
Figure 7.4: Photographic visualisation via light microscopy of the immunohistochemistry antibody expression profiles associated with serine biosynthetic and glycolytic pathways in the tissue sections belongings to patient 88, a grade I meningioma patient (n=1). Antibodies of interest include; p53 (A), PKM2 (B) and Fascin (C). Incubation with DAB (6 minutes) enables antibody presence, appears brown. H&E counterstain followed DAB incubation, appearing blue in color allowing indication of cellular bodies.

A

X10 magnification   X40 magnification

B

X10 magnification   X40 magnification

C

X10 magnification   X40 magnification
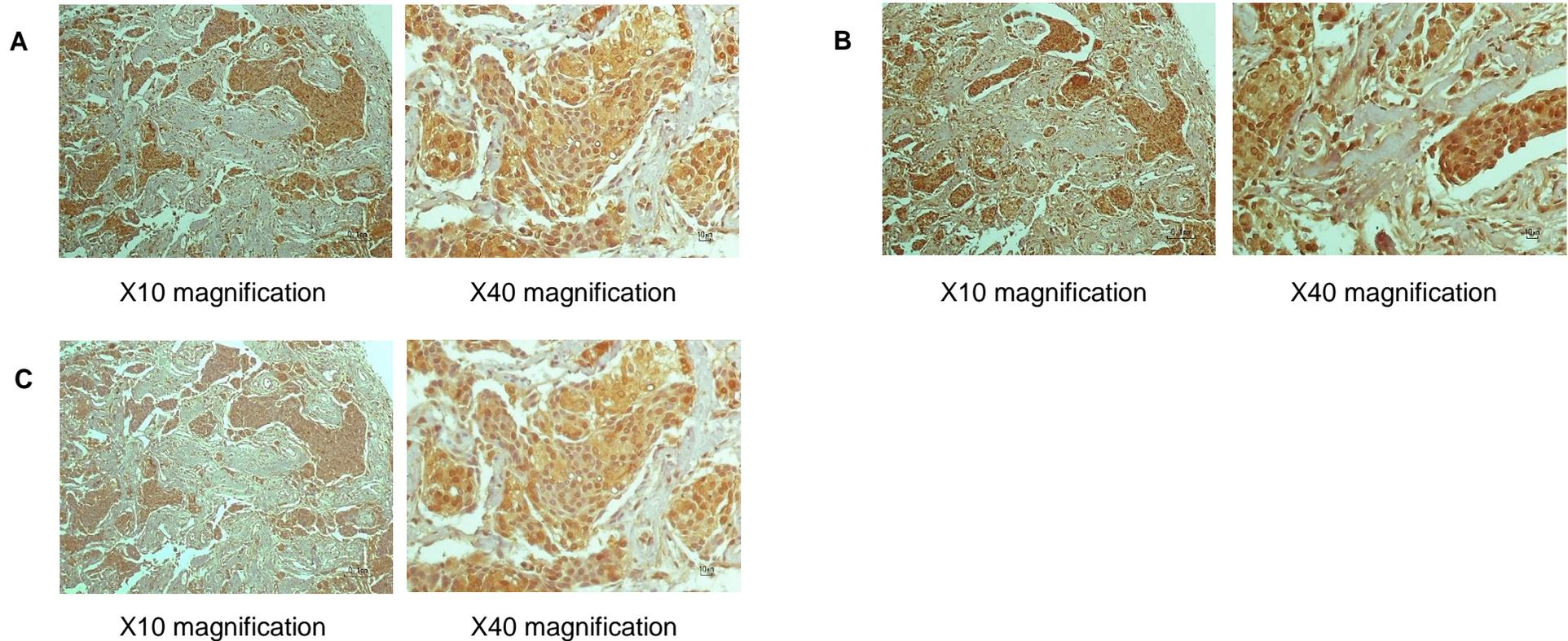
Figure 7.5: Photographic visualisation via light microscopy of the immunohistochemistry antibody expression profiles associated with serine biosynthetic and glycolytic pathways in the tissue sections belongings to patient 91, a grade I meningioma patient (n=1). Antibodies of interest include; p53 (A), PKM2 (B) and Fascin (C). Incubation with DAB (6 minutes) enables antibody presence, appears brown. H&E counterstain followed DAB incubation, appearing blue in color allowing indication of cellular bodies.

A

X10 magnification   X40 magnification

B

X10 magnification   X40 magnification

C

X10 magnification   X40 magnification
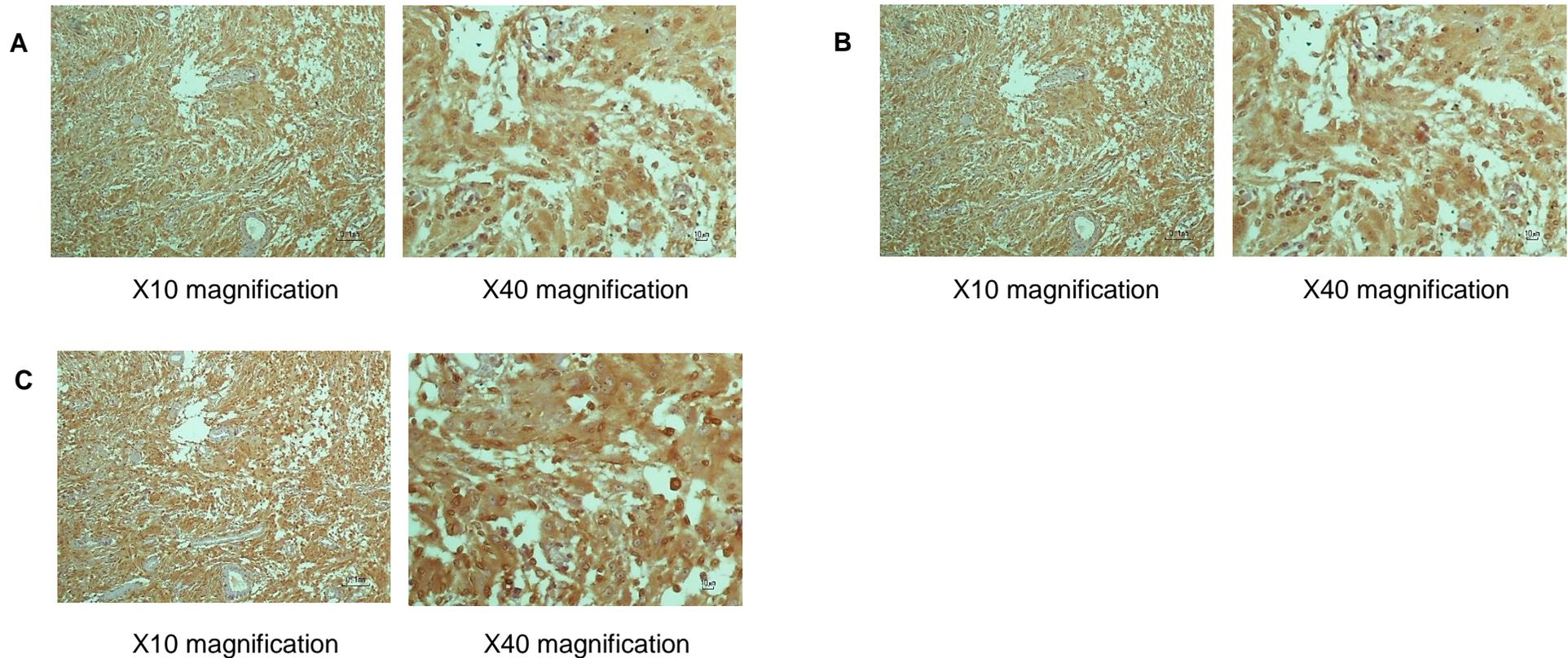
Figure 7.6: Photographic visualisation via light microscopy of the immunohistochemistry antibody expression profiles associated with serine biosynthetic and glycolytic pathways in the tissue sections belongings to patient 95, a grade I meningioma patient (n=1). Antibodies of interest include; p53 (A), PKM2 (B) and Fascin (C). Incubation with DAB (6 minutes) enables antibody presence, appears brown. H&E counterstain followed DAB incubation, appearing blue in color allowing indication of cellular bodies.

A

X10 magnification   X40 magnification

B

X10 magnification   X40 magnification

C

X10 magnification   X40 magnification
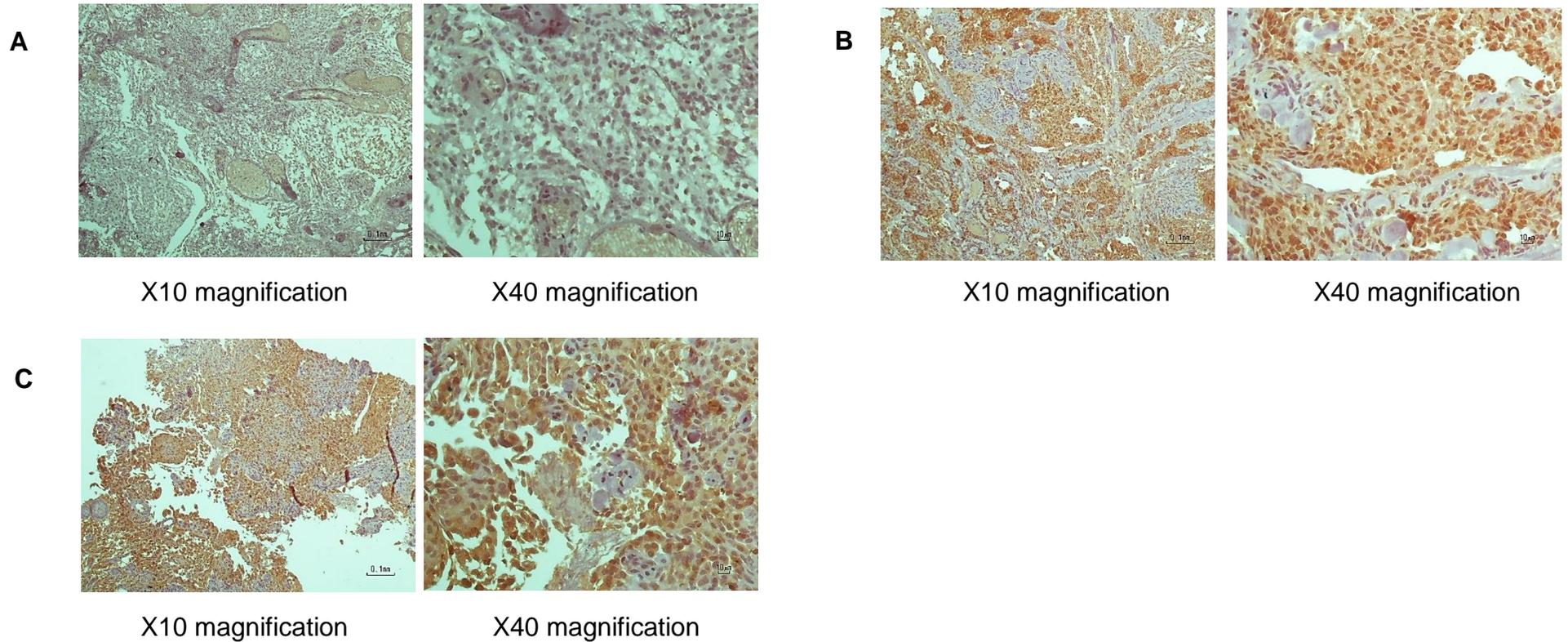
Figure 7.7: Photographic visualisation via light microscopy of the immunohistochemistry antibody expression profiles associated with serine biosynthetic and glycolytic pathways in the tissue sections belongings to patient 99, a grade I meningioma patient (n=1). Antibodies of interest include; p53 (A), PKM2 (B) and Fascin (C). Incubation with DAB (6 minutes) enables antibody presence, appears brown. H&E counterstain followed DAB incubation, appearing blue in color allowing indication of cellular bodies.
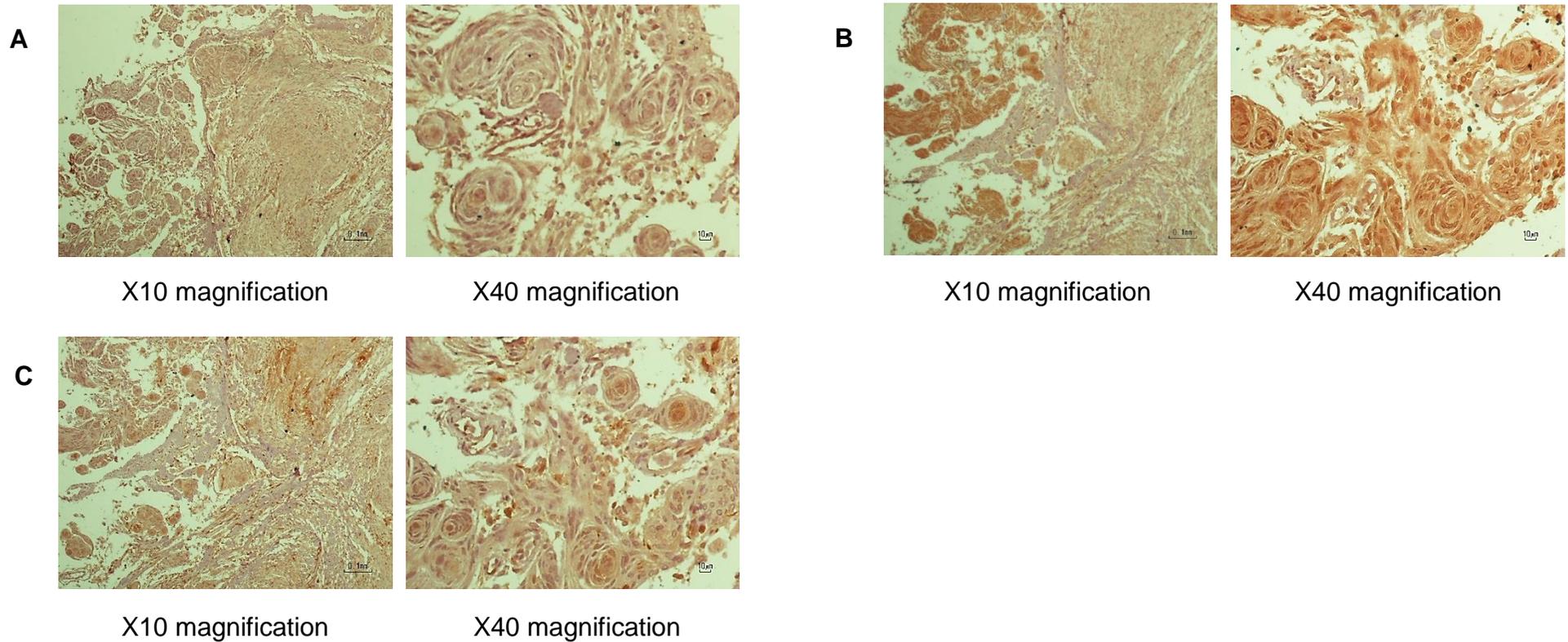
Figure 7.8: Photographic visualisation via light microscopy of the immunohistochemistry antibody expression profiles associated with serine biosynthetic and glycolytic pathways in the tissue sections belongings to patient 118, a grade I meningioma patient (n=1). Antibodies of interest include; p53 (A), PKM2 (B) and Fascin (C). Incubation with DAB (6 minutes) enables antibody presence, appears brown. H&E counterstain followed DAB incubation, appearing blue in color allowing indication of cellular bodies.

A

X10 magnification   X40 magnification

B

X10 magnification   X40 magnification

C

X10 magnification   X40 magnification

D

X10 magnification   X40 magnification
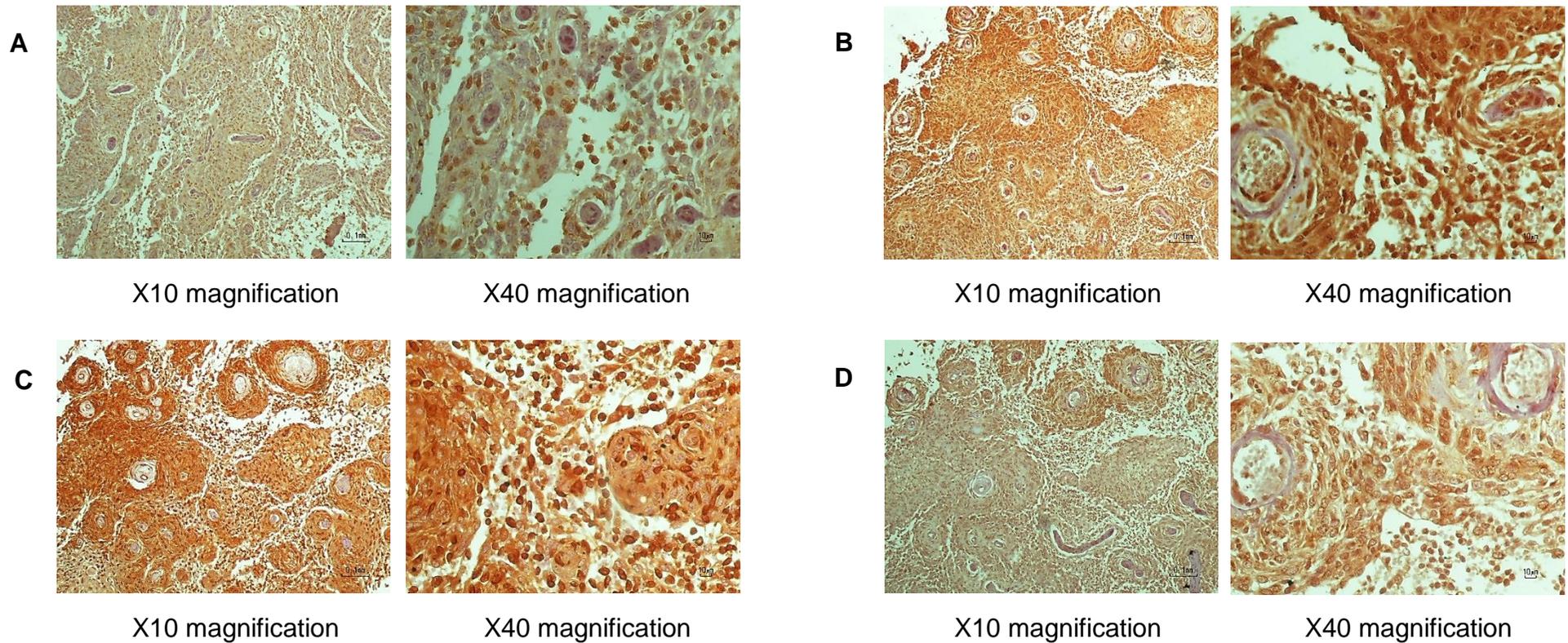
Figure 7.9: Photographic visualisation via light microscopy of the immunohistochemistry antibody expression profiles associated with serine biosynthetic and glycolytic pathways in the tissue sections belongings to patient 145, a grade I meningioma patient (n=1). Antibodies of interest include; p53 (A), PKM2 (B), Fascin (C) and PHGDH (D). Incubation with DAB (6 minutes) enables antibody presence, appears brown. H&E counterstain followed DAB incubation, appearing blue in color allowing indication of cellular bodies.
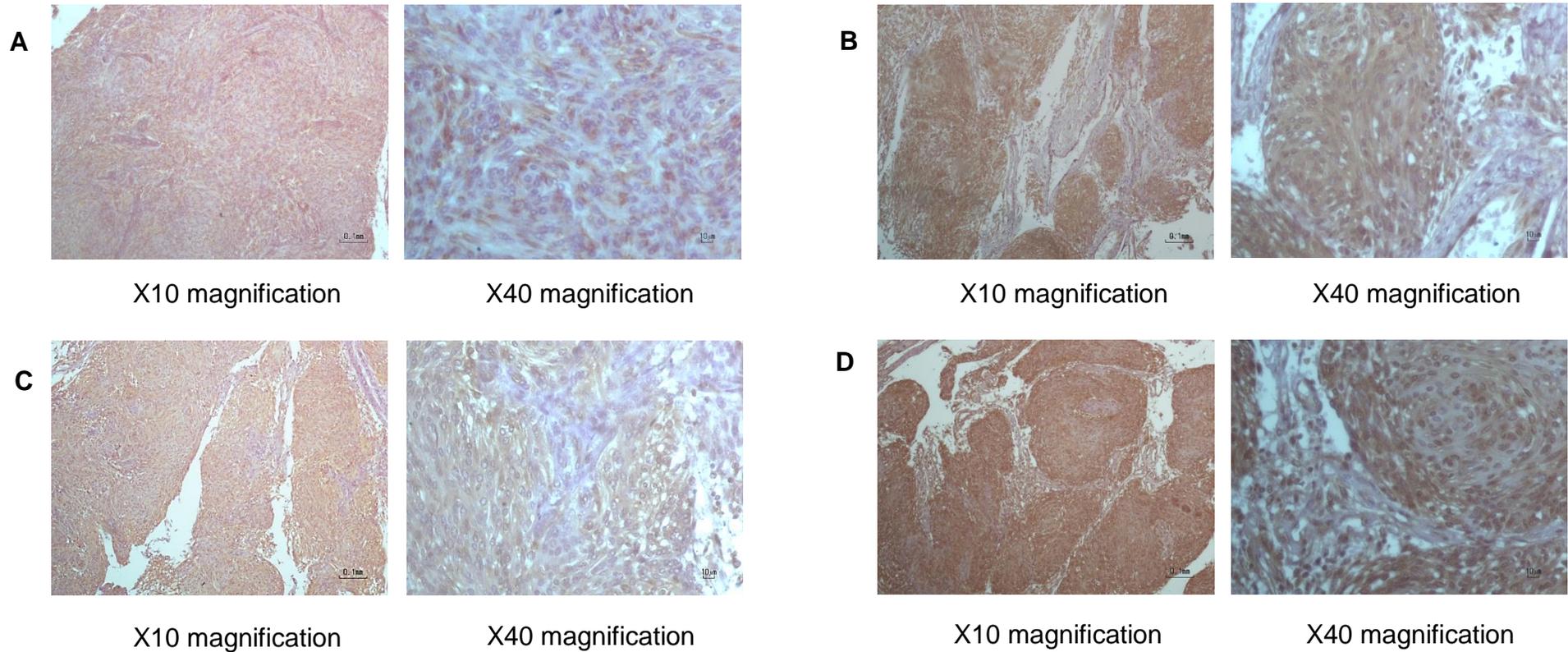
Figure 7.10: Photographic visualisation via light microscopy of the immunohistochemistry antibody expression profiles associated with serine biosynthetic and glycolytic pathways in the tissue sections belongings to patient 36, a grade I meningioma patient (n=1). Antibodies of interest include; p53 (A), PKM2 (B), Fascin (C) and PHGDH (D). Incubation with DAB (6 minutes) enables antibody presence, appears brown. H&E counterstain followed DAB incubation, appearing blue in color allowing indication of cellular bodies.

A

X10 magnification   X40 magnification

B

X10 magnification   X40 magnification

C

X10 magnification   X40 magnification
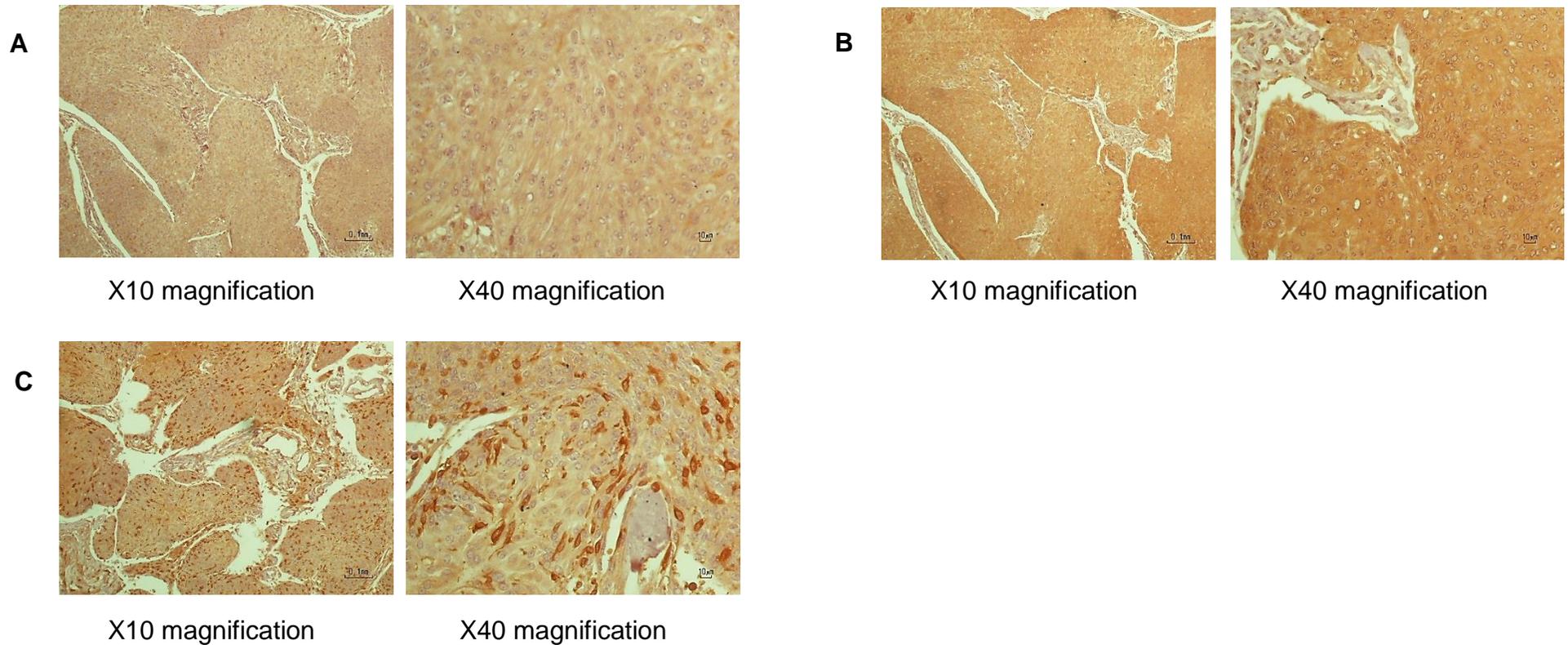
Figure 7.11: Photographic visualisation via light microscopy of the immunohistochemistry antibody expression profiles associated with serine biosynthetic and glycolytic pathways in the tissue sections belongings to patient 395, a grade II meningioma patient (n=1). Antibodies of interest include; p53 (A), PKM2 (B) and Fascin (C). Incubation with DAB (6 minutes) enables antibody presence, appears brown. H&E counterstain followed DAB incubation, appearing blue in color allowing indication of cellular bodies.

A

X10 magnification   X40 magnification

B

X10 magnification   X40 magnification

C

X10 magnification   X40 magnification

D

X10 magnification   X40 magnification
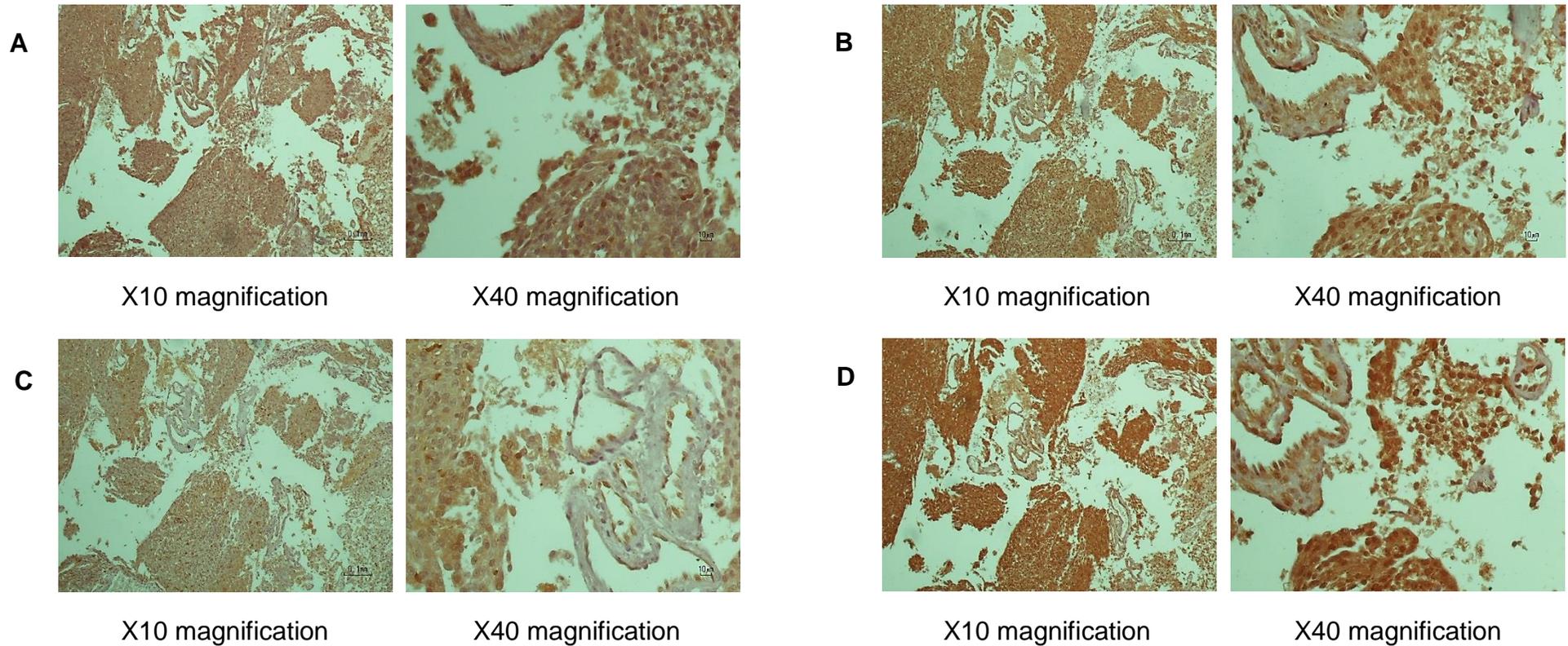
Figure 7.12. Photographic visualisation via light microscopy of the immunohistochemistry antibody expression profiles associated with serine biosynthetic and glycolytic pathways in the tissue sections belongings to patient 457, a grade II meningioma patient (n=1). Antibodies of interest include; p53 (A), PKM2 (B), Fascin (C) and PHGDH (D). Incubation with DAB (6 minutes) enables antibody presence, appears brown. H&E counterstain followed DAB incubation, appearing blue in color allowing indication of cellular bodies.

A

X10 magnification   X40 magnification

B

X10 magnification   X40 magnification

**C**

X10 magnification   X40 magnification
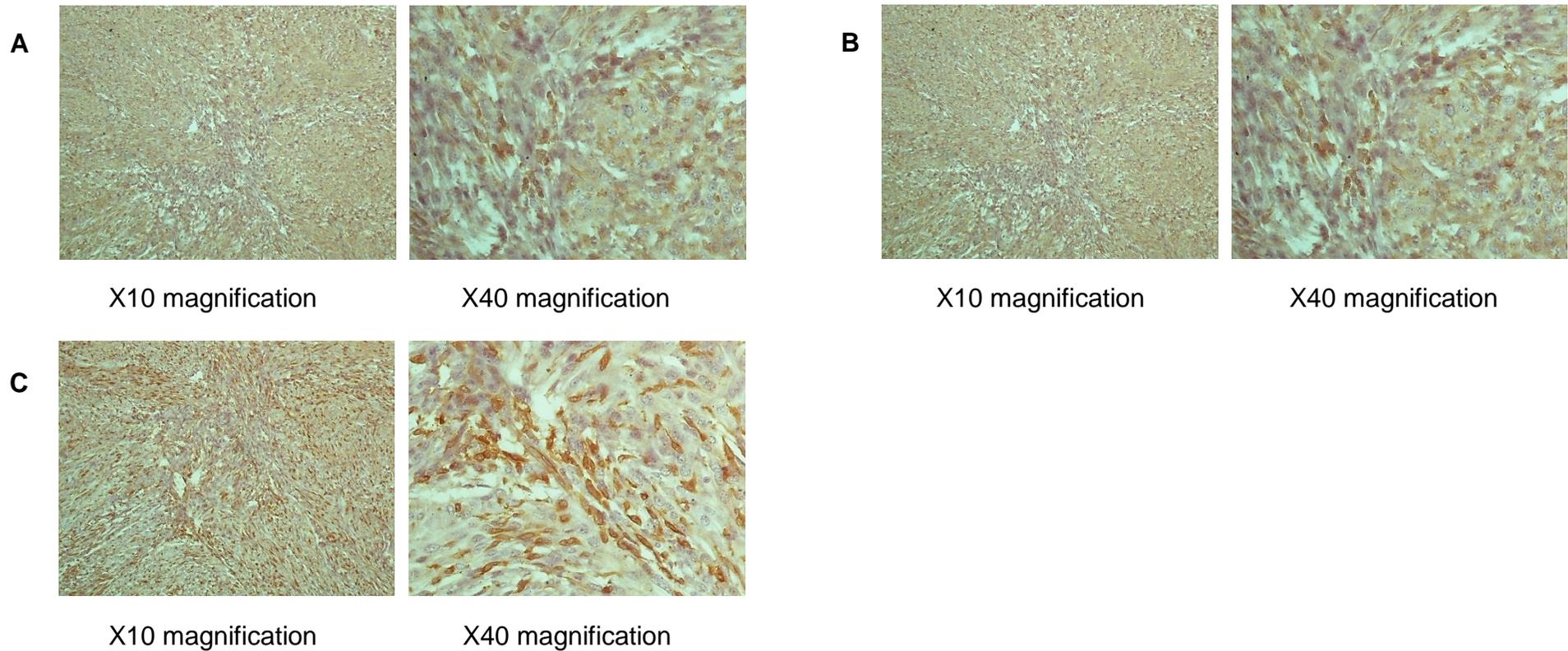
Figure 7.13: Photographic visualisation via light microscopy of the immunohistochemistry antibody expression profiles associated with serine biosynthetic and glycolytic pathways in the tissue sections belongings to patient 677, a grade II meningioma patient (n=1). Antibodies of interest include; p53 (A), PKM2 (B) and Fascin (C). Incubation with DAB (6 minutes) enables antibody presence, appears brown. H&E counterstain followed DAB incubation, appearing blue in color allowing indication of cellular bodies.
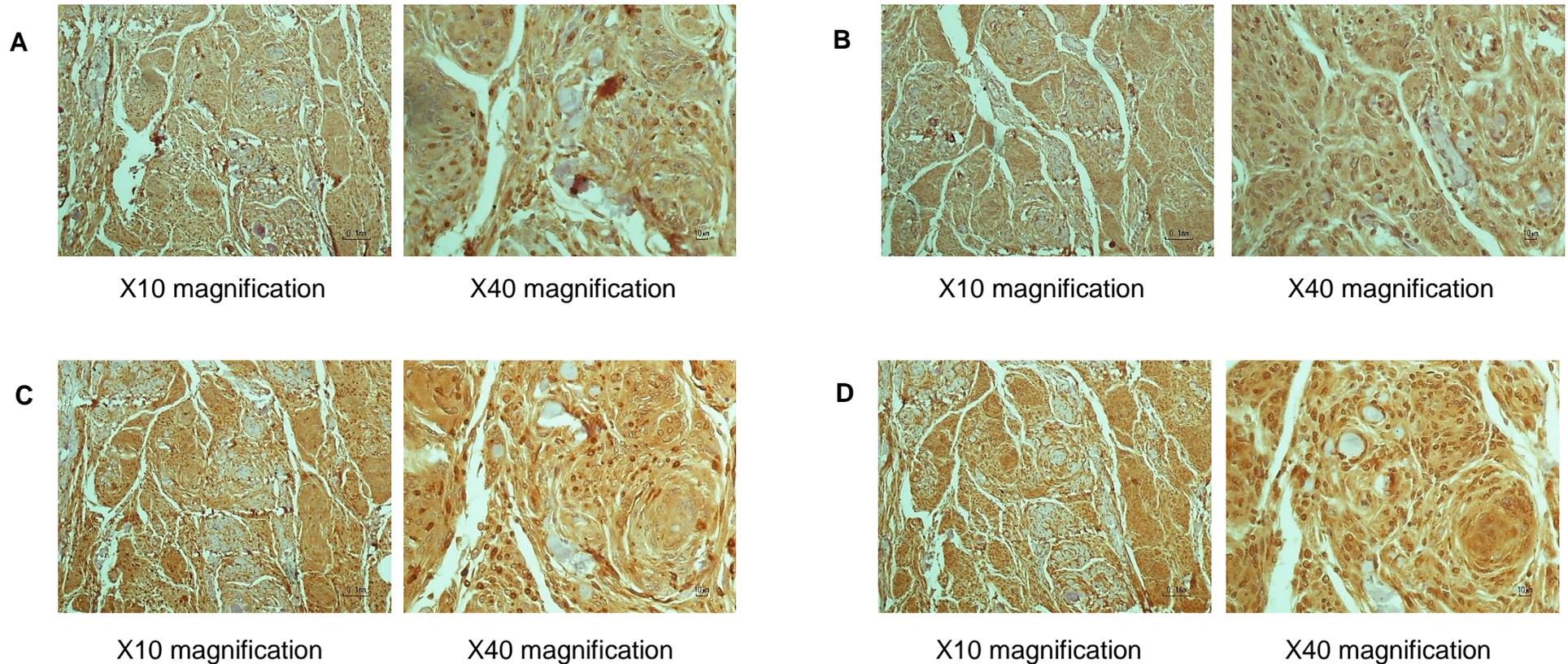
Figure 7.14: Photographic visualisation via light microscopy of the immunohistochemistry antibody expression profiles associated with serine biosynthetic and glycolytic pathways in the tissue sections belongings to patient 708, a grade II meningioma patient (n=1). Antibodies of interest include; p53 (A), PKM2 (B), Fascin (C) and PHGDH (D). Incubation with DAB (6 minutes) enables antibody presence, appears brown. H&E counterstain followed DAB incubation, appearing blue in color allowing indication of cellular bodies.

A

X10 magnification   X40 magnification

B

X10 magnification   X40 magnification

**C**

X10 magnification   X40 magnification
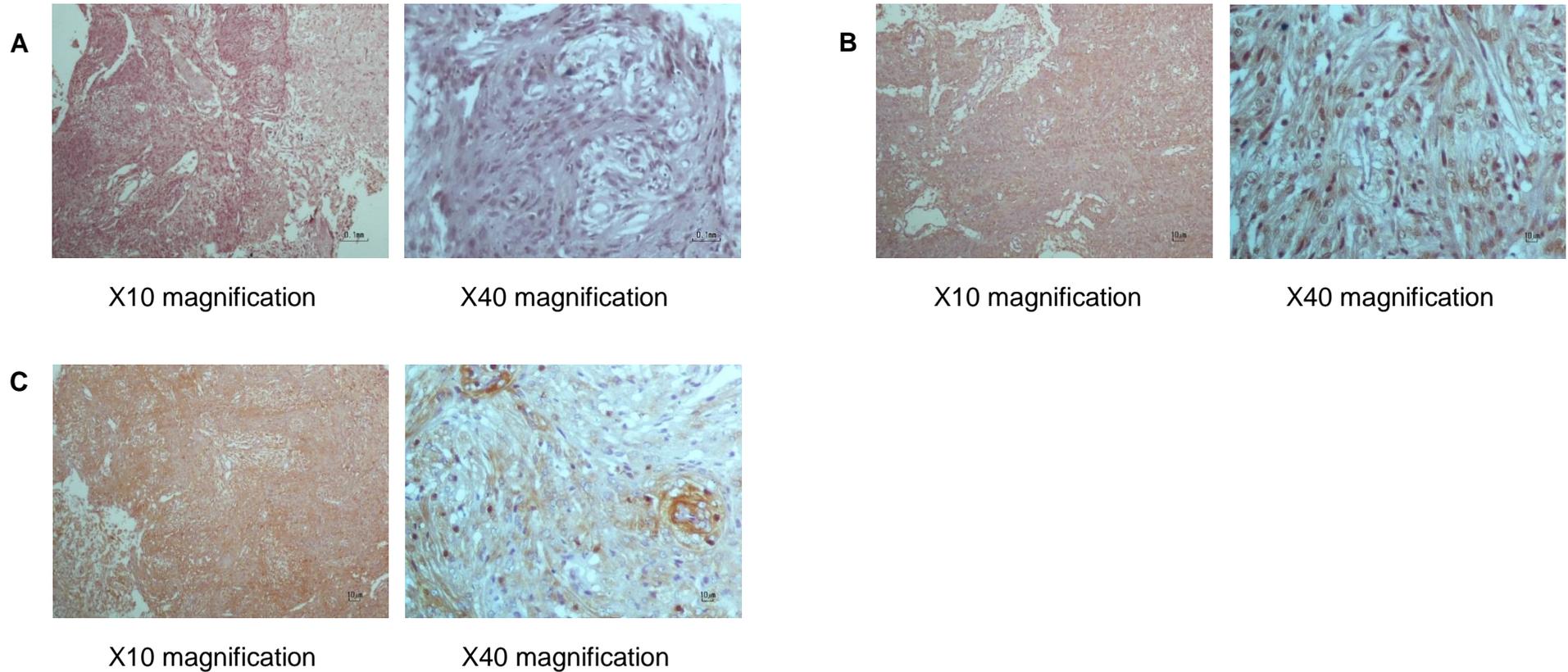
Figure 7.15: Photographic visualisation via light microscopy of the immunohistochemistry antibody expression profiles associated with serine biosynthetic and glycolytic pathways in the tissue sections belongings to patient 286, a grade II meningioma patient (n=1). Antibodies of interest include; p53 (A), PKM2 (B) and Fascin (C). Incubation with DAB (6 minutes) enables antibody presence, appears brown. H&E counterstain followed DAB incubation, appearing blue in color allowing indication of cellular bodies.

A

X10 magnification   X40 magnification

B

X10 magnification   X40 magnification

C

X10 magnification   X40 magnification
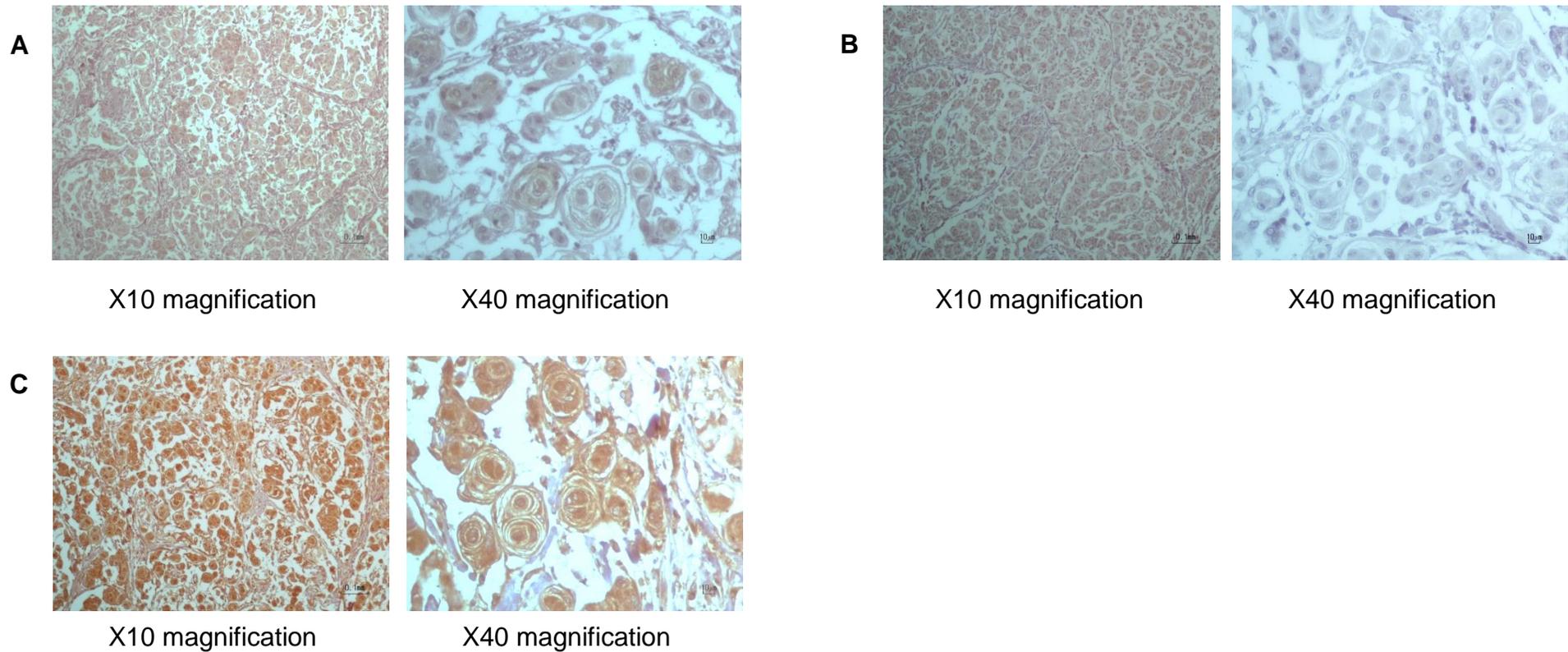
Figure 7.16: Photographic visualisation via light microscopy of the immunohistochemistry antibody expression profiles associated with serine biosynthetic and glycolytic pathways in the tissue sections belongings to patient 198, a grade II meningioma patient (n=1). Antibodies of interest include; p53 (A), PKM2 (B) and Fascin (C). Incubation with DAB (6 minutes) enables antibody presence, appears brown. H&E counterstain followed DAB incubation, appearing blue in color allowing indication of cellular bodies.

A

X10 magnification   X40 magnification

B

X10 magnification   X40 magnification

C

X10 magnification   X40 magnification
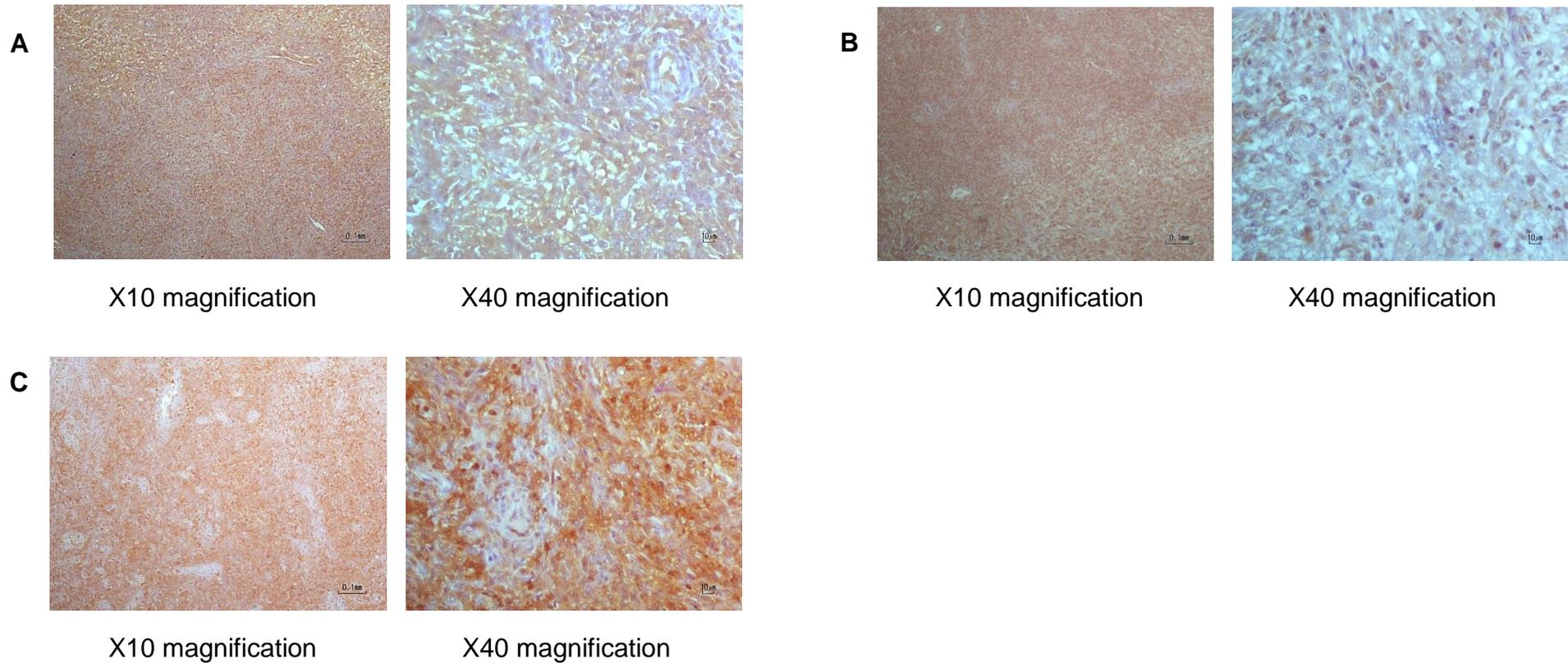
Figure 7.17: Photographic visualisation via light microscopy of the immunohistochemistry antibody expression profiles associated with serine biosynthetic and glycolytic pathways in the tissue sections belongings to patient 143, a grade II meningioma patient (n=1). Antibodies of interest include; p53 (A), PKM2 (B) and Fascin (C). Incubation with DAB (6 minutes) enables antibody presence, appears brown. H&E counterstain followed DAB incubation, appearing blue in color allowing indication of cellular bodies.

A X10 magnification X40 magnification

B X10 magnification X40 magnification

C X10 magnification X40 magnification

**D** X10 magnification X40 magnification
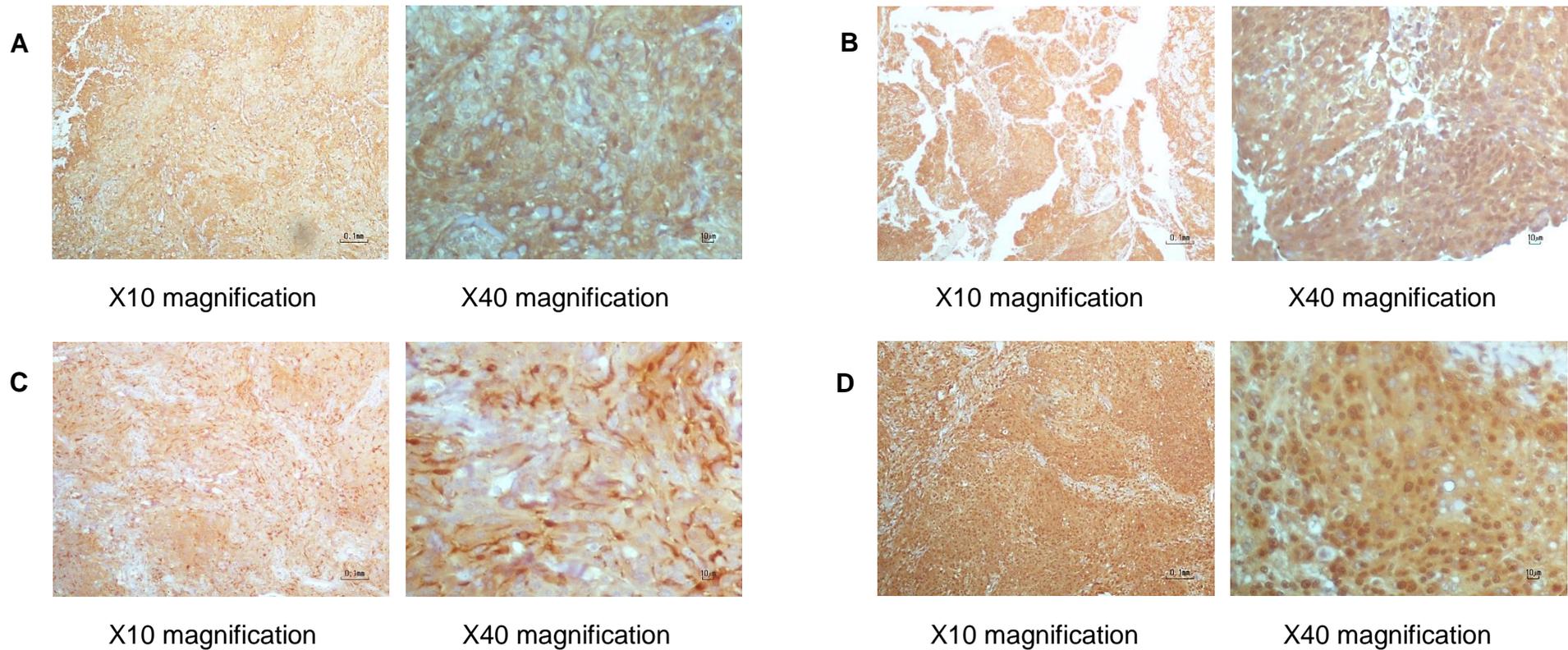
Figure 7.18: Photographic visualisation via light microscopy of the immunohistochemistry antibody expression profiles associated with serine biosynthetic and glycolytic pathways in the tissue sections belongings to patient 392, a grade II meningioma patient (n=1). Antibodies of interest include; p53 (A), PKM2 (B), Fascin (C) and PHGDH (D). Incubation with DAB (6 minutes) enables antibody presence, appears brown. H&E counterstain followed DAB incubation, appearing blue in color allowing indication of cellular bodies.

7.21 APPENDIX 21

7.21.1 Publications

Hatchell H, Hill M, Lawrence C, Rolph C (2014). P45LIPID SIGNATURES IN MENINGIOMA - METABOLIC CLUES TO REVEAL POTENTIAL THERAPEUTIC TARGETS. *Neuro-Oncology.* 2014;16 (Suppl 6):vi7. doi:10.1093/neuonc/nou249.33.

7.21.2 Presentation attended and presented

Hatchell H (2013). Tumour associated lipid signatures: Metabolic clues via yeast paradigms. Brain Tumour North West 7th Annual Retreat.

Hatchell, H (2015). Poster presentation. Sidney Driscoll Foundation Annual Neuroscience Lecture tomorrow based at Royal Preston Hospital.

Hatchell, H (2015). Poster presentation. Sidney Driscoll Foundation Neuroscience Lecture tomorrow based at Royal Preston Hospital.

Attended Brain Tumour North West 9th Annual Retreat (2015).

Attended Brain Tumour North West 10th Annual Retreat (2016).